WORLD CLIMATE RESEARCH PROGRAMME

WORLD OCEAN CIRCULATION EXPERIMENT

Report of the WOCE North Atlantic Workshop

by F. Schott, C. Böning, H. Bryden, R. Molinari,
P. Schlosser, C. Wunsch and L. Stramma

Institut für Meereskunde, Universität Kiel, Germany
23–27 August 1999

WOCE Report No. 169/2000

February 2000, WOCE International Project Office, Southampton

WOCE is a component of the World Climate Research Programme (WCRP), which was established by WMO and ICSU, and is carried out in association with IOC and SCOR. The scientific planning and development of WOCE is under the guidance of the Scientific Steering Group for WOCE, assisted by the WOCE International Project Office.

Report prepared in the WOCE International Project Office

Report Editor: **Roberta Boscolo**

Layout: **Sheelagh Collyer**

BIBLIOGRAPHIC CITATION

WOCE INTERNATIONAL PROJECT OFFICE 2000 Report of the WOCE North Atlantic Workshop, Institut für Meereskunde, Universität Kiel, Germany, 23–27 August 1999. WOCE International Project Office, WOCE Report No. 169/2000, 110pp.

CONTENTS

1. INTRODUCTION AND OVERVIEW

The WOCE North Atlantic Workshop was held at Institut für Meereskunde in Kiel during 23–27 August 1999, with the sessions taking place in the Art Gallery located in close proximity to the Institute. It was opened by the Mayor of Kiel, Mr Norbert Gansel, who welcomed the participants and gave a short background on the history of Kiel and of its association with the sea. Prof. Peter Lemke, Director of the Institut für Meereskunde then gave a welcome address in which he outlined the structure and research missions of the Institute. Dr John Gould, Director of the WOCE International Project Office, briefly reviewed the tasks ahead and summarised the roles of other relevant WOCE Workshops. Finally, Friedrich Schott, Chairman of the Scientific Organising Committee, explained how the specific structure and organisational form of the Workshop was selected and what the expectations were as to accomplishments.

Attendance of the Workshop was about 150, with about half coming from Germany, 35 from North America, 15 from the UK, 10 from the Nordic countries and the rest of the participants from other European countries. A reception was held on Monday aboard the Research Vessel “Alkor” at the Institute dock and a Workshop Dinner on Wednesday in the Kiel Yacht Club.

The Workshop was organised into:

- four main sessions with a total of 30 invited presentations and general discussion periods at the end of each session to identify and discuss overarching questions pertinent to session topics;
- poster displays for each session;
- working group deliberations.

Considering the large observed water mass and circulation variability of the North Atlantic it was decided early in the planning process to put emphasis on decadal variability aspect while at the same time keeping in mind that a WOCE Variability Workshop is being planned for the fall of 2000.

The four main sessions dealt with the following topics:

1. North Atlantic decadal variability and the WOCE period;
2. North Atlantic circulation, pathways and water mass distributions from WOCE observations, altimetry and model results;
3. Thermohaline overturning and flux divergences;
4. Process studies, which was subdivided into four sub-sessions: Overflows; Labrador Sea convection; deep mixing and role of topography; thermocline ventilation.

The detailed agenda is attached in Appendix 1; the abstracts of the invited session presentations are in Section 2 of this report.

In the general discussion periods following each of the sessions, problem areas were identified for further study and taken up subsequently in the Working Group discussions. The Scientific Organising Committee defined four Working Group topics ahead of time and the objectives of each of them were presented on the Workshop web site and again to the participants at opening time.

The number of posters shown at the Workshop was 78 (listed in Appendix 4). Poster abstracts were presented on the Workshop web-site prior to the Workshop and handed out as a printed collection to participants at registration time. The posters were grouped by session topics, and there were about a quarter of the total for each of the four sessions. Posters were displayed in two batches: for sessions 1/2 during Monday/Tuesday, and for sessions 3/4 on Wednesday/Thursday. Poster presenters were given the opportunity to briefly introduce their posters during the discussion periods at the end of each session.

2. ABSTRACTS OF INVITED PRESENTATIONS

2.1 North Atlantic decadal variability and the WOCE period

Interdecadal Variability in Coupled GCMs: Model results versus observations

M. Latif, Max-Planck-Institut für Meteorologie, Hamburg, Germany. latif@dkrz.de

The climate over the North Atlantic Ocean and its adjacent land areas is strongly governed by the North Atlantic Oscillation (NAO). The NAO is characterised by strong year-to-year fluctuations, but it exhibits also some pronounced interdecadal variability. Some recent atmospheric model integrations indicate that the low-frequency changes in the NAO may be forced by low-frequency changes in the underlying SST (e.g. Rodwell et al., 1999).

Global coupled ocean-atmosphere general circulation models (CGCMs) simulate realistically the low-frequency variability in the NAO (e.g. Latif et al., 1997, and references therein). The CGCMs can be used to study the mechanisms that lead to the interdecadal variability. All models indicate that a stochastic concept should be adopted to understand the dynamics of the interdecadal variability, as originally described by Hasselmann (1976). The spectra of quantities simulated by the CGCMs support this simple picture: Atmospheric quantities exhibit almost white spectra, while oceanic quantities are characterised by red spectra (Fig. 1).

Spectral peaks are also found in some model simulations, and these can be understood also within the "stochastic concept": Damped eigenmodes of the ocean or the coupled ocean-atmosphere system may be excited by the stochastic forcing. Consistent with observations generally two types of variables are simulated: Decadal variability and multi-decadal variability. While the decadal variability is associated with time scales of 10–20 years, the multi-decadal variability has characteristic time scales of many decades. The sea surface temperature anomaly (SSTA) structures of the decadal and multi-decadal variabilities differ considerably: While the decadal variability is associated with an SST-tripole, the multi-decadal variability is associated with an SST-monopole in the North Atlantic. There are indications from the models and from observations that the decadal variability is associated with variations in the wind-driven gyres, while the multi-decadal variability is connected to variations of the thermohaline circulation (THC).

References

Hasselmann, K.,1976: Stochastic climate models. Part I: Theory. Tellus, 28, 473–485.

Latif, M.,1997: Dynamics of interdecadal variability in coupled ocean-atmosphere models. J. Climate, 11, 602–624.

Rodwell, M. J., D. P. Rowell, and C. K. Folland, 1999: Oceanic forcing of the wintertime North Atlantic Oscillation and European climate. Nature, 398, 320–323.

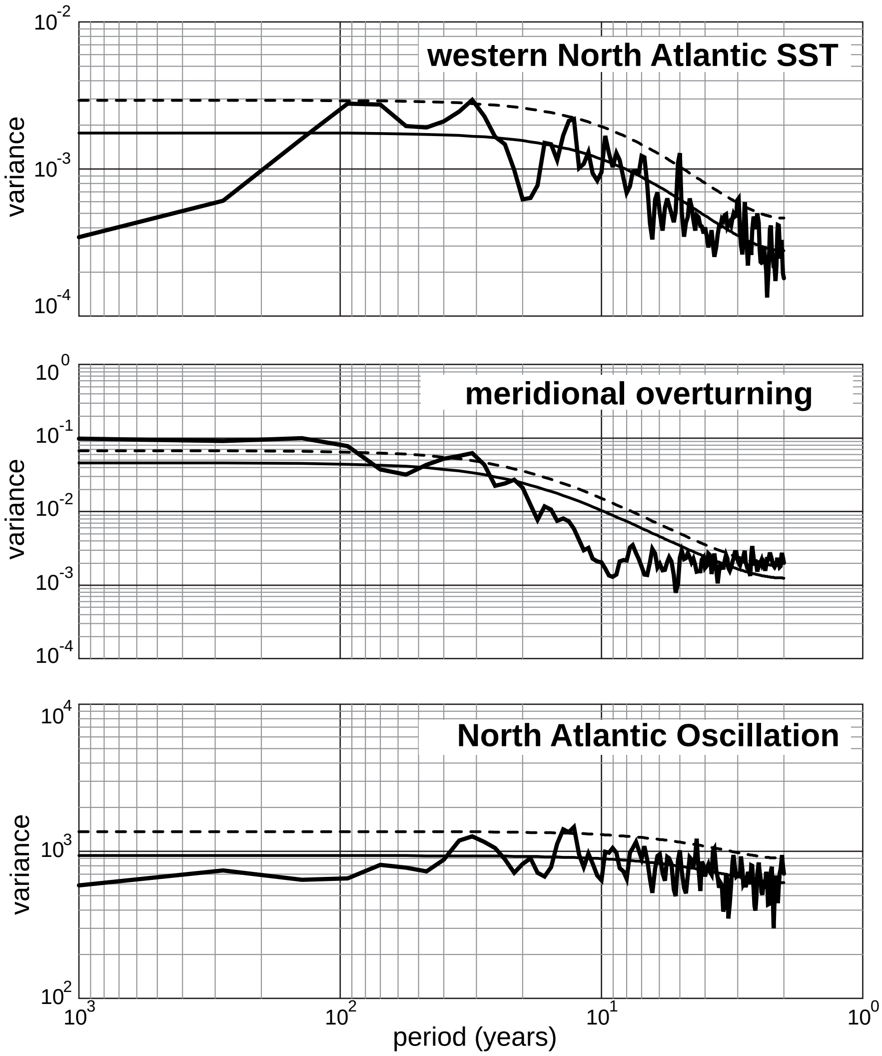

Figure 1. Spectra of the anomalous North Atlantic SST, overturning and the NAO index as simulated by the CGCM ECHAM3/LSG in a 2000-year integration. The solid curves in all three panels show the corresponding AR-1 spectra. The dashed curves indicate the 95% significance levels.

Decadal variability of water masses and circulation in the subpolar North Atlantic

Ruth G. Curry, Woods Hole Oceanographic Institution, USA

The WOCE measurement programme in the 1990s' subpolar gyre recorded an extreme phase in the North Atlantic Ocean's interdecadal fluctuation of thermohaline and gyre circulation, heat content, and property distributions. This oceanic fluctuation is primarily a response to and integration of atmospheric forcing variability dominated by the North Atlantic Oscillation (NAO) mode (or, perhaps more broadly, the Arctic Oscillation (AO) described by Thompson and Wallace, 1998); and to second order, changes in freshwater forcing induced by variations in outflows from the Arctic seas. Characterised by changes in atmospheric mass distributions with centres of action in the Azores high and Iceland low Sea Level Pressure (SLP) cells, the NAO itself has undergone a quasi-decadal fluctuation and multi-decadal modulation in the last half of this century. These are associated with changes of strength and geography of the surface westerlies across the mid-latitude Atlantic Ocean into Europe as well as the intensity of the wintertime polar vortex. Several versions of an NAO index (NAOI) have been generated from differences in wintertime SLP recorded near those action centres (e.g. Hurrell, 1995; Jones et al., 1997). The general patterns of NAO variability reflect noisy, quasi-biennial variations during the 19th century, followed by the development of lower frequency (quasi-decadal) and higher amplitude characteristics since about 1905 (Hurrell and van Loon, 1997). The NAO's most extreme and persistent negative phase dominated the 1950s and 1960s. Circa 1972, the NAO shifted to a persistently high phase that culminated in extreme index values in the late 1980s and early 1990s, but ended with a dramatic drop to its opposite extreme in winter 1995/96. Hydrographic measurements acquired over the past fifty years indicate that, from shallow to deep, the subpolar water masses have been altered by the cumulative effects of wind and surface heat flux patterns associated with the NAO, and further punctuated by intermittent episodes of enhanced ice/freshwater outflow from the Arctic seas and warm/saline waters from the subtropics.

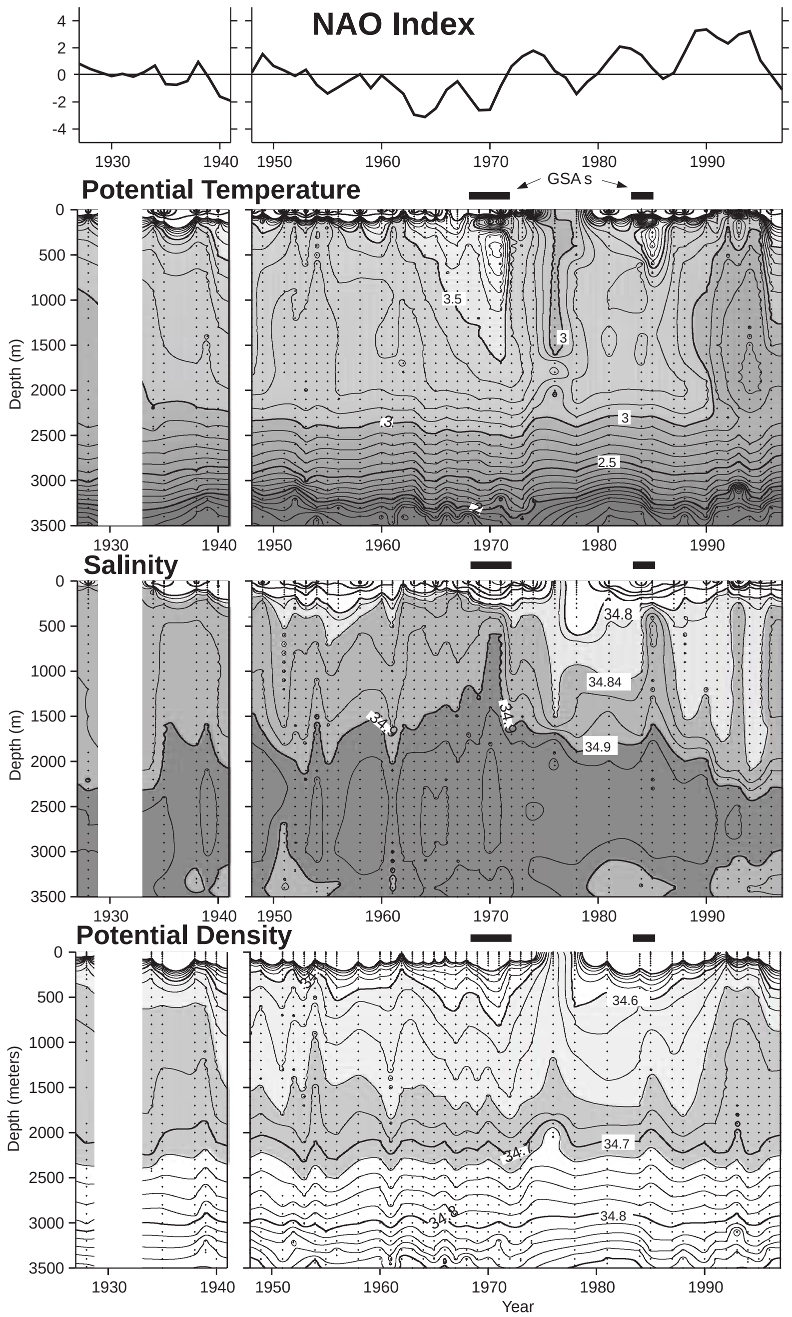

Figure 1. Time series of properties as a function of depth in the central Labrador Basin. Stations were limited to those where seafloor depth exceeded 3500 m. All measurements for each year were isopycnally averaged to produce an annual mean profile. Small crosses indicate years and depths for which data were available. The top panel is an NAO index (Hurrell, 1996) constructed from wintertime SLP differences between Iceland and Portugal and smoothed with a 3-point running mean. Two documented "Great Salinity Anomaly" occupations of the region are denoted by dark bars and labelled GSA. Contour intervals are: potential temperature 0.1˚C, salinity 0.02, potential density (relative to 1500 db) $0.02\,kg/m^3$.

Deep Water production/Labrador Sea Water history

Two major convective centres which form deep waters in the North Atlantic are located in the Greenland Sea and Labrador Basin. Dickson et al. (1996) demonstrated an opposite phasing of convective activity at these sites that was coordinated by NAO atmospheric forcing. During the NAO low phase of the 1960s, ventilation of the Greenland Sea was at a maximum (>3500 m) while the Labrador Sea was tightly capped. After 1972, convective activity in the Greenland Sea steadily diminished with convective exchange restricted to <1000 m by 1993, while Labrador Sea convection intensified in two main stages, reaching >2300 m in 1992. From observed surface heat and freshwater fluxes spanning 1980–95, Labrador Sea Water (LSW) renewal increased from essentially zero in the early 1980s to ~10 Sv in 1990, while Greenland Sea Deep Water (GSDW) declined from ~11 Sv in 1981 to ~3.5 Sv in 1991 (R. Marsh, submitted).

The history of deep water production in the subpolar gyre is recorded in the relatively long time series of measurements in the central Labrador Basin near Ocean Weather Station "Bravo" (Fig. 1). The temperature record (second panel) reflects the quasi-decadal cycles of NAOI-correlated surface heat fluxes (Cayan, 1992): periods of enhanced heat flux and deep convection (colder temperatures between 500–2000 m) in the 1920s, 1950s, 1970s, and 1990s alternating with diminished heat flux and weak convection (warmer temperatures) in the 1940s, 1960s and 1980s. The 1990s stand out in the degree of cooling (<2.7°C) and depth of convection (>2300 m).

The salinity history (third panel, Fig. 1) somewhat echoes these cycles, but also exhibits a longer trend toward increasingly fresh LSW over the past 70 years. The descent of the 34.84 isohaline best describes this trend. In the 1920s, despite strong convection and cold temperatures (<3.0°C), the salinities were relatively high (>34.88) with a diminished gradient between LSW and the underlying Iceland–Scotland overflow waters (ISOW) (>34.92). By 1993, the salinity had dropped below 34.84 all the way down to 2000 m. A slight freshening occurred in the 1950s but the bulk of freshening was incurred by two distinct episodes of enhanced Arctic outflows of ice and freshwater, the "Great Salinity Anomalies" which occupied the Labrador Basin in 1968–72 and again in the early 1980s (Dickson et al., 1988; Belkin et al., 1997). The first pulse of freshwater/sea ice was traced back to the Arctic through Fram Strait; the second entered the Labrador Basin through Davis Strait from Baffin Bay. These fluctuations of Arctic outflow were associated with anomalous northerly winds east of Greenland, in the first event, and off the Canadian Archipelago in the second (Dickson et al., 1988; Hakkinen, 1993; Belkin et al., 1998). The outflows boosted the baroclinic transport of the Labrador slope current (Petrie and Drinkwater, 1993) and the low salinity signal subsequently spread eastward in a pattern consistent with horizontal mixing between the strengthened Labrador slope current and North Atlantic Current (Reverdin et al., 1997).

The decadally varying strength of overturning and associated changes in vertical density structure (bottom panel, Fig. 1) in the Labrador Basin are primarily thermally-driven phenomena. Over the instrumental record, temperature and salinity, vertically averaged over the upper 2000 db water column, changed by approximately 0.8°C and 0.06 respectively. The relative

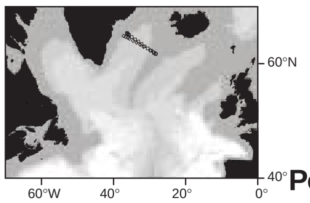

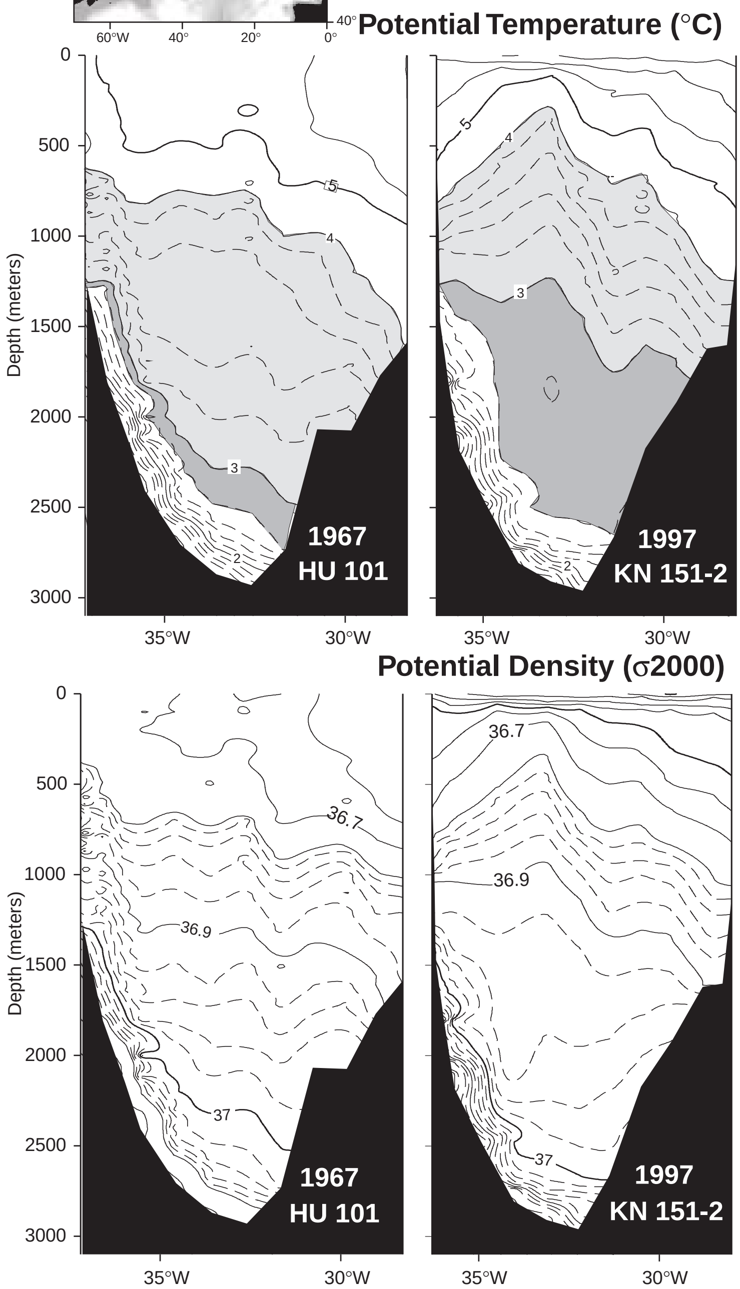

Figure 2. Vertical sections in the Irminger Basin. Top panels are potential temperature sections from Hudson 101 in 1967 (left) and KN151-2 in 1997 (right). Temperatures between 2.8°–4°C have been shaded grey. Bottom panels are potential density sections from the same cruises. The map indicates the location of the sections across the Irminger Basin.

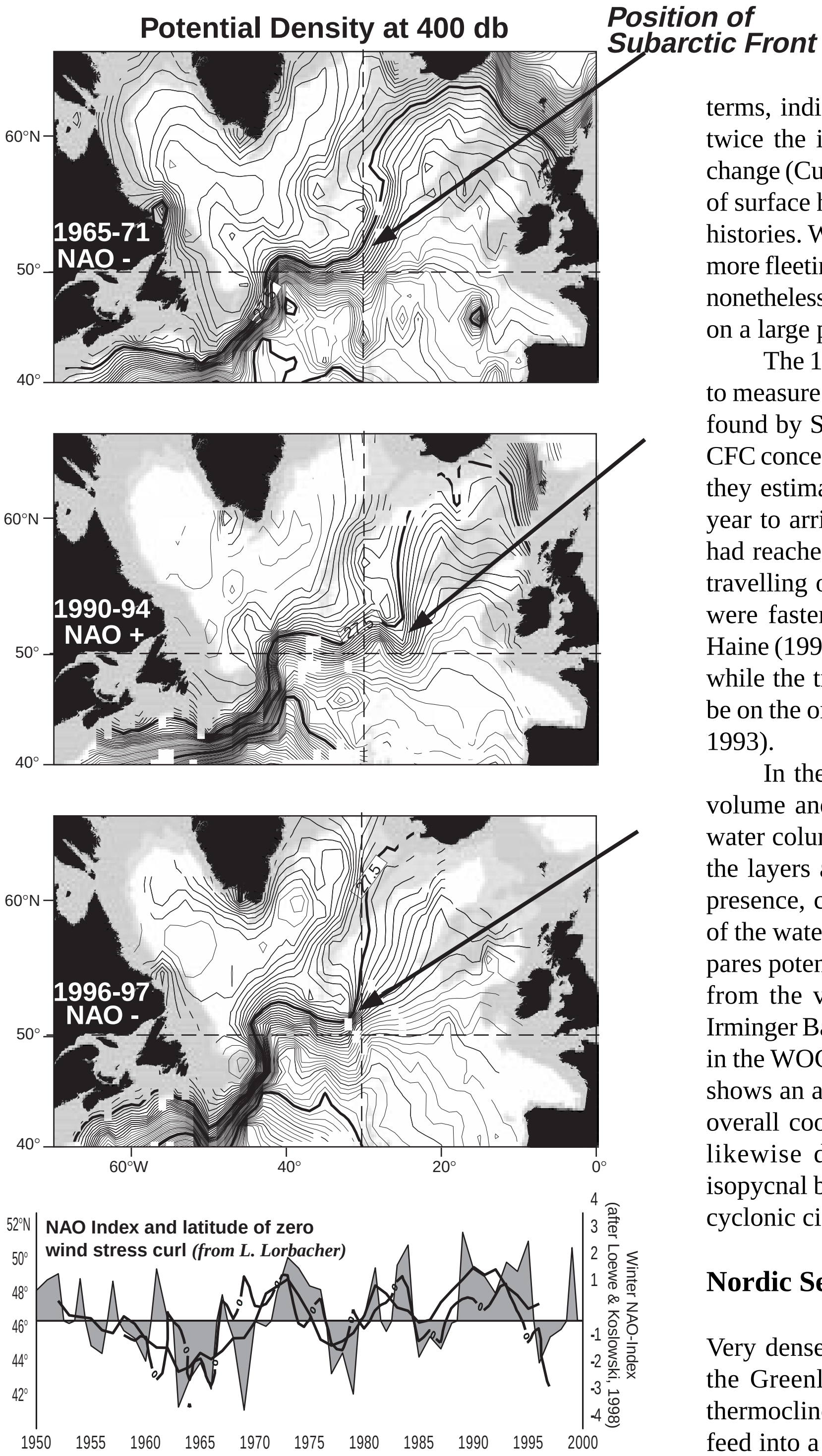

Figure 3. Potential density at 400 db shows location of Subarctic Front in years of extreme negative NAO forcing (top), positive NAO (second panel), and after the precipitous drop of NAO in 1995/96 (third panel). Arrows mark the eastward position of the front. Lines have been drawn at 30°W and 50°N to help visualise the shifted positions. The bottom panel shows the annual mean latitude of the zero wind stress curl (heavy line annotated 0) between longitudes 30°–45°W as computed by K. Lorbacher (pers. comm.). The NAO index (Lowe and Koslowski, 1998) is co-plotted, the thick line being a low-pass filtered version of the thin line.

contributions of temperature and salinity changes to density, determined from the thermal expansion and salinity contraction terms, indicate that the temperature change had roughly twice the impact on LSW density compared to salinity change (Curry and McCartney, in prep.). Thus the intensity of surface heat flux dominates the convection and density histories. While the role of surface salinity anomalies was more fleeting in their influence on convective activity, they nonetheless left a distinct and lasting footprint of freshening on a large portion of the subpolar water column.

The 1990s vintages of LSW provided an opportunity to measure its spreading rate in the subpolar gyre and was found by Sy et al. (1997) to be surprisingly rapid. Using CFC concentrations and temperature/salinity distributions, they estimated that LSW from a particular year took <1 year to arrive in the Irminger Basin. Within 4–5 years it had reached the eastern boundary in the Rockall Trough travelling on average at 1.5–2.0 cm/sec. These estimates were faster than previously believed: Cunningham and Haine (1995) estimated a 1.0–1.5 cm/sec eastward spread, while the transit time to the Rockall area was thought to be on the order of 18 years (Read and Gould, 1992; Ellett, 1993).

In the Irminger and Iceland Basins, the anomalous volume and properties of LSW substantially altered the water column structure. In the Irminger Basin especially, the layers above and below were squeezed by the LSW presence, causing a considerable cooling and freshening of the water properties between 500–2000 m. Fig. 2 compares potential temperature and potential density sections from the very high quality Hudson section across the Irminger Basin in 1967, with the same crossing of the basin in the WOCE programme thirty years later. The later time shows an appreciable doming of the isotherms as well as overall cooling of the basin interior. The isopycnals are likewise domed at shallower levels while the deep isopycnal bowl is steepened, thus translating to a stronger cyclonic circulation in the subpolar gyre of the 1990s.

Nordic Seas Overflows

Very dense waters formed in the Nordic Seas spill over the Greenland–Iceland–Faroe–Scotland Ridge, entrain thermocline and intermediate waters as they descend, and feed into a deep northern boundary current system in the subpolar gyre. Of the two principal Nordic Seas overflows (NSOW), ISOW is the more saline and Denmark Straits Overflow Water (DSOW) is the densest. The combined outflow of NSOW was estimated to be about 6 Sv near the sills, but the entrainment process approximately doubles that transport (Dickson and Brown, 1994). Dickson's direct measurements of the dense boundary current components off Angmagssalik, Greenland from 1986–91 indicated transports of ~11 Sv below $\sigma_\theta = 27.8$ that were remarkably stationary.

It remains unclear to what extent or on what time-scales the intensity of the overflows may vary. Several investigators have documented water mass characteristics in the overflows' density range that are significantly variable (Brewer et al., 1983; Swift, 1984; Lazier, 1988). From a collection of hydrographic sections emanating from Cape Farvel, Greenland, Bacon (1998) inferred a doubling and then halving of the transports of these denser classes of waters on decadal timescales. His analysis suggested a causal link between atmospheric conditions in the Nordic Seas (related to NAOI) and the intensity of the DSOW transports. Dickson et al (1999) recently documented a dramatic warming of the overflow core in 1997 off Angmagssalik. This condition was associated with an apparent upslope migration of the current – although not necessarily a change in flow speeds. They linked this event to atmospheric and hydrographic changes that occurred upstream in the West Spitzbergen Current three years previous, suggesting an element of predictability in the overflow characteristics. Over the same time period, repeat hydrography off Angmagssalik and Cape Farvel in fall 1996, spring 1997, and fall 1997 also noted a progressive uplift of the onshore edge of DSOW over that year (McCartney et al., 1998). The hydrography further indicated a significant freshening and growth of transports in the denser classes of waters. These observations occurred 1–2 years after the precipitous drop of the NAOI in 1995/96, suggesting a possible NSOW response to enhanced buoyancy forcing in the Nordic Seas. However, in the MRI "Faxafloi" section repeated across Denmark Strait from 1997–99, the Icelandic researchers have measured highly variable temperature-salinity properties that do not show any progressional time evolution (H. Valdimarson, pers. comm.).

Thus, questions regarding the nature and timescales of the variability linger. NAO fluctuations of wind speed and direction, air temperature and humidity could conceivably affect the overflow products in several ways. Variable buoyancy forcing could alter the amount and characteristics of water transformed into specific density classes and exported over the sills. Alterations of vertical density structure on either side of the sills might alter the hydraulic control of the overflow intensity. NAO shifts in wind patterns could influence the wind-driven exchanges of warm water between the subpolar gyre and Nordic Seas, or the freshwater/ice outflow from the Arctic. The production rates and characteristics of the subpolar waters that are entrained into the NSOW – which themselves are affected by NAO wind and buoyancy forcing – might also alter the transports and characteristics of the overflow products through time.

Position of the Subarctic Front

The Subarctic Front (SAF) is prominent in subsurface temperature, salinity and density distributions as a meandering but continuous band of strong horizontal gradients. From Flemish Cap to the Charlie Gibbs Fracture Zone (CGFZ) in the Mid Atlantic Ridge (MAR) it is synonymous with the northern branch of the North Atlantic Current (Krauss, 1986). East of the MAR, it makes a sharp turn northward and the strong gradients disappear, replaced by the vertically homogenised deep

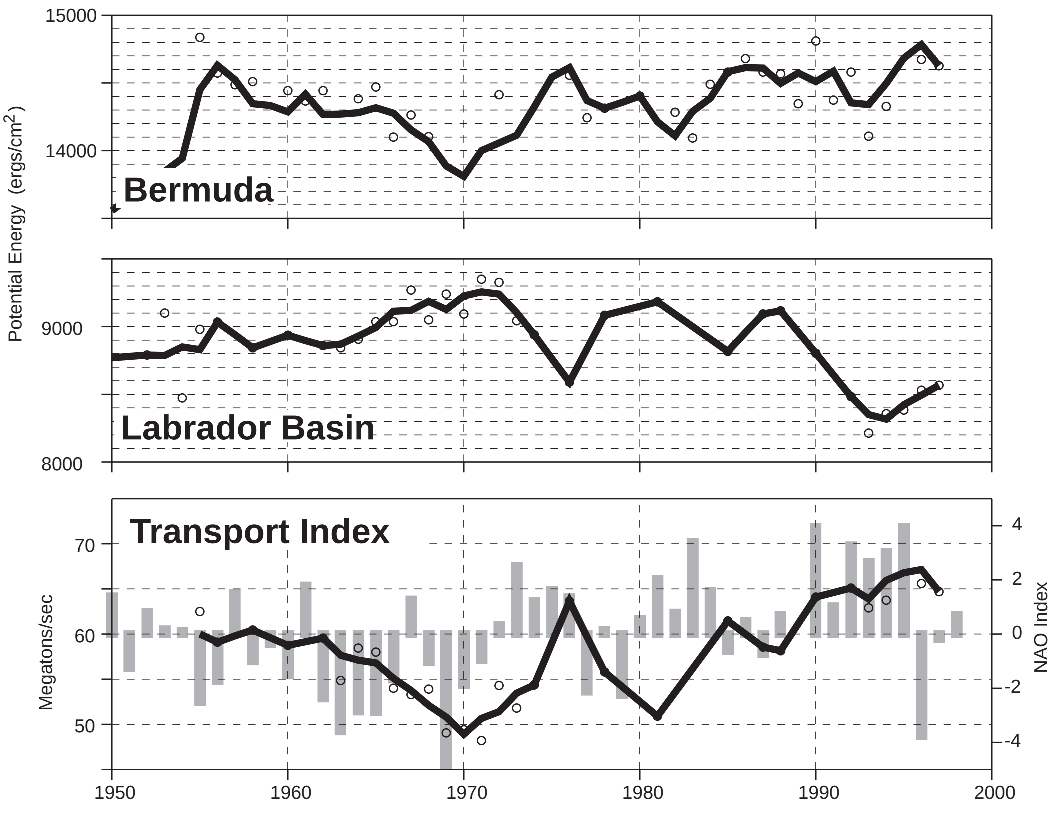

Figure 4. Top panels are time-series of potential energy from the central subtropical gyre (Station "S" near Bermuda) and central subpolar gyre (OWS "Bravo" in the Labrador Basin). Circles are annual values and the black curves are 3-point running means. The bottom panel is an index of the eastward baroclinic mass transport derived from the difference between PE at the gyre centres divided by an appropriate Coriolis parameter (f at latitude 40°N). Circles are the raw annual values, the black curve is a 3-point running mean. The atmospheric NAO index of Hurrell (1995) has been plotted as the grey bars.

winter mixed layers or Subpolar Mode Waters (SPMW). The SAF is a boundary between the warm and saline subtropical components advected in the North Atlantic Current and the cold subpolar gyre water masses. The location of the front is known to meander latitudinally by 200–300 km at frequencies of a few months and to form multiple branches, most likely in response to wind forcing (Belkin and Levitus, 1996).

A substantial east-west shift in the SAF, which occurred around the abrupt drop of the NAOI in winter 1995/96, was documented by hydrography sections along the WOCE A1E line (Bersch et al., 1999) and by XBT lines repeated along the Iceland and Newfoundland WOCE AX2 line (Reverdin et al., 1999). The early 1990s, a time of extreme high NAO, was associated with an eastward extension of the cold, fresh, and dense subpolar water masses across the MAR, with the SAF located near 23°W. After 1995, the low salinity subpolar waters retracted westward of the MAR, the SAF shifted to about 30°W, and warm, saline NAC waters replaced the colder, fresher elements east of the Reykjanes Ridge. A search into the historical record suggest that such shifts are a low frequency feature of the SAF. Fig. 3 shows the position of the SAF in 3 time periods (1965–71, 1990–94, and 1996–97) from the density field at 400 db. It was situated near 30°W in the 1960s' time of extended low NAO.

The low frequency east-west shifts may be partly rationalised through NAOI-correlated shifts of the wind stress fields. K. Lorbacher (pers. comm.) has analysed the annual mean latitudinal position of the zero wind stress curl (τ_0) between longitudes 30°–45°W and found a general correspondence of its position and the NAOI history. Consistent with the NAO SLP patterns, the high phases of NAOI are associated with a northerly position of τ_0 (47°–49°N), and the opposite low phase with a southerly position (43°–46°N – Fig. 3, bottom panel). The shifted zero wind stress curl line and changes in wind strength are likely to alter the meridional transports of the underlying NAC circulation elements. While τ_0 is in its northerly position (positive NAOI), the westerlies are in a strengthened phase, enhancing southward Ekman transports of the upper waters and thereby expanding the subpolar gyre influences. In its southerly position (negative NAOI), both winds and southward Ekman transports are weakened. Sverdrup theory further predicts zero net meridional transport along τ_0, so that when shifted southward, more of the warm NAC circulation elements lie to the north of this line, resulting in enhanced northward geostrophic transports of the warmer, saline components and therefore retraction of the cold subpolar influences. Bersch et al. (1999) further point out that high NAOI conditions force increased Ekman divergence in the subpolar gyre and therefore strengthened Ekman upwelling. This is consistent with the observed eastward expansion and thinning of the gyre SPMW layers. The weakened westerlies associated with low NAOI conditions reduce Ekman upwelling, decrease the doming of the gyre, and permit less dense waters from the margins to advance toward its centre – a westward contraction of the subpolar gyre.

Subpolar Mode Waters

The 1995/96 collapse of the extreme positive NAO was accompanied not only by the westward retraction of the subpolar gyre, but also by an order 1–2°C increase in temperature content of the SPMW layers extending down as far as 1000 m (Bersch et al., 1999; Reverdin et al., 1999). Compared to climatology, the early 1990s' SPMW were running ~1°C cooler and >0.1 psu fresher than usual, while the western subtropical thermocline was in a very warm and saline phase. In the low NAOI years 1965–71, the SPMW were running similarly warmer (~1°C relative to climatology) and more saline (>0.1) everywhere in the subpolar gyre; simultaneously, the western subtropical upper ocean was running 1–2°C cooler. Following the 1972 shift to positive NAOI, the SPMW grew rapidly cooler and fresher.

Although these patterns of warm/cold SPMW could be attributed to the NAOI-correlated surface heat flux anomalies (Cayan, 1992), several pieces of evidence suggest that ocean advection plays a significant role as well.

(1) The episodes of warming and cooling are also mirrored in analyses that show SST anomalies propagating from the western subtropics to eastern subpolar regions (Hansen and Bezkek, 1996; Sutton and Allen, 1997).

(2) Reverdin et al. (1999) and Bersch et al. (1999) both report that the 1990s temperature changes are twice what could be expected from the NAOI change in air-sea heat fluxes.

(3) The warm SPMW, in the late 1990s, was accompanied by increased salinities which would require unrealistic amounts of evaporation were they solely attributable to air-sea fluxes.

(4) The latitudinal shifting of τ_0, described above, is consistent with enhanced northward transport of subtropical waters in negative NAOI, and enhanced southward recirculation of those components in positive NAOI phases. Such patterns in meridional heat transport are reported across 48°N (Koltermann et al., 1999).

(5) From analysis of salinity patterns, Reverdin et al. (1997) concluded that the rapid cooling and freshening of the SPMW observed post-1972 resulted partly from horizontal mixing of anomalously large transports of cold and fresh waters (associated with the GSA) from the Labrador slope into the NAC.

Thus decadal changes in the subpolar upper ocean properties are likely to be incurred not only through altered local forcing conditions (e.g. anomalous surface heat fluxes, Ekman upwelling) but also by enhanced transports of waters from the subtropics and the Labrador slope.

Intensity of the Gyre Circulation

The post-1995 SPMW warming was captured in the altimeter data as a basin-wide rise in subpolar sea-surface height (SSH) of order +8 cm (S. Esselborn, pers. comm.) and in the hydrographic data as a dynamic height anomaly of similar order (Bersch et al., 1999). The warming was synonymous with an eastward-intensified density decrease in the upper 1000 m which was opposite to the western-intensified density increases incurred by the cold, thick LSW between 500–2000 m. The resultant baroclinic restructuring implies an intensification of the subpolar gyre circulation in the 1990s in sharp contrast to the situation circa 1970, at the opposite extreme NAOI.

From observed potential energy (PE) distributions Curry and McCartney (1999) estimate that the 25-year rise of the NAOI to the 1990s' extreme was accompanied by a 30% increase in the total 0–2000 db eastward baroclinic mass transport along the gyre boundary, from approximately 50 Mtons/sec in 1970 to about 65 Mtons/sec circa 1995, Fig. 4. Both subpolar and subtropical gyres contributed equally to the changes in this oceanic transport index. PE reflects the vertical density structure and heat content of the ocean well below the wind-driven layer and the development of deep shear beneath 1000 m accounts for fully half of the interdecadal transport change. The subpolar PE history primarily reflects the local wind and buoyancy forcing, but the passage of the GSAs exerted a damping effect on both convection and transport as they passed through the Labrador Basin. The subtropical PE primarily reflects the first baroclinic mode of response to zonally integrated wind stresses, augmented by the surface heat flux anomalies associated with formation of Eighteen Degree Water. The subtropical and subpolar PE histories are out-of-phase resulting in a north-south dipole in the western basin that either intensified or weakened the PE gradient between the two gyres and therefore the eastward component of the gyre circulation. The heat content anomalies which entered the eastern subpolar region from the subtropics or Labrador slope current created an east–west dipole in the PE distribution as well. Circa 1970 at the time of extended negative NAOI, both north–south and east–west PE gradients were reduced resulting in weakened horizontal gyre circulations. In the 1990s, the western subpolar PE was at an all time low, the western subtropical PE was very high, and extreme north–south and east–west PE gradients resulted. The heat content anomaly which was advected into the eastern subpolar region post-1995 further enhanced the east–west subpolar gradient. Thus the amplification of the NAO to persistent and extreme values has been echoed by a corresponding multi-decadal spin-up of the North Atlantic gyre circulation.

References

Bacon, S., 1998: Decadal variability in the Outflow from the Nordic Seas to the Deep North Atlantic. Nature, 394, 871–874.

Belkin, I. M., and S. Levitus, 1996: Temporal variability of the Subarctic Front near the Charlie Gibbs Fracture Zone. J. Geophys. Res., 10, 28317–28324.

Belkin, I. M., S. Levitus, I. Antonov, and S.-A. Malmberg, 1998: "Great salinity anomalies" in the North Atlantic. Prog. Oceanogr., 41, 1–68.

Bersch, M., J. Meincke, and A. Sy, 1999: Interannual thermohaline changes in the northern North Atlantic 1991–1996. J. Geophys. Res., submitted.

Brewer, P. G., W. S. Broecker, W. J. Jenkins, P. B. Rhines, C. G. Rooth, J. H. Swift, T. Takahashi, and R. T. Williams, 1983: A climatic freshening of the deep Atlantic north of 50°N over the past 20 years. Science, 222, 1237–1239.

Cayan, D. R., 1992: Latent and sensible heat flux anomalies over the northern oceans: Driving the sea surface temperature. J. Phys. Oceanogr., 22, 859–881.

Cunningham, S. A., and T. W. N. Haine, 1995: Labrador Sea Water in the eastern North Atlantic. Part I: A synoptic circulation inferred from a minimum in potential vorticity. J. Phys. Oceanogr., 25, 649–665.

Curry, R. G., and M. S. McCartney, 1999: Ocean gyre circulation changes associated with the North Atlantic Oscillation. In preparation.

Dickson, R. R., J. Meincke, S.-A. Malmberg, and A. J. Lee, 1988: The "Great Salinity Anomaly" in the northern North Atlantic 1968–1982. Prog. Oceanogr., 20, 103–151.

Dickson, R. R, J. Lazier, J. Meincke, P. Rhines, and J. Swift, 1996: Long-term coordinated changes in the convective activity of the North Atlantic. Prog. Oceanogr., 38, 241–195.

Dickson, B., J. Meincke, I. Vassie, J. Jungclaus, and S. Osterhus, 1999: Possible predictability in overflow from the Denmark Strait. Nature, 397, 243–246.

Dickson, R. R., and J. Brown, 1994: The production of North Atlantic Deep Water: Sources, rates, and pathways. J. Geophys. Res., 99, 12319–12341.

Ellett, D. J., 1993: Transit times to the NE Atlantic of Labrador Sea Water signals. ICES, Report C.M. 1993/C: 25: 12pp.

Hakkinen, S., 1993: An Arctic source for the Great Salinity Anomaly: A simulation of the Arctic Ice-Ocean system for 1955–1975. J. Geophys. Res., 98, 16397–16410.

Hansen, D. V., and H. F. Bezdek, 1996: On the nature of decadal anomalies in North Atlantic sea surface temperatures. J. Geophys. Res., 101, 8749–8758.

Hurrell, J. W., 1995: Decadal trends in the North Atlantic Oscillation: regional temperatures and precipitation. Science, 269, 676–679.

Hurrell, J. W., and H. van Loon, 1997: Decadal variations in Climate associated with the North Atlantic Oscillation. Clim. Change, 36, 301–326.

Jones, P. D., T. Jonsson, and D. Wheeler, 1997:. Extension to the North Atlantic Oscillation using early instrumental pressure observations from Gibraltar and SW Iceland. Int. J. Clim., 1433–1450.

Koltermann, K. P., A. V. Sokov, V. P. Tereschenkov, S. A. Dobroliubov, K. Lorbacher, and A. Sy, 1999: Decadal changes in the thermohaline circulation of the North Atlantic. Deep-Sea Res., 46, 109–138.

Krauss, W., 1986: The North Atlantic Current. J. Geophys. Res., 91, 5061–5074.

Lazier, J. R. N., 1988: Temperature and salinity changes in the deep Labrador Sea, 1962–1986. Deep-Sea Res., 35, 1247–1253.

Marsh, R., 1999: Variability of the North Atlantic meridional circulation inferred from surface density forcing over 1980–95. J. Clim., submitted.

McCartney, M. S., K. Donohue, R. Curry, C. Mauritzen, and S. Bacon, 1998: Did the Overflow from the Nordic Seas Intensify in 1996–1997? Int. WOCE Newsl., 31, 3–7.

Petrie, B., and K. Drinkwater, 1993: Temperature and salinity variability on the Scotian shelf and in the Gulf of Maine 1945–1990. J. Geophys. Res., 98, 20079–20089.

Read, J. F., and W. J. Gould, 1992: Cooling and freshening of the subpolar North Atlantic Ocean since the 1960s. Nature, 360, 55–57.

Reverdin, G., D. Cayan, and Y. Kushnir, 1997: Decadal variability in the upper northern North Atlantic in 1948–1990. J. Geophys. Res., 102, 8505–8531.

Reverdin, G., N. Verbrugge, and H. Valdimarsson, 1999: Upper ocean variability between Iceland and Newfoundland 1993–1998. J. Geophys. Res., submitted.

Sutton, R. T., and M. R. Allen, 1997: Decadal predictability in Gulf Stream sea surface temperature. Nature, 388, 563–567.

Swift, J. H., 1984: A recent θ-S shift in the deep water of the northern North Atlantic. In: Climate processes and climate sensitivity, J. E. Hansen and T. Takahashi (eds.) Geophys. Monographs, 29 Maurice Ewing volume 5, Am. Geophys. Union, Washington, DC, pp. 39–47.

Sy, A., M. Rhein, J. Lazier, K. P. Koltermann, J. Meincke, A. Putzka, and M. Bersch, 1997: Surprisingly rapid spreading of newly formed intermediate waters across the North Atlantic Ocean. Nature, 386, 675–679.

Thompson, D. W. J., and J. M. Wallace, 1998: The Arctic Oscillation signature in the wintertime geopotential height and temperature fields. Geophys. Res. Lett., 25, 1297–1300.

Decadal Variability of water masses, overturning and heat transports across 48°N

Klaus Peter Koltermann, Bundesamt für Seeschiffahrt und Hydrographie, Hamburg and Rostock.

The North Atlantic Ocean plays a prominent part in the global thermohaline circulation. The global redistribution of heat and freshwater throughout the water column mostly happens here. It also is the most active ocean part due to its close interaction of atmosphere and ocean. The implications on the meridional transports of heat and freshwater here are as yet unclear. The questions of temporal and spatial stability of the thermohaline circulation have yet to be answered. Model studies have suggested that rapid changes (Manabe and Stouffer, 1988, Fanning and Weaver, 1997) and different mechanisms (Rahmstorf, 1995, 1996) have an effect on long-term temporal changes and changes in the rate of change in the pattern and strength. Evidence from observations is slowly building up (Bryden et al., 1996; Sy et al., 1997; Curry et al., 1998; Molinari et al., 1998; Koltermann et al, 1999).

Changes in the full-depth hydrographical fields of trans-atlantic sections over the last 40 years have been deduced for a coherent set at 24.5°N, 36°N and 48°N latitudes, spanning the time from the International Geophysical Year IGY 1956/7 through the early WOCE years in the 1990s (Koltermann et al., 1999). These changes yield a systematic and coherent picture: at decadal, climate relevant time scales, the variability of the volume transports reflects primarily a bimodal structure of the vertical profile of the Meridional Overturning Circulation (MOC). A single meridional cell is found in 1982 with higher volume transports of the upper and deeper layers than in the intermediate layer and a subsequently reduced export of intermediate water masses. For 1956/7 and 1992/3 there were two meridional cells, with a pronounced LSW transport, and drastically reduced transports in the upper and lower layers. Comparing the volume transport estimates at 36°N and 24.5°N for the same time slices reveals that the transition from the one-cell to the two-cell case is governed by changing overflow transports north of 48°N. Heat transports vary accordingly. The changes are largest at 36°N between 0.47 and 1.29 PW, where changes in the Mediterranean Water component are largest. At 24.5°N they vary between 1.38 and 1.54 PW, but at 48°N the changes are between 0.27 and 0.62 PW (Table 1)

This analysis essentially underlines that the meridional transports of heat and freshwater are not constant, show systematic changes and are related to changes in water mass volumes and properties. The scheme of the meridional overturning circulation, though, implies that for the one-cell case the northward transport of warm and salty Atlantic Water penetrates to the European Polar Seas north of the Greenland–Iceland–Faroe Ridge, supplying this lowly stratified region with additional heat and particularly salt. In this case there is an efficient thermohaline coupling between these two regions, exchanging properties vital for potential large-scale convection processes. For the two-cell case the transports to the European Polar Seas are much reduced. The entire overturning is confined to the region south of the Greenland–Iceland–Faroe Ridge. Now the coupling between the two regions is strongly reduced and the impact of changes in the composition or properties of the Overflow Waters are the only likely link between them.

Table 1. Meridional heat flux in the North Atlantic derived from hydrographic data for different latitudes since 1957.

Year	*Latitude*		
	24° N	*36° N*	*43-48° N*
1957-59	1.38±0.29	0.47±0.24	0.27±0.15
1981-82	1.48±0.20	1.29±0.17	0.62±0.11
1992-93	1.54±0.19	0.70±0.15	0.53±0.12

These observed changes over some 40 years of the thermohaline circulation in the North Atlantic do not yield any insight into the changes of the rate of change nor their origin. There are too few, or no more, observations that would allow to construct a time-series of these meridional transports. At interannual time scales, though, we are able to at least determine the speed of the rate of change and its origin from five repeated sections at 48°N in the 1990s (Lorbacher, 1999).

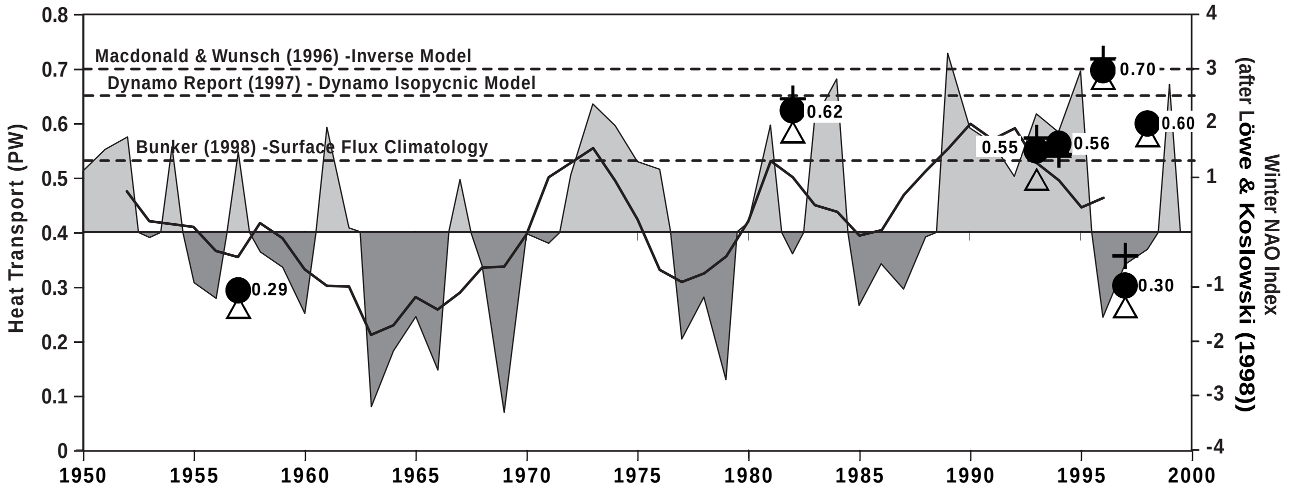

Figure 1. Net meridional heat transport between 42–49°N in the North Atlantic for the period 1957 to 1998. The wind-driven parts of the total transport are estimated with long-term monthly means (dots), with the long-term annual mean (triangles) and with actual monthly means (crosses) of wind stress data from the NCEP/NCAR reanalysis project. Underlying are the winter (DHF) NAO-index after Löwe and Koslowski (shaded) and its five year running mean. Heat transport estimates based on models are also included.

All estimates are given as the sum of the three transport components of a quasi-stationary, large-scale horizontal circulation: the ageostrophic Ekman, and the two geostrophic components, the depth-independent barotropic or Sverdrup and the baroclinic component. To maintain the mass balance over the plane of the section the compensation of each component is assumed. For the baroclinic component the balance is maintained by a suitable choice of a surface of no-motion. The absolute meridional velocity as a function of the zonal distance and depth is therefore the sum of the three components and their compensatory component, respectively at each point of the area integral of the mass transport.

The variability of the MOC shows a rapid response to the external atmospheric forcing. High-frequency, large amplitude fluctuations in the wind-field of the entire North Atlantic – quantified by the North Atlantic Oscillation Index NAO – affect mainly the position of the line of zero wind-stress curl (Table 2). The line of zero wind stress curl shifts with changes in the NAO-Index. This shift produces primarily a deformation and/or an acceleration of the sub-polar gyre or a generation of meanders of the NAC or baroclinic instabilities, ultimately mesoscale hydrographic variability. During a negative NAO-Index (weak westerlies) the subpolar gyre contracts (spins-down) and the subtropical gyre expands (spins-up). In this case the zero-wind stress line has moved further north and the dynamics at 48°N are more influenced by the anticyclonic circulation of the subtropical gyre, resulting in am increased southward transport east of the Western Boundary Current and the associated recirculation. This leads to a reduction of the total northward transport of heat and of the upper layer of the MOC. The dynamic response follows the changes in the NAO-index (Fig. 1) with a time lag of about one year, and was most pronounced in 1995/6 for the largest change in the index since the beginning of the series in 1864. In 1996 we subsequently find a maximum heat transport and overturning rate, and only one year later a reduction by 60% and 40%, respectively. The dynamical response across the 48°N section is most pronounced east of the western boundary current regime. Heat, freshwater and mass transport across the 48°N section are closely related to the NAO-index (Fig. 2). Unclear at present is which part of this shift contributes to the observed temporal transport changes along the 48°N section and how it could explain the observed phase lag between atmospheric forcing and oceanic response.

The biggest uncertainties, due to the use of different values of the two wind-

Table 2. Temporal development of the meridional overturning rate, transports of heat and freshwater and the components of heat transport.

Time	*Heat Transport Components*					*Fresh-water*	*MOC*
	Baro-tropic	*Baroclinic*		*Ekman*	Total		
		Over-turning	*Eddy*				
Apr 1957	-0.012	0.393	-0.049	-0.037	0.294	-0.878	12.7
Apr 1982	-0.020	0.575	0.101	-0.032	0.624	-1.050	20.0
Jul 1993	-0.004	0.566	0.038	-0.048	0.551	-1.071	15.2
Oct-Nov 1994	-0.005	0.609	0.054	-0.096	0.563	-1.015	16.1
May 1996	0.003	0.690	0.060	-0.055	0.698	-1.096	20.1
Jun 1997	-0.018	0.504	-0.133	-0.050	0.303	-0.684	13.3
May 1998	-0.004	0.638	0.021	-0.055	0.600	-1.006	17.8

driven parts of the total heat transport explain only 30% of the observed temporal changes. Therefore the baroclinic part is mainly responsible for the observed changes. It contributes more than 80% to the total heat transport across 48°N.

Changes in salt and heat contents at 48°N during the WOCE period indicate that the temporal variability of heat and freshwater transports is not dominated by advected subtropical temperature and salinity anomalies in the upper layers. Responsible for the observed temporal variability of the transports in the nineties are the changes in the rates of the transported volumes.

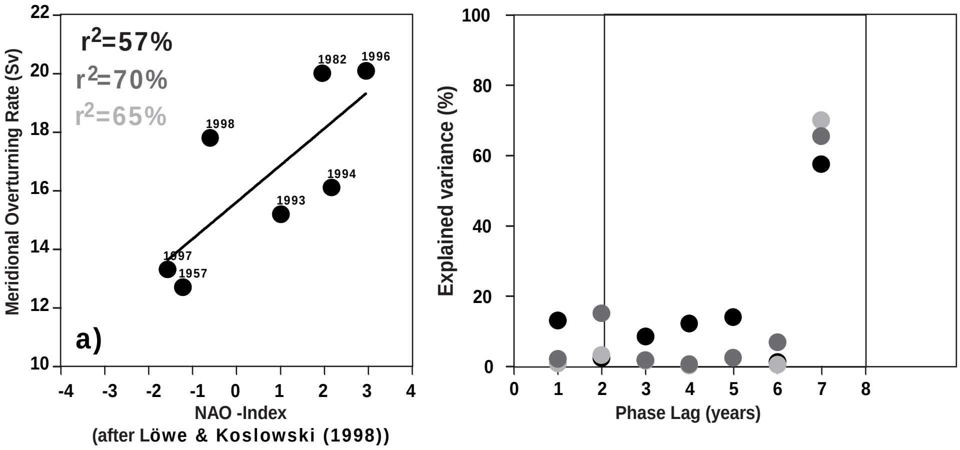

Figure 2. Correlation between the NAO-index and the meridional overturning rate for a phase-lag of one year (a) and the explained variance of the correlation between the NAO-index and the meridional overturning rate (black), the meridional transports of heat (dark grey) and for different phase lags.

References

Bryden, H. L, M. J. Griffiths, A. Lavin, R. C. Millard, G. Parrilla, and W. Smethie, 1996: Decadal changes in water mass characteristics at 24°N in the Subtropical North Atlantic Ocean. J. Clim., 9(12), 3162–3186.

Curry, R. G., M. S. McCartney, and T. M. Joyce, 1998: Oceanic transport of subpolar climate signals to mid-depth subtropical waters. Nature, 391, 575–577.

Fanning, A. F., and A. J. Weaver, 1997: Temporal-geographical meltwater influences on the North Atlantic conveyor: implications for the Younger Dryas. Paleoceanogaphy, 12, 307–320.

Koltermann, K. P., A. Sokov, V. Terechtchenkov, S. Dobroliubov, K. Lorbacher, and A. Sy, 1999: Decadal Changes in the Thermohaline Circulation of the North Atlantic. Deep-Sea Res., Part II, 46(1+2), pp 109–138.

Lorbacher, K., 1999: Niederfrequente Variabilität meridionaler Transporte des Schnittes WOCE/A2 in der Divergenzzone des Nordatlantischen Subtropen- und subpolarwirbels. Diss. Univ. Hamburg.

Manabe, S., and R. J. Stouffer, 1988: Two stable equilibria of a coupled ocean-atmosphere model. J. Clim., 1, 841–866.

Molinari, R. L., R. A. Fine, W. D. Wilson, J. Abell, M. M. McCartney, and R. G. Curry, 1998: A fast track for recently formed Labrador Sea Water: The deep western boundary current of the North Atlantic Ocean. Geophys. Res. Lett.

Rahmstorf, S., 1995: Multiple convection patterns and thermohaline flow in an idealized OGCM. J. Clim., 8, 3028–3039.

Rahmstorf, S., 1996: On the freshwater forcing and transport of the Atlantic thermohaline circulation. Clim. Dyn., 12, 799–811.

Sy, A., M. Rhein, J. R. N. Lazier, K. P. Koltermann, J. Meincke, A. Putzka, and M. Bersch, 1997: Surprisingly rapid cooling of newly formed intermediate water across the North Atlantic Ocean. Nature, 386, 675–679.

Decadal Variability in sea level and its relationship to meridional overturning in the North Atlantic

Sirpa Hakkinen, NASA Goddard Space Flight Center, USA

Summary

Sea level variability investigated here makes use of three factors:

1. sea level in subtropics is a good measure of the oceanic baroclinic dynamics,
2. coastal tide gauge data extends to the early 1900s in many locations around the North Atlantic,
3. altimeter measurements from space can extend these data to the open ocean.

In light of this information the main conclusions concerning the low-frequency variability of the sea level are discussed:

- US SE Coast tide gauge data shows that 10–15% of the monthly variance is on a 12–13 year periodicity.
- The altimeter and model simulated sea surface height (SSH) share the same leading empirical orthogonal function (EOF) mode where the centre of action is along the Gulf Stream and North Atlantic Current.
- Longer hindcast runs are used to make the connection between the time series of the SSH EOF1 and meridional heat transport and as well as with the leading mode of heat flux which is associated with the North Atlantic Oscillation (NAO).

Thus we can have a qualitative estimate of the state of overturning/meridional heat transport based on SSH. The altimeter data suggests that since 1996 the overturning has slowed down from its heights in the early 90s. Decadal variability is prominent only in the quantities related to the thermal forcing and can be found only in very limited regions in the western Atlantic, in the subpolar gyre and in the subsurface between 20°N and 30°N.

Tide Gauge data

The coastal sea level data used here are from the Permanent Service for Mean Sea Level (PSML) in Bidston, UK. The data gaps if less than 2 years are filled with linear interpolation of anomalies. Fig. 1 depicts the low pass filtered (49-month running mean) sea level on the US side with an apparent decadal signal of ±6 cm amplitude. One can count 5–6 occurrences of this signal. In fact, the decadal signal found in most of the US East coast tide gauge stations (e.g. at Charleston) show a prominent decadal signal constituting 10–15% of the monthly variance (Unal and Ghil, 1995; Hakkinen, 1999a). This SSH behaviour is in contrast to the COADS SST variability (Deser and Blackmon, 1993) which do not show a decadal peak above the red noise level. However, the decadal period in sea level is not found everywhere, e.g. the eastern subtropical Atlantic tide gauge stations lack a definite signal. This agrees with the conclusions by Frankignoul et al. (1997) who show that the spectral variability of the sea level in the eastern side of the basin is explained as a red noise response to a white noise atmosphere.

Analysis of model simulated and altimeter SSH

Linking sea level and overturning variability requires the use of numerical model simulations. Three different model experiments are considered in which the basic monthly

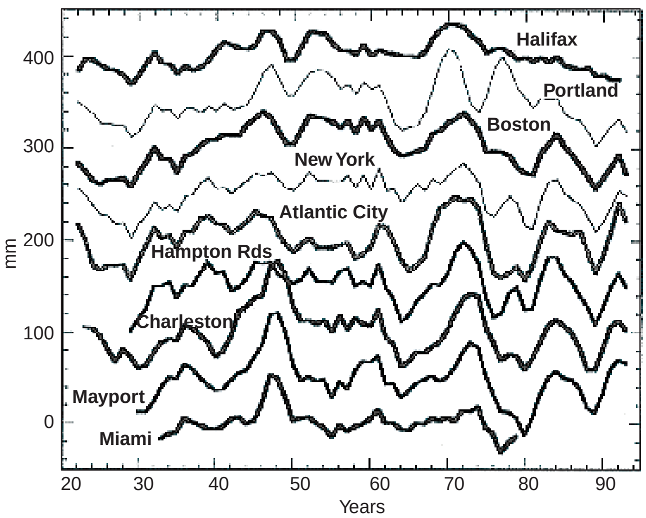

Figure 1. US East Coast tide gauge data, low pass filtered with 49 month running mean, units in mm.

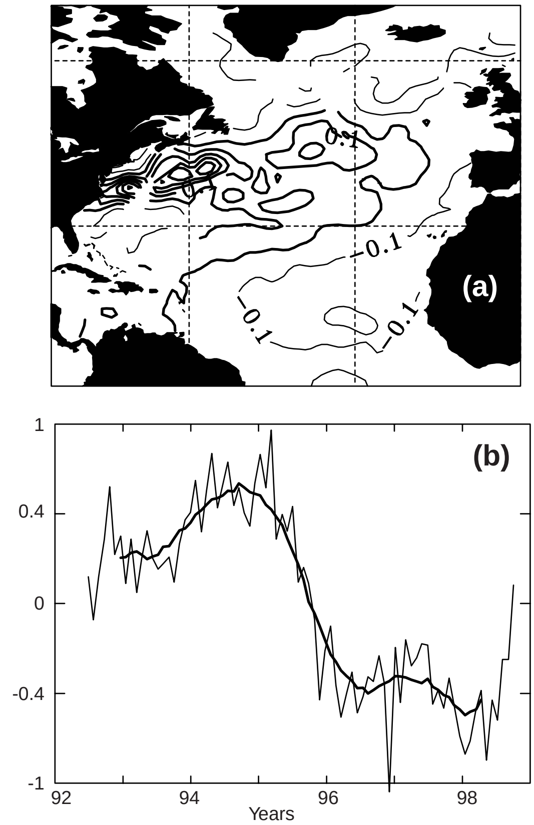

Figure 2. EOF1 (a) and PC1 (b) of the sea surface height from TOPEX/POSEIDON altimeter measurements for period 1992–1998. EOF1 in non-dim. units, interval 0.1. PC1 in units of cm. The difference from February 1995 SSH to January 1997 (or December 1998) at the maximum of the spatial pattern (over the Gulf Stream) is 12 cm. The smooth line is 13 month running mean.

climatological surface forcing is altered by the following anomalies:

1. anomalies in wind and thermal forcing (E1) (Hakkinen, 1999b),
2. anomalies in thermal forcing (E2) and
3. anomalies in wind stress forcing (E3).

The anomalies are from COADS data base (da Silva et al., 1994). Simulation period is 1946–1993.

The EOFs of SSH in all three cases give the leading mode which has an elongated centre along the Gulf Stream and North Atlantic Current with an opposing anomaly extending from the Labrador Sea along the Eastern seaboard (similar to Fig. 2a). However, there are slight differences in the east–west location and the northernmost position of the elongated centre, a manifestation of the effect of wind and thermal forcing on the location of the North Atlantic Current. (These modest differences influence the cross-correlation in this region between E1 and E2 SSH as will be shown). The leading mode of SSH from 6 years of altimeter data shows a similar concentration of variability in the Gulf Stream area with a time series that has much longer term variability than the length of the time series (Figs. 2a,b). The SSH time series from the long simulations contains an apparent decadal

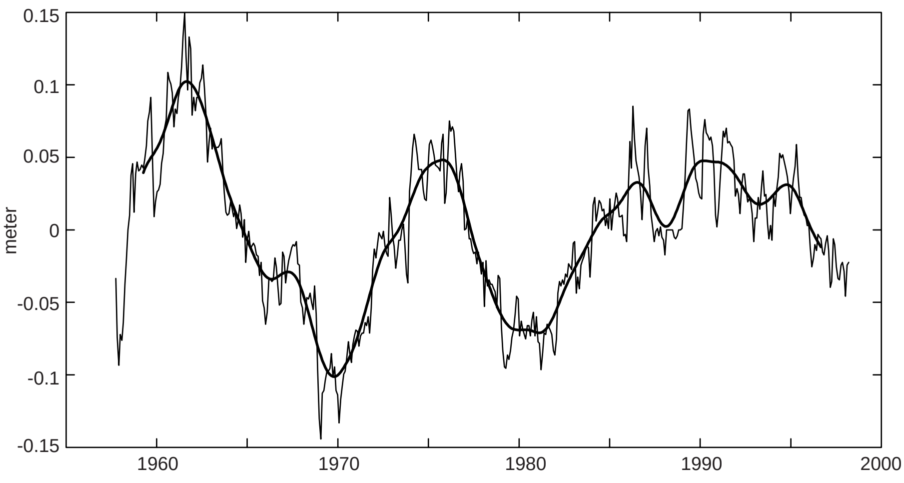

Figure 3. PC1 from model simulation using NCEP Reanalysis data for period 1958–1997. Units in m, smooth line is low-pass filtered form.

periodicity around 12–14 years (Fig. 3). Thus, it is likely that the TOPEX time series could represent a part of such a cycle, which indicates that the meridional overturning is presently in a weak phase.

The model results are used to relate the SSH variability (defined by EOFs) with overturning and meridional heat transport. One such relationship is between the leading modes of the heat flux and SSH: the variations in the SSH model follow within 2 years the variations in the heat flux. Also another, rather obvious relationship can be derived from the model data: meridional heat transport is highly correlated with the time series of the leading heat flux mode. This association of the leading heat flux mode brings in the role of the North Atlantic Oscillation (NAO) in the low frequency variability (Hakkinen 1999b). This relationship is true for simulations E1 and E2, but has no relevance in E3.

The above result may seem contrary to the conclusions of the study by Sturges and Hong (1995) who showed that the low pass filtered sea level in Bermuda can be derived from integrating a planetary wave equation westward including only wind stress curl variability (local and remote). How does one reconcile these results showing either the influence of thermal forcing and the observed strong signal at the US East Coast or wind stress curl on SSH and the results of Frankignoul et al. (1997)? One solution to the dilemma is that the thermally driven and wind stress curl driven SSH changes may occupy mutually exclusive regions. A straightforward computation of cross-correlation can provide further information: The model experiments E1 and E2 give highly correlated sea level variability in areas of mode water formation in the subpolar gyre and subtropics, but E1 and E3 are correlated highly in far more extensive areas of the North Atlantic and especially on the eastern side extending to 60°W at the latitude 30°N (Fig. 4). Thus the Bermuda sea level is mainly affected by the wind stress curl in agreement with Sturges and Hong (1995).

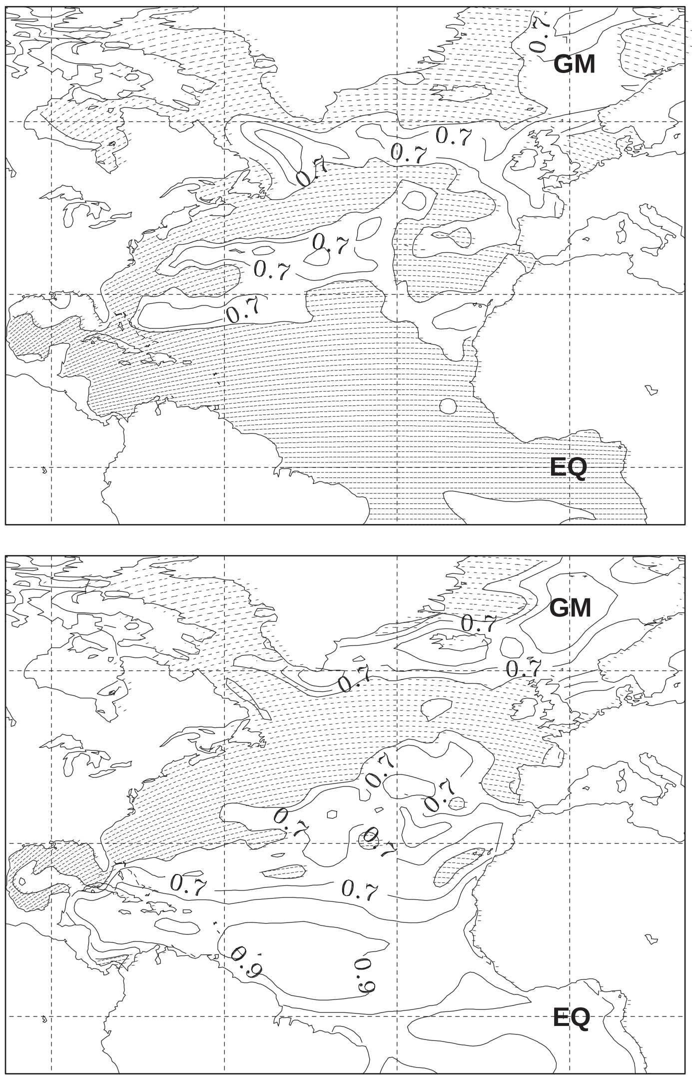

Figure 4. Month to month, point by point cross correlations of experiments (a) E1 and E2, (b) E1 and E3. Contour interval is 0.1, correlation less than 0.6 are shaded.

The wedge where local Ekman pumping and wind-driven Rossby waves contribute the most to the sea level variability has an appearance of a shadow zone of the ventilated thermocline theory. Liu (1993) has shown that local Ekman pumping has to be balanced by Rossby waves in the shadow zone, a self-evident result since the western boundary of the shadow zone is defined by Rossby waves arrested by the gyre circulation. Thus sea level in the eastern basin is determined by wind stress curl which represents a white noise forcing. These two elements enable one to place the conclusions of red noise behaviour in sea level by Frankignoul et al. (1997) into perspective. This also means that the Bermuda sea level represents simply a red noise behaviour and is not indicative of overturning variability. The location of the decadal signal is limited to the western boundary current and coastal region west of it and to the interior of the subpolar gyre.

SSH and the upper ocean heat content: a signal of a coupled cycle?

In the subtropics the sea level is a measure of the upper ocean heat content with the first EOF mode similar to the one of SSH. The second mode of the upper ocean (1000 m) heat content has a bipolar distribution of variance with a northern centre covering the subpolar gyre and an elongated centre with opposing sign between 20°N and 30°N reminiscent of a Rossby wave propagation. In fact their time series are correlated at a lag so that the mode 2 dipole with negative northern centre leads the first mode (with a positive centre in the Gulf Stream) by 2 years, and thus form a propagating pair. At the same time their time series are highly correlated with the time series of the leading heat flux mode (the first one with a two year lag, the second simultaneously). In effect there is a well-defined progression of events on a decadal scale initiated by cooling (heating) in the subpolar gyre and intensification of the thermohaline cell which builds up through Rossby waves in the subtropics to an enhanced (decreased) heat content in the Gulf Stream–North Atlantic Current region.

The regularity of the decadal signal in US SE Coast sea level suggests a stationary process perhaps a part of a coupled cycle where the buoyancy fluxes initiate the cycle of thermohaline cell variability (involves only the Labrador Sea Water). It is suggested that the coupled mode exhibits positive feedback in the subpolar gyre between the atmosphere and ocean (Grotzner et al., 1998; Hakkinen, 1999a). The positive feedback leads to intensification of overturning which has a negative feedback on itself (being thermally driven). Moreover, a coupled mode requires existence of a delayed response between the positive and negative feedbacks which is necessary for the development of an oscillatory behaviour. The baroclinic Rossby waves at latitudes 20°N to 30°N, visible in the upper ocean heat content, are likely to mediate the delayed response.

References

da Silva, A. M, C. C. Young, and S. Levitus, 1994: Atlas of surface marine data 1994, Volume 1, Algorithms and procedures. NOAA Atlas Series.

Deser, C., and M. L. Blackmon, 1993: Surface climate variations over the North Atlantic Ocean during winter 1900–1989. J. Climate, 6, 1743–1753.

Frankignoul, C., P. Muller, and E. Zorita, 1997: A simple model of the decadal response of the ocean to stochastic wind forcing. J. Phys. Oceanogr., 27, 1533–1546.

Grotzner, A., M. Latif, and T. P. Barnett, 1998: A decadal climate cycle in the North Atlantic Ocean as simulated by the ECHO coupled GCM. J. Climate, 11, 831–847.

Hakkinen, S., 1999a: Decadal air-sea interaction in the North Atlantic based on observations and modeling results. J. Climate, to appear.

Hakkinen, S., 1999b: Variability of the simulated meridional heat transport in the North Atlantic for the period 1951–1993. J. Geophys. Res., 104, 10991–11007.

Liu, Z., 1993: Thermocline forced by varying Ekman pumping. Part I: Spinup and spindown. J. Phys. Oceanogr., 23, 2502–2522.

Sturges, W., and B. G. Hong, 1995: Wind forcing of the Atlantic thermocline along 32°N at low frequencies. J. Phys. Oceanogr., 25, 1706–1715.

Unal, Y. S., and M. Ghil, 1995: Interannual and interdecadal oscillation patterns in sea level. Clim. Dyn., 11, 255–278.

Can low frequency variability internal to the atmosphere drive significant interdecadal variability in the ocean and in coupled ocean-atmosphere models?

Richard Greatbatch, Department of Oceanography, Dalhousie University, Canada

A brief overview is given of the so-called “null hypothesis” for interdecadal variability in the North Atlantic climate system. Under the “null hypothesis”, the ocean responds to forcing from the atmosphere, but the associated mid-latitude SST anomalies do not dynamically feedback and change the overlying atmospheric circulation. The “null hypothesis” relies on the observation that atmospheric general circulation models can generate their own interdecadal variability, independent of coupling with the ocean, and also the controversy that surrounds the atmospheric response to North Atlantic SST anomalies. The latter is illustrated by comparing recent results from Rodwell et al. (1999) at the Hadley Centre with the results of similar integrations described by Zwiers et al. (1999) and carried out by Xiaolan Wang at the Canadian Centre for Climate Modelling and Analysis in Victoria, BC.

Work carried out in collaboration with Dr Tom Delworth at GFDL is then described (Delworth and Greatbatch, 1999). It is argued that the interdecadal variability in the GFDL coupled model, and described by Delworth et al. (1993) (see Fig. 1), is an example of the “null hypothesis”; in particular, that the interdecadal variability in that model is not a dynamically coupled phenomenon. Model experiments are used to show that significant interdecadal variability can be generated in an ocean model by low

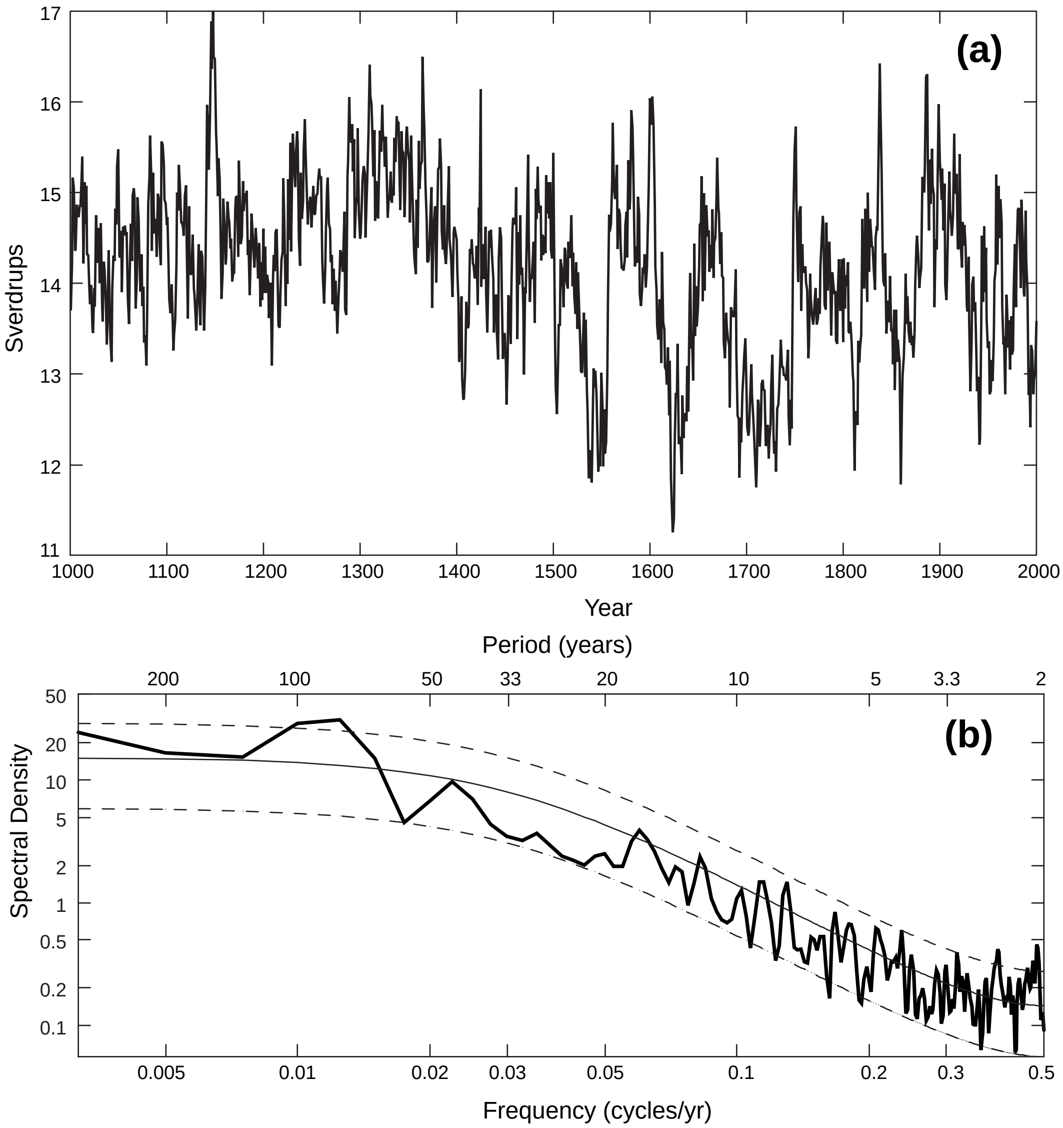

Figure 1. (a) Time series of the intensity of the thermohaline circulation (THC) in the model North Atlantic (referred to as the THC Index). The intensity is defined for each year as the maximum of the meridional overturning streamfunction between 20°N and 90°N. The streamfunction field is computed each year from annual-mean meridional velocities zonally-averaged over the Atlantic basin. (b) Fourier spectrum of the time series in (a). The spectrum was computed by taking the Fourier transform of the lagged autocovariance function, using a Tukey window and a maximum of 200 lags. The heavy, solid line denotes the spectrum, the thin, solid line denotes a fit of a red noise (first-order Markov) process to that spectrum, and the dashed lines denote the 95% confidence interval about the red noise spectrum.

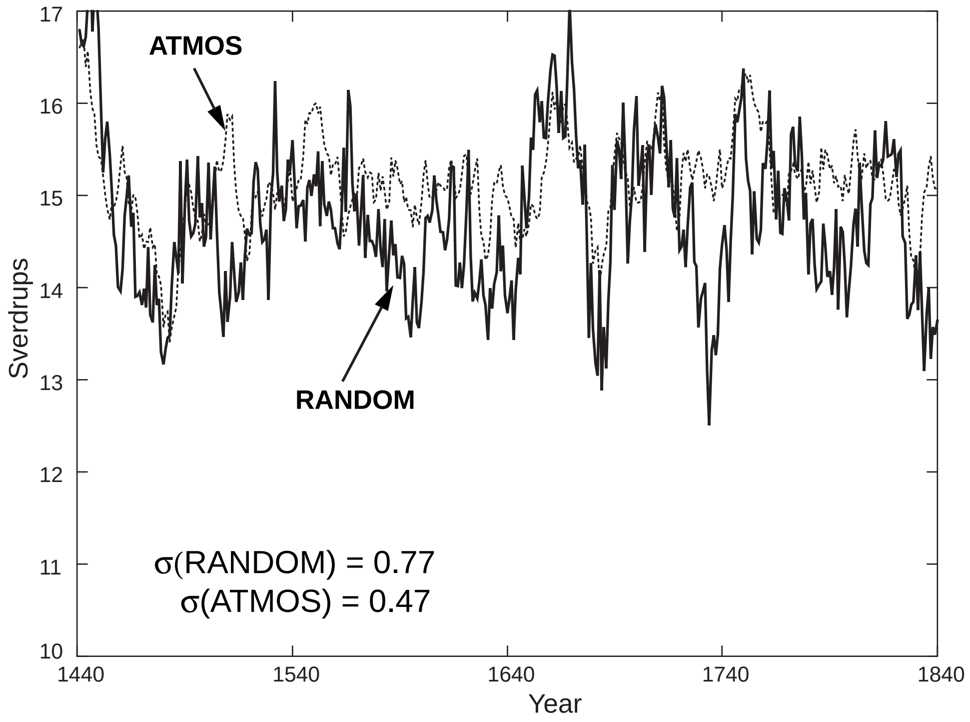

Figure 2. Time series of THC from (i) ocean model driven by annual mean flux anomalies selected randomly from the coupled model output (solid line, RANDOM), and (ii) ocean model driven by annual mean flux anomalies from an extended run of an atmosphere-only model with a prescribed seasonal cycle of SSTs and sea ice (dashed line, ATMOS).

frequency atmospheric forcing that does not rely on dynamical coupling with the ocean (examples are given in Fig. 2). It is also shown that variations in heat flux are the dominant term (relative to the fresh water and momentum fluxes) in driving the THC variability in the GFDL model. In addition, experiments driving the ocean model using either high or low pass filtered fluxes, with a cut-off period of 20 years, show that the multidecadal THC variability in the GFDL model is driven by the low frequency portion of the spectrum of atmospheric flux forcing. Analyses have also revealed that the multidecadal THC fluctuations in the GFDL model are driven by a spatial pattern of surface heat flux variations that bears a strong resemblance to the North Atlantic Oscillation.

References

Delworth, T. L., and R. J. Greatbatch, 1999: Multidecadal thermohaline circulation variability driven by atmospheric surface flux forcing. J. Climate, in press.

Delworth, T. L., S. Manabe, and R. J. Stouffer, 1993: Interdecadal variations of the thermohaline circulation in a coupled ocean-atmosphere model. J. Climate, 6, 1993–2011.

Rodwell, M. J., D. P. Rowell, and C. K. Folland, 1999: Oceanic forcing of the wintertime North Atlantic Oscillation and European climate. Nature, 398, 320–323.

Zwiers, F. W., X. L. Wang, and J. Sheng, 1999: Effects of specifying bottom boundary conditions in an ensemble of atmospheric GCM simulations. J. Geophys. Res. (Atmos.), in press.

Is a steady-state ocean circulation still a useful framework for understanding?

Carl Wunsch, Massachusetts Institute of Technology, USA

One of the major goals of WOCE was to sample the ocean sufficiently well that one could begin to quantify the extent to which the variability present could preclude representing the general circulation quantitatively as a time average flow field. The analogy with the atmosphere is clear: the time-mean atmosphere has Hadley/Halley, Ferrel cells, and other flows, which emerge from heavily time-averaged data, and these produce great insight into how the atmosphere works. But for understanding property transports, and their interannual variability, it is difficult to escape having to integrate through actual weather systems. Is the ocean similar in that regard?

The WOCE field programme did not focus on this objective. Nonetheless, a good deal of data, much of it from TOPEX/POSEIDON has accumulated over the WOCE period, which begins to shed light on the question. As summarised in part by Stammer and Wunsch (1999), a one-year average difference of the absolute sea surface topography between years 1 and 4 shows sub-basin scale changes in the North Atlantic equivalent to 50 Sverdrups transport changes. The mesoscale eddy field exhibits ±30% kinetic energy changes over the same four years. In some regions, there appears to be an annual cycle in the eddy kinetic energy approaching this amplitude as well. These changes are generally consistent with the results from the historical current meter records, and in fact a preliminary "universal" spectral description is now available (Zang, 1999). Changes in the meteorological fields over the ocean are also at least qualitatively consistent with much of the change being a forced response.

The TOPEX/POSEIDON data, and now the modern GCMs, all show a very strong, short-time scale barotropic variability, especially in the sub-polar gyres (illustrated with animation not reproduced here). Although largely invisible in hydrographic data, these motions cause serious problems of interpretation of direct velocity devices, and may well influence the hydrographic state through mixing at topographic features. Experiments with trying to make zonal mass balances in the western North Atlantic using synoptic sections suggest massive imbalances probably associated with large-scale meridional movement of the Gulf Stream.

The data and models all suggest that no part of the circulation is steady, and that there is variability on all time and space scales, and apart perhaps from very long distance integrated quantities, synoptic data differ sometimes greatly from long-term averages. Thus to the extent that one seeks to be truly quantitative in discussing the general circulation and its transport properties, it appears that the data have to be handled almost on a day-by-day basis in some regions, and that drives one towards syntheses in an "assimilation" mode. Fortunately, it appears that the assimilation capability is within reach.

References

Stammer, D., and C. Wunsch, 1999: Temporal change in eddy energy of the oceans. Deep-Sea Res., II, 46, Siedler Vol., 77–108.

Zang, X., 1999: In prep.

2.2 North Atlantic circulation, pathways and water masses – Distributions from WOCE observations, altimetry and model results

Upper layer circulation in the subpolar North Atlantic during the WOCE period

Lynne D. Talley, Scripps Institution of Oceanography, USA

A principal focus of observational upper ocean work in the subpolar North Atlantic is the transformation of inflowing warm, saline subtropical waters into the precursors of intermediate water formed in the Labrador Sea and deep water formed in the Nordic Seas. This constitutes the local upper ocean limb of the meridional overturning circulation whose amplitude is calculated variously at about 15 to 20 Sv. Conventional circulation analyses (e.g. Reid, 1994) show a branching of the Gulf Stream and North Atlantic Current feeding the cyclonic subpolar circulation, which is depicted with broad northward flow in the eastern subpolar region, feeding surface flow into the Norwegian Sea, westward flow along the northern margin and into the Irminger Current which feeds into the Labrador Sea. Some element of the flow following the curve of the Reykjanes Ridge is also indicated, particularly with increasing depth in the water column. Ample evidence for incursion of lower latitude properties has been demonstrated, for instance with the high silica tongue at about 27.5 σ_θ originating from the Gulf Stream and indicating South Atlantic influence moving into the subpolar region (Tsuchiya, 1989). Mass, heat and salt budgets for the transformation of upper ocean waters around the subpolar gyre have been made (e.g. Worthington, 1976; McCartney and Talley, 1984; McCartney 1982; Schmitz and McCartney, 1993). However, the seasonal transformation with careful local flux budgets, and description of the actual transformation process as tied to the fluxes and local circulation has not heretofore been accomplished.

The upper ocean waters of the subpolar gyre are characterised by quite thick layers of low stability, assumed to originate as deep mixed layers in winter. In general these layers are more than 400 m thick, ranging up to more than 600 m, and then to 1500 during intermediate depth convection in the Labrador Sea (McCartney and Talley, 1982). These layers are remarkable on a global scale only in the Antarctic sector of the east Indian and South Pacific Oceans are comparable depths attained (e.g. global mixed layer depth map based on oxygen saturation from Talley, 1999). Because of their thickness and ease of identification, the subpolar mixed layers are termed Subpolar Mode Water (SPMW). The distribution of SPMW based on a relatively sparse 1950s/1960s data set was described by McCartney and Talley (1982). The concept therein was of thick mixed layers moving smoothly eastward and then northward and thence cyclonically around the subpolar gyre into the Labrador Sea, with an initial potential temperature and density of 14°C and 26.9 σ_θ just south of the North Atlantic Current loop, varying smoothly around the gyre to finally arrive at the Labrador Sea Water (LSW) properties of about 3°C/27.84 σ_θ. The North Atlantic Current jet centred at about 52°N was considered the fulcrum of this cyclonic movement. Southward subduction of the 27.1 and 27.2 σ_θ waters of the eastern region into the subtropical gyre is also observed. This set of observations and hypothesis of transformation are items to be tested using the WOCE observations.

Another portion of the upper limb circulation to be tested is the extent to which Mediterranean Water feeds higher salinity into the subpolar gyre. The high salinity of the North Atlantic inflow into the Nordic Seas is a crucial part of the

Table 1. Selected in situ WOCE Observations for the subpolar North Atlantic.

Floats' PI	*Drifters*	*Current Meters (PI)*	*Hydrography (PI)*
Davies (PALACE)	International effort (Niiler)	Canada (Clarke)	Canada (Clarke, Hendry, Lazier)
Owens (PALACE)		Germany (Schott/Fischer)	France (Gaillard, LeCann, Mercier)
Gould (PALACE)		Nordic WOCE (Hansen)	Germany (Bersch, Käse, Koltermann, Meincke, Schott, Sy, Zenk)
LeCann and Speer (ALACE)		United Kingdom (Dickson/Saunders)	Netherlands (van Aken)
Rossby (RAFOS isopycnic)			Nordic WOCE (Blindheim, Østerhus)
Bower and Richardson (RAFOS isopycnic)			Russia (Sokov, Tereshchenkov)
Zenk (RAFOS)			Spain (Parrilla)
			United Kingdom (Bacon, Bryden, Gould, Pollard, Smythe-Wright)
			United States (Curry, Joyce, McCartney, Pickart, Talley)

formation of what becomes North Atlantic Deep Water. The amount of Mediterranean Water influence versus simple incursion of high salinity surface waters is to be quantified. How Mediterranean Water influence spreads northward is to be determined, whether by direct advection in a poleward eastern boundary current or through eddy processes that gradually feed higher salinity northward.

WOCE observations

The WOCE data set for the subpolar North Atlantic is extremely rich, including Lagrangian observations (surface drifters and large numbers of subsurface floats), current meter arrays, and hydrography covering many areas every year since the start of WOCE field observations in 1990. Particularly intensive field observations occurred in 1991 and again in 1997, the latter including many float projects (Table 1). A major observational effort has also been undertaken in the Labrador Sea studying the formation of intermediate water. Challenges for synthesis during the next few years are to gather these data sets from many different investigators and countries and use them to construct the best analyses of the circulation, eddy field, water properties, and transformation/mixing. Because of the major time variations in the subpolar region associated with the North Atlantic Oscillation, care must be taken to examine data sets from uniform time periods. It is hoped that seasonal variation can also be examined for at least the latter years, given the temporal coverage of the data sets.

All results for drifters, floats and current meters described in the next few paragraphs should be referred back to and ascribed to the principal investigator listed for each measurement.

Surface drifter averages for $2° \times 6°$ boxes are possible for all of the region from 1988 to the present, with some regions with coverage sufficient for much higher spatial resolution (P. Niiler, pers. comm.). The drifter averages show the expected elements of the eastward flow of the North Atlantic Current, turning northward into the subpolar region. Average westward flow south of Iceland is remarkably weak. Strong currents resume along the Greenland coast in the Irminger Current, and in the West Greenland and Labrador Currents in the Labrador Sea.

Subsurface floats were deployed in four modes: acoustically tracked (RAFOS) along an isobar, RAFOS along an isopycnal, pop-up without profiling (ALACE), and pop-up with temperature/salinity profiling (PALACE). The first large deployment was of acoustically-tracked floats in the North Atlantic Current at

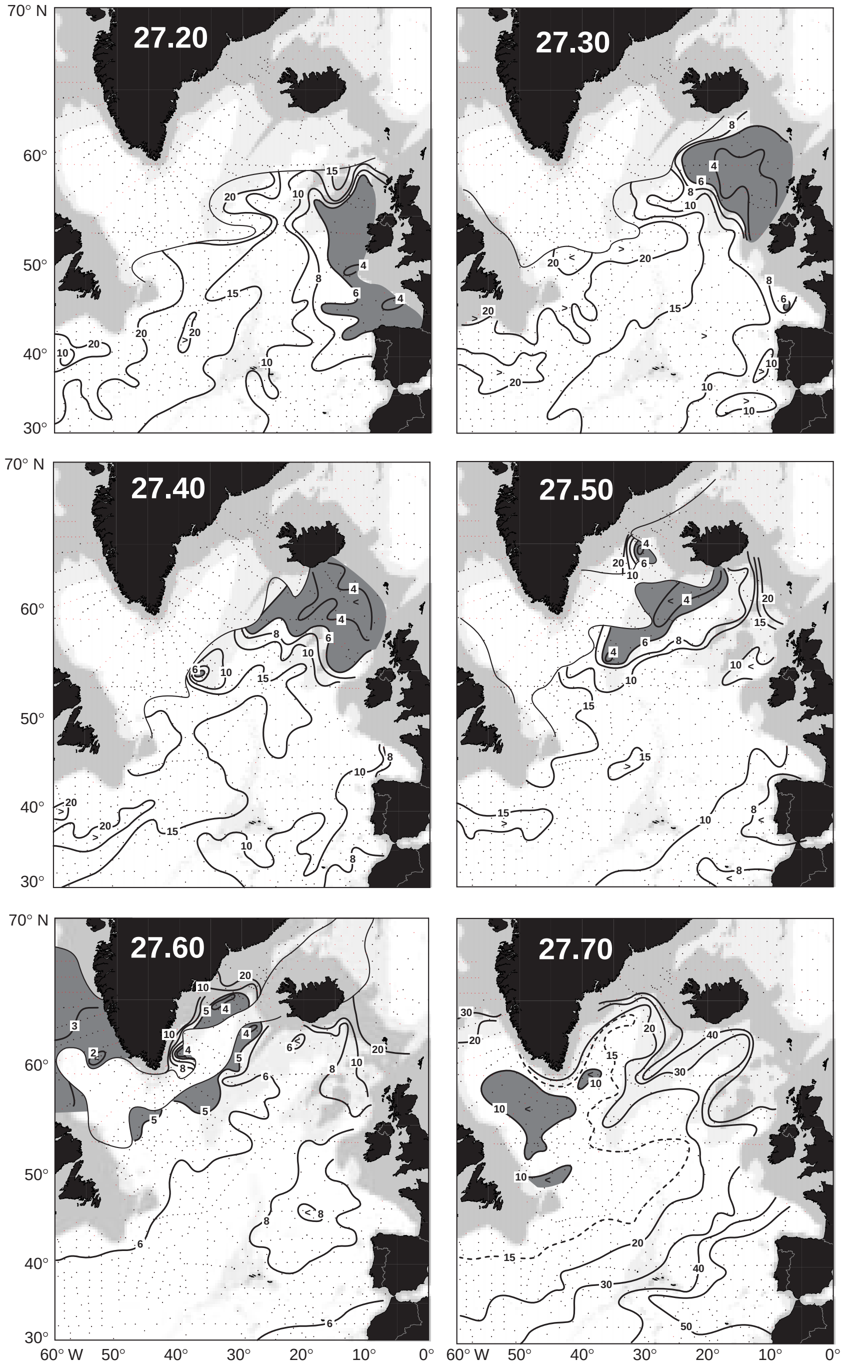

Figure 1. Isopycnic potential vorticity (10^{-13} cm^{-1} sec^{-1}) based on the Reid (1994) data set, most of which was collected in the late 1950s and 1960s, during a period of low North Atlantic Oscillation index. PV less than 4×10^{-13} cm^{-1} sec^{-1} at 27.2 to 27.5 σ_θ is shaded; each of these isopycnals has a similar range of PV. The shaded region at 27.6 σ_θ is less than 5×10^{-13} cm^{-1} sec^{-1}, since PV is somewhat higher on this isopycnal. The shaded region at 27.7 σ_θ is less than 1×10^{-13} cm^{-1} sec^{-1} since PV is generally lower at this density, which lies at the top of the Labrador Sea Water layer.

27.2 and 27.5 σ_θ (Rossby, pers. comm.). (The latter is the density near the base of the thermocline waters feeding into the subpolar region; it outcrops in the eastern Irminger Basin.) The mean velocities from these show a major eddy centred at 42°N, 44°W (Mann Eddy) and describe the loop of the North Atlantic Current into the Labrador Sea. RAFOS floats at 27.5 σ_θ were deployed at and east of the Reykjanes Ridge in 1996–1997, with the first results returning now (Bower and Richardson, pers. comm.), including capture of one float by a meddy near the Goban Spur. RAFOS floats at 1500 dbar east of the Reykjanes Ridge and in the Iceland Basin and Rockall areas show two modes: eddy flow and topography-following flow along Rockall Plateau/Hatton Bank and the Reykjanes Ridge (Zenk, pers. comm.).

PALACE floats have been deployed at 450, 1000 and 1750 dbar east of the Reykjanes Ridge as part of the project ARCANE (LeCann and Speer, pers. comm.). At 450 dbar, the floats describe westward circulation out of the Bay of Biscay and southward flow west of Portugal. At 1000 dbar, the mean vectors describe a poleward current along the eastern boundary along Portugal, the north side of the Bay of Biscay and along the Celtic shelf. They also show an anticyclonic flow (eddy) west of the Celtic shelf and cyclonic flow in the northern part of the Bay of Biscay. PALACE floats have been deployed in the western Labrador Sea at 1500 m (Schott and Fischer, pers. comm.). Most of those that escaped the Labrador Sea did so in the North Atlantic Current or southward around Flemish Cap, but none continued southward into the deep western boundary current. A transport-resolving array in the Labrador Current at 53°N accompanied the float program and showed a southward transport top-to-bottom of 40 to 50 Sv (Schott and Fischer).

PALACE floats deployed in great numbers at 700 and 1500 m in the Labrador Sea (Davis) and with somewhat sparser coverage in the remainder of the subpolar region (Owens) have been used to create a dynamic height map at 700 m, with the use of vertical shear from Levitus climatology to map the deeper float velocities upward. Coverage began in 1994, with a steep ramp-up to a large number of profiles in 1997 and 1998. The Labrador Sea floats describe the outer rim current and a "short circuit" into the Irminger Sea. Of the few floats that rounded Flemish Cap to the south, none continued southward in the deep western boundary current. Floats in the south-eastern region (40 to 50°N and east of 30°W) show weak flow dominated by eddies. One float in the Rockall region managed to pass north of the Iceland-Scotland ridge after grounding and continued vigorously northward along the Norwegian coast. The 700 m dynamic topography reveals a very interesting feature of an anticyclonic flow or countercurrent inshore of the rim current around the Labrador Sea. The low dynamic topography between the rim current and countercurrent may be the site of deeper mixed layers and convection. The two main exit paths from the Labrador Sea are thus due to the countercurrent into the Irminger Basin, south of Greenland, and also along the North Atlantic Current. Elsewhere, flow closely follows the Reykjanes Ridge and is cyclonic in the Iceland Basin and possibly anticyclonic in Rockall Trough. A separate large-scale cyclonic flow is found east of the Reykjanes Ridge and south of the Iceland Basin. The field in the south-eastern region appears dominated by eddies.

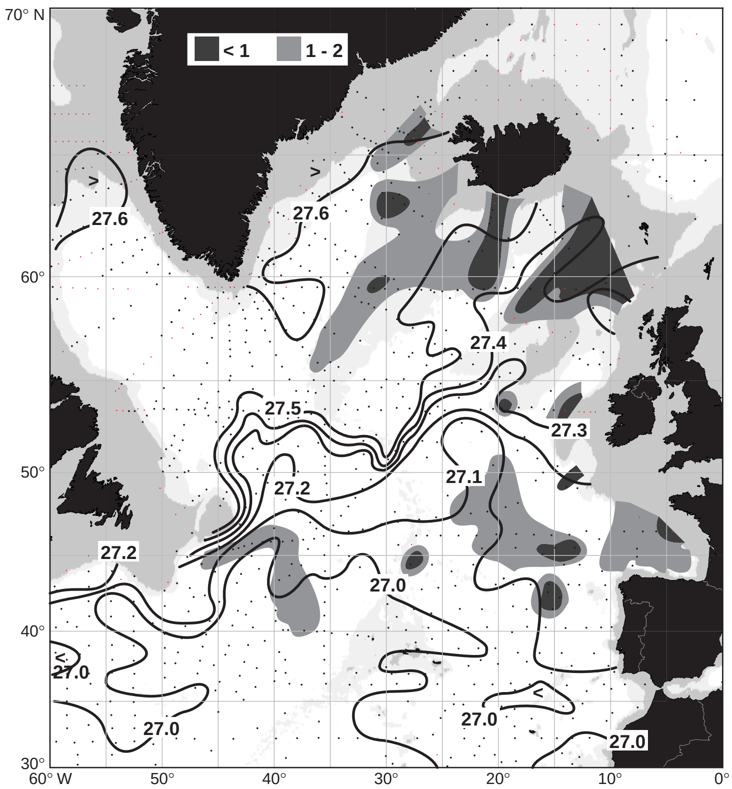

Figure 2. Potential density σ_θ at the absolute potential vorticity minimum (for densities less than 27.65 σ_θ), using the Reid (1994) data set. Regions of potential vorticity of less than 2×10^{-13} cm^{-1} sec^{-1} are shaded (dark and light, respectively).

Observations in the Irminger Basin

Many PALACE floats produce profiles of temperature and salinity. At some point it is presumed that these can be used to augment the hydrographic data set. The total hydrographic data set and many results are much too extensive to be described here. An immediate challenge is to assemble this ongoing data set, which consists of a number of sections that are repeated every year. Because of the large interannual changes in the subpolar regions' water properties, the following analysis of hydrographic data is confined to May–August 1997 when there was reasonably good coverage of the whole region.

Subpolar Mode Water

The data set consisting primarily of stations collected in the 1950s and early 1960s, assembled by Reid (1994) was first used to map the Subpolar Mode Water (SPMW) for that period. During that time, the NAO was in a protracted low phase, and so it is expected

Table 2. WOCE CTD data sources for Figure 3.

A24	Talley	Knorr	June 1997
AR19	Koltermann	Gauss	May 1998
AR7W	Schott	Meteor	July/Aug 1997
A25	Bacon	Discovery	Aug/Sept 1997
	Zenk	Meteor	May 1997

that the data set, while covering many years, is reasonably uniform. It was relatively easy to create maps from the data set, suggesting that indeed the data set was internally consistent. This data set has much better spatial resolution than the more limited data set used in McCartney and Talley (1982) where the SPMW was first described, although both data sets are from about the same time.

Isopycnic potential vorticity ($f\,d\rho\,/\,\rho\,dz$) was calculated from the historical bottle data as outlined first in Talley and McCartney (1982). PV was mapped on isopycnals at every 0.1 σ_θ from 26.8 to 27.7 σ_θ. Maps for 27.2 to 27.7 σ_θ are shown in Fig. 1. Low PV indicates a relatively thick layer. On all isopycnals, low potential vorticity occurs near the isopycnal surface outcrop, and hence is bounded by a high lateral gradient of PV on the outcrop margin. The thickest layers proceed from the Bay of Biscay at 27.2 σ_θ, to Rockall Trough/Plateau at 27.3 σ_θ, to the south side of the Iceland–Scotland Ridge at 27.4 σ_θ, to along the Reykjanes Ridge at 27.5 σ_θ, around the perimeter of the outcrop in the Irminger Basin at 27.6 σ_θ, to the central Labrador Sea at 27.7 σ_θ. The last distribution is very similar to that of the denser LSW (Talley and McCartney, 1982). In contrast to the smooth, wide SPMW distribution shown in McCartney and Talley (1982), these maps show that the deep mixed layers are strongly confined to the boundary regions. The most extreme low PV is mostly associated with topography – the shelf around the UK, Rockall Plateau/Hatton Bank, the Iceland-Scotland Ridge, the Reykjanes Ridge and the Greenland Shelf. This could be due variously to strong eddies forming near the margins or enhanced mixing over topography, possibly due to large tidal dissipation. Measurements do not extend up on to the shelves in general in this data set and so the relative efficacy of mixing on the shelves was not evaluated.

The density of the SPMW potential vorticity minimum (Fig. 2) shows the tight North Atlantic Current, turning northward after crossing the Reykjanes Ridge, and a fanning of isopycnals from this tight feature. In contrast to the picture of McCartney and Talley (1982), this more detailed view suggests that the warmer mode waters south of 50°N (27.0 to 27.15 σ_θ or so) are mainly associated with the subtropical circulation and move southward. The SPMW that proceeds into NADW formation more likely originates directly from the North Atlantic Current waters. Little SPMW is found between 27.2 and 27.3 σ_θ; this is likely the primary bifurcation density between the subtropical and subpolar circulations. A large area of SPMW around 27.4 σ_θ is found in the northeast, and a large area of density 27.5 σ_θ over the western flank of the Reykjanes Ridge and most of the Irminger Basin. The very lowest potential vorticity at the minimum is shaded in the figure, and shows the importance of the ridge complexes.

The WOCE data from May–August 1997 followed a protracted time of high NAO, although the NAO during that particular year was low. Differences in properties of the subpolar region between the 1960s and the mid-1990s have been described elsewhere. From the isopycnals examined here, freshening of the Labrador and Irminger basins is clear, due to increased import of fresh waters from the north. Salinity along the eastern boundary SPMWs, at 27.3 to 27.5 was higher in the eastern boundary region, suggesting increased flow of saline waters from the south. The lowest potential vorticity, indicating a nearby outcrop, for each of the isopycnals is shown in Fig. 3a. As with the earlier data, the importance of the boundary regions and ridges is clear, especially in the extension of the 27.5 σ_θ SPMW southward along the Reykjanes Ridge. In comparison with the 1950s/

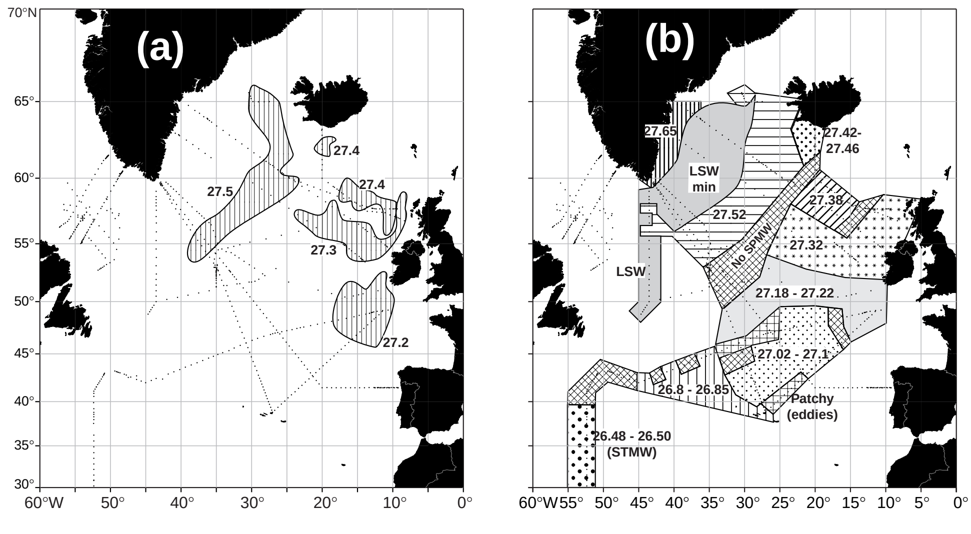

Figure 3. (a) Areas of potential vorticity less than 4×10^{-13} cm^{-1} sec^{-1} for isopycnals 27.2 to 27.7 σ_θ, based on WOCE hydrographic sections collected in May–August 1997. Data sources are listed in Table 2. Data were smoothed CTD profiles, and so the potential vorticity numbers are not precisely comparable with those calculated from bottle data, as in Figs. 1 and 2. (b) Density of the potential vorticity minimum in the SPMW in May–August 1997. Shaded regions indicate where a clear SPMW potential vorticity minimum is not present. Potential density values listed in the various regions are the average SPMW density for that region, about which there is only small variation.

1960s, the SPMW in the eastern subpolar region is somewhat denser, with the 27.3 and 27.4 isopycnals outcropping several degrees of latitude farther south in 1997. The Irminger and Labrador Sea SPMW centres are similar in the two time periods, although the 27.7 σ_θ mode extends more clearly into the Irminger Sea in 1997. This is presumably associated with the average circulation defined by the Labrador Sea PALACE floats, as described above.

Examination of PV along the individual, highly-resolved WOCE sections shows that in general there are large regions of coherently low PV centred at one density or with very slowly varying density, terminating abruptly and switching to another density. It is difficult to depict this building block structure on a contoured horizontal map. Fig. 3 shows the regions as indicated by these sections, with the average densities of the SPMWs in each region listed. Prominent in this SPMW distribution is the North Atlantic Current and its northward extension in the subarctic front, as defined on each section by at least two stations. Within this feature there is no SPMW. South and east of the front, SPMWs fall into five separate density classes, which appear nearly discontinuous. It is not claimed herein that these exact density classes would be found in each year, but the general increase in density towards the north is a robust feature of all data sets, while the probability of quantisation within this general increase is very likely for other years, and should be pursued with data sets from other years. In the southern region, south of about 47°N, the mode waters are broken up by an eddy field. Thus the impression of domination by eddies in this region based on PALACE float data, as described above, extends to hydrography as well. Data from this period were not available along the Iceland–Scotland Ridge and so the final mapping of the northern modes was not possible.

West of the subarctic front, in the eastern Irminger Basin and along the Reykjanes Ridge, the SPMW density is remarkably uniform, centred at 27.52 σ_θ, with none of the progression of densities observed east of the front. Modes at a density of 27.65 σ_θ are found only along the Greenland shelf, and appear to be associated with thick mixed layers formed locally there. The central Irminger Basin is dominated by Labrador Sea Water, and so identification of an SPMW there is not sensible in this data set.

In summary, this initial view of the SPMW distribution based on more detailed analysis of the 1950s/1960s data and WOCE data from summer 1997 suggests major refinements to previous ideas: boundary intensification of the low potential vorticity areas, association of the major SPMW modes with topographic features, a clear demarcation between SPMWs east and west of the subarctic front, quantisation of SPMW densities, with SPMW west of the subarctic front being of nearly uniform density. Much further analysis is required to pursue these SPMW features, to attempt to identify specific formation sites or regions for each SPMW "type" and the connections between them, and hopefully to identify the processes producing such remarkably thick mixed layers. Important adjunct data sets are the floats for the circulation and eddy field, surface fluxes, and high resolution SST and altimetry to better define the horizontal structures and relation to the eddy field and fronts.

References

McCartney, M. S., 1982: The subtropical circulation of Mode Waters. J. Mar. Res., 40(suppl.), 427–464.

McCartney, M. S., and L. D. Talley, 1982: The subpolar mode water of the North Atlantic Ocean. J. Phys. Oceanogr., 12, 1169–1188.

McCartney, M. S., and L. D. Talley, 1984. Warm water to cold water conversion in the northern North Atlantic Ocean. J. Phys. Oceanogr., 14, 922–935.

Reid, J. L., 1994. On the total geostrophic circulation of the North Atlantic Ocean: flow patterns, tracers and transports. Prog. Oceanogr., 33, 1–92.

Schmitz, W. J., and M. S. McCartney, 1993. On the North Atlantic circulation. Rev. Geophys., 31, 29–49.

Talley, L. D., and M. S. McCartney, 1982. Distribution and circulation of Labrador Sea Water. J. Phys. Oceanogr., 12, 1189–1205.

Talley, L. D., 1999: Some aspects of ocean heat transport by the shallow, intermediate and deep overturning circulations. In: Mechanisms of Global Climate Change at Millenial Time Scales, Geophys. Mono. Ser., 112, American Geophysical Union, ed. Clark, Webb and Keigwin, 1–22.

Tsuchiya, M., 1989: Circulation of the Antarctic Intermediate Water in the North Atlantic Ocean. J. Mar. Res., 47, 747–755.

Worthington, L. V., 1976: On the North Atlantic circulation. Johns Hopkins Oceanographic Studies, 6.

Some features of the North Atlantic circulation in high resolution models

A. M. Treguier, LPO, IFREMER, Brest, France

Following the early WOCE Community Model Experiments initiated at NCAR by Holland and Bryan (1989), a large number of models of the North Atlantic circulation have been run during the WOCE years. Those models range from "eddy-permitting" (typically, 1/3° grid size) to what we call today "eddy-resolving" (1/10°).

Much in the same way as weather forecast models, high-resolution ocean models are meant to reach a high degree of realism. With such models it becomes possible to make local, quantitative comparisons with data. When the model fails to represent the details of the observed flows one asks why – something which is not usually done with low-resolution models.

A few model results relative to the North Atlantic circulation are presented here, to illustrate where models can help and how they have improved over the WOCE years. The results come from modelling efforts in many countries: The CME at NCAR (US) and IfM (Germany), the DYNAMO intercomparison project (IFM-Germany, SOC-UK, LEGI-France), the POP models (LANL, US), the MICOM high-resolution model (RSMAS, US), the FLAME project (Germany), the CLIPPER project (France).

The Azores Current

In the first CME eddy-permitting model of the North Atlantic, the Azores Current was too weak and did not penetrate far enough to the east (Spall, 1990). Test of different wind fields made no difference. With a higher resolution of 1/6°, the eddy activity increased but not the mean current (Beckmann et al., 1994). After much speculation, one of the models in the DYNAMO intercomparison project, the 1/3° isopycnic model, succeeded in producing a flow that looked like an Azores Current. This has been analysed by Jia (1999) and shown to result from the dynamics in the Gulf of Cadiz, where a strong relaxation was imposed to simulate the input of Mediterranean water.

The dynamical relationship between the Azores Current and the Mediterranean outflow is confirmed by the French CLIPPER eddy-permitting model (Fig. 1b). The figure shows the profile of zonal velocity for an experiment with open Gibraltar Straits. An eastwards current is found at the location of the Azores front. A previous experiment with closed Gibraltar Straits had produced a weaker flow (similar to the LEVEL model of the DYNAMO intercomparison). However, the results of the Los Alamos POP 1/10° model and 0.28° model (Smith et al., 1999), also presented on Fig. 1 (a and c) suggest that more analysis is needed to understand the respective roles of the Mediterranean outflow and the horizontal resolution. In the higher resolution POP model (top) the current is more intense, and certainly more realistic than in the CLIPPER model. Momentum eddy fluxes intensifying the Azores Current (as happens in the atmospheric jet stream) could explain the difference. On the other hand, the 0.28° POP model also had open Gibraltar Straits (Smith, pers. comm.) but the Azores Current is almost non-existent. A detailed comparison of those models should help understand if the volume of upper layer water entrained in the Gulf of Cadiz controls the strength of the Azores Current, as recently proposed by Özgökmen et al. (1999).

Finally, we note that the models with open Gibraltar Straits produce a cyclonic vertically

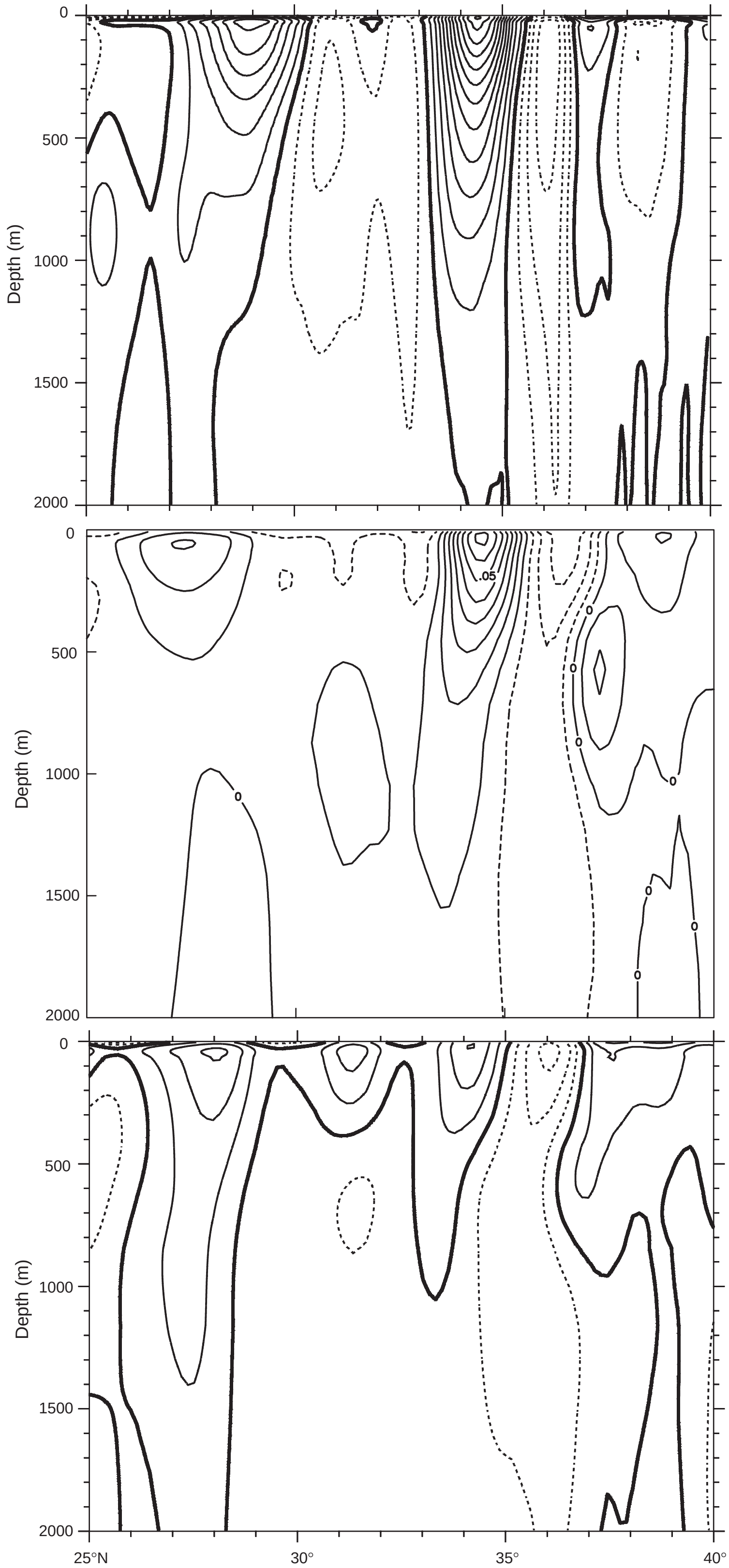

Figure 1. Meridional sections of the time-mean zonal velocity averaged between 35°W and 25°W. Contour interval is 1 cm/s. (a) POP 0.1° run, (c) POP 0.28° run from Smith et al., 1999; (b) CLIPPER 1/3° run.

integrated mass transport of about 4–5 Sverdrups in the Gulf of Cadiz. This is much less intense than the circulation found in the isopycnic models (15 Sv or more) and is not in contradiction with observations.

Deep circulations

The deep circulations have not been analysed in detail in models because of the lack of observations to validate them. Validation will now become easier both by the growth of the observational database and the availability of a large number of model solutions. As an example, we consider the deep anticyclonic gyres in the Canary Basin, already noticed by Spall (1990) in the CME solution. In some models those gyres are correlated with an anticyclonic anomaly of the depth-integrated transport of 5 to 10 Sverdrups. It is the case of the sigma-coordinate models in the DYNAMO intercomparison (Willebrand et al., 1999), and also the CLIPPER 1/3° model. Comparing those solutions should help us understand the origin of those circulations (perhaps the inflow of Antarctic bottom water through the VEMA fracture zone).

The subpolar gyre

The subpolar gyre of the North Atlantic Ocean is probably a key area where global scale climate variations can be generated. The eddy-permitting models have represented this area rather poorly. Many sensitivity experiments (e.g. Doscher et al., 1994) have shown that the meridional overturning and heat transport are sensitive to local features, for example the details of the topography over the sills.

Major flaws were a bad representation of the path of the North Atlantic Current, the loss of deep water down-stream of the sills (or excessive amount of deep water for isopycnic models) and the salinisation of the Labrador Sea (to salinity larger than 35 PSU).

The new high resolution models (MICOM 1/12° and POP 1/10°) reproduce much better the path of the North Atlantic Current, and the salinity field seems more realistic in POP. A more precise analysis of the water masses in those experiments is necessary, to see if indeed high resolution is a remedy to the climatic drift of ocean models.

Conclusion

We have started the WOCE decade with one eddy-permitting 1/3° model of the North Atlantic. Because of the increase in computing power we now have tens, perhaps more than one hundred of experiments at that resolution. From those sensitivity experiments and model intercomparisons modellers have tried to draw conclusions about the ocean dynamics and its sensitivity to the forcing. The conclusions are sometimes questioned because of the lack of realism of the eddy-permitting model solutions.

In the next ten years, if the increase in computing power keeps its pace, we will be able to move in two directions:

- perform sensitivity studies with fully eddy resolving models, rather than eddy-permitting;
- perform long term integration with eddy permitting models, or models with higher resolution of western boundary currents and narrow passages, to better understand the time scales of climatic variability.

References

Döscher, R., C. W. Böning, and P. Herrmann, 1994: Response of circulation and heat transport in the North Atlantic to changes in thermohaline forcing in the northern latitudes: a model study. J. Phys. Oceanogr., 24, 2306–2320.

Spall, M. A., 1990: Circulation in the Canary Basin: A model/data analysis. J. Geophys. Res., 95(C6), 9611–9628.

Beckmann, A., C. W. Böning, C. Koberle, and J. Willebrand, 1994: Effects of increased horizontal resolution in a simulation of the North Atlantic Ocean. J. Phys. Oceanogr., 24, 326–344.

Jia, Y., 1999: On the formation of an Azores current due to Mediterranean overflow in a modelling study of the North Atlantic. J. Phys. Oceanogr., in press.

Özgökmen, T. M., E. P Chassignet, and C. G. H. Rooth, 1999: On the connection between the Mediterranean outflow and the Azores current. In press.

Smith, R. D., M. E. Maltrud, F. O. Bryan, and M. W. Hecht, 1999: Numerical simulation of the North Atlantic Ocean at 1/10°. J. Phys. Oceanogr., in press.

Willebrand, J., B. Barnier, C. Böning, C. Dieterich, P. Herrmann, P. D. Killworth, C. Le Provost, Y. Jia, J. M. Molines, and A. L. New, 1999: Circulation characteristics in three eddy-permitting Models of the North Atlantic. Prog. Oceanogr., submitted.

Gulf Stream modelling: A brief overview

E. P. Chassignet, with contributions from R. Smith, Z. Garraffo, H. Hurlburt, and P. Hogan.

Until recently, most ocean general circulation models (OGCMs) had great difficulties in reproducing the basic pattern of the Gulf Stream. The modelled Gulf Streams had in general the tendency to separate far north of Cape Hatteras and to form a large stationary anticyclonic eddy at the separation latitude (e.g., Beckmann et al., 1994; Bryan et al., 1995; Dengg et al., 1996). Simulations with grid resolution of 1/10° or higher are now able to realistically represent the Gulf Stream separation (Bleck et al., 1995; Paiva et al., 1999; Smith et al., 1999; Hurlburt and Hogan, 1999; Chassignet et al., 1999). These results support the view that an inertial boundary layer (which results from the fine resolution) is an important factor in the separation process (Özgökmen et al., 1997).

Fig. 1 displays the 3-year-mean sea surface height (SSH) from two thermodynamically forced OGCMs with comparable horizontal resolution (on the order of 1/10°). The first simulation (Fig. 1a) was integrated for 10 years (after a 5-year spin-up) with the Los Alamos Parallel Ocean Program (POP; Smith et al., 1992) using 1985–1996 6-hourly ECMWF winds, surface heat flux from Barnier et al. (1995), and restoration to monthly Levitus (1982) surface salinity. The second simulation (Fig. 1b) was integrated for 20 years with the Miami Isopycnic Coordinate Ocean Model (MICOM; Bleck et al., 1992; Bleck and Chassignet, 1994) using monthly climatological forcing from COADS (da Silva et al., 1994). While both integrations exhibit a separated Gulf Stream, there are substantial differences in its path, strength, and variability. In POP, the simulated Gulf Stream flows in a more zonal direction than that observed after separation, resulting in a southward offset of the mean path of 1° to 1.5° latitude. In MICOM, the simulated Gulf Stream path agrees well with observations until the location of the New England Seamounts chain, where it is displaced northward by about 1°. This northward shift is associated with a larger than observed seasonal migration of the path [observed annual signal of up to 100 km, north of the mean from August to November and south of the mean from March to June (Mariano et al., 1999)]. Overall, the modelled Gulf Stream is stronger in POP (maximum surface velocities of 190 cm/s) than in MICOM (maximum surface velocities of 150 cm/s). The SSH variability associated with the meandering stream is also stronger in POP and agrees well with observations (Smith et al., 1999). The lower eddy energy in MICOM may be a result of the mixed layer formulation, which suppress vertical shear, and/or a result of the use of harmonic dissipation (biharmonic in POP) (DYNAMO, 1997).

Several sensitivity experiments with a biharmonic dissipation operator in the momentum equations were therefore performed with MICOM. The resulting mean SSH for two different magnitudes of the dissipation is displayed in Fig. 2. With the higher order operator (biharmonic), the eddies were found to retain their structure for longer periods of time, but with undesirable effects on some features of the large-scale circulation. In Fig. 2a, for example, the western boundary current is seen to separate early from the coast (at the Charleston bump before Cape Hatteras) when a relatively small value of the biharmonic viscosity coefficient is used in MICOM. A similar result was observed with POP during the spin-up phase (Smith et al., 1999), and both the viscosity and diffusion had to be increased by a factor of 3 in an attempt to diminish this problem. An increase in the magnitude of the dissipation operator in MICOM did indeed eliminate the early detachment seen in Fig. 2a, but it also led to the establishment of a permanent eddy north of Cape Hatteras (Fig. 2b). The best separation/penetration results in MICOM were obtained with a combination of the two operators (Fig. 1b).

These results appear to suggest that, even with such a fine grid spacing, the subgrid-scale parameterisation choice is of importance for the large scale circulation. The fact that eddies persist in the same location for years in both simulations with biharmonic operators [Gulf of Mexico for POP (Fig. 1a), north of Cape Hatteras for MICOM (Fig. 2b)] seems to indicate an incorrect representation of the eddy/mean flow and/or of the eddy/topography interactions, possibly because of the scale selectiveness of the higher order operator (biharmonic). A lower level of eddy activity was also observed in North Atlantic simulations performed with the Navy Layered Ocean Model (NLOM) with the same resolution and with a Laplacian operator, but a four-fold increase in resolution with the same operator brought the

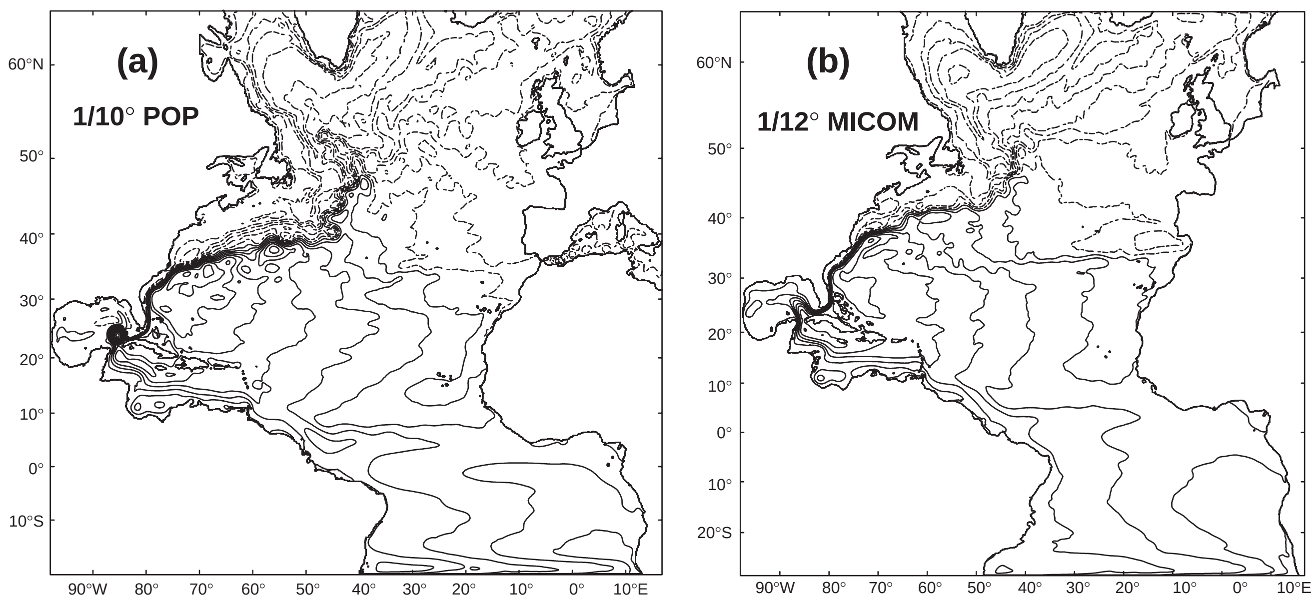

Figure 1. 3-year-mean model SSH field for (a) 1/10° POP and (b) 1/12° MICOM.

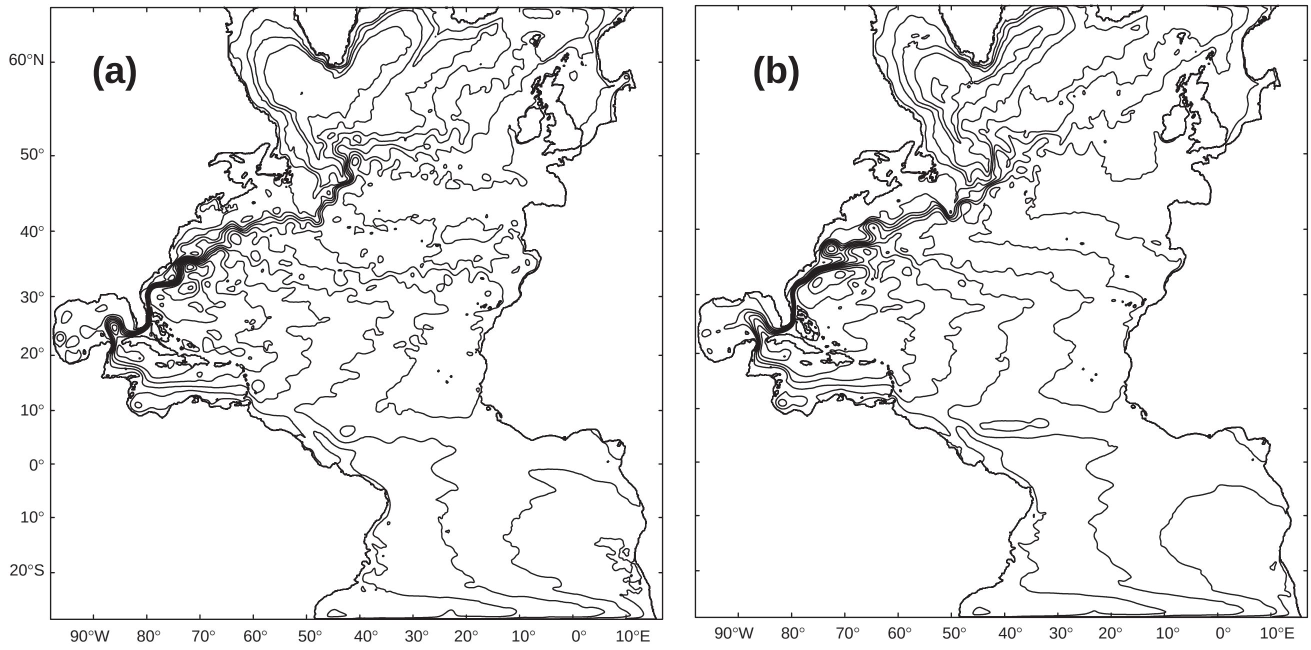

Figure 2. 1-year-mean model SSH field with biharmonic viscosity operator in MICOM: (a) small coefficient; (b) large coefficient.

SSH variability to observed levels without altering the pattern of the large scale circulation (Hurlburt and Hogan, 1999).

Finally, while numerical simulations at the above-noted resolutions are becoming more common, they still demand the latest in computing facilities. Most of the long term global coupled ocean/atmosphere calculations presently underway are limited to fairly coarse resolution ocean models (on the order of 2°), in which a misplacement of the Gulf Stream position has a profound impact on the coupled system. Attempts are being made to reduce the tendency for the coarse resolution western boundary current to follow the coastline. The National Center for Atmospheric Research (NCAR) Climate Group showed some indication of improvement in the separation with a particular form of anisotropic viscosity in a 2° version of the CSM global model. These experiments, however, show rather strong temporal variability in the separation point, and a satisfactory solution has not yet been achieved.

References

Beckmann, A., C. W. Böning, C. Köberle, and J. Willebrand, 1994: Effects of increased horizontal resolution in simulations of the North Atlantic Ocean. J. Phys. Oceanogr., 24, 326–344.

Bleck, R., C. G. H. Rooth, D. Hu, and L. T. Smith, 1992: Salinity-driven transients in a wind- and thermohaline-forced isopycnic coordinate model of the North Atlantic. J. Phys. Oceanogr., 22, 1486–1505.

Bleck, R., and E. P. Chassignet, 1994: Simulating the oceanic circulation with isopycnic coordinate models. The Oceans: Physiochemical Dynamics and Resources. The Pennsylvania Academy of Science, 17–39.

Bleck, R., S. Dean, M. O'Keefe, and A. Sawdey, 1995: A comparison of data-parallel and message-passing versions of the Miami Isopycnic Coordinate Ocean Model (MICOM). Parallel Computing, 21, 1695–1720.

Bryan, F. O., C. W. Böning, and W. R. Holland, 1995: On the midlatitude circulation in a high-resolution model of the North Atlantic. J. Phys. Oceanogr., 25, 289–305.

Chassignet, E. P., Z. D. Garraffo, and A. M. Paiva: Fine-mesh (1/12°) modeling of the North Atlantic: the spin-up phase. In preparation.

da Silva, A. M., C. C. Young, and S. Levitus, 1994: Atlas of surface marine data 1994. Volume 1: Algorithms and procedures. US Department of Commerce, NOAA, NESDIS, 83 pp.

Dengg, J., A. Beckmann, and R. Gerdes, 1996: The Gulf Stream separation problem. In: The Warmwatersphere of the North Atlantic Ocean, W. Krauss, (Ed.), Gebr. Borntraeger, Berlin, 253–290.

DYNAMO, 1997: Dynamics of North Atlantic Models: simulation and assimilation with high resolution models. Technical report, Institut für Meereskunde. 334 pp.

Hurlburt, H. E., and P. J. Hogan, 1999: Impact of 1/8° to 1/64° resolution on Gulf Stream model-data comparisons in basin-scale subtropical Atlantic Ocean models. Deep-Sea Res., accepted.

Mariano, A. J., T. M. Chin, E. H. Ryan, R. Kovach, and O. B. Brown, 1999: On Gulf Stream path variability. To be submitted.

Özgökmen, T., E. P. Chassignet, and A. Paiva, 1997: Impact of wind forcing, bottom topography, and inertia on mid-latitude jet separation in a quasi-geostrophic model. J. Phys. Oceanogr., 27, 2460–2476.

Paiva, A. M., J. T. Hargrove, E. P. Chassignet, and R. Bleck, 1999: Turbulent behaviour of a fine mesh (1/12°) numerical simulation of the North Atlantic. J. Mar. Sys., 21, 307–320.

Smith, R. D., J. K. Dukowicz, and R. C. Malone, 1992: Parallel ocean circulation modelling. Physica D, 60, 38–61.

Smith, R. D., M. E. Maltrud, F. O. Bryan, and M. W. Hecht, 1999: Numerical simulations of the North Atlantic Ocean at 1/10°. J. Phys. Oceanogr., submitted.

Modelling of the Deep Western Boundary Current and offshore recirculation in the North Atlantic Ocean

Mitsuhiro Kawase, University of Washington School of Oceanography, USA.

When Stommel and Arons (1960) developed their model of abyssal circulation, which featured the deep western boundary current (DWBC), it was considered a major triumph of dynamical oceanography. In their view the deep western boundary current was a feature of low-Rossby-number flow on a rotating sphere driven by localised inflow and distributed upwelling. The steady-state model of Stommel and Arons emphasised the deep western boundary current's role in balancing the mass budget of the circulation, and considered it as an essentially passive responder to the interior circulation. Today, after several decades of observation, theoretical analyses and numerical modelling, we recognise the deep western boundary current as something far more complex, possibly having multiple driving mechanisms, and having an important role as an integral part of the oceanic component of the climatic system. My aim in this presentation is a survey of progress in the understanding of deep western boundary currents in the last decade or so and prospecting of future research directions.

Driving mechanisms; adjustment

The traditional view of the deep western boundary current has been that it is the outflowing limb of the thermohaline overturning. Kawase (1987) studied the spin-up of abyssal circulation driven in this manner, and elucidated the fundamental role played by boundary (Kelvin) waves. In his numerical model, a Kelvin wave signal from a localised source of deep water established a boundary current along the western boundary of the ocean down to the equator. Thus, this portion of the deep western boundary current can exist independent of the interior circulation, although the eventual transport in the boundary current in the asymptotic steady state is clearly interior-dependent by the same argument as

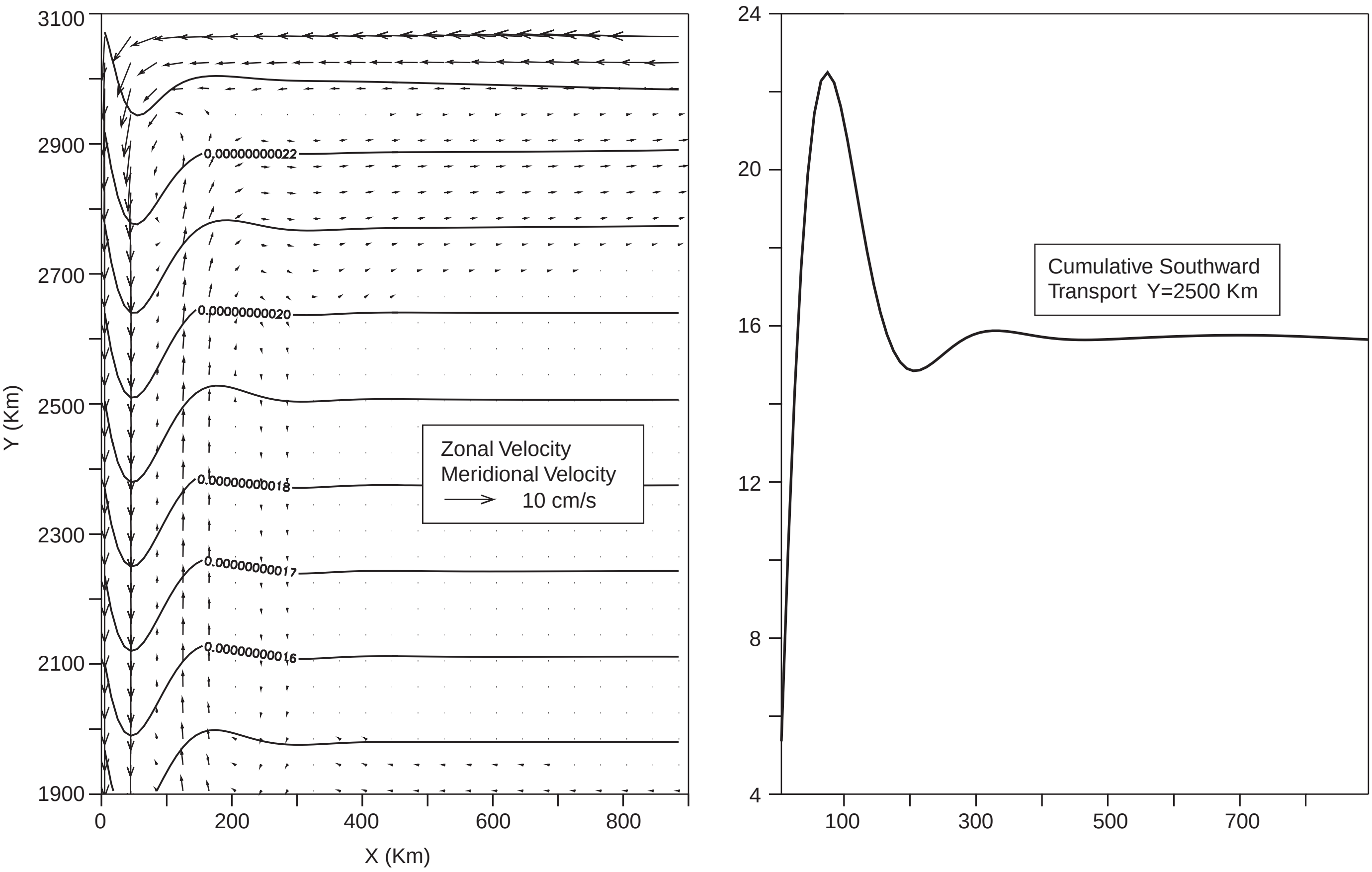

Figure 1. A visco-inertial boundary current driven by a northern mass source in a shallow water (equivalent-barotropic) model. The source drives 15 Sv of southward transport. Left: velocity (vectors) and potential vorticity (contours) around y=2500 km on an equatorial beta-plane. Right: cumulative mass transport at y=2500 km. The recirculating component is about 50% of the net southward transport. Layer depth: 3000 m. Reduced gravity: $8.3 \times 10^{-3}\ m/s^2$. Horizontal eddy viscosity: $4 \times 10^4\ m^2/s$. Model is free-slip.

for the Stommel-Arons model. On the other hand, extension of the deep western boundary current into the opposite hemisphere had to wait for the arrival of the signal from the eastern boundary in the form of long Rossby waves. This portion of the deep western boundary current is closer to that in the original Stommel-Arons model and is crucially dependent on the interior circulation. Another implication of the Kelvin-wave-mediated adjustment is that it would be rapid, with substantial response in a given basin within a few years and globally within a few decades.

Adjustment of thermohaline circulation in response to changes in thermohaline forcing has been studied in realistic context in recent years as the interest is stimulated by the connection between climatic shifts and changes in thermohaline circulation. Karcher and Lippert (1994) used an equivalent barotropic model with realistic Atlantic bathymetry to study the establishment of deep circulation by NADW. Their model shows rapid adjustment of circulation by the Kelvin-Rossby mechanism through the Atlantic in less than a decade. The current work of Goodman (1999) studies the same adjustment in a global context using a coarse-resolution OGCM. The spin-up of thermohaline circulation along the expected Kelvin waveguide is very much in evidence and its influence is felt in all oceans within twenty years of the initiation of deep water production. Exceptions to this are the Antarctic Circumpolar region, which is dynamically isolated from Kelvin waves originating in the North Atlantic, and the corner of recirculation gyre in the North Atlantic which lags substantially behind the surrounding region. The reason for the insensitivity of the latter region is unclear, but it may be due to refraction of baroclinic long Rossby waves, which would carry the information of the adjustment into the interior, by the wind-driven circulation (Luyten and Stommel, 1986). In any case, this rapid dynamical adjustment of circulation is to be contrasted with the slow advective adjustment of the newly formed deep water reaching corners of all basins, which would take five hundred years or more.

An altogether different driving mechanism for intensified currents along continental margins is driving by eddies. Several arguments have been advanced for eddies driving mean flow along the contours of large-scale potential vorticity with magnitudes roughly in proportion to the slope of the topography. Holloway (1992) has advocated inclusion of this effect into models of coarse resolution. His argument is based on “topographic stress” arising from effects of small scale topography on eddies, but similar eddy-rectified currents also occur in models with smooth bathymetry (Spall, 1994; Thompson, 1995). Along the western boundary of the North Atlantic, both the Kelvin and the eddy driving would give the same direction of transport in the boundary current while they would oppose each other in the “non-native” hemisphere for the deep water. Thermohaline driving must account for a substantial portion of the DWBC transport in, for example, the South Atlantic, where the boundary current is in the opposite sense from what is expected from the eddy driving. On the other hand, modern observations of the DWBC point to several features of the current that indicate possibly important contributions from eddy driving. These include the discrepancy between measured and tracer-inferred current speeds; largely barotropic structure of the current below the main thermocline with the vertical scale exceeding that of the tracer features; and measured transport in excess of the estimated thermohaline overturning at many locations. Further research is needed given the uncertain status of our understanding of eddy rectification.

Interaction with the upper ocean, interior, and recirculation

A model study by Thompson and Schmitz (1989) indicated that the deep western boundary current may influence the separation of the Gulf Stream at Cape Hatteras, long a notorious challenge in the simulation of the North Atlantic circulation. Spall (1996a) and Ladd and Thompson (1998) have studied the crossover region using idealised, eddy-resolving models including tracers. Recirculation gyres associated with the Gulf Stream are featured in both models and driven by transfer of momentum from the wind-driven current in the upper layer by form drag of baroclinic eddies (Holland and Rhines, 1980). In both works eddies are seen to play an important role in the crossover region, either for the entrainment of the DWBC water into the recirculation (Spall) and for the continuation of the DWBC south (Ladd and Thompson).

Deep recirculation gyres are not only associated with the Gulf Stream. Long-term measurements of currents along the western boundary and trajectories of neutrally buoyant floats have revealed the existence of recirculating gyres at several latitudes along the western boundary, such that the deep western boundary current may be considered not so much a continuous current as a series of recirculating gyres, each elongated in the alongshore direction. The dynamics of these recirculation gyres have attracted little attention other than those associated with the Gulf Stream. For most of the tropics and the subtropics in the North Atlantic, the surface current is northward and therefore in the wrong direction to drive the southward deep western boundary current via the form drag mechanism responsible for the Gulf Stream recirculations (Holland and Rhines, 1980). A simpler yet more plausible explanation is that these are Munk-type viscous or possibly visco-inertial boundary layers (Cessi et al., 1990) and is a by-product of the thermohaline deep western boundary current. Simple scaling based on the observations of Lee et al. (1996) with current speed (U) of 20 cm/s, gyre width (L) of 150 km at 27°N gives the non-linear parameter $U/\beta L^2$ of 0.4 and horizontal eddy viscosity of $6.7\times10^4\ \mathrm{m}^2/\mathrm{s}$. A simple model calculation based on these parameters (Fig. 1) gives a recirculation gyre with quite a realistic structure, although the magnitude of the recirculatory component is nowhere as large as observed by Lee et al. It is hoped that there will be progress in dynamical understanding of these recirculation gyres in the near future from dynamical analyses of observations and eddy-permitting/resolving models, both idealised and realistic.

Low-frequency variability

From the studies mentioned above it is clear that the deep western boundary current responds rapidly to changes in the thermohaline forcing, and observation of such changes have been claimed in recent years. There may in addition be modes of low-frequency variability in the ocean in which the deep western boundary current play a more active role. In the three-layer model of the crossover region mentioned above, Spall (1996b) noted the circulation alternating between a state with high mean but low eddy kinetic energy with a long zonal penetration of the recirculation gyres and an opposite state with a timescale of roughly a decade. This oscillation, somewhat reminiscent of the high/low index oscillation in the mid-latitude atmospheric circulation, was absent when the transport of upper DWBC was set to zero. During the high-penetration phase, the upper DWBC was almost completely diverted into the eastward limb of the recirculation gyre. Spall attributes this oscillation to intrusion of low potential vorticity water Whether or not such oscillations can exist in more realistic models of the Atlantic circulation, or in reality, is not clear.

Modelling issues

Modelling the western boundary current remains a challenge for simulation of basin-wide ocean circulation. The problem is severe for models used for climate studies (such as in coupled models), since computers are only now reaching the speed required for running eddy-resolving OGCMs fast enough for extensive parameter study. The need for adequate parameterisation of eddy-scale processes is unlikely to go away in the near future. One problem that plagued coarse-resolution models was short-circuiting of the thermohaline circulation due to horizontal mixing of density along the western boundary. This problem has been addressed through the use of flux-correction scheme that mimic the bolus transport associated with baroclinic eddies (Böning et al., 1995). More controversial is representation of eddy rectification in coarse-resolution models. In future, data assimilation would give us formal means of assessing model error and need for parameterisation in such models.

Acknowledgements

I thank Joint Institute of Study of the Atmosphere and the Ocean (JISAO), University of Washington, for hosting me during the preparation of this presentation, and Ed Sarachik, David Battisti, Igor Kamenkovich and in particular Paul Goodman for providing me with ideas and suggestions. I thank Fritz Schott and the IfM Kiel for their invitation to the WOCE North Atlantic Workshop and giving me the opportunity for this presentation.

References

Böning, C. W., W. R. Holland, F. O. Bryan, G. Danabasoglu, and J. C. McWilliams, 1995: J. Clim., 8, 515–523.
Cessi, P., R. V. Condie and W. R. Young, 1990: J. Mar. Res., 48, 677–700.
Goodman, P., 1999: J. Phys. Oceanogr., submitted.
Holland, W. R., and P. B. Rhines, 1980: J. Phys. Oceanogr., 10, 1010–1031.
Holloway, G., 1992: J. Phys. Oceanogr., 22, 1033–1046.
Karcher, M. and Lippert, A., 1994: J. Geophys. Res., 99, 12357–12373.
Kawase, M., 1987: J. Phys. Oceanogr., 17, 2294–2317.
Ladd, C., and L. Thompson, 1998: J. Phys. Oceanogr., 28, 1717–1738.
Lee, T. N., W. E. Johns, R. J. Zantopp, and E. R. Fillenbaum, 1996: J. Phys. Oceanogr., 26, 962–983.
Luyten, J. R., and H. M. Stommel, 1986: Deep-Sea Res., 33, 963–972.
Spall, M.A., 1994: J. Mar. Res., 52, 1051–1080.
Spall, M.A., 1996a: J. Phys. Oceanogr., 26, 2152–2168.
Spall, M.A., 1996b: J. Phys. Oceanogr., 26, 2169–2182.
Stommel, H. M., and A. B. Arons, 1960: Deep-Sea Res., 6, 140–154.
Thompson, J. D., and Schmitz, W. J., 1989: J. Phys. Oceanogr., 19, 791–814.
Thompson, L., 1995: J. Phys. Oceanogr., 25, 1296–1316.

Observations of subtropical/tropical deep circulation

Rana A. Fine, RSMAS, University of Miami, USA

Summary of deep subtropical and tropical circulation

- The CFCs have been transported throughout the western NA on decadal time scales; 2/3 in subpolar, 1/3 in subtropics.
- In addition to the cross-equatorial transport, CFCs and floats show flow at 1–2°S rather than along the equator – the region acts as a buffer zone for cross equatorial exchange.
- Total MOC transport based on hydrography and CFC inventories is 13–15 Sv (colder than 4°C) during the last several decades.
- The DWBC transport is 2–3 times the MOC, the recirculation gyres help to reconcile these differences.
- The recirculation gyres are storage reservoirs-imposing an extended time scale, they integrate and mix properties.
- At the Gulf Stream crossover there is a change in the vertical location of the high mode of DWBC transport from UNADW to LNADW, and in the tropical SA to MNADW.
- There are transformations by mixing in the equatorial region involving at least LNADW/MNADW and LNADW and AABW.

- There are direct measurements in the equatorial region that suggest seasonality in AABW and DWBC transports at all levels.
- There are documented transport and circulation responses to the LSW transient.

Unknown Issues for subtropics and tropics

LSW transient: Is there a concomitant transport increase with the rate increase and arrival of the LSW transient? What is the relationship between formation strengths of ULSW and CLSW? Was ULSW a substitute for CLSW such that the influence of ULSW at lower latitudes will diminish while CLSW influence builds? Or will both strengthen indicative of a strengthening of the UNADW limb of the MOC? What are the circulation changes related to the LSW transient? Are there two pathways southward of the Grand Banks, such that one pathway is favoured under certain forcing (NAO) conditions? What are the atmospheric feedback?

Deep gyres-storage: When will the LSW transient reach the equator? Will the subtropical circulation have to be flushed before the LSW transient anomaly passes downstream to the tropics? What are the flushing and dilution rates of the recirculation gyres? To what degree does the horizontal circulation act like a valve in slowing and diluting the thermohaline transients, so that they basically delay equatorward progression of climate (CO_2, heat, freshwater) anomalies?

DWBC-gyre interactions: What drives the recirculation gyres? What is the role of sub-grid scale processes in altering the circulation and water masses? What are the time and space scales of the variations in the transport, storage and exchange processes?

Cross equatorial: How do the net northward flows of warm and intermediate water and southward flow of UNADW cross the equator? What causes the change in pathway from across to along equator flow or recirculation? What is the role of western intensified recirculation gyres in supplying and receiving the net cross equatorial flows? How does transient information – like the LSW transient – move between hemispheres? What is the equatorial part of the dynamical adjustment process? What is the role of the deep NBC rings in driving the deep "mean" circulation? How stationary are the transequatorial flows of MNADW, LNADW and AABW?

What causes the deep equatorial jets on and off the equator? How coherent and long lived are they? How do the jets connect to the nearby recirculations and the WBC/DWBC crossing the equator? Are there equatorially concentrated counter rotating recirculations to either side of the equator as suggested by the float trajectories, and are these the basic advection field spreading tracers eastward along the equator rather than a monotonic equatorial jet? What is the residence time, or mean speed for particles crossing the equator as a function of water mass/depth?

Equatorial mixing: Is there a concentration of mixing at the equator? Is this deep mixing transferred to the surface layers? What is the relation between small-scale turbulent mixing and the large-scale meridional overturning circulation? What are the relative and absolute magnitudes of lateral and vertical mixing and how do they vary spatially?

What is the rate of the conversion of LNADW to MNADW that is occurring near the equator? What are the 3-D pathways, including mixing processes that drive the conversion/upwelling (e.g., sill overflow effects or rough topography tidal mixing), and horizontal pathways (e.g., whether the eastern basin is playing a big role and why)?

Seasonality: What is the physics of the deep seasonal cycles both on and off the equator? We know there is a DWBC annual cycle that may occur for different reasons in different places, how is it forced, and what are the adjustment processes that take place? What is the role of equatorial wave processes? Are the deep cycle and upper ocean response both closely dynamically linked-and related to the large scale Ekman transport?

What are the energy sources of the ubiquitous 60-day deep oscillations that are observed in the WBL and that may also modulate the sill exchanges between major basins? Is this variability local or interconnected among the regions? Why this 60-day periodicity?

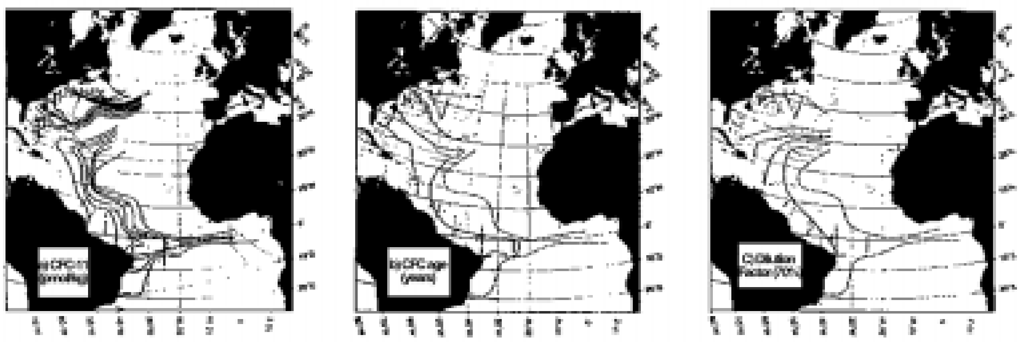

Figure 1. Maps for ULSW of (a) concentration corrected to 1992, age (CFC-11/CFC-12), dilution factor at 70% equilibration (Smethie and Fine, 1999). The dilution factor is calculated by converting CFC ratio derived ages to concentrations using the Northern Hemisphere time history (Walker et al., pers. comm.), and the Warner and Weiss (1985) solubility function at the estimated T-S at time of formation. Dashed curve in Figures (b) and (c) is the 0.02 pmol/kg contour.

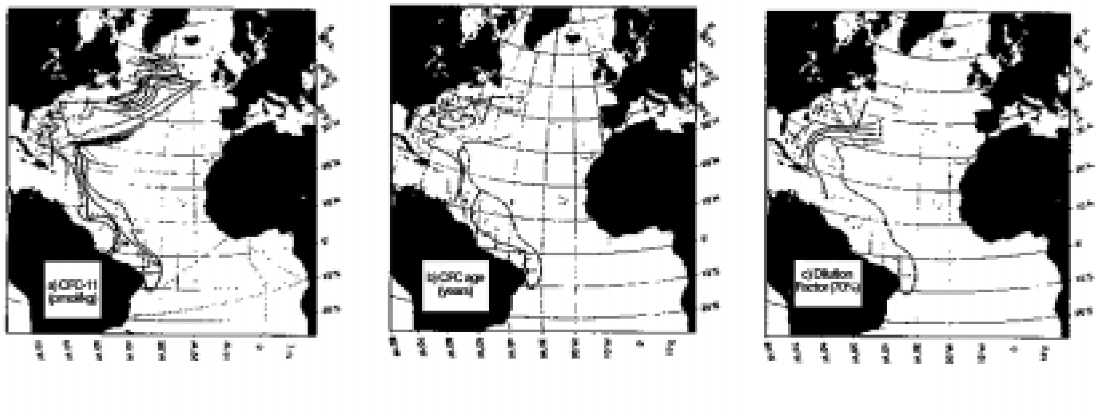

Figure 2. Same as Figure 1 for LNADW.

Biochem: How do extremes in the MOC affect the uptake of CO_2 and biological productivity?

Long-term observations for subtropics and tropics

A purpose of the long-term observations is to assemble a data set that may be used to test and improve models of coupled Atlantic climate variability. The two categories of measurements suggested in the Atlantic Climate Variability Experiment document are appropriate.

(1) The sustained Atlantic wide observing systems in the atmosphere and ocean-these include time series stations and palace floats.

(2) The short term pilot network studies and process studies – these include:

- Re-occupations of key sections with hydrography, current measurements, tracers – inventories and CO_2 – to assess heat and freshwater fluxes, volume changes and formation rates, large scale influences;
- Moored current meter measurements in DWBC of different circulation regimes – temporal variations, dynamics, phase lag of signals; additional stations for monitoring integrated baroclinic transports in the interior.
- Equatorial monitoring strategy to track long-term temperature and transport changes, and confirm seasonality of AABW and NADW.
- Process experiments.

Reference

Warner, M. J., and R. F. Weiss, 1985: Solubilities of chlorofluorocarbons 11 and 12 in water and seawater. Deep-Sea Res., 32A(12), 1485–1497.

Circulation of the tropical Atlantic Ocean

James A. Carton, Department of Meteorology, University of Maryland, USA

The WOCE years have seen a tremendous expansion of observations and theoretical understanding of the tropical Atlantic and its climate. Much of our pre-WOCE understanding was based on successively more concentrated observational programmes examining the mass and momentum fields beginning with the Meteor expeditions of the 1920s followed by GATE and Equalant. These pre-WOCE efforts culminated with the FOCAL/SEQUAL programme of 1982–5, whose goal was to document the seasonal cycle of the upper ocean and lower atmosphere. What they revealed was a very dynamic system with significant year-to-year imposed upon strong seasonal variations.

The interleaving movement of Atlantic water masses characterises the mean circulation of the tropical Atlantic. We won't concern ourselves with the deep circulation here. At mid-depths the temperature and salinity properties of the tropical Atlantic are strongly influenced by the presence of Antarctic Intermediate Water (between the 27.6 and 26.8 σ_θ surfaces). In the western side of the basin the $\sigma = 27.6$ surface occurs near 1000 m depth, while $\sigma = 26.8$ occurs near 250 m depth. At shallower depths high salinity subtropical water is present with somewhat higher salinities for the same density horizon for water of Northern Hemisphere origin. Near-surface water is characterised by reduced salinities due to heavy rainfall as well as Amazon River discharge. The net transport of Southern Hemisphere water northward has been estimated to be approximately 15 Sv.

The strong seasonal cycle present throughout the upper layers of the tropical Atlantic results from the seasonal excursion of the Intertropical Convergence Zone northward and consequent changes in winds, heating, and to a lesser extent, freshwater. Their most striking feature is the appearance in late boreal spring of a zonal ridge-trough variation in the depth of the thermocline (approximately the depth of the 20°C isotherm). The resulting meridional gradient of density leads to a strong eastward flowing North Equatorial Countercurrent spanning much of the basin in a latitude band between 3°N–7°N. This intense thermocline current reaches its maximum speed west of 40°W, gradually decelerating eastward. The seasonal cycle of currents modulates the northward transport of warm water and heat. During boreal winter and spring the northward heat transport across the tropical Atlantic is approximately 1 PW, while by fall there is essentially no cross-equatorial heat transport. A potentially important mechanism for both heat and mass transport northward is the regular production of eddies at the retroflection (beginning) of the North Equatorial countercurrent off Northern Brazil.

The climate of the tropical Atlantic sector is characterised by important long-term changes in rainfall over the surrounding land masses. Studies by Hastenrath in the late 1970s, Hisard, and Moura and Shukla in the early 1980s clearly identified relationships between these changes and patterns of anomalous sea surface temperature. Considerable effort has been expended to identify the causes of these patterns and to determine their relationship to climate variability in the tropical Pacific and midlatitude Atlantic.

An example of the patterns is provided in Fig. 1. This figure, from a recent paper by Ruiz-Barradas et al. (1999) shows the simultaneous spatial patterns of 0/300 m oceanic heat content, surface wind stress, SST, and atmospheric diabatic heating at 500 mb. These patterns have been computed from a combined empirical orthogonal function analysis of historical observations from the UWM-COADS observations, the NCEP re-analysis heating, and the UMD re-analysis heat content.

Interest in characterising and understanding the nature of year-to-year climate variability and its oceanic component has led to an expanded observational array. The observational array began with the Voluntary Observing Ship programme and received a key expansion with the WOCE PALACE float drifting buoys and of course the TOPEX/POSEIDON altimetry. The PALACE floats provide vertical profiles of temperature and in some cases salinity. In the last couple of years the array has expanded with the addition of PIRATA moorings. The PIRATA moorings are instrumented with thermistor chains to 500 m as well as surface meteorological instrumentation.

Future

Many key problems in tropical Atlantic circulation involve coupled interaction between the atmosphere and ocean. There is, for example, significant evidence of the existence of coherent modes of variability, as well as evidence of remote influence. Climate variability in the tropical Atlantic has potentially vast consequences. One example of the latter is the destruction associated with Atlantic hurricanes, which in turn depend sensitively on warm sea surface temperatures in the northern tropics.

A major factor limiting progress on tropical Atlantic variability has been the absence of observations. The

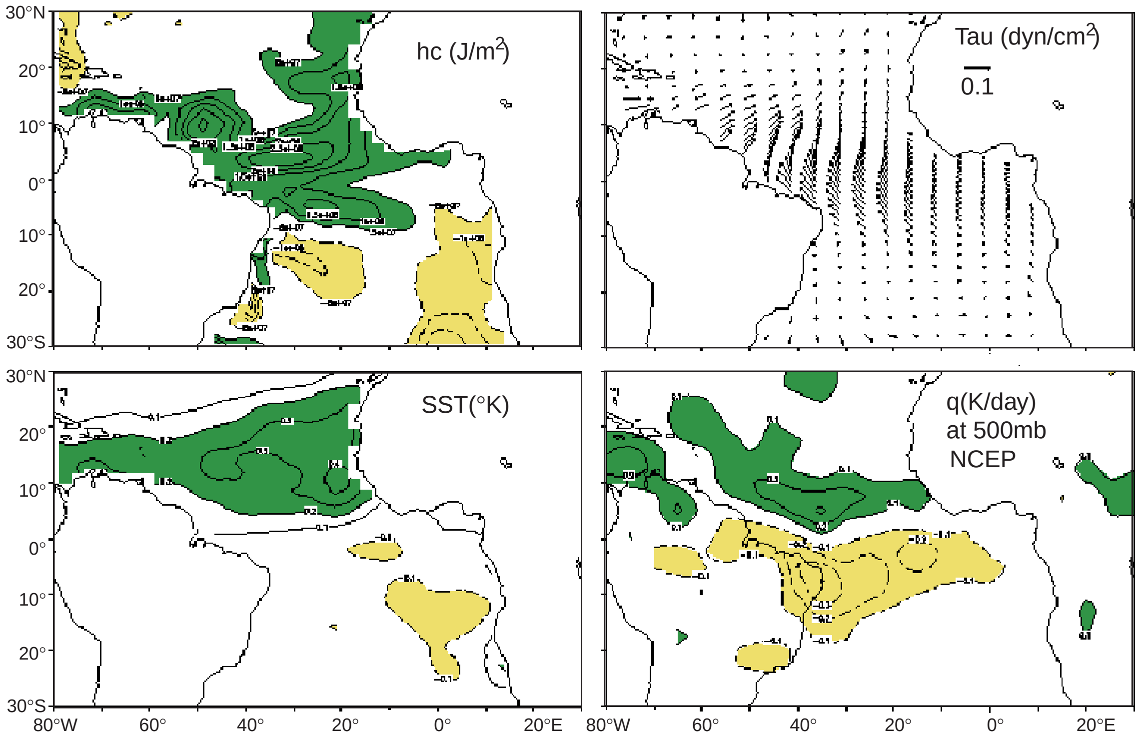

Figure 1. First rotated empirical orthogonal eigenfunction of the combined winds, SST, ocean heat content, and 500 mb diabatic heating based on the full 1957–93 data set from Ruiz-Barradas et al. (1999).

expanding observational array has addressed this problem. Further progress now requires a better theoretical framework to direct observational studies. We can anticipate efforts in this direction in the coming few years.

Reference

Ruiz-Barradas, A., J. A. Carton, and S. Nigam, 1999: Coupled modes in the tropical Atlantic. J. Clim., accepted.

2.3 Thermohaline overturning and flux divergences

Overview of the problem of flux divergences from inverse calculations

Carl Wunsch, Massachusetts Institute of Technology, USA

There are at least three methods for calculating from data the flux divergence of heat energy in the ocean: (1) bulk formulae, (2) atmospheric residuals, (3) direct estimates from the ocean circulation. Others will speak at the meeting about (1) and possibly (2). In reviewing the status of (3), it emerges that we have gradually become more sophisticated over the past 20 years, moving from coarse resolution, linear methods to high density, sometimes non-linear methods, with emerging estimates from full general circulation models. There are now many estimates of the oceanic flux divergence to the atmosphere from all of (1–3). In making comparisons with (3), which I will define as primarily derived from “inverse methods”, one is greatly handicapped by the absence of real error bars for many of the calculations. But the various inverse estimates are gradually converging and the major emerging issues appear to lie with what is probably best regarded as systematic, rather than random, error, and with serious questions about the accuracy of the atmospheric wind fields which govern Ekman components.

Many of these systematic errors appear to lie with the assumption that any particular section can represent the zonal average, particularly at low latitudes, and the related question as to whether estimates based upon climatological hydrography can represent those averages. Experiments with GCMs suggest that the error budgets for the synoptic section approach are considerably larger than previously believed.

The problems of other flux divergences (fresh water, nutrients, oxygen, carbon…) are of equal or greater difficulty. The uncertainties of these results appear to depend directly upon rather subtle understanding of the error budgets of the various properties (e.g., how errors in salinity constraints are related to those in mass constraints).

Remaining almost unexploited for the divergence calculations are the WOCE meridional sections, of which there are a few that could be obtained, and in a very general sense, the transient tracer data remain almost unused. Transient tracers raise some interesting mathematical issues, as the inverse problem for oceanic flow appears to be intrinsically non-linear in contrast to that for steady tracers (in steady flows in both cases). It appears however, that they can be used and may perhaps provide important clues to the systematic errors alluded to above.

Ultimately, probably the best estimates of oceanic flux divergences of all types will come from fully assimilated oceanic general circulation models, but direct use of hydrographic data in these models presents computational difficulties owing to the very long time scale of adjustment to surface boundary conditions.

Fluxes of heat, freshwater, oxygen and nutrients in the North Atlantic from a new global inversion

Alexandre Ganachaud, MIT/WHOI Joint Program, USA. ganacho@mit.edu

One of the motivations for the WOCE programme was to compute global budgets of quantities important to climate. In this study a new, global inversion is used to diagnose fluxes and flux divergences of heat, freshwater, oxygen and nutrients. A linear inverse “box” model is used to combine consistently transoceanic sections, mostly from the WOCE programme. The circulation is geostrophic with an Ekman layer at the surface. Oceanic layers are defined by neutral surfaces. Near conservation of mass, salt and top-to-bottom silica is required and, in addition, heat and the phosphate-oxygen combination ($170[PO_4]+[O_2]$) are conserved in layers that are not in contact with the surface. A solution is sought for a depth-independent adjustment to the thermal wind field, freshwater flux divergences, a correction to the Ekman transport, and the advective and diffusive dianeutral fluxes between layers. The Gauss-Markov method is used to obtain a global estimate of the circulation. The uncertainties take into account both the non-resolved part of the solution and the systematic errors due

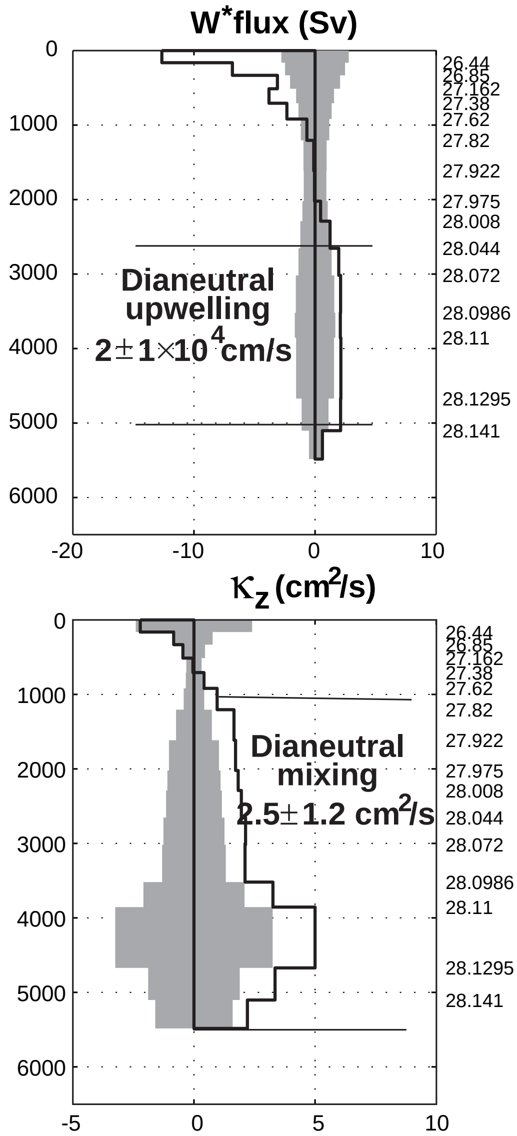

Figure 1. Dianeutral advection and diffusivities in the North Atlantic between 24°N and 48°N. The line indicates the value at the base of each layer. The uncertainty is indicated by the shaded area (one standard deviation).

to the temporal oceanic variability. The meridional overturning shows a southward flow of 14±2 Sv of North Atlantic Deep Water at 48°N and 17±2 Sv at 24°N. Through the use of anomaly equations and the stability of the circulation in the deep layers, dianeutral exchanges are well resolved, indicating an average upwelling of $2 \pm 1 \times 10^{-4}\,\mathrm{cm/s}$ and a diffusivity of $2.5 \pm 1\,\mathrm{cm}^2/\mathrm{s}$ below 2000 dbars (Fig. 1), which are representative of the global average upwelling and diffusivity.

Through the anomaly formulation, tracer divergences are corrected from spurious mass divergences. Energy transports indicate a cooling of the ocean of 0.5±1 PW $(\times 10^{15}\,\mathrm{W})$ between 24°N and 48°N, and a further cooling of 0.56±0.1 PW north of 48°N, while the central Atlantic (30°S to 24°N) indicates a warming of 0.8±0.2 PW. Both warming and cooling are in rough agreement with the conflicting climatology in the Atlantic. No significant freshwater flux is found between 24°N and 48°N (0±0.15 Sv). Previous studies suggested evaporation over this same region, between 0.1 and 0.3 Sv (Macdonald and Wunsch, 1996; Wijffels et al., 1992), thus compatible within two standard deviations with our result. Oxygen and nutrient fluxes and residuals are analysed. From the export production that is associated with biological activity, a sink of dissolved nutrients is expected in the surface layers through consumption and a source in the subsurface layers through remineralisation. However, in the North Atlantic between 24°N and 48°N, a source of nitrate and phosphate is found in the surface layers. The nitrate source is equivalent to $2.3 \pm 0.7\,\mathrm{mol\,C / m^2\,yr}$ while the phosphate source is of $1.5 \pm 0.7\,\mathrm{mol\,C / m^2\,yr}$ thus in Redfield proportions within uncertainties. Such a nitrate source was found in this region by Rintoul and Wunsch (1991). Three possible explanations to this source are suggested:

- advection of dissolved organic matter into the box (i.e., Rintoul and Wunsch, 1991);
- alias of the seasonal cycle in the Ekman transport of nutrients Williams and Follows (1998);
- variability in the nutrient advective fluxes in the upper layers.

Over this same region, there is a net source of oxygen of $1.4 \pm 0.3\,\mathrm{mol\,O_2 / m^2\,yr}$ qualitatively consistent with the cooling that lowers the oceanic partial pressure of oxygen. This study suggests that there is a lack of knowledge about the variability in the advective nutrient fluxes. In particular, it would be useful to monitor the seasonal variations in nutrient concentration in the upper ocean which is affected by seasonal density variations. In addition, there is a lack of recent data across 36°N in the Atlantic, due to at-sea problems during the Russian hydrographic section, and a modern survey is desirable in this region. Simultaneous nutrient and CTD measurements in the Florida Strait are missing during the WOCE period too. Determination of the circulation, heat and nutrient fluxes has been generally based upon zonal and meridional hydrographic surveys. However, heat and primary productivity maps suggest that in many regions the patterns are non-zonal, and a survey could be designed so that it optimises the determination of ocean-atmosphere exchanges.

References

Macdonald, A. M., and C. Wunsch, 1996: An estimate of global ocean circulation and heat fluxes. Nature, 382(6590), 436–439.

Rintoul, S. R., and C. Wunsch, 1991: Mass, heat, oxygen and nutrient fluxes and budget in the North Atlantic Ocean. Deep-Sea Res., 38, Suppl., 355–377.

Wijffels, S. E., R. W. Schmitt, and H. L. Bryden, 1992: Transport of freshwater by the oceans. J. Phys. Oceanogr., 22, 155–162.

Williams, R. G., and M. J. Follows, 1998: The Ekman transfer of nutrients and maintenance of new production over the North Atlantic. Deep-Sea Res., 45(2–3), 461–489.

Seasonal variability of the meridional heat transport and meridional overturning cell

Herlé Mercier, Laboratoire de Physique des Océans, CNRS/IFREMER/UBO, France.

WOCE hydrographic sections are being analysed using inverse models which give estimates of either the circulation at the time of the cruise (synoptic or regional inverse models, e.g. Lux et al., 1999) or the averaged circulation over the observing period (global models, e.g. Ganachaud 1999). None of these models resolve the seasonal cycle. Here, we use an inverse model based on temperature and salinity climatologies to estimate the seasonal cycle of the meridional overturning cell and heat transport in the Atlantic north of 20°S.

The inverse model has been adapted by Larnicol (1998) from Mercier et al.'s (1993) finite difference inverse model. The model resolution is 3° in longitude and 2° in latitude. Hydrographic data are from Reynaud's (1998) Atlas, wind stresses and air–sea heat fluxes from ECMWF. The model satisfies exactly the thermal-wind balance. The Ekman transport in the surface layer is diagnosed from the wind stresses. The model is constrained by mass, heat, and salt conservations and the large-scale vorticity balance. An estimate of the circulation for each season is calculated.

In inverse models, the heat constraint is usually written as a balance between the heat transport divergence and the air-sea heat flux. However, on seasonal time scale, the time change of heat contain is not negligible. Thus, this quantity was added in the heat balance of Larnicol's (1998) inverse model and estimated from Reynaud's climatology.

The total meridional heat transport and the Ekman contribution to the meridional heat transport as diagnosed by the inverse model are presented in Fig. 1 as a function of latitude. A seasonal variability in the heat transport is apparent south of 30°N. A maximum northward heat transport of about 1.5 PW is obtained around 10°N both in fall and winter. At the same latitude, the heat transport falls approximately to zero in summer. This variation is correlated to the change in the Ekman contribution to the meridional heat transport. Similar results were obtained by Böning and Herrmann (1994) but using a prognostic model. The geostrophic circulation contribution to the meridional heat transport (the difference between the total and Ekman meridional heat transports of Fig. 1) varies seasonally in the tropics. Böning and Herrmann (1994) have shown that the seasonal variability of the meridional heat transport in the tropical Atlantic was directly related to that of the meridional overturning cell. Our diagnostic model shows similar results with maximum meridional overturning cell transport in the tropics in fall and winter.

As part of the French contribution to WOCE, zonal hydrographic lines were conducted at 7.5°N and 4.5°S in January–March 1993. A regional box inverse model was built to estimate transports of mass and heat across these two lines (Lux et al., 1999). The estimates of heat transport are 1.35 PW at 7.5°N and 1.09 PW at 4.5°S and agrees well with those of Larnicol (1998) for winter (Fig. 1). Sensitivity studies show that heat transport estimates vary in the range 1.26–1.50 PW at 7.5°N and 0.97–1.29 PW at 4.5°S and thus are only moderately sensitive to the a priori hypotheses and errors in the data.

In the equatorial Atlantic Ocean, the deep circulation is characterised by a conversion of Lower Deep Water into Middle Deep Water (Friedrichs et al., 1994). The inverse model correctly diagnosed this conversion, but shows that its amplitude is quite sensitive to the a priori estimate of the vertical diffusivity in the deep layers. Our best estimate of this conversion is 11 Sv. It is obtained by setting the a priori value of the vertical diffusivity in the deep layers of the

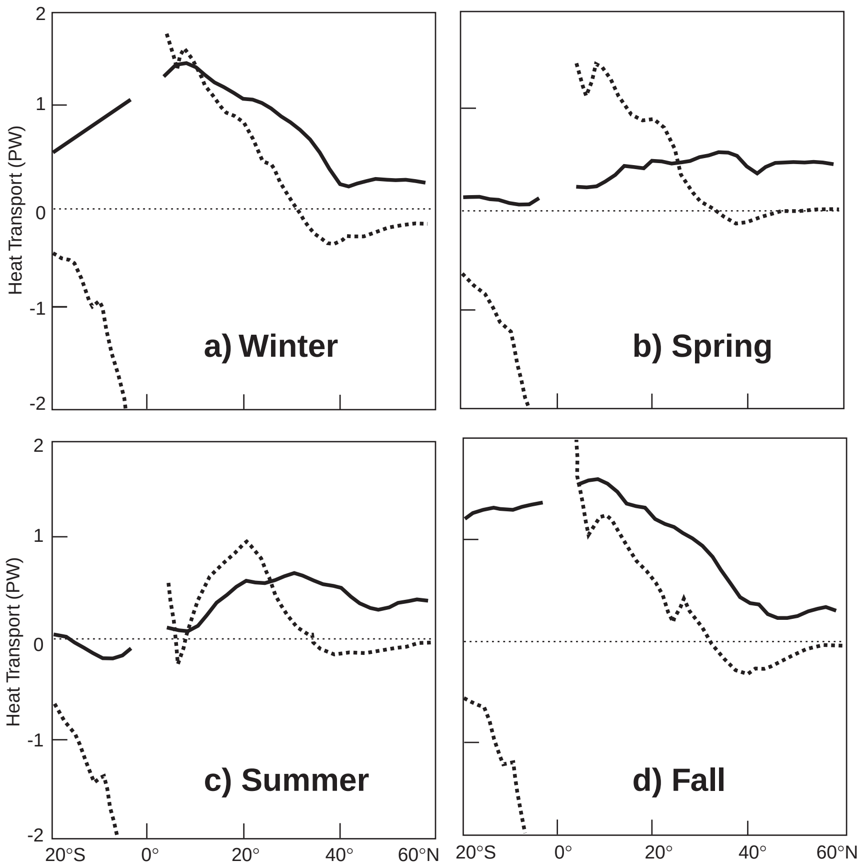

Total meridional heat transport (continuous line) and Ekman contribution to the heat transport (dotted line) as estimated by the finite difference inverse model. (a) Winter (b) Spring (c) Summer (d) Fall.

model to 10×10^{-4} m^2 s^{-1} as suggested by recent indirect estimates given by Ferron et al. (1998) for the Guinea and Sierra Leone basins.

References

Böning, C. W., and P. Herrmann, 1994: Annual cycle of poleward heat transport in the ocean: results from high-resolution modeling of the North and Equatorial Atlantic. J. Phys. Oceanogr., 24, 91–107.

Ferron, B., H. Mercier, K. Speer, K. Polzin, and A. Gargett, 1998: Mixing in the Romanche Fracture Zone. J. Phys. Oceanogr., 28, 1929–1945.

Friedrichs, M. A., M. McCartney, and M. S. Hall, 1994: Hemispheric asymmetry of deep water transport modes. J. Geophys. Res., 99, 25165–25179.

Larnicol, G., 1998: Analyse de la variabilité de l'Océan Atlantique à partir des données altimétriques TOPEX/POSEÏDON et d'un modèle inverse nonlinéaire. PhD thesis, Université de Bretagne Occidentale. Available from Laboratoire de Physique des Océans, Plouzané, France.

Lux, M., H. Mercier, and M. Arhan, 1999: Interhemispheric exchanges of mass and heat in the Atlantic Ocean in January–March 1993. Deep-Sea Res., submitted.

Reynaud, T., P. LeGrand, H. Mercier, and B. Barnier, 1998: A new analysis of hydrographic data and its application to an inverse modelling study. Int. WOCE Newsl., 32, 29–31.

Remarks on meridional transports in ocean models

Jochem Marotzke, Massachusetts Institute of Technology, USA/Southampton Oceanography Centre, UK

Of the various transports of properties by the ocean circulation, the focus has mostly been on the transport of energy, because of its direct influence on sea surface temperature (SST), ocean-atmosphere energy exchange, and climate. However, the community should extend its focus toward:

- Meridional freshwater transport, with its impact on high-latitude salinity, convection, and the large-scale circulation and energy transport. Although this has long been recognised as important, observational estimates of meridional freshwater transport are far less common than those for energy.
- Meridional transport of carbon, with its impact on ocean-atmosphere CO_2 exchange and the radiative forcing of climate.
- Meridional transports of nutrients, which influence the carbon cycle through the biological pump where nutrients are rate-limiting.

Notice that the ocean-atmosphere CO_2 exchange provides a climatically crucial ocean-atmosphere coupling that is NOT exclusively mediated through SST. Hence, there exists a parallel coupling strand, the dynamics of which have remained largely unexplored (see, however, Joos et al., 1999). In contrast to temperature, the maxima in carbon and nutrient concentrations typically occur far away from the sea surface, which immediately makes the deep circulation crucial for climate change. The area of research thus defined should lead to a convergence of interests that were previously either in oceanography or in climate.

Time-mean energy transport

Recent high-resolution (eddy-permitting) Atlantic and global model solutions (The DYNAMO Group, 1997; Parallel Ocean Climate Model, POCM, of B. Semtner and R. Tokmakian, see Jayne, 1999) show quite good agreement with estimates based on observations (e.g., A. Ganachaud, pers. comm., 1999). Major questions arise concerning the models' capability to simulate the mid-latitude convergence of energy transport and resulting loss to the atmosphere, and concerning the influence of the rest of the World Ocean on Atlantic energy transport (incorporated in regional models through southern boundary conditions).

Variability

Jayne (1999) has drawn on previous modelling work of Bryan (1982), Böning and Herrmann (1994), and Lee and Marotzke (1998); the theoretical work of Willebrand et al. (1980) on the ocean's response to wind fluctuations, Schopf's (1980) analogous analysis for low latitudes, Gill's (1980) theoretical model of (among others) equatorial wind fluctuations; and the observational angular momentum analyses of Rosen et al. (1990) and Ponte et al. (1998); to synthesise a reasonably complete theory of seasonal wind-induced heat transport variability. On seasonal and shorter timescales, heat transport variability is dominated by Ekman transport variability and barotropic compensation, as formulated by Bryan (1982) and confirmed in POCM.

Sensitivity and monitoring

In numerical modelling, very often the question arises how a central element of the model solution, such as the strength of the meridional overturning circulation (MOC) or maximum meridional heat transport, depends on the various independent parameters that enter the simulation, such as surface forcing, initial conditions, or diffusion parameters. Typical sensitivity calculations vary one parameter or one group of parameters at a time, which is not very efficient as the number of input parameters grows large. In contrast, the "adjoint" of a model calculates the sensitivity of one output variable, simultaneously to all input variables. Marotzke et al. (1999) have used R. Giering's "Tangent-Linear and Adjoint Model Compiler"

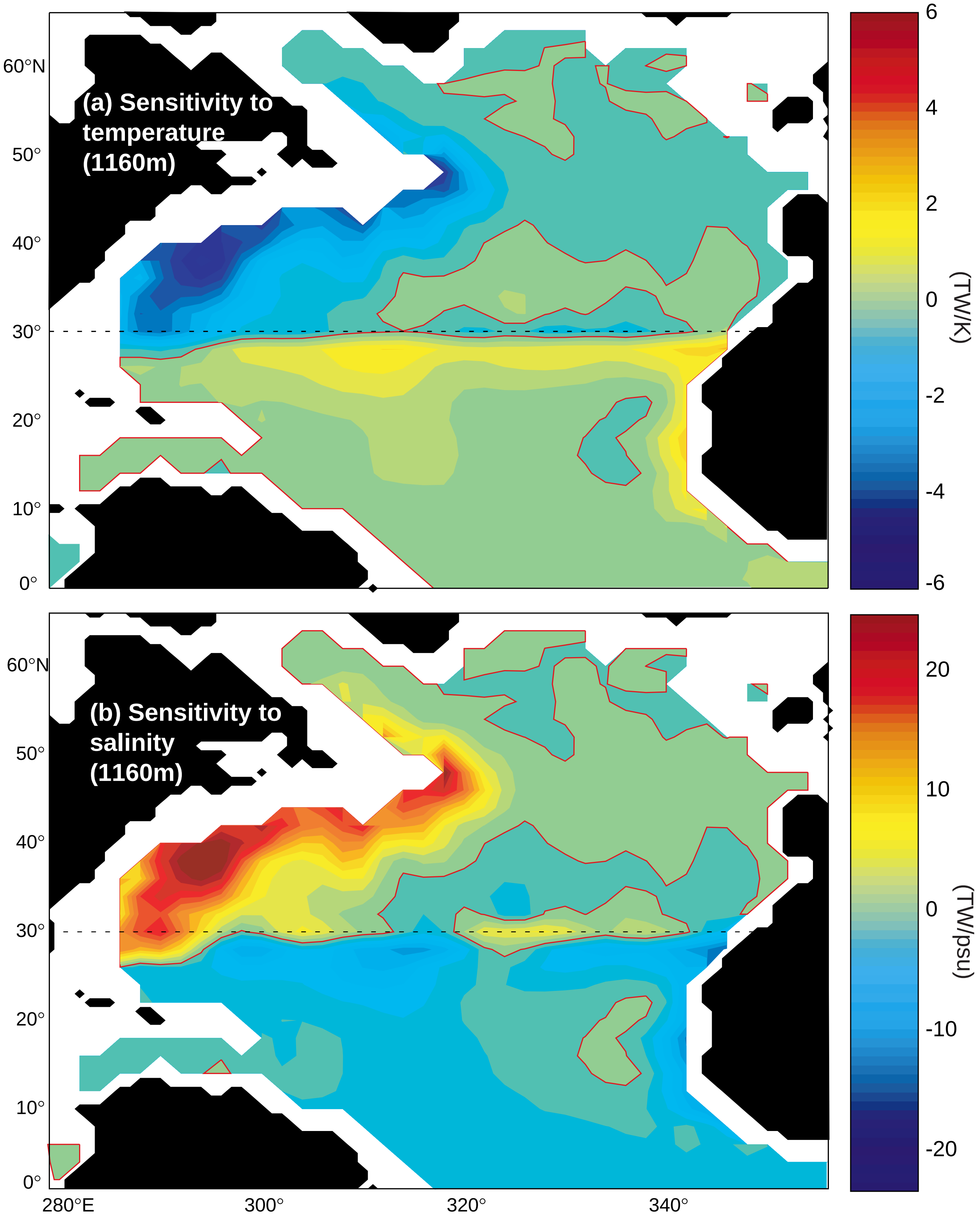

Figure 1. (a) Sensitivity of mean 1993 Atlantic heat transport across 29°N (dotted line), to temperature at 1160 m, on 1 January 1993. Contour interval is 0.5×10^{12} W / K, and the zero contour is drawn in red. (b) Sensitivity of mean 1993 Atlantic heat transport across 29°N (dotted line), to salinity at 1160 m, on 1 January 1993. Contour interval is 2×10^{12} W / psu, and the zero contour is drawn in red (from Marotzke et al., 1999).

(TAMC; Giering and Kaminski, 1998) to create the adjoint to the ocean general circulation model (GCM) of Marshall et al. (1997a,b). A particular application based on the global data assimilation solution of Stammer et al. (1997) for year 1993 is given in Fig. 1. It shows the sensitivity of mean 1993 Atlantic heat transport across 29°N, to temperature and salinity at 1160 m, on 1 January 1993. Most notable is the influence of density anomalies arising from as distant as the Labrador Sea, and its concentration on the zonal boundaries. This latter property is consistent with the concept that the MOC is in thermal-wind balance with the zonal density drop, and suggests that monitoring of the MOC by way of density observations near the boundaries should be a feasible strategy.

References

DYNAMO Group, The, 1997: DYNAMO: Dynamics of North Atlantic Models: Simulation and assimilation with high resolution models. Ber. Inst. Meeresk., 294, 334 pp.

Böning, C. W., and P. Herrmann, 1994: Annual cycle of poleward heat transport in the ocean: results from high-resolution modeling of the North and Equatorial Atlantic. J. Phys. Oceanogr., 24, 91–107.

Bryan, K., 1962: Measurements of meridional heat transport by ocean currents. J. Geophys. Res., 67, 3403–3414.

Giering, R., and T. Kaminski, 1998: Recipes for adjoint code construction. Association for Computing Machinery Transactions on Mathematical Software, 24(4), 437–474.

Gill, A. E., 1980: Some simple solutions for heat-induced tropical circulation. Q. J. R. Meterol. Soc., 10–462.

Jayne, S. R., 1999: The Dynamics of Global Ocean Heat Transport Variability. PhD thesis, 169 pp, MIT-Woods Hole Joint Program in Oceanography.

Joos, F., G.-K. Plattner, T. F. Stocker, O. Marchal, and A. Schmittner, 1999: Global warming and marine carbon cycle feedbacks on future atmospheric CO_2. Science, 284, 464–467.

Lee, T., and J. Marotzke, 1998: Seasonal cycles of meridional overturning and heat transport of the Indian Ocean. J. Phys. Oceanogr., 28, 923–943.

Marotzke, J., R. Giering, K. Q. Zhang, D. Stammer, C. Hill, and T. Lee, 1999: Construction of the adjoint MIT ocean general circulation model and application to Atlantic heat transport sensitivity. J. Geophys. Res., in press.

Marshall, J., A. Adcroft, C. Hill, L. Perelman, and C. Heisey, 1997a: A finite volume, incompressible Navier Stokes model for studies of the ocean on parallel computers. J. Geophys. Res., 102, 5753–5766.

Marshall, J., C. Hill, L. Perelman, and A. Adcroft, 1997b: Hydrostatic, quasi-hydrostatic and non-hydrostatic ocean modeling. J. Geophys. Res., 102, 5733–5752.

Ponte, R. M., D. Stammer, and J. Marshall, 1998: Oceanic signals in observed motions of the Earth's pole of rotation. Nature, 391, 476–479.

Rosen, R. D., D. A. Salstein, and T. M. Wood, 1990: Discrepancies in the Earth–atmosphere angular momentum budget. J. Geophys. Res., 95, 265–279.

Schopf, P. S., 1980: The role of Ekman flow and planetary waves in the oceanic cross-equatorial heat transport. J. Phys. Oceanogr., 10, 330–341.

Stammer, D., C. Wunsch, R. Giering, Q. Zhang, J. Marotzke, J. Marshall, and C. Hill, 1997: The global ocean circulation estimated from TOPEX/POSEIDON altimetry and a general circulation model. Center for Global Change Science Report No. 49, 40 pp, MIT.

Willebrand, J., S. G. H. Philander, and R. C. Pacanowski, 1980: The oceanic response to large-scale atmospheric disturbances. J. Phys. Oceanogr., 10, 411–429.

The export of Atlantic water to the Nordic Seas

Bogi Hansen, Faroe Islands, bogihan@frs.fo; Svein Østerhus, Norway; Bill Turrell, Scotland; Steingrímur Jónsson, Iceland

Together with parts of the Nordic Seas, the north-eastern part of the North Atlantic is much warmer in the surface layers than waters elsewhere at similar latitudes. This is mainly ascribed to the heat carried with the warm, saline water from the Atlantic across the Greenland–Scotland Ridge into the Nordic Seas. Detailed knowledge of the export is therefore necessary to provide boundary conditions for numerical models of the upper layer flows in the north Atlantic. After crossing the ridge, a large part of the exported Atlantic water is furthermore converted to intermediate and deep water in the northern areas and returns to the Atlantic in the form of overflow across the ridge. The characteristics of the exported Atlantic water, especially its salinity, will influence these processes considerably.

The northward export of Atlantic water occurs through three separate branches (Fig. 1) which differ in their origin and water mass characteristics and also deliver their heat and salt content to different areas north of the Ridge where different processes may dominate in the formation of the overflow waters (Hansen and Østerhus, in press).

Of the three branches, the one west of Iceland has been monitored by Icelandic oceanographers and its volume transport of Atlantic water is estimated to be on the order of 1 Sv (Kristmannsson, 1998). The Nordic WOCE project had as one its main aims to determine the fluxes of the other two branches. This effort involved establishing 8 quasi-permanent ADCP mooring sites along two standard sections that have been monitored regularly with CTD observations for many years.

The observation system, established during Nordic WOCE, has been continued within the VEINS programme, and the acquired dataset allows calculation of the fluxes of water, heat and salt carried by the Atlantic water in the two main branches (Hansen et al., 1999). The preliminary results

(Fig. 1) indicate that the Faroe–Shetland Channel dominates over the branch north of the Faroes, but still carries less than 50% of the total volume transport. Since the Atlantic water in the Faroe–Shetland Channel is warmer and saltier than the other branches, this pathway is more important in terms of heat and salt transport.

In the Faroe–Shetland Channel, seasonal variation is seen in the Atlantic water flux over the Scottish slope, but the reverse flow on the Faroe side of the channel varies with about the same amplitude and phase. The net flow through the Faroe–Shetland Channel therefore does not seem to have a large seasonal variation. The branch north of the Faroes does seem to carry somewhat less Atlantic water in late summer and autumn than in spring, but this is the opposite seasonal variation to that seen for the branch passing west of Iceland. The preliminary estimates therefore do not indicate a large seasonal variation in the total volume flux of exported Atlantic water.

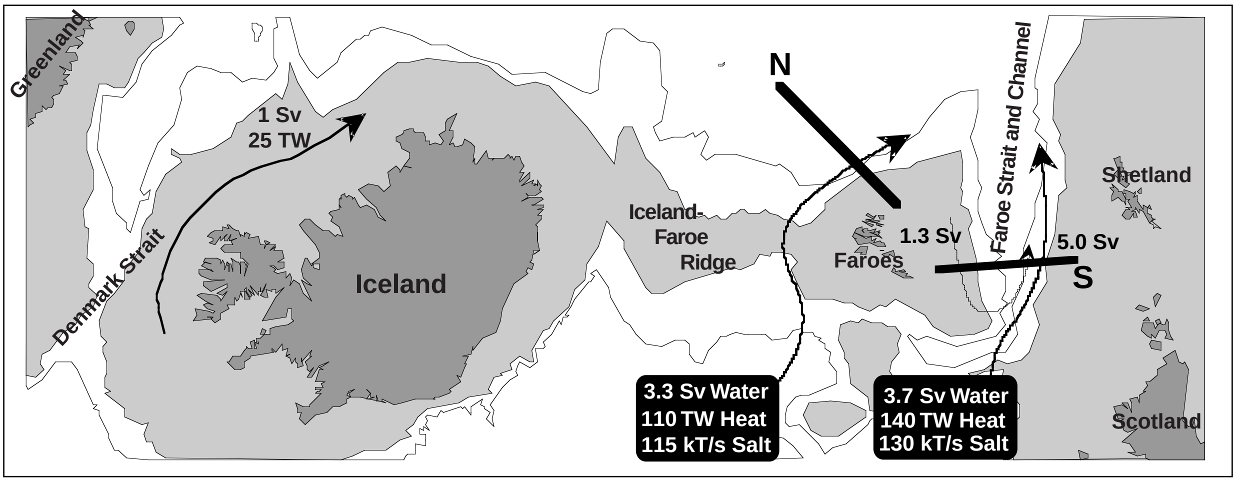

Figure 1. The export of Atlantic water into the Nordic Seas is carried by three branches. Thick lines, labelled N and S, indicate sections across the two main branches which have been monitored with CTD cruises and ADCP moorings in the Nordic WOCE and VEINS projects. The numbers indicate fluxes of water (in SV = 10^6 m^3 / s), heat (in TW = 10^{12} / W), and salt (kiloTonnes per second) for the different branches. In the Faroe–Shetland Channel there is a reverse flow towards the Atlantic on the Faroe side of the channel which reduces the total export through the channel.

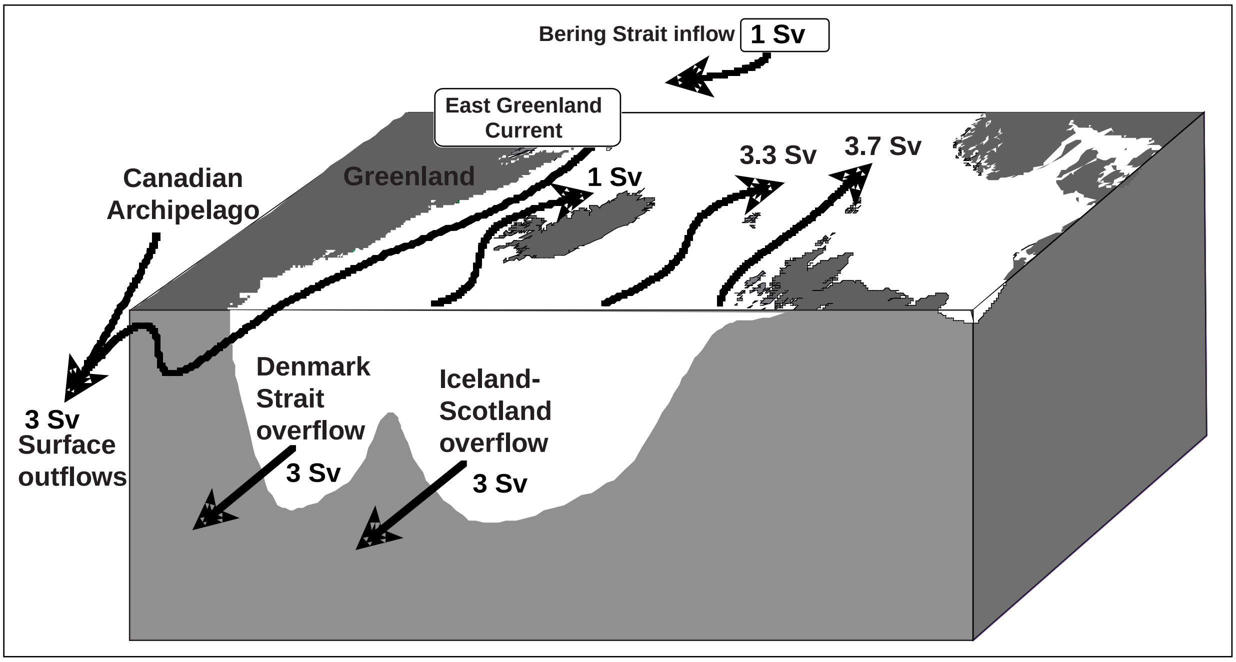

Figure 2. The water budget of the Arctic Mediterranean.

Combining the estimates of the Atlantic water flux with other flux estimates, a budget is found for the Arctic Mediterranean (Nordic Seas and Arctic Ocean) which is close to that suggested by Worthington (1970) although the flow details differ considerably (Fig. 2). In this budget, two thirds of the total inflow and 75% of the Atlantic water export is returned to the Atlantic through the thermohaline loop of the overflows. This, together with the lack of seasonal variation, indicates that the formation of intermediate and deep waters in the Arctic Mediterranean may be more important in driving the Atlantic water export than the direct effect of the wind stress.

References

Hansen, B., K. M. H. Larsen, S. Østerhus, B. Turrell, and S. Jónsson, 1999: The Atlantic Water inflow to the Nordic Seas. Int. WOCE Newsl., 35, 33–35.

Hansen, B., and S. Østerhus, North Atlantic–Norwegian Sea Exchanges. Prog. Oceanogr., accepted

Kristmansson, S. S., 1998: Flow of Atlantic Water into the northern Icelandic shelf area, 1985–1989. ICES Cooperative Research Report No. 225, 124–135.

Worthington, L. V., 1970: The Norwegian Sea as a Mediterranean basin. Deep-Sea Res., 17, 77–84.

Surface heat fluxes and wind stress forcing in the North Atlantic

S. A. Josey, E. C. Kent and P. K. Taylor, Southampton Oceanography Centre, UK.
Simon.A.Josey@soc.soton.ac.uk

The climatological surface heat flux and wind stress forcing of the North Atlantic is reviewed in this paper. In the first section, the various sources of information regarding the flux fields are discussed and the limitations of each considered. Methods by which the accuracy of the surface fluxes may be ascertained are then discussed together with the problems associated with adjusting the heat exchange in order to satisfy ocean heat transport constraints. In the final section, a comparison of the wind stress forcing of the basin during the WOCE period, as represented by the Southampton Oceanography Centre (SOC) climatology, is made with the longer time base climatology of Hellerman and Rosenstein (1983).

Surface flux fields may be determined from three sources: ship meteorological reports, atmospheric model output and satellite observations. Ship based estimates of the fluxes have been obtained from routinely reported meteorological variables using various semi-empirical formulae in a number of studies (e.g. the University of Wisconsin-Milwaukee/Comprehensive Ocean-Atmosphere Data Set (UWM/COADS) climatology, da Silva et al., 1994). The main disadvantage of this approach is the uneven distribution of ship reports which leads to low sampling rates in the tropics and at high latitudes. In addition, it is necessary to correct for various observational biases (Kent et al., 1993) as these can give

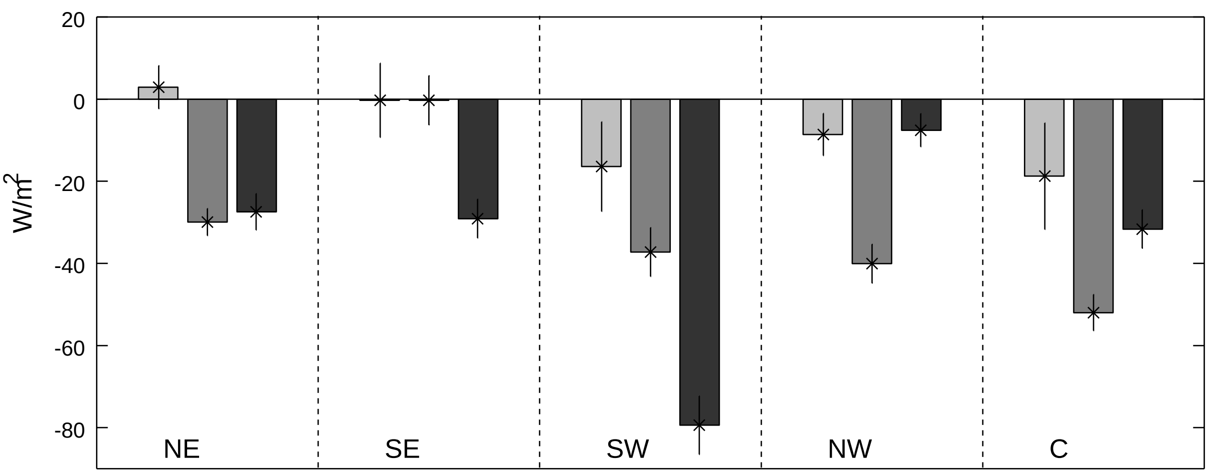

Figure 1. Bar chart representation of the difference (units Wm^{-2}) between the SOC (light grey), ERA (intermediate grey) and NCEP/NCAR (dark grey) buoy net heat fluxes from the Subduction Buoy deployment means at each of the five buoy deployment sites (NE, SE, SW, NW, C). Negative values imply the buoy measures greater ocean heat gain than the comparison dataset estimate.

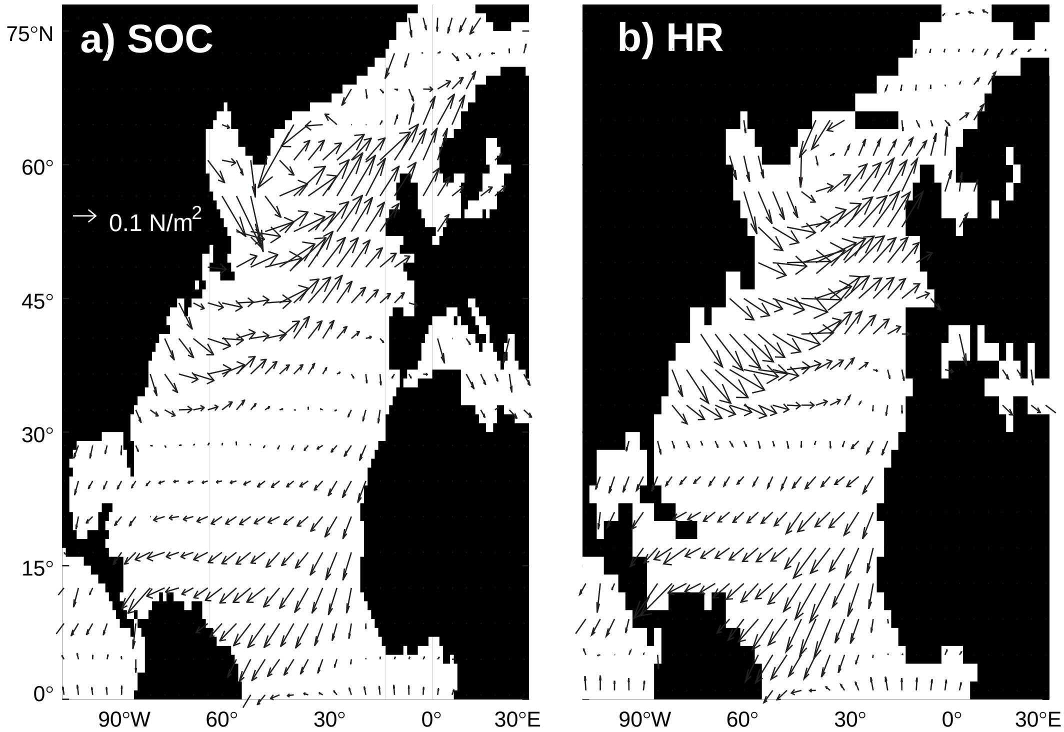

Figure 2. Climatological mean fields for January of the wind stress in the North Atlantic: (a) SOC; (b) HR.

rise to errors of order 10 Wm^{-2} in the monthly mean in either direction (i.e. both enhanced and reduced net heat exchange) which have a complex spatial dependence (Josey et al., 1999). Corrections for these effects have been included for the first time in the Southampton Oceanography Centre (SOC) flux climatology (Josey et al., 1998).

Surface flux fields are also available from various atmospheric models which assimilate reported observations, in particular the re-analysis programmes at the National Center for Environmental Prediction/ National Center for Atmospheric Research (NCEP/ NCAR) and European Centre for Medium Range Weather Forecasting (ECMWF). The advantage of this data source is the uniform spatial coverage and much higher temporal resolution than is possible with ships. However, uncertainties remain in the model physics particularly with regard to the representation of cloud which can give rise to significant shortwave biases.

Satellite observations of cloud cover have been used in radiative transfer models to determine the surface shortwave flux (e.g. Rossow and Zhang, 1995) while estimates of the latent heat flux to an accuracy of 15 Wm^{-2} in the monthly mean are possible using satellite retrieved sea surface temperature and near surface wind speed and humidity (Schulz et al., 1997). Satellites offer greatly improved spatial coverage relative to ships. However, it is not yet possible to accurately retrieve certain surface fields particularly the air temperature which is a key parameter for determining the sensible heat flux and in stability calculations. Finally, surface fluxes may also be obtained as a residual from satellite top of the atmosphere radiative fluxes and atmospheric model heat flux divergences (Trenberth and Solomon, 1994; Keith, 1995) with an inferred accuracy of order 30 Wm^{-2} at 1000 km scales.

North Atlantic annual mean surface net heat flux fields from several climatologies (SOC, UWM/COADS, NCEP/NCAR and ECMWF) are compared. Although qualitatively similar the ship based fields tend to exhibit a net ocean heat gain which is about 30 Wm^{-2} stronger than the re-analysis fields. The implied ocean heat transport for each of the climatologies is compared with hydrographic estimates. The re-analyses transports are in reasonable agreement with the hydrographic values, the ECMWF transport being about 1.0 PW at 20°N. The ship based transport estimates diverge from hydrography with the implication that the surface fluxes are biased towards too much heat gain by the ocean. The heat transport from the version of the UWM/COADS fields that has been adjusted (primarily through a global increase in the latent heat loss by 13% and a reduction in the shortwave by 8%) to satisfy the constraint of zero global mean net heat flux (da Silva et al., 1994) is in good agreement with the hydrographic values.

Assessing the accuracy of heat flux climatologies via the integrated heat transport has the disadvantage that it is difficult to ascertain where the errors arise. Comparisons of the SOC area mean net surface heat flux have been made with hydrographic values for regions that are bound by section estimates (Josey et al., 1999). With this approach regional biases may be identified and it appears that the primary source of error in the ship based estimates in the North Atlantic is an underestimate of the heat loss by of order $50\,Wm^{-2}$ in the annual mean at mid-latitudes.

Large-scale evaluations of surface fluxes should be supplemented by local comparisons against high quality flux measurements from research buoys where available. Results are presented from a comparison with measurements made at the Subduction Buoy array site in the East Atlantic (Moyer and Weller, 1997). The SOC net heat fluxes agree with the Subduction Buoy values to within $15\,Wm^{-2}$ (Fig. 1) which implies that the mid-latitude bias noted above occurs primarily in the western half of the basin. In contrast, the NCEP/NCAR and ECMWF re-analyses underestimate ocean heat gain by $30 - 50\,Wm^{-2}$ at the Subduction Buoy array. Thus, although the reanalysis products provide a reasonable description of the large scale ocean heat transport they appear to contain significant regional biases.

Adjusting the SOC fluxes as suggested by da Silva et al. (1994) leads to underestimates of the ocean heat gain at the various Subduction Buoys by $25 - 50\,Wm^{-2}$. In contrast, limited comparisons with measurements made at the FASINEX array (Weller et al., 1995) in the West Atlantic (27°N, 70°W) show that adjusting the SOC fields leads to improved agreement with the buoy values (Josey et al., 1999). These results suggest that regional rather than global adjustment of ship based climatologies is necessary in order to improve the accuracy of the heat exchange fields. The consequences for the climatologically implied freshwater transport in the Atlantic of increasing the latent heat flux to close the heat budget are briefly considered. It is shown that increases in this term of greater than about 10% lead to discrepancies with the hydrographic freshwater transport estimate in the South Atlantic of Saunders and King (1995).

Potential sources of error in ship based heat fluxes are noted. These comprise inherent uncertainties in the flux formulae, further biases in the reported observations and sampling errors arising from the uneven distribution of ship reports. The use of semi-variogram analysis by Kent et al. (1999) to quantify random observational errors in ship meteorological reports is also discussed.

The wind stress forcing of the North Atlantic in the SOC climatology (which covers 1980–1993) is compared, see Fig. 2, with that from Hellerman and Rosenstein (1983, HR), which is based on a much longer time period (1870–1976). Differences in gyre structure in winter at mid-high latitudes are noted that are consistent with the known variations in the North Atlantic Oscillation which was in a predominantly positive state throughout WOCE and during the period used for the SOC climatology. In particular the sub-polar gyre is stronger in SOC than HR leading to a doubling of the Ekman upwelling velocity in the centre of the gyre from $8.6\ m\ month^{-1}$ for HR to $16.9\ m\ month^{-1}$ for SOC (Josey, Kent and Taylor, manuscript in preparation, to be submitted to JPO). Finally, we note that the differences between the SOC climatology and HR raise the question of how representative is the wind driven ocean circulation in the North Atlantic within the WOCE period of the long term mean?

References

da Silva, A. M., C. C. Young, and S. Levitus, 1994: Atlas of Surface Marine Data Vol. 1: Algorithms and Procedures. NOAA Atlas NESDIS 6, pp.74. US Dept. of Commerce.

Hellerman, S., and M. Rosenstein, 1983: Normal monthly wind stress over the World Ocean with error estimates. J. Phys. Oceanogr., 13, 1093–1104.

Josey, S. A., E. C. Kent, and P. K. Taylor, 1998: The Southampton Oceanography Centre (SOC) Ocean–Atmosphere Heat, Momentum and Freshwater Flux Atlas. Southampton Oceanography Centre Report No. 6, Southampton, UK, 30 pp. & figs.

Josey, S. A., E. C. Kent, and P. K. Taylor, 1999: New insights into the ocean heat budget closure problem from analysis of the SOC air-sea flux climatology. J. Climate, 12(9), 2856–2880.

Keith, D. W., 1995: Meridional energy transport: uncertainty in zonal means. Tellus, 47A, 30–44.

Kent, E. C., P. G. Challenor, and P. K. Taylor, 1999: A statistical determination of the random observational errors present in voluntary observing ships meteorological reports. J. Atmos. Ocean. Tech., 16(7), 905–914.

Kent, E. C., P. K. Taylor, B. S. Truscott, and J. S. Hopkins, 1993: The accuracy of voluntary observing ships meteorological observations – results of the VSOP – NA. J. Atmos. Oceanic Technol., 10(4), 591–608.

Moyer, K. A., and R. A. Weller, 1997: Observations of surface forcing from the subduction experiment: a comparison with global model products and climatological data sets. J. Clim., 10(11), 2725–2742.

Rossow, W. B., and Y.-C. Zhang, 1995: Calculation of surface and top of atmosphere radiative fluxes from physical quantities based on ISCCP datasets, 2. Validation and first results. J. Geophys. Res., 100, 1167–1197.

Saunders, P. M., and B. A. King, 1995: Oceanic fluxes on the WOCE A11 section. J. Phys. Oceanogr., 25(9), 1942-1958.

Schulz, J., J. Meywerk, S. Ewald, and P. Schlussel, 1997: Evaluation of satellite derived latent heat fluxes. J. Clim., 10(11), 2782–2795.

Trenberth, K. E., and A. Solomon, 1994: The global ocean heat balance: heat transports in the atmosphere and ocean. Clim. Dyn., 10, 107–134.

Weller, R. A., D. L. Rudnick, and N. J. Brink, 1995: Meteorological variability and air–sea fluxes at a closely spaced array of surface moorings. J. Geophys. Res., 100(C3), 4867–4883.

2.4a North Atlantic water mass modification processes: Overflows

Flow through sills and straits

Peter D. Killworth, Southampton Oceanography Centre, UK

The problem of hydraulic control has been studied for over a century. Despite this, understanding of the problem in an oceanic context, where stratification and rotation may both be important, is lacking. Stratified flows have almost exclusively been treated in a layered context. Continuous stratification has been treated mainly as a similarity problem. There are very few studies of the behaviour of a fully stratified fluid, although multiple layer approaches can yield similar answers.

These papers all related to non-rotating fluids. The problem becomes considerably more difficult when rotation is added, since cross-sill variability appears. Pratt and Lundberg (1991) give a review, and Whitehead (1998) gives a partial review of more recent work as well as a summary of flows through nine sills. Almost all work in situations other than single layer channel flow has needed gross simplifications, the most popular being a restriction of the potential vorticity to a uniform value, either zero or some arbitrary constant. Neither of these choices are physically realistic, since they necessarily imply changes in along-sill velocity across the sill whose values are much higher than observed. Killworth and McDonald (1993), Killworth (1994, 1995) address maximum principles in a single rotating layer with arbitrary potential vorticity distribution, and show that the Whitehead et al. (1974) laboratory results form an achievable upper bound to the sill throughflow for such configurations. Almost no work addresses the effects of friction. Effects familiar from non-rotating studies such as shock fronts, etc., remain far from understood. Exclusively, no attempt has been made to include the barotropic flow component, which will react with the topography and stratification on length scales which differ from either those of the topography itself or the internal deformation radii. Few papers even extend consideration to two active layers.

Another fundamental difference between rotating and non-rotating flows is the manner in which the upstream (and downstream) flow approaches the sill. In non-rotating fluids this occurs as a wide slowly varying, usually subcritical, flow. In a rotating fluid, for most extant solutions, the upstream flow is confined to a boundary layer, so that upstream flow, and geometry, details are not only important, but can dominate the solution. Outflows can modify the flow in an enclosed basin.

A major omission in most theories is that of time dependence. Flows through sills are unsteady for two reasons: first, they are naturally unsteady because of internal dynamics such as instabilities; and second, they are unsteady because of externally varying forcing such as tides, seasonal variability, etc. In natural situations in which rotation plays only a minor role (such as the Gibraltar throughflow) tides often induce major variability. In particular, the interface between in- and outflow rises and falls at the sill during the tidal cycle. Helfrich (1995) showed that the effects of such forcing were important in a two-layer non-rotating model when particle excursion or signal propagation during a period of the forcing was of the order of the along-sill length scale, and unimportant either in the limit of little or very large excursion. In other words, rapidly varying forcing 'averaged out', while slowly varying forcing had a response that resembled the local steady state at that part of the cycle. Helfrich also found that, unlike most theories of hydraulic control, geometric details of the entire sill area affected the throughflow. Recent work by Helfrich, Kuo and Pratt is beginning a thorough examination of time-dependence in dam-break one-layer flow in a channel using advanced numerical methods.

A separate approach is that of Pratt and Chechelnitsky (1997), who seek dynamical formulae relating inflow and layer depth upstream of some unresolved sill, with the fluid restricted to uniform potential vorticity. This approach seems promising, although it is not tested in models to our knowledge.

The theories above possess fundamental limitations:

- the sills are assumed to be 'slowly varying' along the sill, in the sense that across-sill variations are much more rapid than along-sill
- flows are assumed laminar, despite observations of various instabilities in sills
- the dynamics are largely assumed to be those of a perfect fluid, with little extant work on effects of mixing of water masses and of momentum, despite clear observations that mixing is important in most sills.

To date, we have a variety of formulae representing flow over sills:

- Non-rotating, one-layer, reduced gravity flow of fluid whose surface upstream is a height h above the height of the 'saddle' of the sill. There is a hydraulically controlled flux of $W(g'(2h/3)^3)^{1/2}$, where g' is a reduced gravity for the layer and W the sill width
- Non-rotating two-layer exchange flow (e.g. Gibraltar in- and out-flow) has a maximum controlled flux of $0.25WH(g'H)^{1/2}$ where W and H are the width and depth of the sill, assumed rectangular
- Rotating, one-layer, reduced gravity flow in the same configuration has a maximum controlled flux of $g'h^2/2f$, where f is the Coriolis parameter
- There are no extant formulae for rotating, stratified fluid flow at sills.

Application of such formulae in coarse resolution models has not been productive to date. The Pratt and Chechelnitsky (1997) approach, as noted, has not apparently been tested. Attempts to use maximum bound formulae has yielded severe numerical noise, essentially because the coarse model is attempting to handle fine-resolution results and cannot easily do so without heavy frictional damping.

Sills in numerical models

To date, even the finest resolution global models cannot resolve the sill flows adequately; for example, the DYNAMO (1997) intercomparison of three eddy-permitting N. Atlantic models (the DAMAE intercomparison was similar) showed large differences between the three model responses in the Denmark Strait, despite – formally, at least – the models possessing the same forcing and topography. The Denmark Strait, furthermore, is wide and so apparently resolved by these models. For the foreseeable future, even eddy-permitting models, to function adequately, will need parameterisations of some kind to represent sill flow correctly; the problem is far more urgent for the ocean component of coarse resolution climate models, which usually have to undertake major excisions of ocean floor even to possess a sill between basins at all.

Coarse resolution models

Climate models possess the coarsest resolutions, and so are the most sensitive to details near sills. Roberts and Wood (1997) give an enlightening example from the Greenland–Iceland–Scotland ridge in the Met. Office coarse resolution z-coordinate model climate model. The original topography employed resulted in no net flow across the ridge. Changes in topography by as little as one grid box resulted in gross changes not only to cross-ridge flux (12 Sv being achieved) but also to the location of this flux, and to the composition of the water mass actually crossing the sill. Put another way, a 50% change in heat flux at the GIS ridge latitude can be achieved by the addition or subtraction of a single grid box. It is unclear whether the most realistic results are given by excavating to the deepest, widest, or deepest and widest, points. Certainly current practice of taking median or (worse) mean depth over the grid point using a source of fine resolution depth data is flawed if used in coarse models.

Medium-resolution process models

Medium-resolution models gave valuable input as to why these models were so sensitive. Process models of flows over simple ridges demonstrated how easily flow patterns became complex near the ridge, with mixing slightly upstream of the sill. This, in a coarse resolution model, would not occur easily. Yet columns are squeezed as they pass over the sill and so generate relative vorticity in such process models. Coarse resolution models cannot easily generate relative vorticity and so require large amounts of mixing, which may be erroneous. The dependence on upstream conditions and mixing means that observations within and downstream of sills may not give sufficient information to determine the physics within the sill.

There are results involving parameterised outflow as a relaxation towards observations (designed to simulate, but not explain, sill flow). Simple relaxation to observations needs careful tuning: too weak a relaxation has no effect, while too strong a relaxation forces flow around, rather than through, the relaxed area. Numerical experiments by Gerdes and Beckmann show that inflow must be explicitly included to reach the correct amount of water in a given class.

Fine-resolution models

Two fine-resolution studies, simulating the Vema Channel and Romanche Fracture Zones, were mentioned. In both cases, it was possible to obtain an accurate simulation with sufficient resolution. In the Vema Channel simulation by Jungclaus and Vanicek, the float behaviour observed by Hogg was reproduced, with the flow switching sides within the channel (as predicted in theory by Straub 1998). Again, there was strong mixing and recirculation present. Ferron's (1998) Romanche Fracture Zone study used high vertical resolution (and free slip on the vertical walls to lessen frictional retardation) and a realistic mixing scheme (Mellor-Yamada). High vertical mixing rates ($0.1\mathrm{m}^2\,\mathrm{s}^{-1}$) are found downstream of the sills.

Thus *there are examples when numerical modelling with 'adequate' resolution has been capable of reproducing reality*. However, (a) this resolution is far beyond the ability of any climate model in the foreseeable future, and (b) without either data or large resources, it is impossible to determine what constitutes 'adequate' resolution.

The question of identification of sills which are hydraulically controlled was also raised. Process studies at high resolution demonstrated that Ekman sidewall effects, combined with MacCready and Rhines shutdown, yield a similar cross-stream structure to hydraulic control. Accordingly, accurate determination of the physics is necessary to distinguish these two cases.

References

DYNAMO Group, 1997: Final report to EC. Institüt für Meereskunde, University of Kiel.

Ferron, B., 1998: Écoulement de l'Eau Antarctique de Fond dans la Zone de Fracture Romanche, Ph.D. Thesis Dissertation #552, Université de Bretagne Occidentale, Brest, 167pp.

Helfrich, K. R., 1995: Time-dependent two-layer hydraulic exchange flows. J. Phys. Oceanogr., 25, 359-373.

Killworth, P. D., 1992: On hydraulic control in a stratified fluid. J. Fluid Mech., 237, 605–626.

Killworth, P. D., 1994: On reduced-gravity flow through sills. Geophys. Astrophys. Fl. Dyn., 75, 91–106.

Killworth, P. D., 1995: Hydraulic control and maximal flow in rotating stratified hydraulics. Deep-Sea Res., 42, 859–871.

Killworth, P. D., and N. R. McDonald, 1993: Maximal reduced-gravity flux in rotating, stratified hydraulics. Geophys. Astrophys. Fl. Dyn., 70, 31–40.

Pratt, L. J., and M. Chechelnitsky, 1997: Principles for capturing the upstream effects of deep sills in low resolution ocean models. Dyn. Atmos. Ocean., 26, 1–25.

Pratt, L. J., and P.A. Lundberg, 1991: Hydraulics of rotating strait and sill flow. Ann. Rev. Fluid Mech., 23, 81–106.

Roberts, M. J., and R.A. Wood, 1997: Topography sensitivity studies with a Bryan-Cox type ocean model. J. Phys. Oceanogr., 27, 823–836.
Straub, D. N., 1998: Simple models of flow over deep ocean sills: planetary and semi-geostrophic solutions. J. Phys. Oceanogr., 28, 971–983.
Whitehead, J. A., 1998: Topographic Control of Ocean Flows in Deep Passages and Straits. Rev. Geophys. Space Phys., 36, 423–440.
Whitehead, J. A., A. Leetmaa, and R. A. Knox, 1974: Rotating hydraulics of strait and sill flows. Geophys. Fl. Dyn., 6, 101–125.

Review of the exchange between the Mediterranean and Atlantic through the Strait of Gibraltar

Harry L. Bryden, Southampton Oceanography Centre, UK

The outflow of Mediterranean Water over the sill in the Strait of Gibraltar represents a major input of high salinity water to the interior North Atlantic Ocean. The effects of this high salinity water on the circulation of the North Atlantic are many and often controversial. Mediterranean water cascading over the sill and down into the North Atlantic adds a high salinity signature to the intermediate waters of the Atlantic (Worthington, 1976). This high salinity water arguably leads to the formation of North Atlantic Deep Water in the Norwegian Sea and Antarctic Bottom Water in the Atlantic sector of the Antarctic and hence determines the nature of the global thermohaline circulation (Reid, 1979, 1994). In a model study, Jia (1999) finds the mixing of the descending outflow west of Gibraltar affects the size of the Azores Current. Variations in the amount and salinity of Mediterranean water entering the Atlantic over long time scales are said to be related to the initiation of ice ages (Johnson, 1997). Until recently (Slater and Bryden, 1999), there have been few quantitative estimates of how much of the Mediterranean water goes north and how much west through the Atlantic. In terms of Mediterranean circulation, the inflowing Atlantic water jet through the Strait leads to the formation of the Alboran Sea gyre (Speich, Madec and Crepon, 1996). On larger scale, the Strait may exert an overall control on the salinity of the Mediterranean Sea so that any change in the net evaporation over the basin leads to a change in Mediterranean salinity (Rohling and Bryden, 1992). Changes in sill depth of the connection between the Atlantic and Mediterranean can have dramatic effects on the Mediterranean circulation. For example, a relatively shallow connection of order 20 m depth or less is the likely explanation for the drying up of the Mediterranean 6 million years ago.

The Strait of Gibraltar is a narrow and shallow connection between the Mediterranean and Atlantic. The classical method for estimating the inflow of Atlantic water and outflow of Mediterranean water through the Strait is to use the Knudsen relations based on mass and salt conservation statements for the Mediterranean basin with measurements of the salinities of the inflowing and outflowing waters in the Strait and an estimate of the net evaporation over the Mediterranean. Because the Strait is a bottleneck that restricts how much water can enter or leave, two-layer hydraulic control models have been developed to predict the maximum amount of exchange that can occur between the Atlantic and Mediterranean through the physical configuration of the Strait (Farmer and Armi, 1986). Such predictions are in reasonable agreement with estimates of the exchange from measurements at the Gibraltar sill (Armi and Farmer, 1988). Whether or not the Gibraltar exchange is continuously maximal remains a controversial topic (Garrett, Bormans and Thompson, 1990). Seasonal variation of the surface currents deduced from sea level data suggests that the exchange is maximal only during part of the year. Long-term direct measurements of the exchange, however, are needed to establish whether or not there are seasonal or longer term variations in the exchange.

There are strong tidal fluctuations in the Strait of Gibraltar that effect approximately half of the exchange between the Mediterranean and Atlantic. Time-averaged currents at fixed depth suggest a surprisingly small outflow or inflow of Mediterranean or Atlantic waters, of order 0.35 Sv. Tidal flows contribute an equal amount to the exchange because a large pulse of Mediterranean water crosses the sill into the Atlantic on the outflowing tide when the interface is relatively shallow and a large pulse of Atlantic water enters the Mediterranean on the inflowing tide when the interface is deep. Overall from time series measurements of the exchange, the average outflow of effectively pure (38.4 psu) Mediterranean water is estimated to be 0.7 Sv, with a slightly larger inflow of Atlantic water required to balance mass and salt for the Mediterranean basin (Bryden, Candela and Kinder, 1994).

Barotropic fluctuations in the exchange have been related to fluctuations in the atmospheric pressure over the Mediterranean basin (Candela, Winant and Bryden, 1989). In an inverse barometer argument, high atmospheric pressure depresses Mediterranean sea level so that water is ejected out through the Strait into the Atlantic; low atmospheric pressure raises sea level so that water must be imported from the Atlantic into the Mediterranean. The model response to observed atmospheric pressure fluctuations exhibits strong correlation to observational estimates of the total Gibraltar exchange over time scales longer than 5 days.

Early estimates suggested that there was a fortnightly signal in the exchange with stronger surface inflow and stronger deep outflow evident in daily averaged currents during neap tides (Candela, Winant and Bryden, 1989). Continuous estimates of the inflow of Atlantic water above the interface and outflow of Mediterranean water below the interface, however, exhibit no such fortnightly cycle in the exchange (Bryden, Candela and Kinder, 1994). The explanation appears to be that during spring tides the tidal flux is larger while the mean baroclinic exchange is weaker and during neap tides the tidal flux is weaker so the mean baroclinic exchange builds up so that there is no overall change in the exchange over the fortnightly cycle in tidal current intensity. Similar calculations must be done over longer time periods to determine whether or not the seasonal cycle in the strength of the surface currents is somehow compensated by fluctuations in the depth of the interface between the Atlantic inflow and Mediterranean outflow.

During the WOCE time period, long-term (order 4 years) monitoring of the Gibraltar exchange was attempted by Julio Candela and by a European consortium under the CANIGO project. The long-term measurements are based on a strategy of current meter moorings across the sill section and across the eastern entrance to the Strait and of deep pressure gauges and sea level gauges on the northern and southern sides of the Strait. Because of strong currents and heavy fishing and shipping activities, data recovery rates can be quite low making estimation of the monthly to interannual variations in the exchange through the Strait of Gibraltar difficult.

References

Armi, L., and D. M. Farmer, 1988: The flow of Mediterranean Water through the Strait of Gibraltar. Prog. Oceanogr., 21, 1–105.

Bryden, H. L., J. Candela, and T. H. Kinder, 1994: Exchange through the Strait of Gibraltar. Prog. Oceanogr., 33, 201–248.

Candela, J., C. D. Winant, and H. L. Bryden, 1989: Meteorologically forced subinertial flows through the Strait of Gibraltar. J. Geophys. Res., 94, 12667–12679.

Farmer, D. M., and L. Armi, 1986: Maximal two-layer exchange over a sill and through the combination of a sill and contraction with barotropic flow. J. Fluid Mech., 164, 53–76.

Garrett, C., M. Bormans, and K. Thompson, 1990: Is the exchange through the Strait of Gibraltar maximal or submaximal? In: The Physical Oceanography of Sea Straits, edited by L. Pratt, pp. 271–294, Kluwer, Boston.

Jia, Y., 1999: On the formation of an Azores Current due to Mediterranean overflow in a modelling study of the North Atlantic. J. Phys. Oceanogr., submitted.

Johnson, R. G., 1997: Climate control requires a dam at the Strait of Gibraltar. Eos, 78 (27, July 8), 277+280–281.

Reid, J. L., 1979: On the contribution of the Mediterranean Sea outflow to the Norwegian–Greenland Sea. Deep-Sea Res., 26A, 1199–1223.

Reid, J. L., 1994: On the total geostrophic circulation of the North Atlantic Ocean: Flow patterns, tracers and transports. Prog. Oceanogr., 33, 1–92.

Rohling, E. J., and H. L. Bryden, 1992: Man-induced salinity and temperature increases in western Mediterranean deep water. J. Geophys. Res., 97, 11191–11198.

Slater, D., and H. Bryden, 1999: On the transport of Mediterranean outflow water. Poster presented at the WOCE North Atlantic Workshop, Kiel, August 1999.

Speich, S., G. Madec, and M. Crepon, 1996: A strait outflow circulation process study: The case of the Alboran Sea. J. Phys. Oceanogr., 26, 320–340.

Worthington, L. V., 1976: On the North Atlantic Circulation. The Johns Hopkins Oceanographic Studies, Vol. 6, 110 pp.

Some results from long-term observations of the deep-water flux through the Faroe Bank Channel

Peter Lundberg, Stockholm University; Karin Borenäs, Göteborg University; Bogi Hansen, Fisheries Laboratory, Faroe Islands; Irene Lake, Stockholm University; and Svein Østerhus, Bergen University

The Faroe Bank Channel was not discovered until 1943, but has attracted much attention since this time. Already in the 1950s it was recognised that it plays an important role for the deep-water flow from the Norwegian Sea into the North Atlantic proper, and in 1960 ICES launched its first overflow study to examine this process. This pioneering survey was followed by other exploratory work in the 1960s, ultimately leading to the first Norwegian Sea budget being established by Worthington (1970). ICES also conducted the large-scale experiment “Overflow-73”. This was followed up by other work of more-or-less sporadic nature, conducted by a number of research groups in various countries. A particularly important investigation was undertaken by IOS in the late 1980s, with the aim of obtaining long-term records of the deep-water flow through the passage, cf. Saunders (1990).

The Faroe Bank Channel is more than 200 m deeper than any other passage across the Greenland–Scotland Ridge (Fig. 1). Hence it is the main outlet for the densest overflow of cold water from the Arctic Mediterranean (viz. the Nordic Seas and the Arctic Ocean) to the North Atlantic proper and is estimated to carry about one third of the total deep-water flux across the ridge (Hansen et al., 1998).

Since 1988 the Faroese Fisheries Laboratory has monitored the hydrography of the channel on the basis of regular CTD cruises along a standard section somewhat south-east of the sill and since 1995 the Nordic WOCE and later the VEINS programmes have maintained a 75 kHz ADCP (Acoustic Doppler Current Profiler) mooring at the channel sill. To study the cross-sectional variation of the velocity field, a dedicated experiment was conducted in 1998 where the long-term ADCP mooring was supplemented by two additional 75 kHz ADCPs. These were deployed on each side of the “standard position” during a period lasting about two months from July to September 1998. This undertaking was combined with CTD observations on three cruises.

Vertical profiles

Fig. 2 shows the average velocity profiles from four ADCP deployments at the central mooring site of the channel covering a period of almost three years as well as a sample temperature profile from that site obtained during the special deployment period. Cold water dominates the deepest 200–300 m of the channel and at the central site this cold water flows north-westwards with average velocities exceeding 1 m/sec in the core, centred around 120 m above the bottom.

Cross-sectional variation

The cross-sectional variation is shown in Fig. 3 as an average velocity section across the channel for the July–September 1998 special deployment period. The graph demonstrates that the high-speed core of the flow is located on the south-western side of the channel. Along this slope of the Faroe Bank, the overflow current only extended a little more than 200 m above the bottom.

On the Faroe side of the channel, the velocities adjacent to the bottom were smaller, but the flow extended much higher on to the slope of the Faroe Plateau. Fig. 3 also includes an observed temperature distribution across the channel, and it is recognised that to a large extent the isotherms followed the velocity field.

Flux calculations

To utilise the long-term observations at the central ADCP site, the flux of the deep water through the channel has been calculated by dividing the cross-sectional area of the channel into a number of boxes, each of which is assumed to have the same along-channel velocity as one of the 25 m bins (depth intervals) measured by the ADCP at the central site. The flux calculations have been done both with boxes neglecting the cross-sectional variations of the flow and with boxes designed on the basis of the average properties visible in Fig. 3.

The total water transport through the depths of the channel is of considerable interest, but more important is perhaps the flux of specific water masses. The cold-water core is constituted by two different water masses (Hansen et al., 1998): Norwegian Sea Deep Water (NSDW) colder than -0.5°C, and Norwegian Sea Arctic Intermediate Water (NSAIW) between -0.5°C and +0.5°C. In the literature, water colder than 3°C is often denoted ISOW, viz. “Iceland–Scotland Overflow Water”. (Although peripheral to the main thrust of the present study it can also be mentioned that an analysis of the long-term hydrographic observations indicated that an intermediate water mass consisting of North Icelandic/Arctic Intermediate water also frequently forms a part of the overflow. This may contribute to the characteristic isotherm pinching often visible in the channel.) The water-mass distribution in the boxes associated with each ADCP bin can be determined from the temperature field. Figs. 2 and 3 indicate a relationship between the temperature field and the velocity field. Further study is presently under way to clarify over which time-scales these two fields co-vary. The preliminary calculations reported here have been undertaken for a constant water-mass distribution as well as for one which was associated with the velocity distribution.

Long-term fluxes of the overflow

On the basis of the almost three-year long time series from the central ADCP site, average fluxes have been calculated. These were found to be 2.5 Sv (10^6 m^3 / s) for the total volume flux below 450 m depth, 1.9 Sv for ISOW, and 1.5 Sv of water colder than +0.5°C (NSDW + NWSAIW). These estimates are somewhat preliminary, since a detailed analysis of the data sets has not yet been completed.

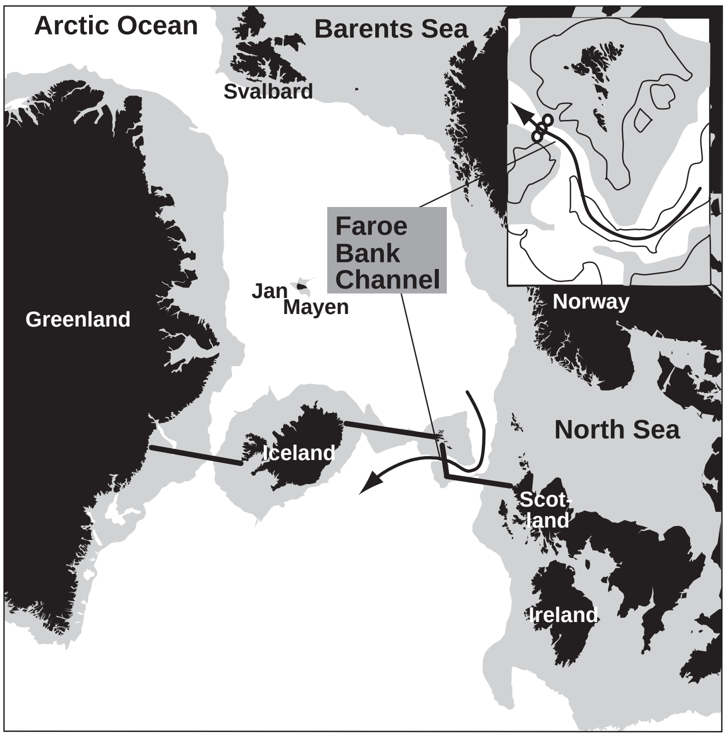

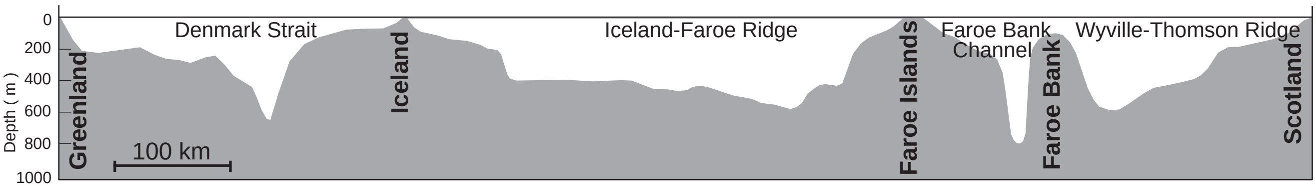

Figure 1. Map of the bathymetry of the Greenland-Scotland Ridge (left) with areas shallower than 1000 m lightly shaded. The insert shows the region around the Faroe Bank Channel with areas shallower than 500 m lightly shaded and ADCP mooring sites indicated by circles. Arrows indicate the path of the overflow through the channel. The section below follows the crest of the ridge along the trace shown on the map.

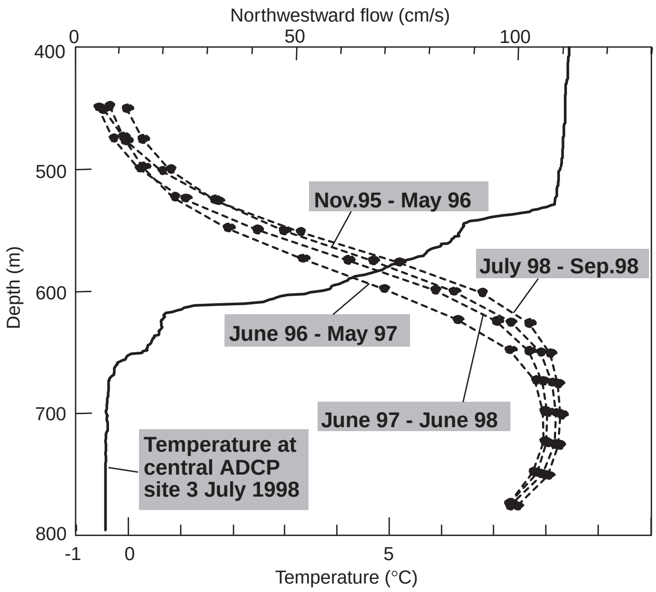

Figure 2. Vectorially averaged velocity profiles along the axis of the channel (cardinal direction 304°) for four ADCP deployments in the middle of the Faroe Bank Channel. Each filled circle indicates the average velocity in a 25 m layer (bin) from measurements every 15 or 20 minutes. The continuous curve shows the temperature profile from a CTD cast at this site.

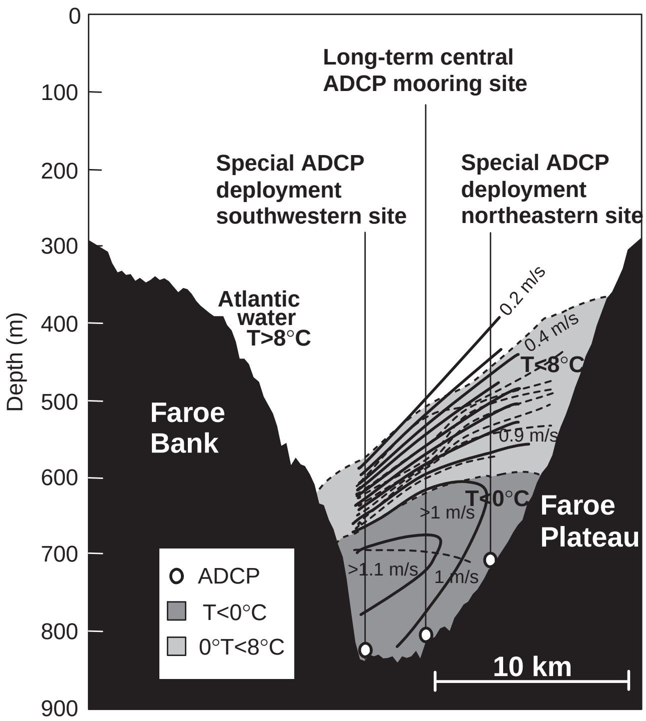

Figure 3. A section across the channel in the sill region with the average along-channel velocity distribution during the special deployment period and a temperature distribution from a CTD section taken towards the end of this period. Water colder than 0°C is strongly shaded, whereas temperatures between 0°C and 8°C are more lightly shaded. Circles indicate the location of the three ADCPs.

However, the numbers were not found to depend critically on cross-sectional variations or the coupling between the velocity and temperature fields. The estimates are hence not expected to be drastically revised by the more refined analysis in progress. These fluxes are largely consistent with previous, less data intensive, estimates (Borenäs and Lundberg, 1988; Saunders, 1990). The temporal evolution of the core velocity at the central ADCP site and of the transport of Iceland–Scotland Overflow Water (ISOW) during the three-year observational period are shown in Fig. 4. Over monthly timescales fairly large variations are seen, but no systematic seasonal signal is obvious from the data. This graph possibly also might reflect a slightly decreasing tendency of the ISOW transport. If so, this would be consistent with long-term trends that have been reported for the region (Østerhus and Gammelsrød, in press; Turrell et al., in press) and for the Faroe Bank Channel itself (Hansen and Kristiansen, in press). As yet, however, the ADCP measurements in the Faroe Bank Channel are of too short duration to permit any conclusions as regards this important question.

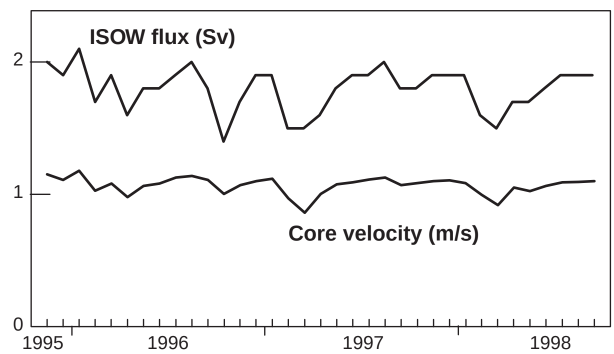

Figure 4. The upper curve shows the monthly averaged along-channel velocity at the core of the flow (117 m above the bottom) from the central ADCP site. The estimated volume flux of ISOW water through the Faroe Bank Channel from November 1995 to September 1998 is shown in the lower curve, based on the assumption of a constant cross-sectional velocity variation and temperature field.

References

Borenäs, K. M., and P. A. Lundberg, 1988: On the Deep-Water Flow Through the Faroe Bank Channel. J. Geophys. Res., 93 (C2), 1281–1292.

Hansen, B., and R. Kristiansen, 1999: Variations of the Faroe Bank Channel Overflow. Rit Fiskideildar, in press.

Hansen, B., S. Østerhus, H. D. Dooley, W. J. Gould, and L. J. Rickards, 1998: North Atlantic–Norwegian Sea Exchanges. The ICES NANSEN Project. ICES Coop. Res. Rep. No. 225.

Østerhus, S,. and T. Gammelsrød, 1999: The Abyss of the Nordic Seas is warming. J. Clim., in press.

Saunders, P. M., 1990: Cold Outflow from the Faroe Bank Channel. J. Phys. Oceanogr., 20, 28–43

Turrell, W. R., G. Slesser, R. D. Adams, R. Payne, and P. A. Gillibrand, 1999: Decadal variability in the composition of Faroe Shetland Channel bottom water. Deep-Sea Res., I, 46, 1–25.

Worthington, L. V., 1970: The Norwegian Sea as a Mediterranean basin. Deep-Sea Res., 17, 77–84.

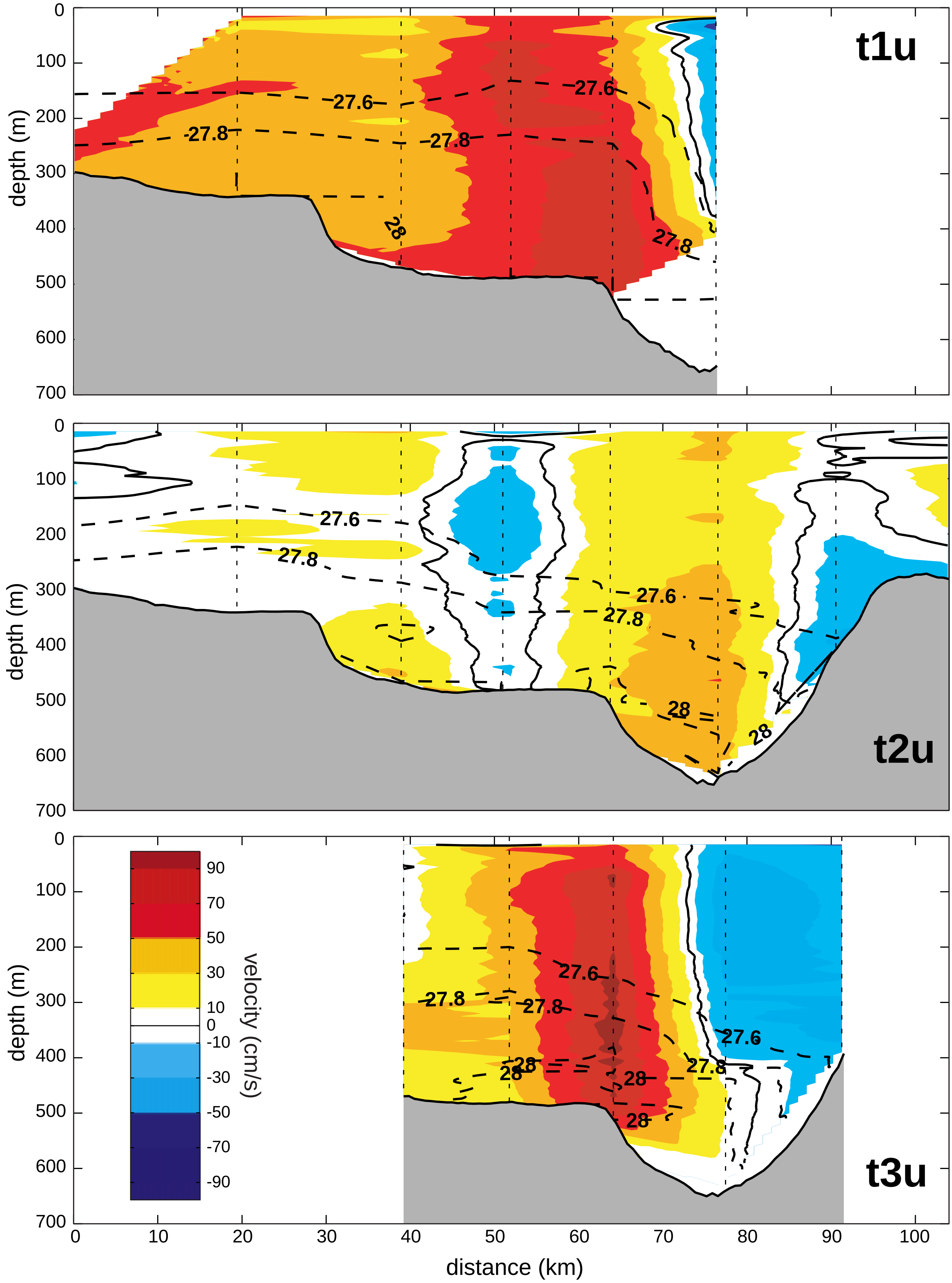

Figure 1. South-westward velocity maps (cm/s) relative to the three occupations across Denmark Strait.

Velocity structure of the Denmark Strait Overflow: New measurements and models

James B. Girton, Rolf H. Käse and Thomas B. Sanford

The dense overflow through the Denmark Strait forms a primary ingredient of North Atlantic deep water and an important part of the global thermohaline circulation. Long-term current meter moorings have characterised the transport of this flow as vigorous and rapidly-varying on timescales of a few days, but very few measurements have been made of the velocity structure at the sill. Numerical models have given a wide variety of descriptions of the overflow, but have largely been of insufficient resolution or area extent to capture the observed structure and estimate the sill flow.

In September 1998, a programme of measurements using expendable and ship-lowered instrumentation was carried out in the Denmark Strait from the RV Poseidon, including a total of 110 expendable current profiler (XCP) and 76 expendable CTD (XCTD) probes. The XCPs, in conjunction with global positioning system (GPS) and acoustic Doppler current profiler (ADCP) instrumentation on board the Poseidon gave full-depth profiles of water temperature and velocity, including within the turbulent bottom boundary layer. The XCTDs provided essential measurements of salinity at an accuracy just adequate for the characterisation of watermass content and density class transport. Three occupations of a section across the Denmark Strait sill revealed a strongly barotropic velocity structure, often concentrated into a thin jet with speeds of up to $90\,\mathrm{cm\,s^{-1}}$ and recirculations on both sides (Fig. 1). The density front between the overflow water (mostly on the Greenland side) and the warmer Atlantic water on the Iceland side is often nearly vertical, but sometimes has a more noticeable slope, giving a baroclinic structure to the velocity. We estimate the transport of water denser than 27.8 (27.6) $\mathrm{kg\,m^{-3}}$ on the three sections at 7.2 (10.0), 2.2 (3.2) and 3.4 (4.6) Sv, respectively. Alternatively, using temperature, the transports of water colder than 2°C are 11.8, 4.2 and 4.0 Sv. Each of these is substantially larger than the commonly used estimate, based on current meter moorings, of 2.9 Sv of water colder than 2°C. However, the local coverage of the earlier measurements makes them not exactly comparable to our profiles. Although these three sections alone cannot give an accurate mean transport value, they do indicate at least that the overflow transport has not decreased substantially from the previously observed value, and may have increased. The observed patterns of variability and paths of overflow water are reproduced quite well by a regional sigma-coordinate model of hydraulic exchange with realistic topography. The model illustrates the barotropic nature of the flow as well as the recirculations on both sides. In addition, the path taken by the main overflow jet moves from one side of the channel to the other as it transits the sill, in agreement with hydraulic predictions. However, the magnitudes of velocities and transports in the model remain smaller than those observed. This difference is being investigated.

2.4b North Atlantic water mass modification processes: Labrador Sea convection

Labrador Sea Water Mass Variability during the WOCE period

R. Allyn Clarke, John R. N. Lazier, and Igor Yashayaev, Ocean Sciences Division, Bedford Institute of Oceanography, Canada

The multiple branches of the North Atlantic Current bring heat and salt to the Nordic, Irminger and Labrador Seas where winter cooling, convection and mixing produce the water masses that form the intermediate and deep waters of the North Atlantic. The current branches that enter the Nordic seas, convect to form the densest water masses in the world ocean form in the Nordic Seas. These then overflow the Shetland–Faroe–Iceland–Greenland ridges and enter the North Atlantic and eventually flow cyclonically around the Labrador Sea in a Deep Western Boundary Current. Another branch of the North Atlantic Current passes through the Irminger Sea and enters the Labrador Sea becoming cooler, fresher and denser as it moves. Convection in the Labrador Sea forms the intermediate water mass known as Labrador Sea Water (LSW) that forms a thick layer of low stability and salinity throughout the Labrador Sea and the North Atlantic Sub Polar Gyre.

The WHP repeat section, AR7W, was established to observe the year to year changes of all the components of North Atlantic deep and intermediate waters. This section was occupied early every summer (mid May to mid July) from 1990 through to 1999. During 1996 to 1998, the section was occupied more frequently with additional occupations in the fall of 1996 (October), the winters of 1997 and 1998 and the summers of 1996 to 1999. During 1996 to 1998, additional hydrographic sections were occupied to map the entire Labrador Sea before, during and after the winter cooling period.

The variability in the LSW should be examined in

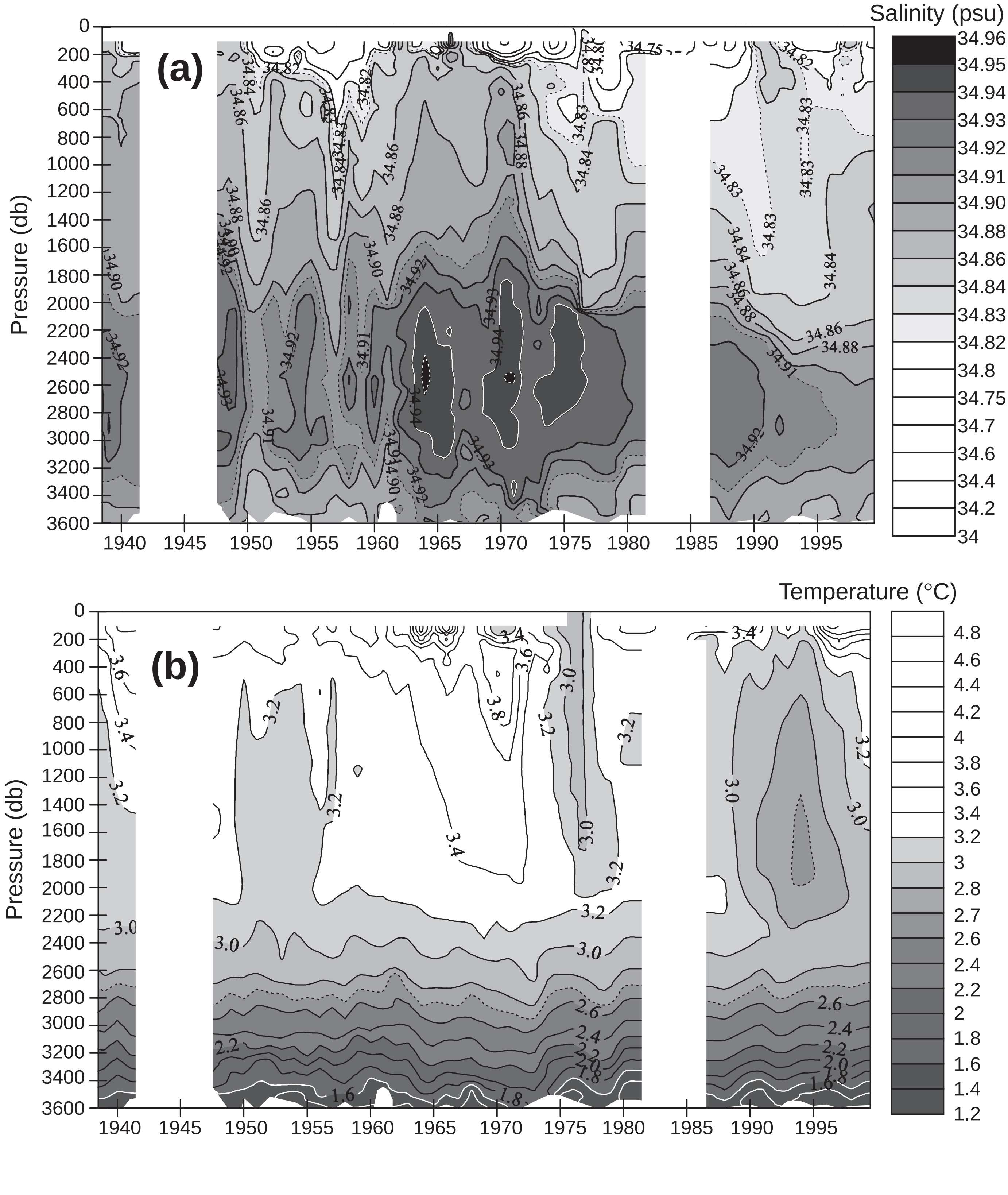

Figure 1. (a) Salinity, (b) Temperature, (c) σ_2, (d) d p/d σ_2 vs. pressure for the central Labrador Sea, 1938 to 1999.

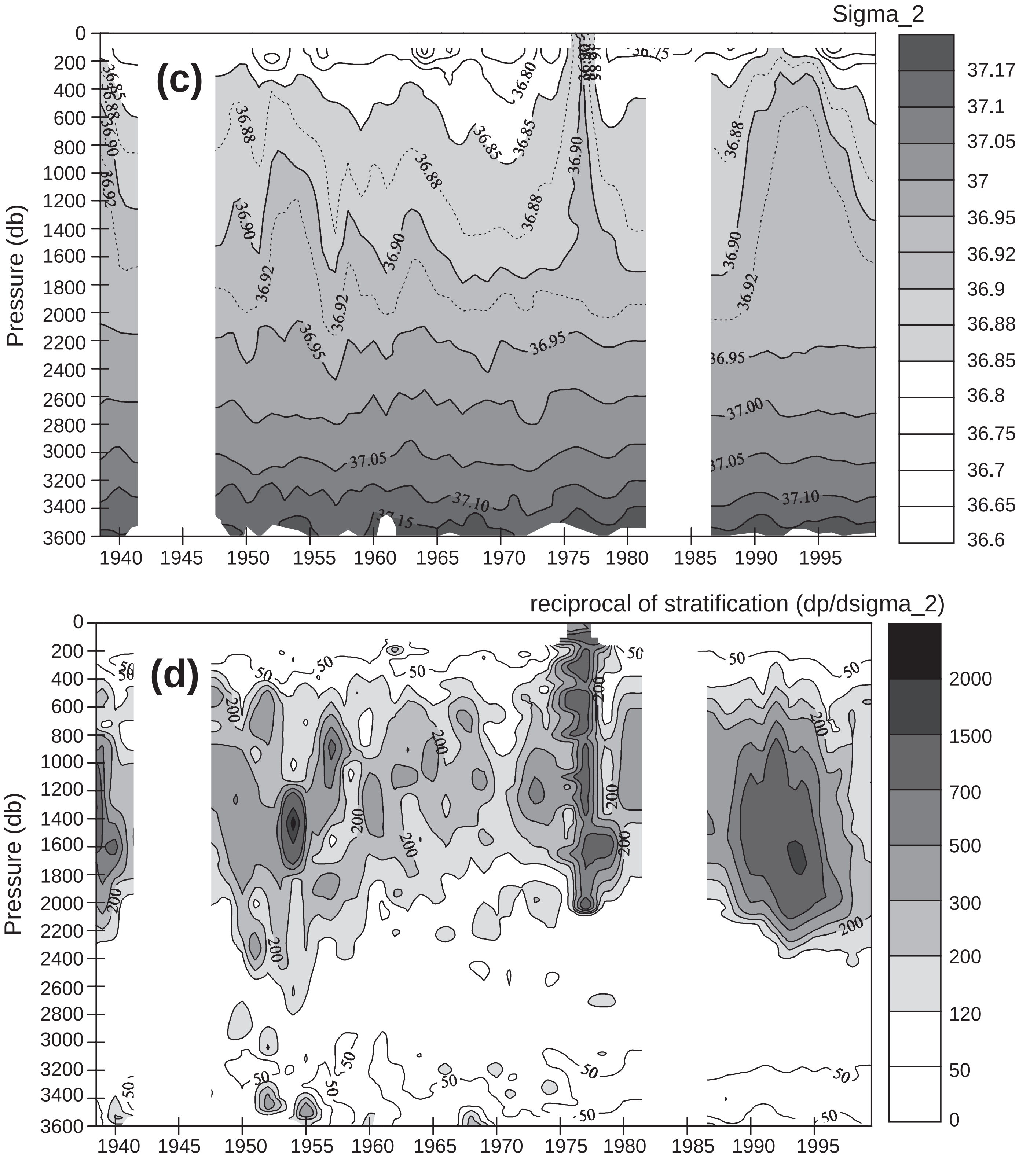

Figure 1. (a) Salinity, (b) Temperature, (c) σ_2, (d) d p/d σ_2 vs. pressure for the central Labrador Sea, 1938 to 1999.

the context of its variability over the longer record. The regular hydrographic sampling from the vessels occupying Ocean Weather Station Bravo in the central Labrador Sea was initiated in the late 1940s and continued to 1974. Bedford Institute of Oceanography carried out surveys during 1976 to 1978 but there were few observations through the 1980s.

Looking at the record from the 1940s to the present, we see that the 1990s represent the strongest sustained period of renewal and modification of LSW in the record. The LSW formed in 1993 and 1994 is the densest and coldest and of the lowest salinity that has been documented (Fig. 1). This period of strengthening convection from 1990 to 1994 was only documented by annual spring/early summer occupations of AR7W.

In June 1994, a heavily instrumented current meter mooring was established near the old OWS Bravo site on the AR7W section. This mooring was equipped with current meters and T,S,P recorders from the bottom to a depth of 75 m with the heaviest concentration of instruments in the upper 1000 m. This mooring has been maintained continuously at this site from 1994 to the present; however, most of the instruments from the spring 1995 through fall of 1996 deployment were lost during recovery.

More intensive hydrographic and other observations began in 1996 with both the Labrador Sea Convection experiment and the beginning of the IfM Kiel hydrographic and mooring programmes in the region. This period of more intense observations was also a period of weaker convection resulting in the re-stratification and re-salination of the water column. While the winter of 1996/97 is characterised as weaker convection by the standards of the 1990s, convection to reach to the order of 1400 m and this would be considered high convection if one considers the entire period since 1948.

Over the fall, winter, spring, summer of the 1996/97 cooling and re-stratification cycle, the hydrographic fields of the Labrador Sea were mapped five times. In addition, a large number of profiling ALACE floats, moorings, other float systems and surface drifters were making measurements within the LSW depth range throughout the sea. When all these data are collected together, we should be able to define the seasonal cycle during 1996/97 and perhaps on through 1997/98. However, to truly understand how the Labrador Sea responds to the wide variety of different atmospheric conditions, we will continue to need to go back to the Bravo period and the mapping of the Labrador Sea done by the ICES Polar Front surveys of 1956/57 and John Lazier's survey of 1966/67.

The change in the LSW from the 1970s to the 1990s is remarkable. The thickness of the layer defined by $27.78 \geq \sigma_\theta \geq 27.72$ (this includes both the classical LSW and the upper LSW) increased from 700 to 800 m to 1100 to 1400 m. In the Newfoundland Basin, this same layer increased its thickness from 400–500 m to 600–800 m. BIO's hydrographic section along 50°W in fall 1993, fall 1994 and spring 1995 showed increasing amounts of new LSW entering the sub tropical gyre in 1994 and 1995 when our programme in this area ended. The analysis of the WOCE North Atlantic intensive data sets collected in the sub-tropical gyre in 1997 should look for the spreading of this new cold and dense LSW along the western boundary.

The Labrador Sea Deep Convection Experiment

Martin Visbeck, LDEO, Columbia University, USA

Deep convection in the ocean is an important process for deep-water ventilation and part of the global thermohaline circulation. However, several aspects of the convective process are not fully understood which warranted a focused process study using observation, models and theory. The representation of deep convection and its interaction with the mesoscale circulation in ocean circulation models is of questionable fidelity and in need of improvement. The Labrador Sea Convection Experiment was designed to fulfil several objectives:

- Improve our understanding of the dynamics of the convective elements, which have length scales of a few hundreds of meter and timescales of a few hours. In particular the role of the earth's rotation as a limiting factor was of interest.
- Investigate the interaction of the mesoscale with the convective elements and the larger scale circulation. How does the mesoscale influence the preconditioning, violent mixing and re-stratification phase? And are mesoscale eddies the rate limiting factor for the export of newly ventilated water?
- Assess the importance of the basin scale circulation on the convective process. Is the advection of anomalous water masses crucially influencing the convective process? Or are changes in the strength of the atmospheric forcing predominately important for the interannual variability of deep convection?

After a few years of intensive planing we mounted a field campaign in the Labrador Sea over two consecutive winter seasons from the fall of 1996 until the early summer of 1998. It was decided to invest significant resources into a new technology, neutrally buoyant floats, which would be able to monitor the upper ocean (down to a depth of ~1500 m) and at the same time measure the vertical velocity and large and mesoscale circulation. Three different float types were used:

- True Lagrangian floats that are able to follow water parcels in all directions and would give new insights into the three dimensional structure of the convective elements.

- Acoustically tracked RAFOS floats with the added ability to profile the upper 1000 m.
- Profiling ALACE floats which drift at a fixed depth for about one week and the obtain a temperature and salinity profile on the way to the surface where they relay their data through a satellite system in almost real time.

The float measurements were augmented by moored observations which measured the Eulerian circulation and stratification changes at several locations along a section between the Labrador shelf and the region where the maximum convective activity was suspected. A few of the moorings hosted a tomographic array to measure the integral heat content changes.

Finally, ship board CTD/LADCP surveys were conducted each winter and early summer to map the large scale density and tracer field.

During those cruises substantial efforts were made to obtain high quality air-sea flux measurements which then were used to calibrate the flux maps obtained from operational centres. Also during one airplane transect at the time of a strong cold air outbreak yielded valuable high quality heat flux measurements from the marginal ice zone into the interior of the Labrador Sea.

A detailed description of some of the early findings of the experiments can be found in a group publication by the Labrador Sea Group (1998). In the following I will highlight a few aspects of the early results.

(A) The profiling floats in combination with the hydrographic surveys allowed us to map the maximal depth of the late winter convection and its regional extent. During the winter of 1996–1997 deep convection reached to 1500–2000 m depth. In particular the Month of February showed strong heat losses to the atmosphere. However, the winter average heat loss was less that in the early 1990s. The second winter (1997–1998) was even weaker and the maximum convection rarely exceeded 1000 m depth.

(B) Vertical float trajectories from the Lagrangian floats showed nicely the deepening of the well mixed layer and allowed to estimate plume turnover times. It is not clear yet to what extend the earth's rotation limits the efficiency of the convective mixing.

(C) Horizontal float trajectories, when averaged over the two years, were able to map the basin scale circulation in the Labrador Sea. As expected, the largest currents are found near the continental margin. However, there is evidence for extended recirculation just offshore of the boundary current. Moreover, the floats that started in the interior of the Labrador Sea are exported by two pathways. The majority of the floats became entrained into the boundary current and followed it southward. But some also left the Labrador Sea on a more north-easterly track toward the Irminger Basin.

(D) The hydrographic survey showed that two distinct types of newly ventilated water masses were formed. The denser one was found offshore of the Labrador Current close to the position of the former weather ship BRAVO. However, significant quantities of a lighter variety were found within the boundary current region. The proximity to the boundary current allows a rapid export of this newly ventilated water mass.

(E) All floats showed significant mesoscale energy in the Labrador Sea consistent with satellite based estimates. It is not clear yet if the mesoscale energy has a strong seasonal cycle and/or is regionally variable.

In summary, the Labrador Sea Convection Experiment was a very successful enterprise and we expect more exciting results in the next few years when all the data will be fully analysed.

Reference

The Labrador Sea Group, 1998: The Labrador Sea Deep Convection Experiment. BAMS, 79.

Variability of deep convection and boundary circulation 1996–1999

U. Send, F. Schott, C. Mertens, D. Kindler, and J. Fischer.

Moored observations in the Labrador Sea are available now for summer 1996 until summer 1999 from the special research initiative (SFB) running in Kiel (which studies the dynamics of thermohaline circulation variability) and for the year 1994–1995 from a joint IfM/BIO-UW mooring deployment (with P. Rhines, J. Lazier). The SFB years include convection moorings with ADCP and Seacat instruments in the interior and the boundary current, and 3–4 acoustic tomography moorings for sensing the larger-scale evolution of the stratification, Fig. 1.

The convection variability from year to year is well documented using depth-time contour plots of the temperature time series (surface to 2500 m) from the central Labrador Sea (K1/K11/K21). The observed convection depths in the different years were 94/95: 1800 m, 96/97: 1500 m, 97/98: 700 m, 98/99: 400 m. Comparison with surface heat fluxes shows a strong influence regarding the timing of convection, but the total November–March buoyancy loss each winter is not well related to the convection strength, 94/95: $0.56\,m^2/s^2$, 96/97: $0.69\,m^2/s^2$, 97/98: $0.47\,m^2/s^2$, 98/99: $0.50\,m^2/s^2$.

The horizontal extent of the convectively mixed cold region can be estimated using the horizontal temperature averages from tomography paths and the temperature information at the end points. This yields upper limits of 40 km toward the boundary current (K11–K12) and approx.

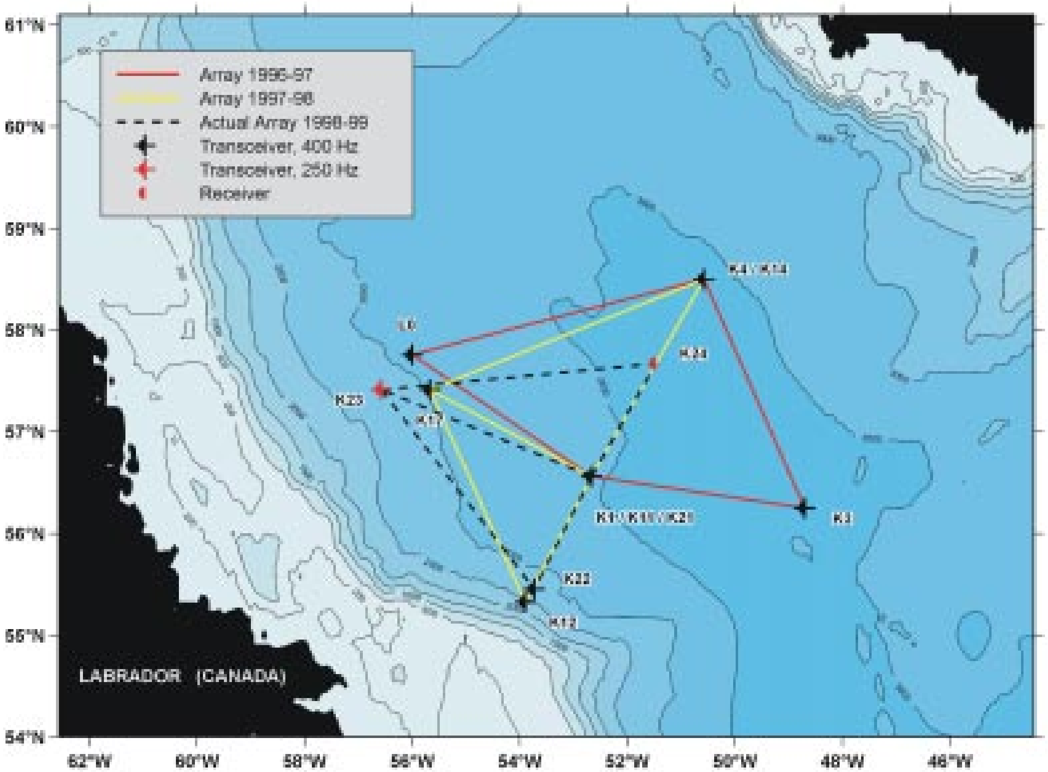

Figure 1. Location of SFB convection moorings (K1/K11/K21, K2/K12/K22) and tomography sampling paths (solid and dashed lines) for the first 3 years of the SFB.

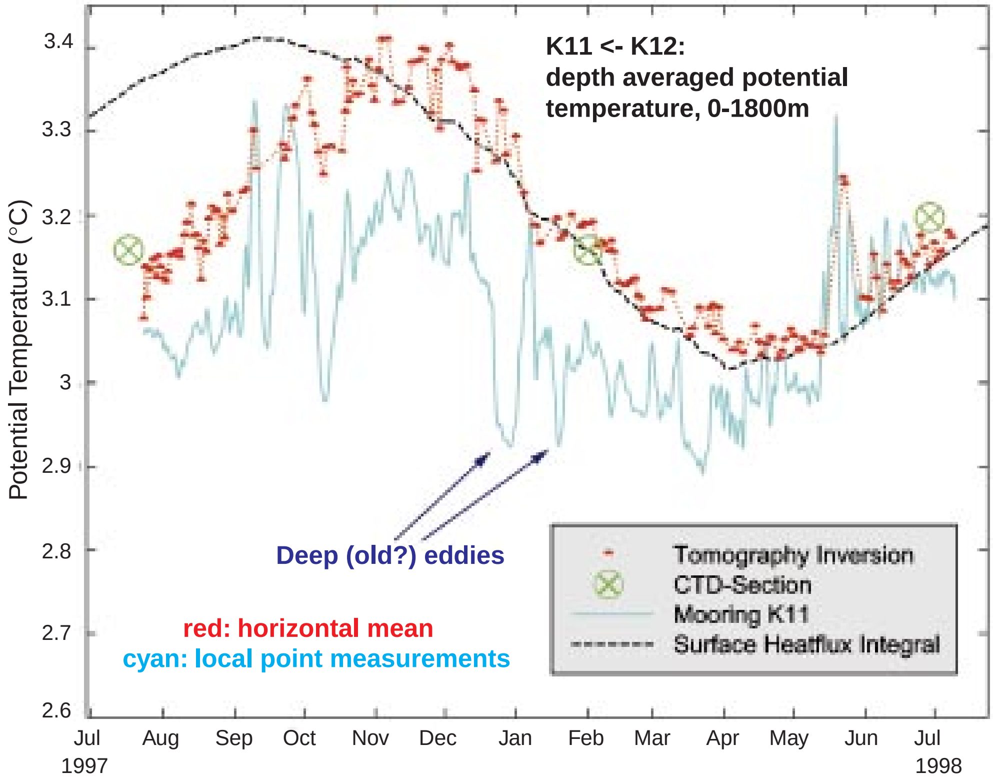

Figure 2. Comparison of NCEP surface heat flux integral (dashed) and heat content evolution averaged between the central mooring K11 and the boundary current mooring K12 (dotted line with large points). Starting in December, both the cooling and warming phase appear to follow a 1-D heat balance, while locally at K11 there is warming after deep convection (April) which is much larger than surface heat fluxes can explain.

100 km toward the interior (K11–K14) using data from 1997/98.

To investigate causes for the interannual variability other than the surface buoyancy flux, the initial stratification (here from our summer cruises) may be considered, as well as variability in the horizontal mixing/advection processes during mixed-layer deepening. It turns out that the summer stratification can qualitatively explain the apparent discrepancies between convection depth and winter buoyancy loss, e.g. the convection in 96/97 was only to 1500 m in spite of very large buoyancy loss because of rather high initial stratification. On the other hand, the horizontal advection of buoyancy during the cooling phase seems to be small, as judged from 1-D heat budgets, both local (at one mooring) and in the horizontal averages (from tomography).

The export of the convectively cooled water probably takes place mainly by lateral mixing/advection processes after the convective phase. Between the central mooring and the interior basin (K11-K14), large horizontal advection of heat takes place after the convection has ceased, with much faster warming than expected from surface heat fluxes. Along the line between the central mooring and the boundary current however (K11–K12), the horizontal average of heat remains constant while the boundary cools and the interior warms see Fig. 2. This is indicative of mixing exchange between the boundary and the central mooring. Indeed, the boundary mooring shows cooling signals after the interior convection, which cannot be locally generated and thus are consistent with, exchange with the basin interior. The boundary current also shows an increase in eddy kinetic energy at about the convection season, but whether this is related or fortuitous remains unclear an this point. No convection within the boundary current itself was observed so far (at the site of our mooring).

Labrador Sea convection in models and its relation to the large-scale thermohaline overturning circulation variability: A brief overview

E. P. Chassignet, with contributions from C. Böning, J. Dengg, A. Paiva, L. Smith, and A. M. Treguier

Very large differences in North Atlantic winter mixed layer depths are observed not only among simulations carried out with models of different architectures, but also among realisations performed with the same model but with different forcing, domain size, subgridscale parameterisations, etc…

In some cases, the sinking in the deep winter mixed layer regions contributes significantly to the overturning circulation. The following questions then arise:

- What are the factors responsible for the observed differences in model winter mixed layer depths?
- What are the physical processes behind the sinking in the deep winter mixed layer regions? Does the sinking contribute significantly to the overturning circulation?

This brief overview focuses primarily on the series of North Atlantic basin experiment comparisons performed in the framework of the CME (Community Modelling Experiment) and of DYNAMO (DYnamics of North Atlantic MOdels). The differences between the DYNAMO and CME experiments lie mainly in the domain configuration (inclusion of the overflows in DYNAMO vs. buffer zone at 65°N in CME), in the forcing (ECMWF in DYNAMO vs. Hellerman-Rosenstein Han in CME), and in the variety of models (LEVEL, ISOPYCNIC, and SIGMA in DYNAMO vs. LEVEL and ISOPYCNIC in CME)*.

Fig. 1 illustrates the variety of solutions that can arise when all models are configured as similarly as possible (DYNAMO, 1997). The region in which the model results differ most significantly is the Labrador Sea (Willebrand et

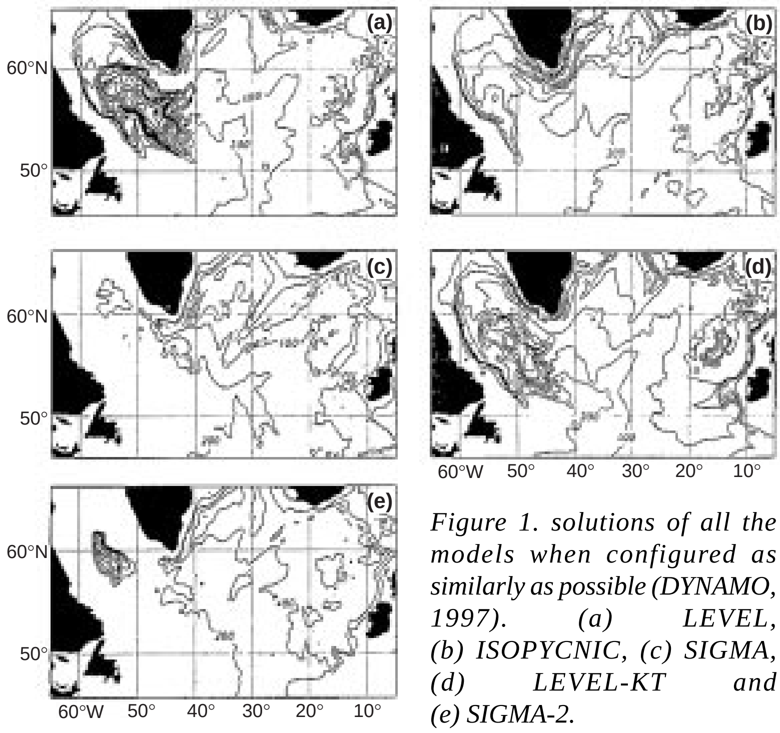

Figure 1. solutions of all the models when configured as similarly as possible (DYNAMO, 1997). (a) LEVEL, (b) ISOPYCNIC, (c) SIGMA, (d) LEVEL-KT and (e) SIGMA-2.

* LEVEL: GFDL-MOM code (Cox, 1984)
ISOPYCNIC: MICOM code (Bleck et al., 1992)
SIGMA: SPEM code (Haidvogel et al., 1991)

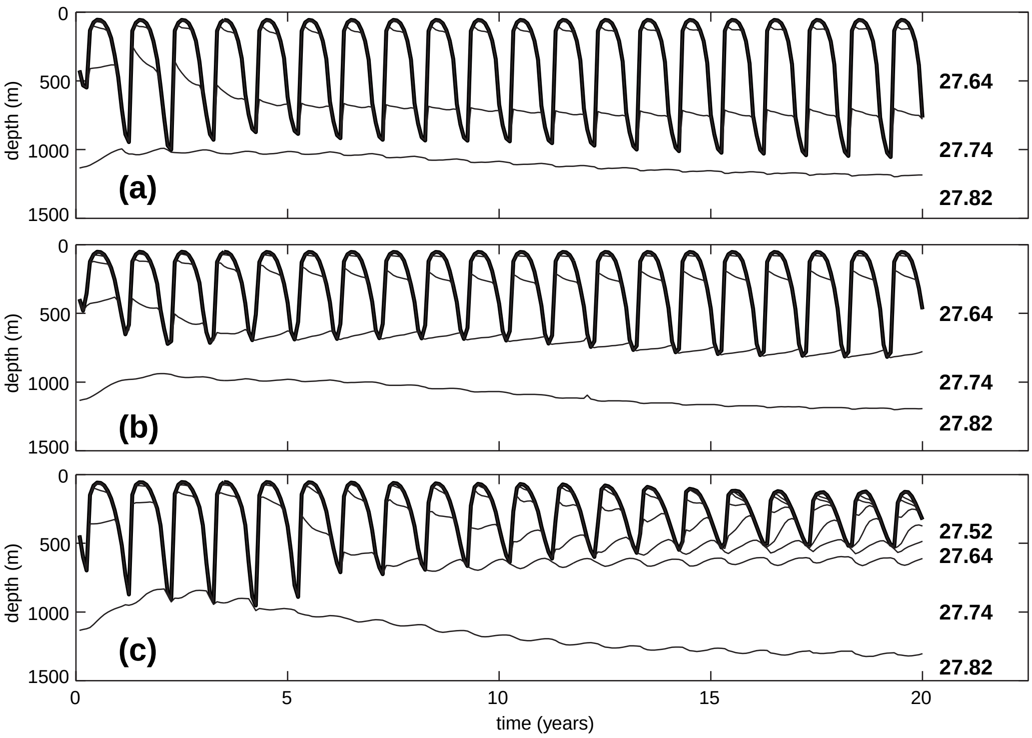

Figure 2. Time evolution of the layer interface depths in the central Labrador Sea. The surface forcing are: (a) prescribed E-P and a linear bulk formula for the heat flux, (b) prescribed E-P and the full bulk formulas for the heat flux and (c) relaxation to Levitus surface salinity and a linear bulk formula for the heat flux.

al., 1999). The winter mixed layer in LEVEL (Fig. 1a) is deeper than 1000 m over much of the region, reaching the bottom at the centre of the cyclonic gyre. In contrast, SIGMA (Fig. 1c) has a shallow winter mixed layer without any sign of deep convection. ISOPYCNIC (Fig. 1b) falls in between, with winter mixed layer depths ranging from 250 to 750 m over most of the region, exceeding 1000 m only within the boundary current. Small changes within a particular model can strongly influence the Labrador Sea mixed layer behaviour: a modified topography in SIGMA-2 (Fig. 1e) allows much stronger and deeper convection, while a Kraus-Turner mixed layer parameterisation in LEVEL-KT (Fig. 1d) reduces the maximum depth to 2500 m. Considerable changes are also observed in LEVEL as a consequence of modification of the lateral mixing scheme: a switch to isopycnal mixing from horizontal mixing produces deep convection patterns that resemble those observed in ISOPYCNIC.

Sensitivity experiments for ISOPYCNIC in the CME domain, carried out with various surface boundary conditions, also reveal substantial differences in the convection patterns. In Smith et al. (1999) with Hellerman and Rosenstein (1983) winds, Han (1984) linear bulk formula for the heat flux formulation, and relaxation to Levitus surface salinity, deep convection occurs both in the Labrador and Irminger basins down to 3000 metres. A similar pattern is seen in the corresponding LEVEL experiment (Böning et al., 1996), although the Irminger mixed layer depth in this case is relatively shallow (~700 metres). In ISOPYCNIC, however, despite relaxation to Levitus surface salinity, relatively salty water reaches the model Irminger basin via westward flow along the northern wall east of Greenland, destabilising the water column and permitting the onset of deep mixing.

The importance of the freshwater boundary conditions is further illustrated in a series of experiments performed by Paiva and Chassignet (1999) in the same CME configuration, except for the surface forcing which is based on COADS (Comprehensive Ocean-Atmosphere Data Set; da Silva et al., 1994). Fig. 2 shows the time evolution of the layer interface depths in the central Labrador Sea (averaged within latitudes 56–58°N and longitudes 50–52°W) for three experiments. The surface forcing consists of:

- prescribed E-P (evaporation minus precipitation) and a linear bulk formula for the heat flux (Fig. 2a)
- prescribed E-P and the full bulk formulas for the heat flux (Fig. 2b)
- relaxation to Levitus surface salinity and a linear bulk formula for the heat flux (Fig. 2c).

With prescribed E-P forcing, the mixed layer depth reaches 1000 m (Figs. 2a,b). With surface restoring conditions for salinity (Fig. 2c), a freshening of the surface layer leads to a shift from a regime with deep convection in the initial five years of the simulation, to one in which convection is restricted to the upper 500 m. This last result resembles in many aspects the interruption of convection observed in the 1960s (Talley and McCartney, 1982) associated with the Great Salinity Anomaly. In the model, however, the surface fresh water needed to inhibit convection originates at the inner edge of the North Atlantic current (Paiva, 1999).

In all these model results, there is very little correlation between mixed layer depths and overturning circulation strength. For example, the overturning circulation in SIGMA-2 is weaker than that in SIGMA despite the more intense convective events in the former (Fig. 1c,e). The contribution to the deep southward transport from sinking in the Labrador Sea is generally found to be weak in most LEVEL experiments (~1 Sv). However, this contribution increases to 3 Sv for cases with isopycnic mixing, Gent and McWilliams (1990) parameterisation, and a Kraus-Turner mixed layer. Contributions of 3 Sv magnitude are observed in ISOPYCNIC for the same horizontal resolution (Smith et al., 1999).

In summary, convection in the Labrador Sea takes many shapes and forms depending not only on the intrinsic model architecture, but also on factors such as surface forcing, advection of outside properties, boundary conditions, lateral mixing parameterisations, etc… In order to unravel this complex behaviour and understand the processes behind the differences, one must first perform model comparisons in a controlled environment, i.e., a process study of the Labrador Sea, in which all of the above effects can be analysed independently of the large scale circulation. The impact of the above-noted effects on the large-scale circulation is, however, significant, and also must be assessed.

References

Bleck, R., C. Rooth, D. Hu, and L. T. Smith, 1992: Salinity-driven transients in a wind- and thermohaline-forced isopycnic co-ordinate model of the North Atlantic. J. Phys. Oceanogr, 22, 1486–1505.

Böning, C. W., F. O. Bryan, W. R. Holland, and R. Döscher, 1996: Thermohaline circulation and poleward heat transport in a high-resolution model of the North Atlantic. J. Phys. Oceanogr., 26, 1142–1164.

Cox, M. D., 1984: A primitive equation three-dimensional model of the ocean. Tech. Rep., 1, GFDL, NOAA, Princeton University.

da Silva, A. M., C. C. Young, and S. Levitus, 1994: Atlas of surface marine data 1994. Volume 1: Algorithms and procedures. US Department of Commerce, NOAA, NESDIS, 83 pp.

DYNAMO, 1997: Dynamics of North Atlantic Models: simulation and assimilation with high resolution models. Technical report, Institut für Meereskunde. 334 pp.

Gent, P. R., and J. C. McWilliams, 1990: Isopycnal mixing in ocean circulation models. J. Phys. Oceanogr., 20, 150–155.

Haidvogel, D. B., J. L. Wilkin, and R. Young, 1991: A semi-spectral primitive equation ocean circulation model using vertical sigma and orthogonal curvilinear horizontal co-ordinates. J. Comput. Phys., 94, 151–185.

Han, Y-J., 1984: A numerical world ocean general circulation model. Part II: A baroclinic experiment. Dyn. Atm. Oceans, 8, 141–172.

Hellerman, S., and M. Rosenstein, 1983: Normal monthly wind stress over the world ocean with error estimates. J. Phys. Oceanogr., 13, 1093–1104.

Paiva, A. M., 1999: The impact of surface buoyancy flux variability on water mass formation in North Atlantic numerical simulations. PhD dissertation, Univ. of Miami, 135 pp.

Paiva, A. M., and E. P. Chassignet, 1999: Impact of surface flux parameterisations on North Atlantic simulations. To be submitted.

Smith, L. T., E. P. Chassignet, and R. Bleck, 1999: The impact of lateral boundary conditions and horizontal resolution on North Atlantic water mass transformations and pathways in an isopycnic coordinate ocean model. J. Phys. Oceanogr., in press.

Talley, L. D., and M. S. McCartney, 1982: Distribution and circulation of Labrador Sea Water. J. Phys. Oceanogr., 12, 1189–1205.

Willebrand, J., B. Barnier, C. Böning, C. Dietrich, P. Herrmann, P. D. Killworth, C. LeProvost, Y. Jia, J-M. Molines, and A. New: Circulation characteristics of three eddy-permitting models of the North Atlantic. Prog. Oceanogr., submitted.

2.4c North Atlantic water mass modification processes: Deep mixing and role of topography

Topographic effects on eddies and mixing in the Denmark Strait overflow plume

Rolf H. Käse, IfM Kiel, Germany.

IfM Kiel has surveyed the overflow region in eddy-resolving experiments for three consecutive years 1996–1998. The following findings may be important for the discussion of variability on scales that relate to long-term climate changes:

- Individual sections show large variations in plume thickness and core temperature,
- Maximum bottom density drops sharply within a few Rossby radii from the sill, while diminishing more slowly further downstream indicating different mixing mechanisms in the near and far field,
- Thin layers (<100 m) exist with velocities O(1 m/s) in the cross-slope flow region, but little entrainment is observed, indicating laminar flow with Froude numbers <4. Thin, cold but less fast layers are also found in the bottom parallel regime,
- Chains of cyclones and anticyclones develop further downstream and travel along the topography.

From the observed spatial variability it is concluded that dramatic warming events as reported by Dickson et al. (1999) are within the general variability limits and most likely are caused by entrainment of Irminger Sea water into the plume via the eddy chains and not by changes in the overflow sources.

Numerical simulations with a sigma-coordinate high resolution process model (Käse and Oschlies, 1999) are in good agreement with the observations regarding transport variability, eddy formation and role of eddies in water mass transformation.

Maximum core velocities are found at the maximum bottom slope, a consequence of the fact that patches tend to

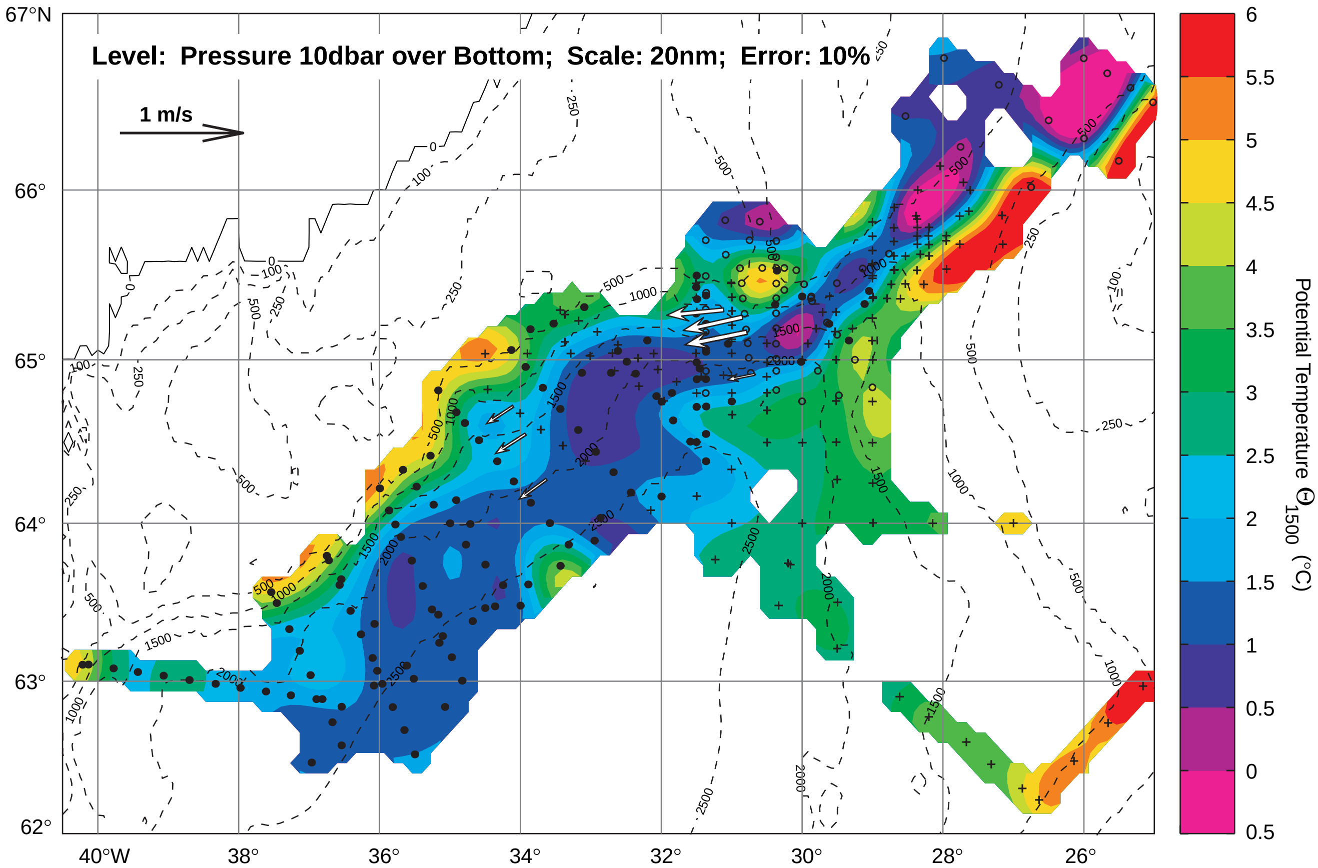

Figure 1. Bottom temperature from all three Poseidon cruises (CTD only) and some mean vectors from historical current meter records.

stretch quicker along strong topographic gradients. The observed probability density function of overflow thickness has the same character as the simulation, showing a maximum at 100–150 m and a secondary maximum near 300 m, the latter being related to doming in the cyclonic eddies.

References

Dickson, B., J. Meincke, I. Vassie, J. Jungclaus and S. Østerhus, 1999: Possible predictability in overflow from the Denmark Strait. Nature, 397, 243-246

Käse, R., and A. Oschlies, 1999: Flow through Denmark Strait. J. Geophys. Res., submitted.

Mixing and buoyancy forcing in an abyssal basin

Louis C. St. Laurent, J. M. Toole, K. L. Polzin, R. W. Schmitt, and J. R. Ledwell, Woods Hole Oceanographic Institution, USA

Observations of turbulence occurring above rough bathymetry in the abyssal Brazil Basin are considered. Levels of enhanced dissipation (ε) are clearly related to height above bottom (h_{ab}); and both spatial and temporal trends are present. The mixing levels along sloping bathymetry exceed the levels observed on ridge crests and canyon floors. Additionally, mixing levels modulate in phase with the spring–neap cycle of tides. Internal waves generated by barotropic tidal–flow over topography are the only mechanism capable of supplying the energy needed to support the observed dissipation rates; frictional boundary layer processes are not significant. A model of the dissipation rate $\varepsilon(h_{ab})$ is derived from data that was temporally de-aliased using an internal–wave energy scaling with a record of the barotropic tides, and the model retains a spatial dependence associated with the distribution of sloping bathymetry. The modelled dissipation rates are used to specify the turbulent diffusivity and constrain the diapycnal advection $(\omega*)$ in an inverse model for the steady circulation. This inverse model uses both beta-spiral and integrated forms of the advective budgets for heat, mass and vorticity, and provides sufficient information to resolve the full three–dimensional flow. The inverse model solution reveals the presence of a deep circulation with zonal character. On isopycnals above the level of fracture–zone crests, flow is westward and fluid is downwelled at rates of $\omega* = -(10-20)\,\mathrm{m}/\mathrm{yr}$. Along deeper isopycnals, fluid is carried eastward in canyons exceeding $\omega* = 30\,\mathrm{m}/\mathrm{yr}$ where the abyssal bottom shoals to meet the Mid Atlantic Ridge. This circulation accounts for $(0.3 \pm 0.1)\times 10^6\ \mathrm{m}^3\,\mathrm{s}^{-1}$ of local upwelling for the water class with potential temperature $\theta < 0.8$°C. These results suggest that mixing in abyssal canyons plays an important role in the mass budget of Antarctic Bottom Water.

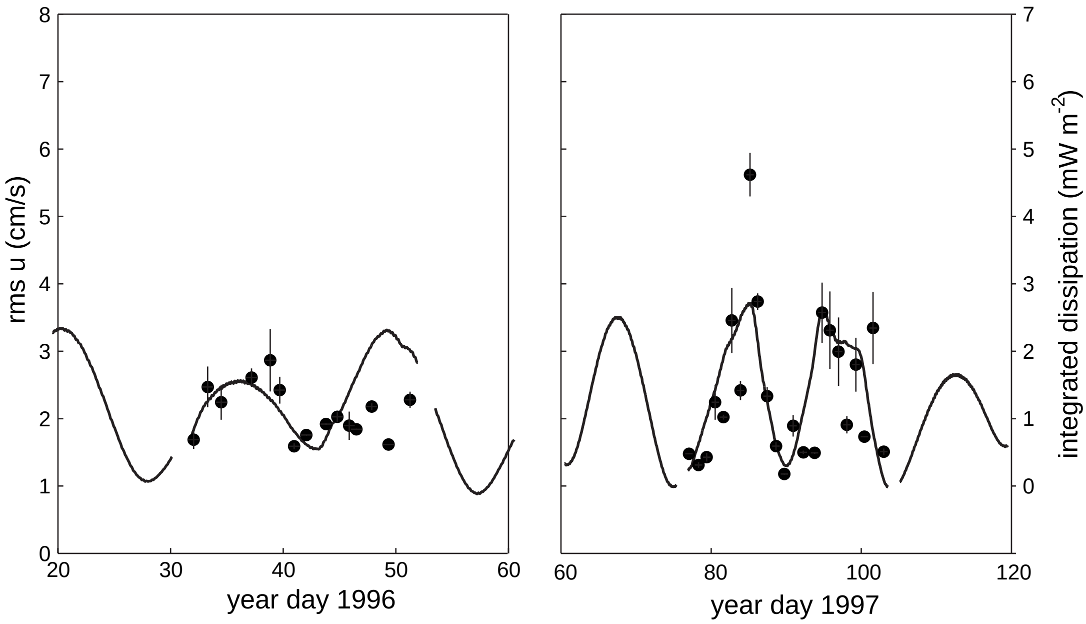

Figure 1. Comparison of column-integrated dissipation with estimates of barotropic tidal speed. The dissipation data ρεwere integrated to 2000 m height above bottom, and daily averages with standard errors are shown. The tidal velocity record was estimated using the TPXO model of Egbert et al. (J. Geophys. Res., 99, 24821–24852, 1994).

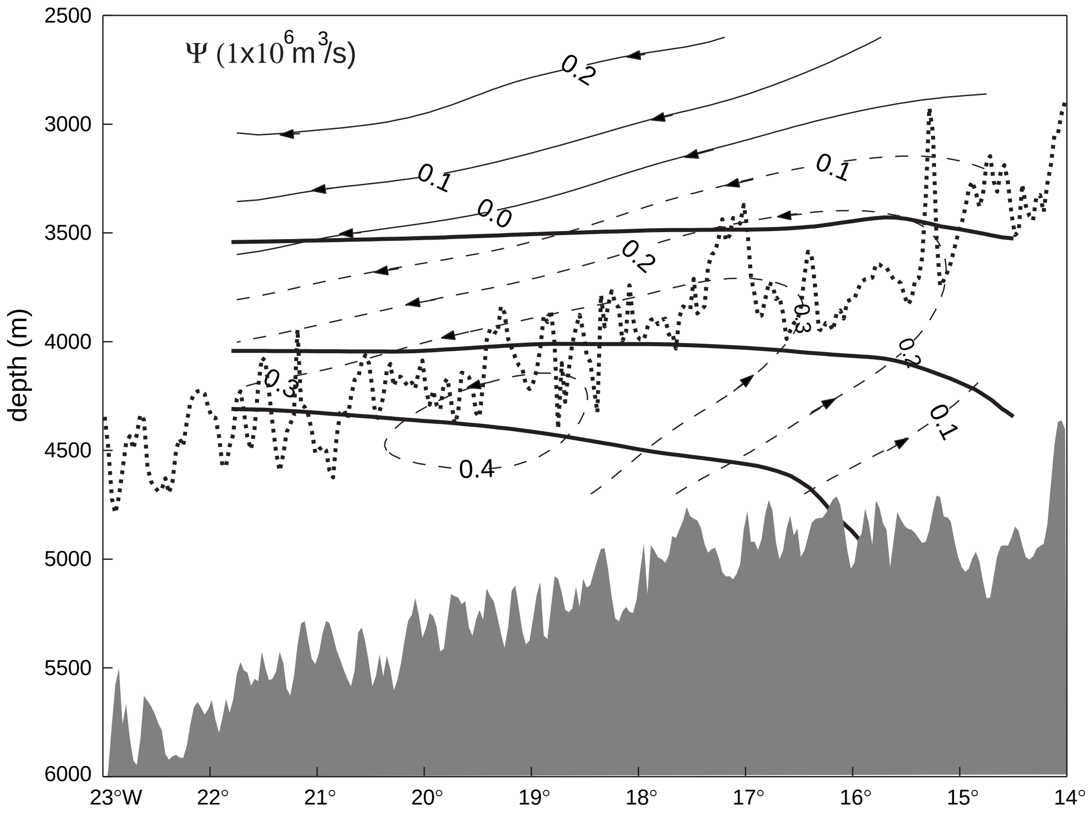

Figure 2. The meridionally integrated stream function as estimated through objective analysis of the inverse model solution. Representative bathymetry of canyon floors (shaded) and ridge crests (dotted) is shown, as are three deep isopycnals (thick lines). The deepest isopycnal corresponds to the 0.8°C isotherm, and (0.3±0.1) Sv of net up welling occurs across this surface in the region of the tracer release experiment.

2.4d North Atlantic water mass modification processes: Thermocline ventilation

Physics of thermocline ventilation in the North Atlantic

David P. Marshall, Department of Meteorology, University of Reading, UK. D.P.Marshall@met.reading.ac.uk

Ventilation is the primary process by which the atmosphere communicates with the ocean interior. Once subducted into the main thermocline, a water mass is shielded from atmospheric influence and may preserve its properties over great distances. A quantitative understanding of thermocline ventilation is thus important both for understanding the role of air–sea forcing in setting the structure of the thermocline, and for determining the rate at which heat, salt, carbon, and other tracers are transferred into the ocean interior.

Subduction

Ventilation of the main thermocline is associated with the transfer of fluid from through the base of the winter mixed layer into the main thermocline. Since the winter mixed layer depth varies from tens of metres in the tropics, to several hundred metres at high latitudes, ventilation is significantly enhanced through lateral transfer across the sloping mixed layer base, in addition to vertical transfer. Marshall et al. (1993) estimated the annual subduction rate from hydrographic and wind–stress climatologies in the North Atlantic (Fig. 1). They found subduction rates approaching 100 m over the subtropical gyre, roughly twice the maximum rate of Ekman pumping, a result that is confirmed by numerical models (e.g., New et al., 1995; DYNAMO Group, 1997). However, far than being spatially uniform, the subduction is generally concentrated into a narrow "subduction zone", associated with a sharp gradient in mixed layer depth running southwest–northeast across the subtropical gyre (Fig. 1). A consequence of this localisation is the subduction of weakly–stratified mode waters.

Subduction is not a year–round process. As first noted by Iselin (1939), the properties of the main thermocline match those of the winter mixed layer, rather than annual–mean mixed layer. Stommel (1979) explained this result in terms of a "mixed layer demon". The mixed layer undergoes a seasonal cycle, shallowing in summer and deepening in winter. Fluid parcels subducting from the shallow summer mixed layer are re–entrained when the mixed layer next deepens during the subsequent winter; only fluid parcels subducted in late winter can escape irreversibly into the main thermocline. Williams et al. (1995) tested Stommel's demon

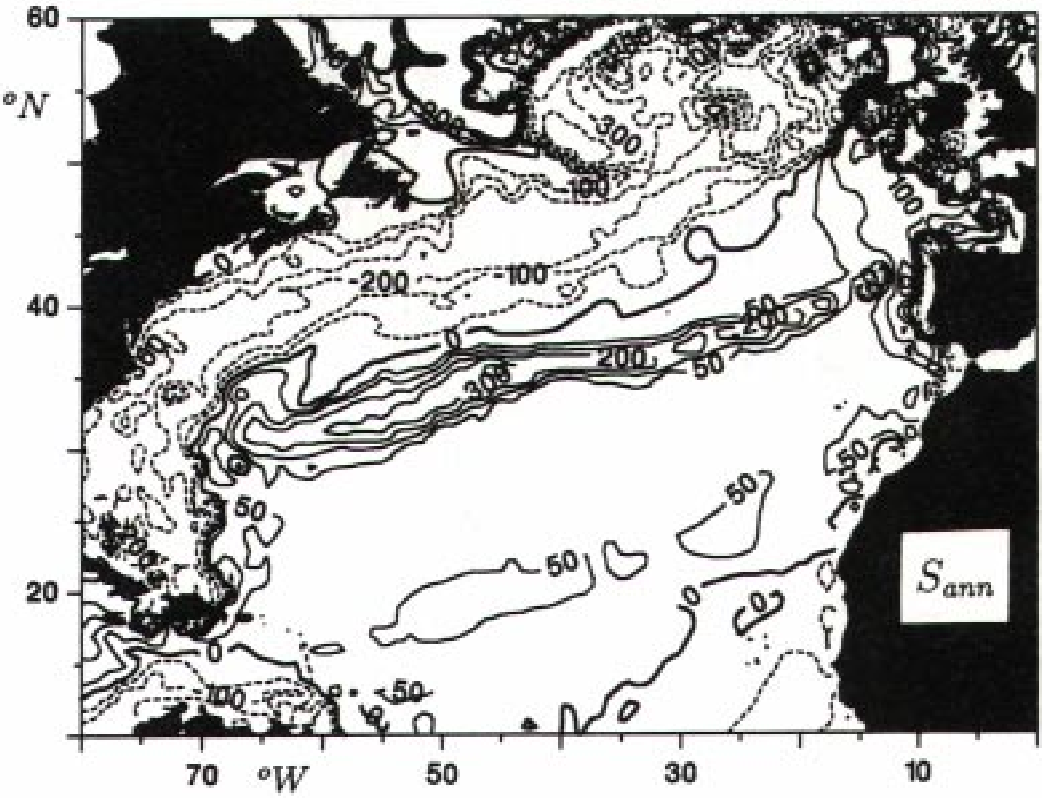

Figure 1. The annual subduction rate (m/yr) diagnosed by Williams et al. (1995) from the 1° CME model. The subduction is concentrated into a sharp "subduction zone" running southwest–northeast across the subtropical gyre.

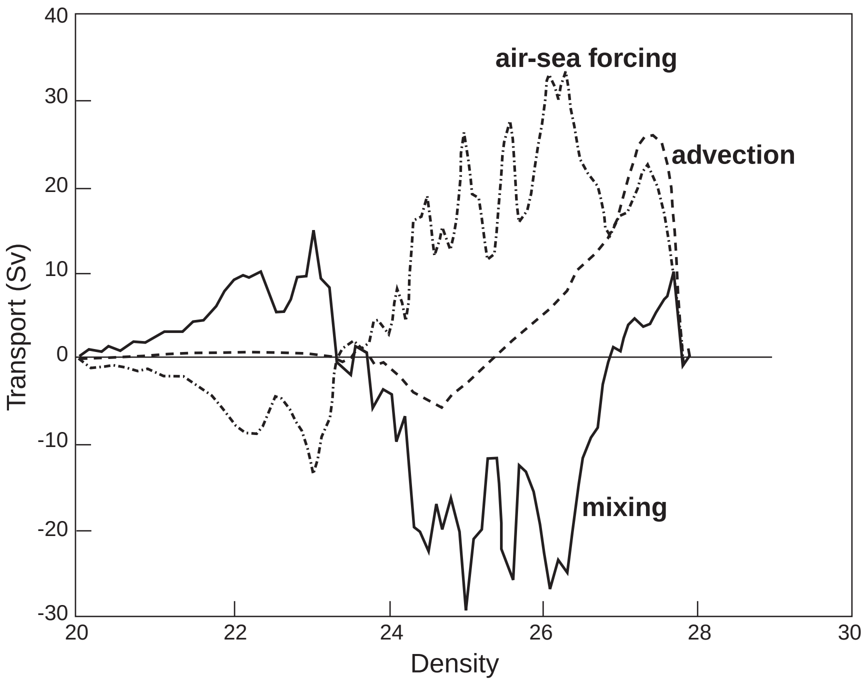

Figure 2. Water mass transformation inferred by Speer (1998) from Isemer and Hasse air–sea fluxes (dot–dashed line) and from hydrographic data at 11°S (dashed line). The difference can be attributed either to mixing or calculation uncertainty (solid line).

mechanism through a diagnostic analysis of the 1° CME model. In particular, using an idealised "date tracer", they found that fluid subducts into the main thermocline during a relatively short "subduction period" of about one month in late winter.

More recently, attention has turned to the role of mesoscale eddies in subduction. The impact of eddies on subducted water masses is clearly seen in the recent DYNAMO model experiments (DYNAMO Group, 1997): the subduction of low potential vorticity water is somewhat sporadic, and, in contrast to the laminar ventilated thermocline model of Luyten et al. (1983), the subducted potential vorticity anomaly is efficiently eroded through the action of the eddies. Such behaviour is consistent with findings from the recent "Subduction Experiment" (e.g., Joyce et al., 1998). However eddies do not merely modify the properties of subducted water masses, but may indeed modify the rate at which a water mass is subducted. The "eddy subduction" can be identified with the transfer of fluid into the main thermocline by the eddy–induced "bolus velocity" (Marshall, 1997), a secondary circulation associated with the flattening of isopycnals in baroclinic instability (Gent et al., 1995). In an idealised numerical experiment, Hazeleger and Drijfhout (1999) estimate that the eddy subduction may reach 100 m/yr in the subtropical gyre, enhancing the annual subduction by almost a factor of two. More work is required to determine the applicability of such results to the North Atlantic, but it seems likely that eddies may significantly modify subduction rates in frontal regions, such as the Azores Current.

Water mass formation

An alternative, but complimentary, approach to investigating thermocline ventilation is provided by the concept of "water mass formation" (Walin, 1982). The idea is that buoyancy fluxes transform water masses from one density class to another; the convergence of these transformation fluxes gives the net rate of water mass formation.

If water mass transformation within the surface mixed layer is associated purely with air–sea buoyancy fluxes, then one can infer water mass formation rates from climatological data. Using Isemer and Hasse surface fluxes, Speer and Tziperman (1992) found a net formation in two water mass classes, corresponding respectively to subtropical and subpolar mode water. The uncertainties associated with such calculations are large, both due to assumptions made in the methodology, as well as uncertainties in the climatological data. Nevertheless qualitatively similar results are obtained for different flux climatologies.

A large uncertainty with such estimates concerns the role of diapycnal mixing. Speer (1998) compared updated estimates of air–sea transformation rates with an independent dynamical estimate, obtained by evaluating the net northward volume transport within each density class at 11°S; the difference can be attributed either to calculation errors, or to diapycnal mixing (Fig. 2). Speer found the two estimates to be consistent within the main thermocline ($26.6 < \sigma < 27.6$), but that large mixing is required on lower density classes in the tropics, and also on higher density classes, most likely associated with the dense water overflows.

However such calculations cannot distinguish between mixing within the main thermocline, and mixing within the surface layer of the ocean. The latter is particularly important because, by modifying the buoyancy forcing of the surface mixed layer, it directly modifies water mass transformation rates (Garrett and Tandon, 1997). This issue was addressed in a numerical calculation by Marshall et al. (1999). Using data from a 1° resolution version of the MIT Ocean Model, Marshall et al. independently evaluated the diapycnal volume fluxes across density surfaces within the surface mixed layer, and compared these with the water mass transformation suggested by air–sea fluxes of heat and freshwater alone. They found significant discrepancies, that could be attributed to vertical mixing within the seasonal thermocline at low– and mid–latitudes, with lateral diapycnal fluxes also playing a role at high–latitudes. Further work is required to determine whether such findings carry over to eddy–resolving models.

Future issues

As we approach the end of the WOCE programme, I believe that we have obtained a good diagnostic understanding of thermocline ventilation, albeit with some significant uncertainties concerning the role of geostrophic eddies and diapycnal mixing. However, I am less convinced that we have an adequate prognostic understanding of thermocline ventilation. The spatial structure of the winter mixed layer is dynamically coupled with the underlying circulation. As already been remarked, it is the spatial inhomogeneities in mixing that give rise to the occurrence of mode waters. How will the spatial structure of the mixed layer change under different surface forcing? What are the consequences for the properties and ventilation rates of mode waters? What are the implications for decadal variability? These will be key issues over the next few years.

References

DYNAMO Group, 1997: DYNAMO. Dynamics of North Atlantic Models. Simulation and Assimilation with High Resolution Models. Institut für Meereskunde, Christian–Albrechts Universität, Kiel, 334 pp.

Garrett, C., and A. Tandon, 1997: The effects of water mass formation of surface mixed layer time–dependence and entrainment fluxes. Deep-Sea Res., 44, 1991–2006.

Gent, P. R., J. Willebrand, T. J. McDougall, and J. C. McWilliams, 1995: Parameterizing eddy–induced tracer transports in ocean circulation models. J. Phys. Oceanogr., 25, 463–474.

Hazeleger, W., and S. S. Drijfhout, 1999: Eddy subduction in a model of the subtropical gyre. J. Phys. Oceanogr., in press.

Iselin, C. O'D., 1939: The influence of vertical and lateral turbulence on the characteristics of waters at mid–depths. Trans. Amer. Geophys. Union, 20, 414–417.

Joyce, T., M., J. R. Luyten, A. Kubryakov, F. B. Bahr, and J. S. Pallant, 1998: Meso– to large–scale structure of subducting water in the subtropical gyre of the eastern North Atlantic Ocean. J. Phys. Oceanogr., 29, 40–61.

Luyten, J. R., J. Pedlosky, and H. Stommel, 1983: The ventilated thermocline. J. Phys. Oceanogr., 13, 292–309.

Marshall, D. P., 1997: Subduction of water masses in an eddying ocean. J. Mar. Res., 55, 201–222.

Marshall, J. C., D. Jamous, and J. Nilsson, 1999: Reconciling thermodynamic and dynamic methods of computation of water–mass transformation rates. Deep-Sea Res., 46, 545–572.

Marshall, J. C., A. J. G. Nurser, and R. G. Williams, 1993: Inferring the subduction rate and period over the North Atlantic. J. Phys. Oceanogr., 23, 1315–1329.

New, A. L., R. Bleck, Y. Jia, R. Marsh, M. Huddleston, and S. Barnard, 1995: An isopycnic model study of the North Atlantic. Part I: Model experiment. J. Phys. Oceanogr., 25, 2667–2699.

Speer, K. G., and E. Tziperman, 1992: Rates of water mass formation in the North Atlantic Ocean. J. Phys. Oceanogr., 22, 93–104.

Speer, K. G., 1997: A note on average cross–isopycnal mixing in the North Atlantic Ocean. Deep-Sea Res., 44, 1981–1990.

Stommel, H., 1979: Determination of water mass properties of water pumped down from the Ekman layer to the geostrophic layer below. Proc. Nat. Acad. Sci., 76, 3051–3055.

Walin, G., 1982: On the relation between sea–surface heat flow and thermal circulation in the ocean. Tellus, 34, 187–195.

Williams, R. G., M. A. Spall, and J. C. Marshall, 1995: Does Stommel's mixed layer "demon" work? J. Phys. Oceanogr., 25, 3089–3102.

The use of tracers to study thermocline ventilation

W. J. Jenkins, School of Ocean and Earth Sciences, Southampton University, UK.

Because of their basic similarities, the distributions of transient tracers tend to look similar. The 1988 meridional sections of CFC-11, CFC-12 and tritium along ~20°W presented by Doney et al. (1996) share many common features, especially the way that they outline the leading edge of the transient tracer front as it dyes the meridional overturning cell, and their downward penetration into the main thermocline. Such observations provide

(1) a direct visualisation of the pathways and magnitude of ventilation.

There are important differences, however, which are driven by the fact that each tracer has its own unique boundary conditions and time history. The CFCs, for example, have relatively latitude-independent, monotonically increasing atmospheric concentrations, and significant equilibrium solubility temperature dependence. Tritium, on the other hand exhibits a pronounced latitudinal gradient, a more impulse-like time history, and a vapour-precipitation coupled deposition. Such differences, although complicating tracer distribution interpretation, are

(2) a source of information regarding the mechanisms of ventilation.

Several approaches have been used to construct "Tracer Ages" based on a variety of simple concept models. Such quantities provide immediate and direct qualitative assessment of water mass ages, but have subtleties: in the presence of significant mixing, they become non-linearly biased estimates of "true" age. Thus it must be stressed that

(3) tracer age systems must be used with caution.

Having admitted this, however, one might add that inasmuch as such systems are influenced by mixing, consideration of

(4) deviations from "ideality" or differences between tracer ages may yield information about the relative roles of mixing and advection in ventilation.

This paper presents some specific examples of these points, including results from the Subduction Experiment performed in the Eastern North Atlantic in the early 1990s (e.g. see Jenkins, 1998).

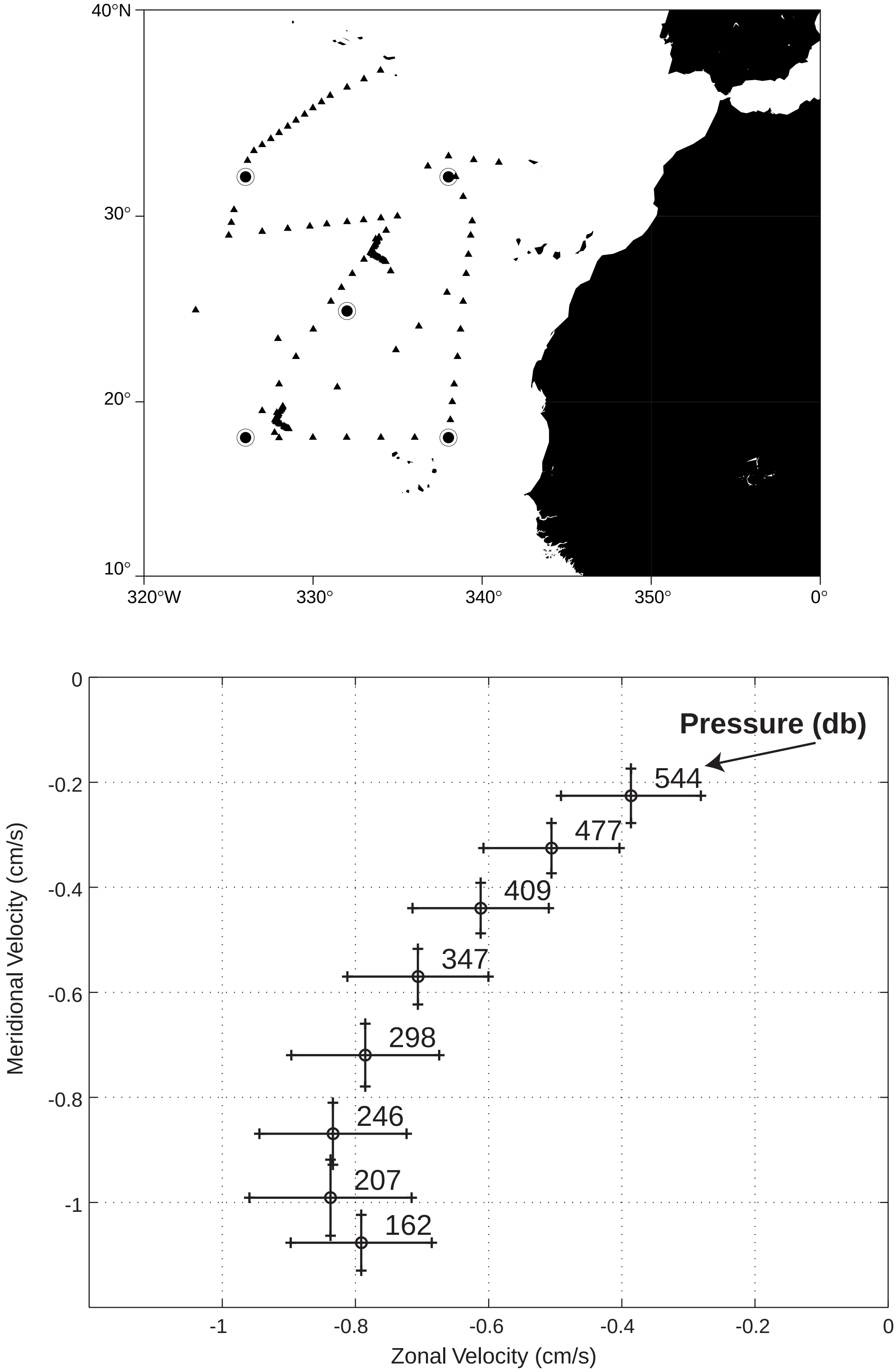

Figure 1. Subduction Experiment Station Locations (top) and Diagnosed absolute velocity spiral (bottom).

On shallow isopycnal surfaces ($\sigma_0 < 26.7\,\mathrm{kg\,m^{-3}}$) in the Subduction Area, tritium-^{3}He age has been combined with salinity and geostrophic balance to determine the reference level velocity and hence an absolute velocity spiral to an accuracy of $1\,\mathrm{mm\,s^{-1}}$ (Jenkins, 1998 and Fig. 1). The technique also yields vertical velocity estimates that are quantitatively consistent with large-scale vorticity balance, two estimates made from isotherm-following floats, and extrapolates to ECMWF-derived Ekman pumping rates at the base of the mixed layer (Jenkins, 1998). Further, the technique estimates isopycnal diffusivities and oxygen consumption rates.

The Subduction Area inversion described above takes into account all the non-linear terms in the age equation, and is thus a complete treatment of the problems associated with that age tracer. The non-linear terms are less than 10% throughout the thermocline, but the unsteady (time-dependent) term increases with depth, exceeding 20% on the deeper isopycnals ($\sigma_0 > 26.7\,\mathrm{kg\,m^{-3}}$) and approaches 50% at 600 m depth. That is, the deeper ages are increasing at the rate of several months per year. The increase can be shown, using AOU distributions to be a characteristic of the age-tracer "dynamics", rather than any secular change in water mass age (Robbins and Jenkins, 1998). This time dependent behaviour of the tracer age is a distinct signature throughout the deep thermocline of the entire subtropical gyre and must be due to a diffusive, non-advective ventilation of these isopycnal surfaces across the Azores Front (Robbins et al., 1999). This interpretation is further supported on the basis three additional lines of evidence:

- The gyre scale tritium-^{3}He scatter plot is consistent with a low peclet-number stream-tube simulation (Jenkins, 1988),
- The maximum gyre "stable tritium" values are only about one third the historical maximum surface water values (Jenkins, 1998),
- There is a distinct bend in the tritium-^{3}He vs. P_{CFC} age curves presented by Doney et al. (1996) for these isopycnals.

We then ask how such inter-gyre exchange might be accomplished? There is a fundamental conundrum that we must face. Sarmiento's (1983) calculation, based on the observed inventory of tritium in the North Atlantic main thermocline, requires a "net" surface water subduction of approximately 40 Sv, yet direct Ekman pumping accounts for only about 1/4 to 1/3 of this volume flux. It is tempting to rely on lateral induction mechanisms to achieve this extra flux, and indeed the large-scale topography of North Atlantic winter mixed layer depths seems consistent with such a conclusion. However, the strong diffusive signature in the tracer fields denies such an advective mechanism. Moreover, consideration of the climatological Montgomery stream-lines for the area show no significant meridional advection across the Azores Front. Robbins et al. (1999) suggest eddy transport across the Front as the means of ventilation for the deeper isopycnals, but I suggest here an additional candidate process. A simple, idealised model calculation reveals the potential significance of this mechanism.

Consider here a double Stommel gyre, corresponding to the subpolar and subtropical gyres, driven by a simple wind stress described by

$$\tau = \cos[\pi(y - y_0(t)],$$

where the zero-curl latitude $y_0(\mathrm{t})$ time dependent, here given by the simple function

$$y_0(t) = \Delta y \sin(\omega t).$$

As the zero-curl latitude migrates, those waters whose meridional velocity is smaller than the propagation velocity of the zero-curl latitude are in effect "captured" by the other gyre, and exchanged across the boundary. We can thus compute the mass flux between the critical latitude and the zero-curl latitude as

$$M = \Delta y \omega H \Delta x \cos \omega t,$$

where H is the basin depth (about 1 km) and ΔX is the basin width (about 4000 km). For an annual migration (Δy) of 50 km, this leads to a r.m.s. mass-exchange of about 25 Sv. Larger amplitude, but slower inter-annual migrations, such as those associated with NAO events may in fact lead to similar scale gyre exchanges. While the above schematic calculation is overly simplistic, it does illustrate an additional mechanism of gyre exchange.

In summary, tracers provide direct visualisation and quantification of circulation and ventilation rates within the main thermocline. Furthermore, coupling of tracer systems allow a determination of the mechanics of ventilation. Consideration of tracer and tracer-age systematics in the Eastern Subtropical North Atlantic reveal that the upper main thermocline is advectively ventilated, while diffusive ventilation appears important for the lower thermocline.

Acknowledgement

The author thanks R. X. Huang for invaluable guidance in the gyre exchange calculation.

References

Doney, S. C., W. J. Jenkins, and J. L. Bullister, 1996: A comparison of ocean tracer dating techniques on a meridional section in the Eastern North Atlantic. Deep-Sea Res., 44, 603–626.

Jenkins, W. J., 1988: The use of anthropogenic tritium and helium-3 to study subtropical gyre ventilation and circulation. Phil. Trans. Roy. Soc. (London) A, 325, 43–61.

Jenkins, W. J., 1998: Studying thermocline ventilation and circulation using tritium and ^{3}He. J. Geophys. Res., 103, 15817–15831.

Robbins, P. E., and W. J. Jenkins, 1998: Observations of temporal changes in tritium-^{3}He age in the Eastern North Atlantic thermocline: evidence for changes in ventilation? J. Mar. Res., 56, 1125–1161.

Robbins, P. E., J. R. Price, H. B. Owens, and W. J. Jenkins, 1999: On the importance of lateral diffusion for the ventilation of the lower thermocline in the subtropical North Atlantic. J. Phys. Oceanogr., 29, in press.

Sarmiento, J. L., 1983: A tritium box model of the North Atlantic thermocline. J. Phys. Oceanogr., 13, 1269–1274.

3. WORKING GROUP REPORTS

3.1 WG 1: WOCE synthesis products
(co-chairs: J. Marotzke and L. Talley)

3.1.1 Towards WOCE Synthesis

The following informal classification of synthesis products was considered (C. Wunsch):

- Level I: Result of assembly/quality control of a single data type;
- Level II: Atlases, maps, etc. (combination of data and statistical assumptions);
- Level III: Assimilation product; consistent with data and model dynamics; time-dependent (the analogue to the atmospheric "reanalysis")

The WG1 felt that there were no fundamental conceptual obstacles to the WOCE synthesis effort. While there are significant challenges (see below), synthesis is ongoing at all levels. In particular, with the recent decision to fund at least one continuing global data assimilation effort through the US National Ocean Partnership Program (NOPP), Level-III type synthesis has started.

Points that were discussed explicitly (from Level I to Level III):

- **Level I,** Compilation and quality control of tracer data: Well underway, no significant problems anticipated (R. Fine). However, the "float dataset" was discussed in detail, because it was felt that it posed the biggest challenge from a single type of platform. Float data are so heterogeneous in every respect that one can hardly speak of a "float dataset" as such. Sampling is inhomogeneous in space and in time. The basic analysis yields trajectories, Eulerian (box) averages of first and second statistical moments, hydrographic profiles, or along-track hydrography, or some combination of these. Important identified issues were: data release and submission policies, the use of trajectory information in quantitative model-data comparisons (difficult because of the chaotic nature of trajectories), and (related) to ensure that the trajectory information is archived properly, even though it might not enter current Level-III-type synthesis efforts
- **Level II,** Hydrographic atlases: Several efforts are underway (see Table 1). The potential of redundancy was discussed, but it was felt that the possibility of comparing differing approaches justified parallel efforts.
- **Level-III-type synthesis:** The largest unsolved scientific problem is the lack of accurate error characterisations in both model and data. This point is central since one must state how well a model is supposed to fit observations. Fundamental issues are systematic model errors and error correlation structures.

3.1.2 Need for adequate supercomputing support

Computing was identified as the largest PRACTICAL problem encountered by WOCE synthesis efforts. In the US, the lack of adequate supercomputer support has reached critical dimensions. The NSF-funded supercomputer centres are hopelessly oversubscribed, and NSF is unwilling to support local mini-supercomputer purchases, which currently seem the only strategy by which Level-III-type synthesis could be performed. In Europe, the situation is somewhat better since there is no embargo against Japanese vector computers, but support of high-end supercomputing has not been sufficient either. It was suggested that WOCE (or CLIVAR) must make its voice heard toward increased high-end computing support for the ocean sciences.

3.2 WG 2: Improved parameterisations for large-scale models
(co-chairs: A.-M. Treguier and C. Böning)

The objective of WG2 was to revisit those issues most relevant to the North Atlantic circulation, building upon the information provided by the talks and posters during the previous days. The aims were to propose strategies to improve large scale climate models, and suggest which observations and datasets could best provide guidance and help validate the model results.

Table 1. Overview of various Hydrographic Climatology efforts (to be extended). The climatology of A. McDonald is summed under Hydrobase (K. Jancke, August 1999).

	Levitus 1x1	*Levitus .25x.25*	*SAC*	*Hydrobase*	*Reynaud*
Region	Worldwide	Worldwide	South of 70° N	Worldwide	Atlantic
Horizontal resolution	1x1 deg	.25x.25 deg	1x1 deg, other grids upon request	.5x.5 deg, potential for any gridscale	1x1 deg
Time resolution	Monthly	Seasonal?	Steady (monthly soon)	Monthly, Annual, Composites of years	Seasonal
Vertical resolution			45	As many as desired	72
Interpolation level type	Isobaric	Isobaric	Isopycnal	Isopycnal (mixed layer model at surface)	Isobaric
Interpolation method	Optimal interpolation	Optimal interpolation	Optimal interpolation	Optimal interpolation, direct integration	Averaging, varying region size
Parameters	TSO_2, Nuts	TS???	TSO_2, (Nuts)	TSO_2, Nutrients, Tracers	TS
Data basis	WOA	WOA	WOA, WOCE, SODB, pers. comm.	WOA, WOCE, ICES, pers. comm	WOA
Quality control	Std	Std	Statistics of theta-property	Statistics of theta-property	Extended

A list of critical processes was identified: flow over sills and through narrow passages, downslope flow of dense water masses and near-bottom mixing, convection, and parameterisation of eddies. Additional potentially important processes were tidal mixing; the representation of western boundary currents and the residual mean circulation.

Before talking about improvement of climate models it is best to agree on which physical processes are important for climate on the decadal time scales. The sill and overflow problems were unanimously found important, but the effects of different parameterisations of convection and deep mixing on the circulation were less clear. A more structured discussion on this issue was not possible for lack of time.

3.2.1 Flow over sills and through narrow passages

The problem can be set in the following way (P. Killworth): knowing the profiles of temperature and salinity on each side of the sill, predict the depth of the layer of fluid that goes in one direction and the other (that is, the position of the interface assuming a two-layer fluid); predict the volume fluxes F in each direction, and if mixing is important the transformed properties of the water downstream. There is no general analytical solution, especially in the rotating case. Probably, if more manpower can be devoted to the problem, semi-empirical formulae may be found for the most important sills. Such studies must rely on observations and high resolution model experiments.

It was suggested to concentrate efforts on the sills that have potentially the largest effect at decadal scales: in the North Atlantic, the Denmark Strait, Faroe Bank Channel and Strait of Gibraltar are the most obvious candidates. Observations upstream and downstream of the sills exist and could be compiled. However there are no clear observations of what is needed the most, namely the tendencies: for example, how do the properties downstream of Denmark Strait vary when the upstream properties change?

3.2.2. Downslope flow of dense water

Present climate models and even eddy permitting models (e.g., the DYNAMO intercomparison) do not represent the downslope flows correctly. Horizontal and terrain-following co-ordinate models (for different reasons) exaggerate the mixing of water masses as they flow down; isopycnic models have too little mixing. Several parameterisation schemes have been proposed recently: bottom boundary layer schemes for level models, and Richardson-number dependent mixing for isopycnic co-ordinates models. A few teams are proposing an intercomparison of those schemes in different models, at the local (one sill) and global scale. The recommendation of the working group is to publicise this intercomparison, to open it to other teams, and to document the model configurations so that new parameterisations can be tested later under the same conditions.

Such intercomparisons need to include a realistic configuration (Denmark Strait is proposed) to allow the use of oceanic data to validate the models. High-resolution models are not sufficient: they produce different solutions according to the details of their mixing schemes. The recommendation is to quantitatively evaluate and compare the volume flux of dense waters downstream of the sills. The properties of the sill flow and the properties of the water it mixes with must also be considered.

3.2.3 Convection

A variety of results about deep convection in the Labrador Sea were presented during the main sessions and poster presentations. Different models forced with similar climatological fluxes reveal large differences in the depth and horizontal patterns of convection in the Labrador Sea. On the other hand, models forced with time varying fluxes (i.e., based on reanalysis products) indicate an interannual variability of convection depth not unlike the observations. The two main questions identified were: what are the reasons for the existing big model differences in the simulation of convection properties; and what is the impact of changes in deep convection properties on the large-scale circulation.

Present model results suggest that there is only a small dynamical response outside of the subpolar gyre (e.g., on the meridional overturning circulation) of temporal changes in convection properties or, similarly, of the existing large model-model differences in these properties. Systematic model problems cannot be ruled out, however; e.g., observations underline the importance of the exchanges with the boundary current. It was recommended therefore to restrict model evaluations not to the depth and area of deep winter mixing, but also quantify the export of newly formed LSW out of a control volume (to be defined) which may not be directly related to the depth or extent of the convective region.

If other climatic factors are considered (carbon uptake by the ocean) then convection in the deep mixed layers of the subpolar gyre outside of the Labrador Sea may be quantitatively more important than the deep Labrador Sea convection. Key parameters to measure in the models are the depths of those mixed layers and the time during which they exist. In general, more analysis is needed to understand why models have very different convection patterns in the Labrador and Irminger Seas, i.e. what are the respective roles of air-sea fluxes, model resolution and parameterisations.

3.2.4 Deep mixing

There is evidence for increased vertical mixing above rough topography (St Laurent). Does the amount and distribution of diapycnic mixing matter over time scales shorter than 100 years? It remains to be demonstrated for the variability, but of course it effects the time-equilibrium solution of climate models. A parameterisation of the process should take into account tidal energy, bottom roughness, and deep stratification. Mixing coefficients can (perhaps) be derived from “classical” data (ADCP, CTD) with assumptions about the internal waves providing constraints for the parameterisations.

3.3 WG 3: Description of decadal North Atlantic variability *(co-chairs: M. Latif and J. Willebrand)*

3.3.1 Description of decadal North Atlantic variability

Decadal variability in the North Atlantic Ocean shows a number of features which appear to be robust from both observations and models. While the temporal variability shows a continuous red spectrum, with no preferred periods, the spatial patterns of surface temperature and ocean heat content, however, are clearly dependent on the time scale. At decadal time scales (10–20 years), a North Atlantic tripole structure is apparent, with positively correlated regions between 50° and 15°N, and a negative correlation around 30°–40°N. At multidecadal time scales, this pattern is replaced by an Atlantic dipole, with positive correlation over most of the North Atlantic, and negative correlation in the South Atlantic. In models this dipole pattern is correlated with Thermohaline Circulation (THC) variability.

The variability of the THC is not well known. Models show generally weak variations of the meridional overturning (max. ±2 Sv). While direct observations of Meridional Overturning Cell (MOC) variability are not available, estimates suggest considerably larger variations. In order to test the assumptions used for the observational estimates, it was suggested to apply the estimation procedure to the output of a high-resolution ocean circulation model. Decadal changes in convection and watermass formation are well described, in particular in the Labrador Sea, where convection has the opposite phase compared with the Greenland Sea. There is little evidence for decadal variations of the overflows through Denmark Strait and the Iceland–Scotland regions.

Ocean models forced by observed air-sea fluxes over the last 40 years show very similar responses, which largely agree with the available upper ocean observations and observed deep watermass formation rates. On the other hand, decadal fluctuations in coupled models show a strong dependence on the effective strength of ocean-atmosphere coupling, in particular through the heat flux. While SST-patterns in most models are rather similar, and in rough agreement with observations, the time scales of THC-variations in models are very different, with dominant periods between 10 and 50 years. The reasons for this difference is unknown and likely related to different generation mechanisms. Model intercomparison projects and sensitivity studies focusing on decadal variability will be necessary to clarify causes. These projects will need to include both the oceanographic and atmospheric communities.

When considering observations of decadal variability, one has to remember that it takes decades to obtain new observations. It is therefore important to design new observations in such a way that also facilitates the use and interpretation of existing historical data sets. As an example, the possible relation of the thickness of the cold bottom layer to the strength of the overflow should be investigated, both through observational and/or modelling studies. If such a relationship can be found, it would give a ‘proxy’ for the THC strength, which would allow inferences back over several decades. There was agreement that direct observations of the THC are urgently needed. Their feasibility should be studied, in particular possible errors due to strong barotropic recirculation systems.

3.3.2 Mechanisms of decadal variability

The oceanic reaction to the North Atlantic Oscillation (NAO) is rather well understood, both from observations and model studies. Much of the observed ocean variability, including the SST-tripole and the phases of convection in the Labrador and Greenland Seas, can be explained as forced by the NAO. There is, however, an open question related to the relative roles of local vs. remote wind forcing in the western subtropical gyre. Dynamical considerations suggest remote forcing, whereas observations indicate local forcing. Variations in wind stress and in heat flux are important as forcing mechanisms; the latter are relatively stronger at longer time scales. Changes in the buoyancy flux over the Labrador Sea have a direct influence on variations in the THC which are, however, restricted in models to north of 45°N. The variability of LSW export as estimated from buoyancy fluxes is of the order of 10 Sv, which is significantly larger than the THC variability in models (1–2 Sv); the difference is likely due to lateral processes which need better understanding. Some evidence exists for an influence of LSW production on the Gulf Stream position, and models have shown some sensitivity of the Gulf Stream separation to the strength of the DWBC. The question whether this is important on decadal time scales, however, remains open and cannot be investigated with models of the present resolution.

The question to what degree the decadal mid-latitude ocean variability can feed back onto the atmosphere is highly controversial, and was identified as a primary research issue for the coming years. Results from ocean models suggest a very weak feedback on time scales of 1 to 2 years, and a somewhat larger oceanic influence on time scales of 30 years and longer. It was noted that the ocean influences the atmosphere not only through direct dynamical coupling via SST and sea ice, and that indirect influences through changes in carbon uptake and ocean biology also need to be considered.

The question whether or to what degree the tropic-subtropics variability is influenced by changes in subpolar latitudes was discussed. Such an oceanic ‘bridge’ would be potentially important, as the atmosphere is known to be sensitive to tropical SST variations. One relationship between high and low latitudes exists through the SST-tripole; its causes, however, are unknown and could involve ocean waves, advection through western boundary currents, as well as atmospheric pathways.

3.4 WG 4: Requirements for future observations
(co-chairs: U. Send and M. Visbeck)

The topic of this working group is an issue that many other bodies had previously addressed and drafted recommendations for, e.g. within the framework of CLIVAR and GOOS. Thus, requirements and plans for future observations in the Atlantic exist already from several other sources, and implementation for a number of these is well under way. In view of this and of the short time available for the working group discussion and the large number of participants, it seemed impossible, and in fact inappropriate, to start from scratch with discussions about future observations. A more constructive discussion was expected by starting from the current state of observing (systems) plans, as a strawman structure, and to seek input, criticism, suggestions from the working group about the various points, in the light of the presentations at the conference. A full discussion did not always develop, and was also not possible, for all types of observations planned. However, broad agreement on an issue implies that it is consistent with the current knowledge of ocean processes (or our lack thereof).

Before the observations themselves were touched upon, a certain amount of discussion developed around the question of whether the group should be talking about ‘observations’ or ‘observing systems’. The latter would imply routine, operational, real-time and low-cost approaches. The general conclusion in the group was that, while the design and implementation of observing systems may be the long-term goal, the currently planned observations are more science-driven and also funded this way. When these research-based observations have proven useful and feasible, and when we have learned how to carry them out efficiently, they may evolve into elements of a future observing system. This is the spirit in which most of the observations were discussed.

In order to organise the discussion; the draft observational requirements had been grouped into six categories. This structure will be followed in the report given here.

3.4.1 The Upper Ocean Network

Observations in the upper part of the water column are required for studying climate phenomena like the NAO and tropical Atlantic variability, but also to quantify other key parameter such as the rate at which water masses are formed. Aside from the various SST observing systems (surface drifter, ships of opportunity and satellites) the main existing (and operational) element of an upper ocean network are XBT lines. An international working group recently decided that the high-density lines, which have proven very valuable during WOCE, will be maintained but the remainder should be gradually reduced, once the low-resolution observations are carried out routinely by the float network ARGO. A concern raised repeatedly in this connection at the workshop was that we do not yet know how well ARGO will do the job it is expected to do and that we should therefore be careful about decisions that (eventually) remove a well-proven system. Also, floats will not sample regions with shallow topography and with strong currents properly, while XBTs lines include these parts in a natural way.

An important contribution to upper ocean observations is expected to come from extensive float networks in the future. The working group acknowledged the desirability and expected impact from especially the international ARGO float effort, which might eventually deploy (and maintain?) on the order of 700 floats in the Atlantic. Concrete plans for the North Atlantic are under way in the US and Europe, with proposals to both national and EU agencies pending. A short discussion developed about the issue of parking depths for the ARGO floats, and especially whether a single depth should be prescribed and enforced. A consensus was not reached, but it was pointed out that the current philosophy of ARGO would most likely require a single depth (e.g. to provide a reference flow field). Only floats following this and other specifications would probably qualify as ARGO floats. The same also applies to the requirement for immediate data dissemination via the Global Telecommunication System. The group emphasised that float studies other than ARGO will remain important observational elements like process-targeted applications using different parking depths or different float techniques (e.g. RAFOS).

Eulerian time-series stations, like Bravo and Bermuda, and more recently multiyear-moored systems, have provided important insights into the variability of the upper ocean, including air–sea interaction and water mass formation. Such sites will continue to be an essential element of future upper-ocean observations in the North Atlantic, where a number of oceanographic issues lend themselves to investigation by this method. Sites of particular relevance in view of the workshop are the water mass formation areas (Labrador Sea, Irminger Sea, Nordic Seas, 18° water), tropical regions (PIRATA array plus extensions), and large-scale baroclinic indexing locations (Bermuda–Cape Cod–Bravo–Canary Islands). The discussion emphasised that ship-occupied stations should not be forgotten, since mooring technology cannot sample all variables of interest.

Finally, an upper-ocean network for salinity observations is urgently needed. This will partly be covered by the ARGO profiling floats, and also by the Eulerian time-series stations. However, the working group recommended that volunteer observing ships should be equipped with instrumentation to measure sea surface salinity (at the cooling water intake).

3.4.2 An MOC Observing System

Various topics in relation to the thermohaline overturning circulation played a prominent role at the workshop, like overflows, deep convection, and variability in the thermohaline circulation and its water masses. Thus, future observations addressing these issues have a particular relevance for the workshop.

The classical system for observing the MOC consists of basin-wide hydrographic repeat sections. It turns out, as was reported to the working group, that many groups have strong interests in several such sections, such that a large number of repeat sections in the North Atlantic are more or less committed already. These include the zonal lines 75°N, Greenland–Iceland–UK, AR7W/E, UK–Rockall–Iceland, 48°N, 36°/24°N, 7.5°N, equatorial sections, and the meridional lines 20°W, Cape Farvel–Spain, 52°W, 66°W. In addition, some boundary current repeat lines are expected off Abaco, New York–Bermuda, and in the Denmark Strait area. The repeat interval for these lines varies between biannually to once a decade, which is currently determined by the resources and interests of the involved institutions. The working group emphasised that these line should be carried out as closely as possible to the WOCE one-time survey sections and that tracer measurements should be included wherever possible. Also, the importance of repeat CO_2 inventories will provide new opportunities for joint efforts and new funding resources. Some worry was aired that this large number of repeat sections is merely a ‘shopping list’, but since there are groups for each line which are interested or committed to carry them out, one should hardly discourage them. In fact, the list given corresponds to the plan to be presented at the OceanObs’99 conference in St. Raphael in October 1999. What is needed is a critical assessment of the proposed sections in light of their ability to constrain estimates of MOC variability.

An alternative ‘more direct’ way of observing aspects of the thermohaline circulation consists of moored transport arrays across boundary currents and overflows. Places of particular relevance to the workshop topics are located in various parts along the path of the deep southward flow of NADW and its origins. Thus, transport arrays are essential at the overflows (Denmark Strait and Iceland–Scotland), the exit of the Labrador Sea, and at 2–3 locations along the North American coast and the Caribbean Sea. The arrays can consist of discrete current meter moorings, E-M methods using existing cables, geostrophic transport integrals using dynamic height moorings and acoustic methods. Such observations, however, need to be long-term, in order to be useful, which can pose a problem in terms of funding and scientific pay-off. Most of the mentioned transports sites are already under way or committed, but attention was drawn to the fact they are all operating in an exploratory research mode and it will be years until they have proven themselves and the approaches may become operational in the GOOS sense. A concern was aired that those transport arrays might have to be densely instrumented in order to be able to measure the expected MOC variability on the order of 10–20% of the mean.

3.4.3 Air–Sea Fluxes

Air–sea fluxes are an essential element in future studies of the ocean and climate. At present, very few sites exist which can be used to calibrate reanalysis, remote-sensing and bulk-formula approaches to air–sea flux estimates. Thus, a particular effort is recommended for implementing various options for enhancing the referencing/ calibration possibilities. Moored (time-series) stations are the prime candidates for such measurements, but other options should also be pursued. Vessels of opportunity can be part of such a system, as was pointed out in the working group. Another option mentioned was the use of surface drifters for some of the variables needed. Regarding the moored stations, two philosophies were mentioned in the working group. If used in a reference sense, they should remain in place and be always available for cross-checking other methods. In a calibrations mode, they could be moved around from site to site, after e.g. remote sensing techniques have been tuned/verified.

3.4.4 Process Studies

In view of the workshop presentations, it was clear that particular emphasis in future North Atlantic observations should be on studying some governing but poorly understood processes, relevant to the dynamics and our modelling capabilities. In particular, overflows and bottom boundary layers are still notoriously difficult to represent in numerical models, and the observational base is frequently lacking to determine parameter dependence and variability of these processes, as well as their effect on the larger scale system. The overflows of major importance in the North Atlantic are, of course, in the Denmark Strait and the Iceland–Scotland overflow. Bottom boundary layers appear to be particularly critical in the downslope descent and entrainment region of the water masses having flowed over the above sills. The working group recommended continued and special observational efforts concerning these processes, some of which are under way or planned already.

3.4.5 Satellite Observations

Satellite observations are certain to play an essential role in the future observations of the North Atlantic, among which altimetry features prominently, as highlighted also by workshop presentations. Therefore, (TOPEX/POSEIDON) Jason and ERS follow-up missions will be a crucial element of the future observing system. Similarly important is knowledge of the forcing functions. Here wind observations via scatterometer are considered a necessary input, and were thus also endorsed by the working group. Other variables that were discussed and recommended for satellite observations are sea surface temperature, ice cover and precipitation, all being carried out more or less routinely at present.

The working group further stressed the desirability of salinity measurements from space. However, NASA involvement in a mission for this has been postponed, and hopes are directed at ESA now. There was a degree of dispute regarding the usefulness of salinity data with very low accuracy, but the hope is that, as the system matures, the accuracy will increase.

Some interest was also expressed at the working group in satellite observation of ocean colour and gas exchange.

3.4.6 Input to an Assimilation System

The working group highlighted the importance of feeding observational data to numerical circulation models via an assimilation system (such as it is planned for GODAE). It will be important to learn in the years to come, which observations are most useful in terms of constraining models or filling gaps in the information available to models. Apart from using actual data collected for such investigations, some of the work can be carried out in terms of impact assessment studies. These could also identify additional observations which are missing from the observing system but which would be useful in providing additional information needed for successful model simulations. A comment was also made emphasising the usefulness of models in general for guiding or at least helping the design of observational programmes.

In conclusion, the working group tried to evaluate the various components of the observing system being planned for the North Atlantic. Some of the elements are already ‘on track’ like the float network ARGO and various satellite missions. Therefore, particular emphasis and endorsement was expressed concerning other critical observations like time-series stations, transport arrays, and basin-wide repeat sections. Most of the individual components of the future observing system will have their own presentations at the OceanObs’99 conference in St. Rafael. An issue that will require additional attention in the future is a policy on data submission and quality control.

4. CLOSURE DISCUSSIONS AND OUTLOOK

In plenary session on Friday morning, the WG reports were received and discussed. It was found that the immediate main objective of a WOCE/AIMS synthesis activity, i.e. the production of atlases and maps that can serve as basis for future model and inverse analysis studies was considered well under way based on the activities presented in WG1. Computing was identified as the largest practical problem for synthesis. Internationally, the lack of adequate supercomputer support has reached critical dimensions. As to the model development and parameterisation reviewed by WG2, active group co-operations are under way and co-ordinated activities continue in the WOCE Ocean Model Development WG (chaired by C. Böning). The model comparisons and evaluations recommended by WG3 were endorsed and the need expressed by modelling participants of WG3 for establishing decadal ocean observations was noted. WG4 recommendations were developed from existing plans and expanded based on requirements derived from Workshop topics with the intent to merge this into the papers to be prepared for the OceanObs'99 Conference in St. Raphael. In relation to future observations, some participants expressed concern about the fact that a data management structure for such observations still needs to be established. It was emphasised that existing WOCE structures should be reviewed and maintained if suitable for CLIVAR/GOOS purposes.

A number of group cooperations for model-observation synthesis were established during the Workshop, in particular on Labrador Sea convection and resulting large-scale effects on the overturning circulation. Regarding future observations, a group meeting was organised on Wednesday, 25th August, by Y. Desaubies to work out a co-ordinated proposal for profiling float deployments within ARGO in the context of the EU 5th Framework funding initiative. Another such EU proposal initiative discussed by members of the Nordic WOCE group, and other potential partners, was on the exchange between the Atlantic and the Norwegian/Iceland Sea.

Several possible milestones for more formal future cooperations and interactions were discussed such as special sessions at AGU or EGS and presentations in relevant sessions of the upcoming Ocean Sciences Meeting. Concerning focused publications on Workshop topics, participants were made aware that a special issue of JPO on Labrador Sea convection is being assembled, but other possible options for collections of future synthesis papers were also discussed.

PROGRAMME

Monday, 23 August

9.00 Welcome
Mr Norbert Gansel, Oberbürgermeister of Kiel
Prof. Peter Lemke, Director IfM Kiel,
Dr John Gould, Director International WOCE/CLIVAR Office
Workshop Outline
F. Schott, Chairman, Scientific Organising Committee
10.00 Session 1: North Atlantic decadal variability and the WOCE period
Co-Chairs: C. Böning and F. Schott
Interdecadal variability in coupled GCMs: Model results versus observations (*M. Latif)*
10.30 Coffee Break
11.00 Decadal variability of water masses and circulation in the subpolar North Atlantic *(R. Curry)*
Decadal variability of water masses, overturning and heat transport across 48°N *(P. Koltermann)*
Decadal variability in the North Atlantic: relationships between overturning and sea level variations (*S. Hakkinen)*
Can low frequency variability internal to the atmosphere drive significant interdecadal variability in the ocean and in coupled ocean-atmosphere models? *(R. Greatbatch)*
12.40 Lunch
14.00 Is a steady-state ocean circulation still a useful framework for understanding? *(C. Wunch)*
Discussion session 1 and posters info
15.30 Coffee Break
16.00 Posters info
16.30 Posters Presentations
18.00 Ice Breaker Party, RV Alkor, IfM Dock

Tuesday, 24 August

9.00 Session 2: North Atlantic circulation, pathways and water mass distributions from WOCE observations, altimetry and model results
Co-Chairs: R. Molinari and P. Schlosser
Upper-layer circulation within and north of the Gulf Stream (*L. Talley)*
Upper-layer circulation in high-resolution models *(A.-M. Treguier)*
Gulf Stream Modelling *(E. Chassignet)*
10.15 Coffee Break
10.45 Modelling the DWBC and recirculation *(M. Kawase)*
Observations of Subtropical/Tropical Deep Circulation *(R. Fine)*
Decadal variability in the North Atlantic: relationships between overturning and sea level variations *(S. Hakkinen)*
Coupling to the tropics *(J. Carton)*
Discussion session 2 and posters info
12.30 Lunch
14.00 Session 4a: North Atlantic water mass modification processes: Overflows
Co-Chairs: P. Killworth and R. Käse
Modelling flows through sills and straits and related large scale effects in models (*P. Killworth)*
Review of the exchange between the Mediterranean and the Atlantic through the Straits of Gibraltar *(H. Bryden)*
Some results from long-term observations of the deep-water flux through the Faroe-Bank Channel *(P. Lundberg, K. Borenäs, B. Hansen, I. Lake and S. Østerhus)*
15.15 Coffee Break
15.45 New measurements of the velocity structure of the Denmark Strait Overflow currents and eddies *(J. Girton)*
Discussion session 4a and posters info
16.30 Posters Presentations

Wednesday, 25 August

9.00 Session 3: Thermohaline overturning and flux divergences
Co-Chairs: H. Bryden and C. Wunsch
Overview on the problem of flux divergences (*C. Wunsch)*
Fluxes heat, freshwater, oxygen and nutrients in the North Atlantic from a new global inversion *(A. Ganachaud)*
Section inverse analysis results *(H. Mercier)*
10.15 Coffee Break
10.45 Model-derived meridional mass and heat transports and their variability *(J. Marotzke)*
The export of Atlantic water to the Nordic Seas *(B. Hansen, S. Østerhus, B. Turrell and S. Jonsson)*
Surface heat fluxes and wind stress forcing in the North Atlantic *(S. Josey, E. Kent and P. Taylor)*
Discussion session 3 and posters info
12.30 Lunch
14.00 Session 4b: Labrador Sea convection
Co-Chairs: M. Visbeck and F. Schott
Labrador Sea water mass variability during the WOCE period (*A. Clarke)*
The deep convection experiment of winter 1996/97 *(M. Visbeck)*
Variability of deep convection and boundary circulation 1996–98 *(U. Send, F. Schott, D. Kindler, C. Mertens and J. Fischer)*
15.15 Coffee Break
15.45 Labrador Sea convection in models and relation to THC variability *(E. Chassignet)*
Discussion session 4b and posters info
16.30 Posters Presentations

Thursday, 26 August

9.00 Session 4c: Deep mixing and role of topography
Chair: P. Malanotte-Rizzoli
Modelling the role of topographic interaction (*R. Käse)*
Synthesis of the Deep Basin tracer release experiment *(L. St. Laurent)*
Discussion session 4c
10.15 Changes to working groups
10.30 Coffee Break
11.00 Working groups, batch I
13.00 Lunch
14.00 Session 4d: Thermocline ventilation
Chair: D. Marshall
Physics of thermocline ventilation (*D. Marshall)*
The use of tracers to study thermocline ventilation *(W. Jenkins)*
Discussion session 4d
15.15 Coffee Break
15.45 Working Groups, batch II

Friday, 27 August

8.30 Working Groups continued
9.30 Working Groups reports to plenary
10.30 Coffee Break
11.00 Plenary Discussion, conclusion
13.00 Close of North Atlantic Workshop
14.30 Workshop report activities, Synthesis group co-operation continued

WORKSHOP ORGANISATION

Scientific Organising Committee:

Claus Böning, IfM Kiel/Germany
Harry Bryden, SOC Southampton/UK
Robert Molinari, NOAA/AOML Miami/USA
Gilles Reverdin, CNES, Toulouse/France (unable to attend)
Peter Schlosser, Lamont-Doherty, Palisades/USA
Friedrich Schott, IfM Kiel, Germany (Chairman)
Carl Wunsch, MIT, Cambridge/USA

Local Organising Committee:

Jürgen Kielmann
Sigrun Komander
Thomas Müller
Friedrich Schott
Lothar Stramma (Chairman)
(All IfM Kiel)

Workshop Secretaries:

Kristin Maass
Sigrun Komander

Workshop Website

http://www.ifm.uni-kiel.de/ro/naws.html

LIST OF PARTICIPANTS

Affler, Karina
Institut für Meereskunde Kiel
Düsternbrooker Weg 20
24105 Kiel
Germany
kaffler@ifm.uni-kiel.de

Becker, Sylvia
Institut für Meereskunde Kiel
Düsternbrooker Weg 20
24105 Kiel
Germany
Tel: 49 431 597 3896
Fax: 49 431 597 3891
sbecker@ifm.uni-kiel.de

Berndt, Hauke
Institut für Meereskunde Kiel
Düsternbrooker Weg 20
24105 Kiel
Germany
Tel: 49 431 597 3974
Fax: 49 431 565 876
hberndt@ifm.uni-kiel.de

Bersch, Manfred
Institut für Meereskunde Hamburg
Troplowitzstr. 7
22529 Hamburg
Germany
Tel: 49 40 42838 5748
Fax: 49 40 560 57 24
bersch@ifm.uni-hamburg.de

Biastoch, Arne
Institut für Meereskunde Kiel
Düsternbrooker Weg 20
24105 Kiel
Germany
Tel: 49 431 597 3804
Fax: 49 431 565 876
abiastoch@ifm.uni-kiel.de

Böning, Claus
Institut für Meereskunde Kiel
Düsternbrooker Weg 20
24105 Kiel
Germany
Tel: 49 431 597 3979
Fax: 49 431 565 876
cboening@ifm.uni-kiel.de

Brandt, Peter
Institut für Meereskunde Kiel
Düsternbrooker Weg 20
24105 Kiel
Germany
Tel: 49 431 597 3827
Fax: 49 431 597 3821
pbrandt@ifm.uni-kiel.de

Bryan, Frank
National Center for Atmospheric Research
P.O. Box 3000
Boulder, CO 80307
USA
Tel: 1 303 497 1394
Fax: 1 303 497 1700
bryan@ncar.ucar.edu

Bryden, Harry
Southampton Oceanogr. Centre
Empress Dock
Southampton SO14 3ZH
UK
Tel: 44 2380 59 64 37
Fax: 44 2380 59 62 04
h.bryden@soc.soton.ac.uk

Bumke, Kai
Institut für Meereskunde Kiel
Düsternbrooker Weg 20
24105 Kiel
Germany
Tel: 49 431 597 3874
Fax: 49 431 565 876
kbumke@ifm.uni-kiel.de

Carton, J.
Department of Meteorology
University of Maryland
2417 Computer & Space Science Bldg.
College Park, MD 20742
USA
Tel: 1 301 405 5365
Fax: 1 301 314 9482
carton@atmos.umd.edu

Chassignet, Eric
University of Miami
RSMAS/MPO
4600 Rickenbacker Causeway
Miami, FL 33149
USA
Tel: 1 305 361 4041
Fax: 1 305 361 4696
echassignet@rsmas.miami.edu

Clarke, R. Allyn
Bedford Institute of Oceanogr.
PO Box 1006
Dartmouth, NS B24 4A2
Canada
Tel: 1 902 426 4880
Fax: 1 902 426 7827
clarkea@mar.dfo-mpo.gc.ca

Coldewey, Melanie
Institut für Meereskunde Kiel
Düsternbrooker Weg 20
24105 Kiel
Germany
Tel: 49 431 597
Fax: 49 431 565 876
mcoldewey@ifm.uni-kiel.de

Curry, Ruth
Woods Hole Oceanogr. Institute
MS 21/WHOI
Woods Hole, MA 02543
USA
Tel: 1 508 289 2799
Fax: 1 508 457 2181
rcurry@whoi.edu

Czerniak, Andreas
Institut für Meereskunde Kiel
Düsternbrooker Weg 20
24105 Kiel
Germany

deBoer, Christjan
Institut für Meereskunde Kiel
Düsternbrooker Weg 20
24105 Kiel
Germany
Tel: 49 431 597 3805
Fax: 49 431 597 3821

Dengg, Joachim
Institut für Meereskunde Kiel
Düsternbrooker Weg 20
24105 Kiel
Germany
Tel: 49 431 597 3882
Fax: 49 431 565 876
jdengg@ifm.uni-kiel.de

Desaubies, Yves
Lab. Phys. Océans - IFREMER
BP 70
29200 Plouzané
France
Tel: 33 298 22 42 75
Fax: 33 298 22 44 96
yd@ifremer.fr

Dieterich, Christian
Alfred-Wegener Institut
Bürgermeister-Smidt-Straße 20
27568 Bremerhaven
Germany
Tel: 49 471 4831 752
Fax: 49 471 4831 797
cdieterich@awi-bremerhaven.de

Dietze, Heiner
Institut für Meereskunde Kiel
Düsternbrooker Weg 20
24105 Kiel
Germany
Tel: 49 431 597 3973
Fax: 49 431 565 876
hdietze@ifm.uni-kiel.de

Diggs, Stephen
Scripps Institution of Oceanogr.
9500 Gilman Dr.
La Jolla, CA 92093-0214
USA
Tel: 1 858 534 1108
Fax: 1 858 534 7383
sdiggs@ucsd.edu

Dobrindt, Uwe
Alfred-Wegener Institut
Bürgermeister-Smidt-Straße 20
27568 Bremerhaven
Germany
Tel: 49 471 4831 764
Fax: 49 471 4831 797
udobrindt@awi-bremerhaven.de

Dobroliubov, Sergey
Moscow State University
Vorobiervy Gory
Moscow 117234
Russia
Tel: 7 095 932 8838
Fax: 7 095 932 8836
science@geogr.msu.ru

Dullo, Wolf-Christian
Geomar, Wischhofstraße 1-3
24148 Kiel
Germany
Tel: 49 431 600 2215
Fax: 49 431 600 2925
cdullo@ifm.uni-kiel.de

Eden, Carsten
Institut für Meereskunde Kiel
Düsternbrooker Weg 20
24105 Kiel
Germany
Tel: 49 431 597 3879
Fax: 49 431 565 876
cede,n@ifm.uni-kiel.de

Ernst, Ute
Institut für Meereskunde Kiel
Düsternbrooker Weg 20
24105 Kiel
Germany
Tel: 49 431 597 3973
Fax: 49 431 565 876
uernst@ifm.uni-kiel.de

Esselborn, S.
Institut für Meereskunde Hamburg
Troplowitzstr. 7
22529 Hamburg
Germany
Tel: 49 40 42838 5457
Fax: 49 40 42838 5713
esselborn@ifm.uni-hamburg.de

Fine, Rana
RSMAS, MAC, University of Miami
4600 Rickenbacker Causeway
Miami, FL 33149
USA
Tel: 1 305 361 4722
Fax: 1 305 361 4689
rfine@rsmas.miami.edu

Fischer, Jürgen
Institut für Meereskunde Kiel
Düsternbrooker Weg 20
24105 Kiel
Germany
Tel: 49 431 597 3823
Fax: 49 431 597 3821
jfischer@ifm.uni-kiel.de

Fleischmann, Uli
Universität Bremen, IUP,
Tracer-Oz., P.O. Box 330 440
28334 Bremen
Germany
Tel: 49 421 218 4317
Fax: 49 421 218 7018
ufleisch@physik.uni-bremen.de

Ganachaud, Alexandre
MIT/WHOI Joint Program
MIT 54-1517, 77 Mass Ave
Cambridge, MA 02119
USA
Tel: 1 617 253 21 77
Fax: 1 617 253 1164
ganacho@mit.edu

Gerdes, R.
Alfred-Wegener Institut
Am Handelshafen 12
27570 Bremerhaven
Germany
Tel: 49 471 4831 827
Fax: 49 471 4831 425
rgerdes@awi-bremerhaven.de

Girton, James B.
Applied Physics Lab
University of Washington
1013 NE 40th Street
Seattle, WA 98105-6698
USA
Tel: 1 206 685-9670
Fax: 1 206 543 6785
girton@ocean.washington.edu

Gould, John
Southampton Oceanogr. Centre
Empress Dock
Southampton SO14 3ZH
UK
Tel: 44 2380 596 208
Fax: 44 2380 596 204
wjg@soc.soton.ac.uk

Gouretski, Victor
BSH Hamburg
Bernhard-Nocht-Str. 78
20359 Hamburg
Germany
Tel: 49 40 3190 3541
Fax: 49 40 3190 5000
victor.gouretski@bsh.d400.de

Greatbatch, Richard
Dalhousie University
Dept. Oceanogr.
Dalhousie University
Halifax B3H 4JI N.S.
Canada
Tel: 1 902 494 6674
Fax: 1 902 494 2885
rgreat@phys.ocean.dal.ca

Grootes, Pieter M.
Leibniz-Labor für Altersbestimmung
und Isotopenforschung
Max-Eyth-Str. 11-13
24118 Kiel
Germany
Tel: 49 431 880 3894
Fax: 49 431 880 3356
pgrootes@leibniz.uni-kiel.de

Hagedorn, Renate
Institut für Meereskunde Kiel
Düsternbrooker Weg 20
24105 Kiel
Germany

Haine, Thomas
Dept. Physics, Oxford University
AOPP, Clarendon Lab., Parks Road
Oxford OX1 3PU
UK
Tel: 44 1865 27 20 87
Fax: 44 1865 27 29 23
t.haine1@physics.ox.ac.uk

Hakkinen, Sirpa
NASA Goddard Space Flight Center
Code 971
Greenbelt, MD 20769
USA
Tel: 1 301 614 5712
Fax: 1 301 614 5644
hakkinen@gsfc.nasa.gov

Hamann, Meike
Institut für Meereskunde Kiel
Düsternbrooker Weg 20
24105 Kiel
Germany
Tel: 49 431 597 3819
Fax: 49 431 597 3821
mhamann@ifm.uni-kiel.de

Hansen, Bogi
Fishery Laboratory, Faroe
Box 3051
FO-110 Torshavn
Faroe Islands
Tel: 298 315 092
Fax: 298 318 264
bogihan@frs.fo

Hauser, Janko
Institut für Meereskunde Kiel
Düsternbrooker Weg 20
24105 Kiel
Germany
Tel: 49 431 597 3989
Fax: 49 431 565 876
jhauser@ifm.uni-kiel.de

Hausschildt, Heike
Institut für Meereskunde Kiel
Düsternbrooker Weg 20
24105 Kiel
Germany
Tel: 49 431 597 4014
Fax: 49 431 565 876

Hilmer, Michael
Institut für Meereskunde Kiel
Düsternbrooker Weg 20
24105 Kiel
Germany
Tel: 49 431 597 4003
Fax: 49 431 565 876
mhilmer@ifm.uni-kiel.de

Holliday, Penny N.
WOCE IPO, SOC
European Way
Southampton SO14 3ZH
UK
Tel: 44 2380 596 206
Fax: 44 2380 596 204
nph@soc.soton.ac.uk

Jancke, Kai
BSH Hamburg
Bernhard-Nocht-Str. 78
20359 Hamburg
Germany
Tel: 49 40 3190 0
Fax: 49 40 3190 5000
jancke@bsh.d400.de

Jenkins, William
Southampton Oceanogr. Centre
Empress Dock
Southampton SO14 3ZH
UK
Tel: 44 2380 596 573
Fax: 44 2380 593 052
w.jenkins@soc.soton.ac.uk

Jochum, Markus
MIT
Dept of Earth, Atm & Plan Sciences
77 Massachusetts Avenue
Cambridge, MA 02139-4307
USA
Tel: 1 617 253 2922
Fax: 1 617 253 4464
mjochum@mit.edu

Josey, Simon A.
Southampton Oceanogr. Centre
European Way
Southampton SO14 3ZH
UK
Tel: 44 2380 596 409
Fax: 44 2380 596 400
simon.a.josey@soc.soton.ac.uk

Juncheng, Zuo
Institut für Meereskunde Kiel
Düsternbrooker Weg 20
24105 Kiel
Germany
Tel: 49 431 597 3824
Fax: 49 431 5973821
zjuncheng@ifm.uni-kiel.de

Jung, Thomas
Institut für Meereskunde Kiel
Düsternbrooker Weg 20
24105 Kiel
Germany
Tel: 49 431 597 4003
Fax: 49 431 565 876
tjung@ifm.uni-kiel.de

Jungclaus, Johann
Max-Planck-Inst. für Meteorologie
Bundesstr. 55
20146 Hamburg
Germany
Tel: 49 40 411 73 109
Fax: 49 40 411 73 298
jungclaus@dkrz.de

Käse, Rolf H.
Institut für Meereskunde Kiel
Düsternbrooker Weg 20
24105 Kiel
Germany
Tel: 49 431 597 3881
Fax: 49 431 565 876
rkaese@ifm.uni-kiel.de

Kawase, Mitsuhiro
University of Washington
Box 35 79 40
Seattle, WA 98195
USA
Tel: 1 206 543 0766
Fax: 1 206 685 3354
kawase@ocean.washington.edu

Kieke, Dagmar
Institut für Meereskunde Kiel
Düsternbrooker Weg 20
24105 Kiel
Germany
Tel: 49 431 597 3856
Fax: 49 431 565 876
dkieke@ifm.uni-kiel.de

Kielmann, Jürgen
Institut für Meereskunde Kiel
Düsternbrooker Weg 20
24105 Kiel
Germany
Tel: 49 431 597 3883
Fax: 49 431 565 876
jkielmann@ifm.uni-kiel.de

Killworth, Peter D.
Southampton Oceanogr. Centre
Empress Dock
Southampton SO14 3ZH
UK
Tel: 44 2380 596 202
Fax: 44 2380 596 204
p.killworth@soc.soton.ac.uk

Kindler, Detlef
Institut für Meereskunde Kiel
Düsternbrooker Weg 20
24105 Kiel
Germany
Tel: 49 431 597 3896
Fax: 49 431 565 876
dkindler@ifm.uni-kiel.de

Kivman, Gennady
Alfred-Wegener Institut
Columbusstr., Postfach 12 01 61
27515 Bremerhaven
Germany
Tel: 49 471 4831 783
Fax: 49 471 1700 538
gkivman@awi-bremerhaven.de

Köberle, Cornelia
Alfred-Wegener Institut
Bürgermeister-Smidt-Straße 20
27568 Bremerhaven
Germany
Tel: 49 471 4831 825
Fax: 49 471 4831 797
ckoeberl@awi-bremerhaven.de

Köhl, A. Armin
Institut für Meereskunde Kiel
Düsternbrooker Weg 20
24105 Kiel
Germany
Tel: 49 431 597 3986
Fax: 49 431 565 876
akoehl@ifm.uni-kiel.de

Koltermann, Klaus-Peter
BSH Hamburg
Bernhard-Nocht-Str. 78
20359 Hamburg
Germany
Tel: 49 40 3190 3540
Fax: 49 40 3190 5000
koltermann@bsh.d400.de

Krebs, Uta
Institut für Meereskunde Kiel
Düsternbrooker Weg 20
24105 Kiel
Germany

Kröger, Jürgen
Institut für Meereskunde Kiel
Düsternbrooker Weg 20
24105 Kiel
Germany
Tel: 49 431 597 3884
Fax: 49 431 565 876
jkroeger@ifm.uni-kiel.de

Larsen,Karin M. H.
Fishery Laboratory, Faroe
Noarun 1
100 Torshavn
Faroe Islands
Tel: 298 315 092
Fax: 298 318 264
karinl@frs.fo

Latif, Mojib
Max-Planck-Institut für
Meteorologie
Bundesstr. 55
20146 Hamburg
Germany
Tel: 49 40 411 73 248
Fax: 49 40 411 73 173
latif@dkrz.de

Lavin, Alicia
Instituto Espanol de Oceanografia
Ap. 240
39080 Santander
Spain
Tel: 34 942 291 060
Fax: 34 942 275 072
alicia.lavin@st.ieo.es

Leaman, Kevin
RSMAS, Div. MPO
4600 Rickenbacker Causeway
Miami, FL 33149
USA
Tel: 1 305 361 4058
Fax: 1 305 361 4696
kleaman@rsmas.miami.edu

Lemke, Peter
Institut für Meereskunde Kiel
Düsternbrooker Weg 20
24105 Kiel
Germany
Tel: 49 431 597 3870
Fax: 49 431 565 876
plemke@ifm.uni-kiel.de

Lilly, Jonathan
School of Oceanography
University of Washington
Box 357940
Seattle, WA 98195-7940
USA
Tel: 1 206 543 0767
Fax: 1 206 328 3445
lilly@jaeger.ocean.washington.edu

Lohmann, Katja
Institut für Meereskunde Kiel
Düsternbrooker Weg 20
24105 Kiel
Germany
Tel: 49 431 597 3805
Fax: 49 431 565 876
klohmann@ifm.uni-kiel.de

Lorbacher, Katja
BSH Hamburg
Bernhard-Nocht-Str. 78
20359 Hamburg
Germany
Tel: 49 40 3190 3259
Fax: 49 40 3190 5000
katja.lorbacher@bsh.d400.de

Losch, Martin
Alfred-Wegener Institut
Postfach 12 01 61
27515 Bremerhaven
Germany
Tel: 49 471 4831 765
Fax: 49 471 4831 797
mlosch@awi-bremerhaven.de

Lundberg, Peter
Stockholm University
Dept of Meteorology
Arrhenius Laboratory
Stockholm, S-10691
Sweden
Tel: 46 8 161 735
Fax: 46 9 157 956
peter@misu.su.se

Malanotte-Rizzoli, Paola
MIT
Dept of Earth, Atm & Plan Sciences
77 Massachusetts Avenue
Cambridge, MA 02139-4307
USA
Tel: 1 617 253 2451
Fax: 1 617 253 4464
rizzoli@ocean.mit.edu

Malmberg, Svend-Aage
Marine Research Institute
Skulagata 4
121 Reykjavik
Iceland
Tel: 354 552 02 40
Fax: 354 562 37 90
svam@hafro.is

Marotzke, Jochem
Southampton Oceanogr. Centre
Empress Dock
Southampton SO14 3ZH
UK
Tel: 44 2380 593 755
Fax: 44 2380 593 052
jochem.marotzke@soc.soton.ac.uk

Marsh, Robert
Southampton Oceanogr. Centre
Empress Dock
Southampton SO14 3ZH
UK
Tel: 44 2380 596 214
Fax: 44 2380 596 204
rma@soc.soton.ac.uk

Marshall, David
Univ. of Reading
Dept. Meteorology
PO Box 243, Earley Gate
Reading RG6 6BB
UK
Tel: 44 118 931 8952
Fax: 44 118 931 8905
davidm@met.reading.ac.uk

Martins, Sena Carlos
Institut für Meereskunde Kiel
Düsternbrooker Weg 20
24105 Kiel
Germany
Tel: 49 431 597 3825
Fax: 49 431 597 3821
csena@ifm.uni-kiel.de

Mercier, Herlé
IFREMER, Centre de Brest
BP. 70 Pointe de diable
29280 Plouzané
France
Tel: 33 2 98 22 42 86
Fax: 33 2 98 22 44 96
herle.mercier@ifremer.fr

Mertens, Christian
Institut für Meereskunde Kiel
Düsternbrooker Weg 20
24105 Kiel
Germany
Tel: 49 431 597 3822
Fax: 49 431 565 876
cmertens@ifm.uni-kiel.de

Mikolajewicz, U.
Max-Planck-Institut für Meteorologie
Bundesstr. 55
20146 Hamburg
Germany
Tel: 49 40 411 73 243
Fax: 49 40 411 73 366
mikolajewicz@dkrz.de

Mintrop Ludger
Institut für Meereskunde Kiel
Düsternbrooker Weg 20
24105 Kiel
Germany
Tel: 49 431 597 4023
Fax: 49 431 565 876
lmintrop@ifm.uni-kiel.de

Molinari, Robert
NOAA/AOML
4301 Rickenbacker Causeway
Miami, FL 33149
USA
Tel: 1 305 361 4344
Fax: 1 305 361 4392
molinari@aoml.noaa.gov

Morsdorf, Felix
Institut für Meereskunde Kiel
Düsternbrooker Weg 20
24105 Kiel
Germany
Tel: 49 431 597 3825
Fax: 49 431 597 3821
fmorsdorf@ifm.uni-kiel.de

Mortensen, John
Marine Research Institute
Skulagata 4
121 Reykjavik
Iceland
Tel: 354 5520 240
Fax: 354 5623 790
johnm@hafro.is

Müller, Tom
Institut für Meereskunde Kiel
Düsternbrooker Weg 20
24105 Kiel
Germany
Tel: 49 431 597 3799
Fax: 49 431 565 876
tmueller@ifm.uni-kiel.de

New, Adrian
Southampton Oceanogr. Centre
Empress Dock
Southampton SO14 3ZH
UK
Tel: 44 2380 596 173
Fax: 44 2380 596 204
a.new@soc.soton.ac.uk

O'Dwyer, Jane
Norwegian Polar Institute
Polar Environment Centre
9296 Tromso
Norway
Tel: 47 77 750 555
Fax: 47 77 750 501
jane@npolar.no

Østerhus, Svein
Univ. of Bergen
Allegt. 70
5007 Bergen
Norway
Tel: 47 55 582 607
Fax: 47 55 589 883
svein.osterhus@gfi.uib.no

Olbers, Dirk
Alfred-Wegener Institut
Columbusstr., Postfach 12 01 61
27515 Bremerhaven
Germany
Tel: 49 471 4831 761
Fax: 49 471 4831 797
dolbers@bremerhaven.de

Oschlies, Andreas
Institut für Meereskunde Kiel
Düsternbrooker Weg 20
24105 Kiel
Germany
Tel: 49 431 597 3885
Fax: 49 431 565 876
aoschlies@ifm.uni-kiel.de

Perez-Brunius, P.
University of Rhode Island
Narragansett Bay Campus 224
Box 200
Narragansett, RI 02882
USA
Tel: 1 401 874 6518
paula@rafos.gso.uri.edu

Pollard, Raymond T.
Southampton Oceanogr. Centre
Empress Dock
Southampton SO14 3ZH
UK
Tel: 44 2380 596 433
Fax: 44 2380 596 204
raymond.t.pollard@soc.soton.ac.uk

Quadfasel, Detlef
Niels Bohr Institute for Astr.,
Physics and Geoph.,
Univ. of Copenhagen
Juliane Maries Vej 30
2100 Copenhagen M-X
Denmark
Tel: 45 35 32 06 09
Fax: 45 35 36 53 57
dq@dcess.ku.dk

Read, Jane
Southampton Oceanogr. Centre
Empress Dock
Southampton SO14 3ZH
UK
Tel: 44 2380 596 432
Fax: 44 2380 596 204
j.read@soc.soton.ac.uk

Rhein, Monika
Institut für Ostseeforschung
Seestraße 15
18119 Rostock
Germany
Tel: 49 381 51 97 120
Fax: 49 381 51 97 114
monika.rhein@io-warnemuende.de

Roether, Wolfgang
Institut für Umweltphysik, Univ.
Bremen
Postfach 33 04 40
28334 Bremen
Germany
Tel: 49 421 218 3511
Fax: 49 421 218 7018
wroether@physik.uni-bremen.de

Ruprecht ,Eberhard
Institut für Meereskunde Kiel
Düsternbrooker Weg 20
24105 Kiel
Germany
Tel: 49 431 597 3872
Fax: 49 431 565 876
eruprecht@ifm.uni-kiel.de

Saunders, Peter
Southampton Oceanogr. Centre
European Way
Southampton SO14 3ZH
UK
Tel: 44 2380 596 205
Fax: 44 2380 596 204
peter.saunders@soc.soton.ac.uk

Scheinert, Markus
Institut für Meereskunde Kiel
Düsternbrooker Weg 20
24105 Kiel
Germany
Tel: 49 431 597 3821
Fax: 49 431 597 3821
mscheinert@ifm.uni-kiel.de

Schlosser, Peter
Lamont-Doherty Earth Observatory
Columbia University, Route 9W
Palisades, NY 10964-8000
USA
Tel: 1 914 365 8707
Fax: 1 914 365 8155
peters@ldeo.columbia.edu

Schmith, Torben
Danish Climate Centre
Danish Meteorological Institute
Lyngbyvej 100
2100 Copenhagen O
Denmark
Tel: 45 39 15 74 44
ts@dmi.dk

Schott, F.Friedrich
Institut für Meereskunde Kiel
Düsternbrooker Weg 20
24105 Kiel
Germany
Tel: 49 431 597 3820
Fax: 49 431 565 876
fschott@ifm.uni-kiel.de

Schröter, Jens
Alfred-Wegener Institut
Columbusstr., Postfach 12 01 61
27515 Bremerhaven
Germany
Tel: 49 471 4831 762
Fax: 49 471 4831 797
jschroete@awi-bremerhaven.de

Schulz-Bull, Detlef
Institut für Meereskunde Kiel
Düsternbrooker Weg 20
24105 Kiel
Germany
Tel: 49 431 597 3812
Fax: 49 431 565 876
dbull@ifm.uni-kiel.de

Schweckendiek, Ulf
Institut für Meereskunde Kiel
Düsternbrooker Weg 20
24105 Kiel
Germany
Tel: 49 431 597 3886
Fax: 49 431 565 876
uschweckendiek@ifm.uni-kiel.de

Selten, Frank
KNMI
PO Box 201
3730 AE De Bilt
Netherlands
Tel. 31 30 2206 761
Fax: 31 30 2202 570
selten@knmi.nl

Send, Uwe
Institut für Meereskunde Kiel
Düsternbrooker Weg 20
24105 Kiel
Germany
Tel: 49 431 597 3890
Fax: 49 431 565 876
usend@ifm.uni-kiel.de

Siedler, Gerold
Institut für Meereskunde Kiel
Düsternbrooker Weg 20
24105 Kiel
Germany
Tel: 49 431 596 3899
Fax: 49 431 565 876
gsiedler@ifm.uni-kiel.de

Skagseth, O.
Univ. of Bergen
Allegt. 70
5007 Bergen
Norway
skagseth@gfi.uib.no

Slater, Deb
Southampton Oceanogr. Centre
Empress Dock
Southampton SO14 3ZH
UK
Tel: 44 2380 596 497
Fax: 44 2380 596 204
drs1@soc.soton.ac.uk

Smethie, Jr., William M.
Lamont-Doherty Earth Observatory
Columbia University, Route 9W
Palisades, NY 10964-8000
USA
Tel: 1 914 365 8566
Fax: 1 914 365 8155
bsmeth@ldeo.columbia.edu

Smith, Richard D.
Los Alamos National Laboratory
B-216
Los Alamos, NM 87545
USA
Tel: 1 505 667 7744
Fax: 1 505 665 5926
rdsmith@lanl.gov

Smythe-Wright, Denise
Southampton Oceanogr. Centre
Empress Dock
Southampton SO14 3ZH
UK
Tel: 44 2380 596 439
Fax: 44 2380 596 204
denise.smythe-wright@soc.soton.ac.uk

Sokov, Alexey
P.P. Shirshov Institute of Oceanogr.
Nakhimovski pr. 36
Moscow, 117218
Russia
Tel: 95 129 6192
Fax: 95 129 6192
sokov@gulev.sio.rssi.ru

St. Laurent, Louis
Woods Hole Oceanogr. Institute
Mail Stop 21
Woods Hole, MA 02543
USA
Tel: 1 508 289 3321
Fax: 1 508 457 2181
lstlaurent@whoi.edu

Steffen, Elizabeth L.
Applied Physics Lab
University of Washington
1013 NE 40th Street
Seattle, WA 98105
USA
Tel: 1 206 543 1399
Fax: 1 206 543 6785
steffen@apl.washington.edu

Stolley, M.
BSH Hamburg
Bernhard-Nocht-Str. 78
20359 Hamburg
Germany
Tel: 49 40 3190 3259
Fax: 49 40 3190 5000
martin.stolley@bsh.d400.de

Stramma, Lothar
Institut für Meereskunde Kiel
Düsternbrooker Weg 20
24105 Kiel
Germany
Tel: 49 431 597 3818
Fax: 49 431 565 876
lstramma@ifm.uni-kiel.de

Swift, James H.
UCSD
Scripps Institution of Oceanogr.
Mail Code 0214/9500 Gilman Dr.
La Jolla, CA 92093-0214
USA
Tel: 1 858 534 3387
Fax: 1 858 534 7383
jswift@ucsd.edu

Sy, Alexander
BSH Hamburg
Bernhard-Nocht-Str. 78
20359 Hamburg
Germany
Tel: 49 40 3190 3430
Fax: 49 40 4190 5000
alexander.sy@bsh.d400.de

Talley, Lynne
UCSD
Scripps Institution of Oceanogr.
9500 Gilman Dr.
La Jolla, CA 92093-0230
USA
Tel: 1 858 534 6610
Fax: 1 858 534 9820
ltalley@ucsd.edu

Tereschenkov, Vladimir
P.P. Shirshov Institute of Oceanogr.
Nakhimovski pr. 36
Moscow, 117218
Russia
Tel: 95 124 7928
Fax: 95 124 5983
boba@gulev.sio.rssi.ru

Thompson, Bert
WOCE DIU
502 S. Hanover St.
Baltimore, MD 21201
USA
Tel: 1 410 234 0787
bert@diu.cms.udel.edu

Thorsen, Sannie V.
Danmarks Meteorologiske Institut
Lyngbyvej 100
2100 Copenhagen
Denmark
Tel: 45 39 15 74 07
svt@dmi.dk

Timm, Oliver
Institut für Meereskunde Kiel
Düsternbrooker Weg 20
24105 Kiel
Germany
Tel: 49 431 597 3808
Fax: 49 431 565 876
otimm@ifm.uni-kiel.de

Timmermann, Axel
Royal Dutch Meteorological Inst.
Postbus 201
3730 AE De Bilt
Netherlands
Tel: 31 30 2206 765
timmera@knmi.nl

Todd, James F.
NOAA Office of Global Programs
1100 Wayne Avenue, Suite 1225
Silver Spring, MD 20910
USA
Tel: 1 301 427 2089
Fax: 1 301 427 2073
todd@ogp.noaa.gov

Tokmakian, Robin
Naval Postgraduate School
Dept. Oceanogr.
833 Dyer Rd, Rm328, Bldg. 232
Monterey, CA 93943-5122
USA
Tel: 1 831 656 3255
Fax: 1 831 656 2712
robint@ucar.edu

Treguier, Anne-Marie
IFREMER, Centre de Brest
BP. 70 (Pointe du diable)
29280 Plouzané, France
Tel: 33 2 98 22 42 96
Fax: 33 2 98 22 44 96
anne.marie.treguier@ifremer.fr

Ubl, Sandy
Institut für Meereskunde Kiel
Düsternbrooker Weg 20
24105 Kiel
Germany

van Aken, Hendrik M.
Netherlands Institute for Sea Research
PO Box 59
Den Burg/Texel AB 1790
Netherlands
Tel: 31 222 369 416
Fax: 31 222 319 674
aken@nioz.nl

Visbeck, Martin
Lamont-Doherty Earth Observatory
Columbia University, Route 9W
Palisades, NY 10964-8000
USA
Tel: 1 914 365 8531
Fax: 1 914 365 8157
visbeck@ldeo.columbia.edu

Voelker, Christoph
Institut für Meereskunde Kiel
Düsternbrooker Weg 20
24105 Kiel
Germany
Tel: 49 431 597 3877
Fax: 49 431 565 876
cvoelker@ifm.uni-kiel.de

Walter, Maren
Institut für Meereskunde Kiel
Düsternbrooker Weg 20
24105 Kiel
Germany
Tel: 49 431 597 3822
Fax: 49 431 597 3821
mwalter@ifm.uni-kiel.de

Webb, David
Southampton Oceanogr. Centre
Empress Dock
Southampton SO14 3ZH
UK
Tel: 44 2380 596 199
Fax: 44 2380 596 204
david.webb@soc.soton.ac.uk

Wenzel, Manfred
Alfred-Wegener Institut
Bürgermeister-Smidt-Straße 20
27568 Bremerhaven
Germany
Tel: 49 471 4831 763
Fax: 49 471 4831 797
mwenzel@awi-bremerhaven.de

White, K.

Willebrand, J. Jürgen
Institut für Meereskunde Kiel
Düsternbrooker Weg 20
24105 Kiel
Germany
Tel: 49 431 597 3800
Fax: 49 431 565 876
jwillebrand@ifm.uni-kiel.de

Wilhelm, Dietmar
Institut für Meereskunde Kiel
Düsternbrooker Weg 20
24105 Kiel
Germany
Tel: 49 431 597 3797
Fax: 49 431 597 3821
dwilhelm@ifm.uni-kiel.de

Wilson, Doug
NOAA/AOML/PhOD
4301 Rickenbacker Causeway
Miami, FL 33149
USA
Tel: 1 305 361 4352
Fax: 1 305 361 4412
wilson@aoml.noaa.gov

Wirth, A.
Institut für Meereskunde Kiel
Düsternbrooker Weg 20
24105 Kiel
Germany
Tel: 49 431 597
Fax: 49 431 565 876
awirth@ifm.uni-kiel.de

Woelk, S.
Institut für Meereskunde Hamburg
Troplowitzstr. 7
22529 Hamburg
Germany
Tel: 49 40 42838 2990
Fax: 49 40 560 57 24
woelk@ifm.uni-hamburg.de

Wu Peili
Hadley Centre
London Road
Bracknell RG12 2SY
UK
Tel: 44 1344 854916
Fax: 44 1344 854898
pwu@meto.gov.uk

Wunsch, Carl
MIT
Dept of Earth, Atm & Plan Sciences
77 Massachusetts Avenue
Cambridge, MA 02139
USA
Tel: 1 617 253 5937
Fax: 1 617 253 4464
cwunsch@pond.mit.edu

Zenk, Walter
Institut für Meereskunde Kiel
Düsternbrooker Weg 20
24105 Kiel
Germany
Tel: 49 431 597 3892
Fax: 49 431 565 876
wzenk@ifm.uni-kiel.de

LIST OF POSTERS PRESENTED

The WOCE Hydrographic Programme Office
Danielle M. Bartolacci, Stephen C. Diggs, Jerry L. Kappa, James H. Swift and Lynne D. Talley

The WOCE Hydrographic Programme Office provides data and information services to investigators participating in the field phase of the WOCE Hydrographic Programme and to investigators interested in data from that programme. Data originator and cruise support includes a repository for all WHP data, "behind-the-scenes" assistance with data and documentation files, and a secure area for non-public data. WHP science support includes providing cruise information and data on-line. The WHPO also supports the SAC and investigators who are creating data products such as basin data sets and electronic atlases. The WHPO web site (http://whpo.ucsd.edu) contains nearly complete data and documentation files for the WHP, although some of the more recent files are preliminary and/or non-public. Data held by the WHPO but which are not public are available only via use of passwords whose distribution is controlled by the data originators. Contact information for the data originators is provided by the WHPO.

The role of sea ice variability for the exchange of water and energy between ocean and atmosphere
H. Berndt, M. Hilmer, P. Lemke and E. Ruprecht

Variations of the thermohaline circulation (THC) are essentially driven by fluctuations of the fluxes at the sea surface. Today's knowledge of the surface fluxes in polar latitudes and the impact of sea ice on these fluxes is insufficient. Therefor the role of sea ice variability for the exchange of water and energy between ocean and atmosphere is investigated. Additionally the relative contribution of the sea ice transport to the fresh water budget is estimated and compared to precipitation. Different regional models for the simulation of the climate subsystems are used for this investigation. After adapting the model to the new environment a fully coupled atmosphere–sea ice–ocean simulation will be developed.

The model domain, resolved with a mesh size of 0.5°, is covering an area of about 55 Million km^2. North of 35°N in the North Atlantic the model grid extends across the whole Arctic. Since the Arctic is included into the model domain, realistic boundary conditions for the sea ice export out of the Greenland-Iceland-Norwegian-Seas can be estimated.

The three components precipitation-evaporation, surface runoff and net melting rate show a high input into the Labrador Sea and the Denmark Strait. Freshwater has a strong impact on the stratification of the ocean surface layer. Input of freshwater reduces the salinity and therefor strengthens the stability; deep convection is weakened in those areas.

With a mean transport of 0.114 Sv (@ 3600 km^2/year) the sea ice export out of the Arctic is the highest freshwater input into the Greenland–Iceland–Norwegian Seas and after the Amazon the second largest freshwater flux of our planet. Since there is a good correspondence between model results and observations the ice export was simulated for a time period of 40 years. The annual sea ice export, separated into Fram, Denmark, and Davis Strait shows high interannual variability. Maximum exports can be found in the Fram Strait in 1968 and 1995 with values up to 0.128 Sv. Transports in the Denmark and Davis Strait are one order of magnitude smaller.

Atmosphere and sea ice modelling in polar latitudes
H. Berndt, M. Hilmer, P. Lemke and E. Ruprecht

The physical processes governing the atmosphere–sea ice–ocean interaction in polar latitudes are investigated by regional models for the atmosphere and sea ice. The atmosphere is modelled with the REgional MOdel (REMO), which is a joint development of the Deutsches Klimarechenzentrum (DKRZ), Deutscher Wetterdienst (DWD), and the Forschungszentrum Geesthacht (GKSS). For the simulation of sea ice a Hibler-type dynamic-thermodynamic sea ice model with a viscous-plastic rheology is used. As boundary conditions datasets of atmospheric reanalysis projects are used.

Due to a small number of direct observations of only a few parameters of the Arctic climate system these models are used to obtain physically based estimates of various quantities of interest. For example the accumulation rate of snow and ice on the Greenland ice sheet, which is determined by melting processes and hydrology, cannot sufficiently be obtained by direct measurements.

For the sea ice there have been many efforts during the last two decades in observing its drift and concentration by using satellites and drifting buoys. Other quantities, like for instance the ice thickness, are only sporadically observed. The sea ice model, validated with the available datasets, is used to study the interannual to decadal variability of the ice thickness and the ice volume transports out of the Arctic in response to the atmospheric forcing data.

NAO-induced variability of water masses and transports in the upper layer of the northern North Atlantic
Manfred Bersch and Jens Meincke

Hydrographic observations along WOCE section A1E (Greenland-Ireland) between 1991 and 1999 show a pronounced warming, salinization, and thickening of the Subpolar Mode Water (SPMW) east of the Reykjanes Ridge after the winter 1995/96, when the Westerlies weakened drastically and the North Atlantic Oscillation (NAO) turned from a high phase during the first half of the 1990s to a low phase. Recent hydrographic data from May 1999 reveal a return of the SPMW to colder and fresher conditions. The changes of its heat and salt content amount to 17% and 10%, respectively, for the whole section and are mainly due to thickness variations of the layer.

The magnitude of the thermohaline changes is too large to be explained by altered fluxes of heat and freshwater at the sea surface only. To a large degree the changes result from an expansion/contraction of the subpolar gyre east of the Reykjanes Ridge during NAO high/low phases. When the Westerlies are strong, the eastward transport of cold and fresh subarctic surface and intermediate waters into the Iceland Basin and the region of the Rockall Plateau is increased. Despite this, the total heat and salt transport slightly increases in this region due to the enhanced volume transport. On the other hand, weak Westerlies favour the northward spreading of warm and saline SPMW from the North Atlantic Current into the Iceland Basin and the Rockall Channel, though the transport of volume, heat, and salt drops to a minimum east of the Reykjanes Ridge as was the case in 1996.

Co-variability of sea level pressure and upper ocean heat storage of the North Atlantic, 1948–1998
T. P. Boyer, J. Antonov, S. Levitus and C. Stephens

Since its discovery by Walker (1924) the North Atlantic Oscillation (NAO) in atmospheric sea level pressure (SLP) has been studied extensively . The existence of such a mode of oscillation of sea level pressure (SLP) suggests the possibility of prediction of the future state of the atmosphere in a statistical sense. Dickson et al. (1996) have linked variability of the NAO to changes in ocean convection regimes of the North Atlantic. A second mode of variability of SLP known as the East Atlantic Oscillation (EATL) was described by Rogers (1990). Levitus et al. (1994;1995) identified a mode of variability of upper ocean temperature for the North Atlantic Ocean and linked it to the EATL.

The first step in examining the role of the ocean in climate change is to build the appropriate databases and construct the data and analysis fields that can be used to describe ocean variability. Until the last fifteen years subsurface oceanographic data were not reported in real-time as has been the case with much meteorological data. Levitus et al. (1994a, 1999) describe projects that have resulted in a large increase in the historical upper ocean thermal data available to examine the interannual variability of the upper ocean. Levitus et al. (1994) prepared and distributed gridded analyses of upper ocean temperature anomaly fields for individual years for the 1960–1990 period. We have used a more recent database (Levitus et al., 1998a,b; Boyer et al., 1998; Boyer et al., 1998b) to prepare yearly temperature anomaly fields. In this paper we describe the co-variation of upper ocean heat storage and the North Atlantic and East Atlantic oscillations in sea level pressure for the 1948–98) period.

In addition we described the rate of change of heat storage for the North Atlantic during the 1965–1998 period. NODC Home Page: www.nodc.noaa.gov

North Atlantic circulation, pathways and water mass distributions from WOCE observations, altimetry and model results
V. I. Byshev and Yu. A. Romanov

The structure and the dynamic of the North-Atlantic Current (NAC) in May–June 1990 were studied on the base of the data received by research vessels “Akademik Kurchatov”, “Vityaz” and “Professor Shtockman” in the Soviet expedition “Atlantex-90” carried out on the WOCE programme and the national programme “Sections”. The data of 17 XBT and STD sections in the Newfoundland energy-active zone (45–53°N, 36–45°W) made across the main jets of the NAC and the results of the about one month long instruments of the sea currents at the 14 buoys placed along the meridian 36°W (47–53°N) at horizons 100, 400, 1000, 2000 and 3500 m were analysed. It was shown that the three main branches of the NAC characterised by the strong frontal zones were identified on the SST charts in the June of 1990 by the isotherms 6°C (northern branch of the NAC), 10°C (central branch of the NAC) and 14°C (southern branch of the NAC). Spatial and time variability of the central and the southern branches of the NAC was analysed by tracing of their characteristic isotherms on the facsimile SST charts. It was shown that the Central branch of the NAC was the more stable than the southern one in June of 1990. The strong connection of the stream structure at the meridian 36°W with the underwater sea-mount (2600 m) discovered in this expedition at 49°N, 36°W was revealed. This sea-mount was generating in the stream the quasi-stationary topographic meanders and vortexes. Discharge of different branches of the NAC across the meridian 36°W estimated by the direct current measurements changed from some tens Sv to 100–120 Sv and more.

The studies of NAC system in May–June 1990 present a special interest because of the anomalous condition of the Newfoundland energy-active zone in this period. The negative SST anomaly (-3°C) and the relative low heat content of the upper 1000 m ocean layer was observed to the north and northwest of the subpolar front and positive SST anomaly was observed to the south and southeast of the front. Under such condition the subpolar front was sharpening and North Atlantic current was intensifying. The investigation was party supported by the Russian Foundation for Basic research.

Circulation and conditions in the Irminger Sea from PALACE floats
Luca Centurioni, Sheldon Bacon and W. John Gould

Seven PALACE floats (four C-T-D, three T-D) deployed in October 1996 have revealed seasonal changes in stratification in the Irminger Sea and around the margins of the Labrador Sea. Detailed comparisons with in situ CTD data have allowed calibration of the float FSI CTD sensors and have shown some to be stable to ±0.005 for periods of 2 years. By mid 1999, four floats continue to provide data. The poster shows float tracks, temperature and salinity profile time series and calibration data.

FLAME - A model hierarchy for the Atlantic Ocean
The FLAME Group: C. Böning, J. Dengg, C. Dieteric, C. Eden, U. Ernst, J. Kröger, R. Redler and C. Voelker

FLAME (Family of Linked Atlantic Model Experiments) is a numerical modelling effort focused on the large-scale circulation and biogeochemistry of the Atlantic Ocean. All models that are part of FLAME are built on a common physical and numerical basis (GFDL MOM primitive equation model), and share a common set of initialisation and forcing data. This creates the opportunity for a direct exchange of experiences and new developments between the participating projects. FLAME projects presented on this poster concentrate on: an eddy-permitting simulation of the Atlantic Ocean, water mass formation in a regional model of the Subpolar North Atlantic, variations of the deep cross-equatorial flow in a regional model of the Tropical Atlantic and decadal variation in a coarse-resolution Atlantic model.

Effects of an improved model representation of overflow water on the subpolar North Atlantic
J. Dengg, R. Redler, U. Ernst, C. Böning and A. Beckmann

To improve the representation of overflow water masses in the Denmark Strait and across the Iceland-Scotland Ridge, a recent bottom boundary layer parameterisation (Beckmann and Doescher, 1997) is tested in different configurations and with different resolutions of a z-coordinate model of the subpolar North Atlantic. It is shown that the most critical restriction on the performance of this submodel is imposed by the lateral-mixing scheme used in the GCM. While horizontal mixing destroys the overflow signal completely, isopycnal mixing favours the downhill flow of dense water. The large-scale water mass distribution in the models is improved by the BBL scheme, but the dynamical implications are not as straightforward. Effects on the deep western boundary current and water mass formation (deep convection) in the Irminger and Labrador Sea are examined and conclusions are drawn on the implications for coarse-resolution climate models.

Variations in models of the North Atlantic Ocean circulation forced by observed surface fluxes
Carsten Eden and Jürgen Willebrand

The interannual to interdecadal variability of the North Atlantic Ocean circulation caused by atmospheric surface flux variations has been investigated with a medium-resolution model (4/3 degree horizontal mesh) of the Atlantic Ocean, forced with surface fluxes from the NCEP-reanalysis dataset. In addition, an eddy-permitting resolution (1/3 degree) was used to explore the influence of resolution on model variability.

The model thermohaline circulation (THC) was found to be particular sensitive to heat flux anomalies over the Labrador Sea. Mixed-layer depth variations in that region are correlated with THC-anomalies. These circulation anomalies propagate southwards into the subtropical gyre, resembling a first baroclinic mode boundary wave like structure. The meridional heat transport near the subpolar front is influenced by anomalies of both the THC as well as the horizontal subpolar gyre circulation.

The oceanic transient model response suggests the possibility of a positive feedback in connection with the North Atlantic Oscillation (NAO). Windstress change due to a high NAO weakens the subpolar horizontal circulation and reduces the gyre component of the oceanic heat transport within a few weeks. Together with enhanced southward Ekman heat transport, this leads to colder subpolar SST and could result in a strengthening of the NAO. The subsequent spin-up of the subpolar gyre and enhanced overturning due to anomalous heat fluxes and convection in the Labrador Sea leads however to a negative feedback which dominates after several years.

Interannual changes of sea surface height and geostrophic surface circulation in the North Atlantic as measured by satellite altimetry
Saskia Esselborn, Laury Miller and Bob Cheney

The interannual variability of the Sea Surface Height and of the geostrophic surface circulation in the North Atlantic is investigated using TOPEX/POSEIDON, ERS-1, and ERS-2 altimeter data. We have analysed altimetric data from these 3 satellites between 20°–70°N and 0°–80°W for the period of October 1992 to September 1997. Substantial changes of SSH as well as of strength and position of major geostrophic surface currents occurred in winter 1995/96 when the North Atlantic Oscillation (NAO)-Index dropped abruptly from a strongly positive to a negative value. The SSH in the subpolar gyre rose about 4 cm after the drop of the NAO-Index while the SSH decreased by up to 15 cm in the Gulf Stream Extension at the same time. The changes of SSH are mainly of steric origin – at least in the subpolar region where SSH and dynamic height at WOCE repeat section AR7E between Ireland and the southern tip of Greenland are in good agreement. After winter 1995/96 the geostrophic surface transport of the North Atlantic Current and most of its branches is weakened. This can be explained by the diminished SSH gradient between subtropical and subpolar gyre and by decreased wind forcing. In addition we have observed a southward shift of the Gulf Stream Extension and also of the Azores Current by about 2° during the period of negative NAO-Index.

Boundary current variability in the western subpolar North Atlantic – 1996 to 1998
J. Fischer, F. Schott, C. Mertens, P. Rhines, and J. Lazier

The boundary circulation of deep-water masses in the western subpolar North Atlantic and Labrador Sea is investigated on the basis of moored current meter records, shipboard measurements of hydrography and currents, and on PALACE-Float trajectories. The focus is on spatial (horizontal and vertical) structures of the deep boundary current at key locations around the Labrador Sea, and on flow variability at time scales from weeks to annual.

Both the deep and the shallow flow is cyclonic around the Labrador Sea and the barotropic component contributes most to the deep boundary current transport. Shipboard current measurements and PALACE float trajectories show a well defined deep boundary current of about 100 km width and core speeds of about 15 to 20 cm/s near Hamilton Bank. Shear zones are confined to the shallow Labrador Current at the shelf edge and the deepest part of the deep boundary current, the DSOW layer. A seasonal signal of about 4 cm/s is observed at the seaward extension of the shallow Labrador Current, whereas at depth a seasonal signal is barely detectable in the current meter records (less than 10% of the mean flow). However, the flow variability at depth is dominated by intraseasonal fluctuations in the period range 5 to 20 days, and their intensity has a seasonal modulation with an associated peak in fluctuate kinetic energy (FKE) in late winter. The temperature evolution in the boundary current shows some interesting relation to the flow variability, as almost simultaneously with the increase in FKE a sudden temperature drop is observed, with some indications of a horizontal temperature front inside the boundary current.

Transport of Iceland–Scotland Overflow Water from the Iceland Basin to the West European Basin
Ulrich Fleischmann, Hauke Hillebrand, Alfred Putzka and Reinhold Bayer

Increased values of freon (CFC-11) and tritium at the western flank of the Mid Atlantic Ridge at 48°N (WHP A2 section) hint to newly ventilated Iceland Scotland Overflow Water (ISOW). This water has passed the Gibbs Fracture Zone (52°N) and flows topographically leaded towards the south along the Mid Atlantic Ridge. By comparison of the tracer concentrations in the eastern and western part of the eastern basin a surplus of tracers is determined. This surplus is used to calculate a CFC-11/tritium ratio age for the ISOW, which is compared with the CFC-11/tritium ratio age of the ISOW on the section WHP A1 (58°N) situated north of the Gibbs Fracture Zone in the Iceland Basin. The age difference, the distance of the two sections, the area covered by the measurements with a tracer surplus on the WHP A2 section and the fraction of ISOW resulting from the ratio dating on A2 result in a lower limit for the transport of newly ventilated ISOW past the Gibbs Fracture Zone of (1.08±0.20) Sv.

Velocity surveying of the Denmark Strait Overflow and eddies
James B. Girton, Thomas B. Sanford, Rolf H. Käse and Janko Hauser

A programme of measurements to study the Denmark Strait Overflow using expendable and ship-lowered instrumentation was carried out from the RV Poseidon in September 1998, including a total of 110 XCPs and 76 XCTDs. The XCTDs provided important measurements of salinity for the identification of watermass characteristics, but are not included in this poster. The XCPs, in conjunction with GPS and ADCP instrumentation on board the Poseidon give a full-depth profile of water temperature and velocity, and are able to measure quite close (<1 m) to the ocean floor. They are therefore useful for studying transport and bulk overflow characteristics as well as smaller scale phenomena such as internal waves and the turbulent bottom boundary layer. An eddy sampled by multiple profiles during the second week of the cruise clearly shows a cyclonic upper-layer circulation in connection with cold surface water, as expected from the satellite images. The mean upper-layer water velocity of 50 cm s^{-1} is in agreement with observed eddy propagation speeds, while the lower-layer water velocities are up to three times greater. In addition, bottom layer changes often seem to occur downstream (south-west) of those in the upper layer. Cross-stream sections reveal a combination of barotropic and baroclinic situations at different water depths.

North Atlantic ocean variability on decadal timescales in the Hadley Centre coupled model
Chris Gordon and Claire Cooper

The simulation of decadal variations in the North Atlantic Oscillation (NAO) and related ocean phenomena in a multi-century integration of the latest Hadley Centre coupled model which does not use flux adjustment will be described. Where possible the model simulation is compared with available observations. The ocean component of the model has a 1.25° resolution, which allows a better representation of the North Atlantic Current (NAC) than in many of the earlier coarser resolution climate models. It has also enabled the relationship between the NAO, high latitude convection and the strength and path of the NAC to be explored in detail. It is shown that the model realistically simulates the NAO in both spatial pattern and time variability and, in addition, the ocean component confirms the observed relationship between convection in the Labrador and Greenland Sea and the phase of the NAO. The model also has propagating decadal timescale sea surface temperature anomalies, similar to those found in the historical observations. The mechanisms of propagation of these anomalies in the coupled model will be discussed.

WOCE Atlas for the Atlantic Ocean
V. V. Gouretski, K. Jancke and K.-P. Koltermann

A preliminary electronic version and sample paper copies of the WOCE Atlantic Atlas is presented. The data shown are based on public WOCE data. These data are adjusted according to the “cruise offsets” determined by Gouretski. The version presented is restricted to classical hydrographic parameters.

Maps are produced by optimal interpolation methods based on adjusted pre-WOCE data used for first guess fields, using gamma-n as density coordinate. Sections are presented in a consistent scale and uniform colouring scheme, contoured by objective methods. Cruise data are shown in property-property plots. Comments and critical input for improvement are welcome.

Deep Water Property Comparison for the WOCE and pre-WOCE Atlantic Hydrographic Datasets: Natural variability versus systematic errors
Viktor Gouretski and Kai Jancke

Unprecedented high quality and consistency of the WOCE hydrographic dataset allows a more precise estimate of the natural variability in the deep ocean. However, the problem of systematic differences between cruises must be addressed in order to distinguish between the natural variability and observational artefacts. Here we use a complete Atlantic WOCE hydrography along with a large number of selected pre-WOCE cruises to estimate systematic errors in the data. Property offsets, calculated within respective crossover areas, are decomposed into parts due to systematic errors and due to space/time variability within crossover areas. Analysis shows that the calculated offsets are in general systematic and do not exhibit significant correlation in time and space. The set of cruises yields about 1500 crossover offset estimates, which result in a system of algebraic equations to calculate systematic errors for individual cruises. Applying corrections for systematic errors significantly reduces inter-cruise offsets (by a factor of 2 to 5 depending on parameter), so that the apparent deep water property variability may be explained largely by systematic errors in the data. We provide examples where differences between particular cruises obviously due to systematic errors were interpreted as a consequence of natural variability. Our results allow a more precise estimate of the upper bounds of the deep water property variability on the decadal time scale, and provide a method for improving existing ocean climatology.

North Atlantic DIC ^{14}C Profiles: First Results
Pieter M. Grootes, Marie-Josée Nadeau, Helmut Erlenkeuser, Ludger Mintrop, Arne Körtzinger, and the Leibniz-Team*

The Leibniz-Labor HVEE Tandetron AMS system measured ocean water ^{14}C profiles, sampled during Meteor cruise M36-3 in July–August 1996 in the Nordic Seas and during Meteor M39-3 in July 1997 in the northern North Atlantic Ocean. CO_2 was extracted from 100 ml sample aliquots in the automated DICI-extraction system, developed in the Leibniz-Labor, and split for stable isotope mass spectrometry and AMS ^{14}C analysis. The profiles show, as expected, the penetration of bomb-^{14}C into the deep ocean as different ^{14}C concentrations in various water masses, identified by their different temperature, salinity, and chemistry. Combination of the data with earlier GEOSECS, TTO, and WOCE profiles from the "same" or nearby locations, where available, reveals the uptake of bomb-produced ^{14}C by different parts of the ocean over the intervening time periods. Due to the relatively long ^{14}C exchange time between the surface ocean and the atmosphere, the ocean still shows the transient system response to the atmospheric ^{14}C spike. The ^{14}C tracer data provide a check on calculations of the uptake of anthropogenic excess CO_2 by the ocean based on measured increases of total dissolved organic carbon (DIC) and/or changes in DIC d^{13}C. The data were obtained as part of SFB 313 "Veränderungen der Umwelt: Der nördliche Nordatlantik", (Teilprojekt B2), and the ongoing SFB 460 "Dynamik thermohaliner Zirkulationsschwankungen", (Teilprojekt A5).
*Leibniz-Team: Malte Bitterling, Frank Bruhn, Pieter M. Grootes, Katja Harmel, Peter Hasselberg, Annette Mintrop, Marie-Josée Nadeau, Angelika Oriwall, Anke Rieck and Corinna Tschorn

Variability of Sea-Air Fluxes in the North Atlantic
Sergey Gulev, Thomas Jung and Eberhard Ruprecht

On the basis of six hourly NCEP/NCAR Reanalysis surface flux fields, 40 year (1958–1997) time series of the net sea-air flux and its components as well as wind stress have been evaluated in the North Atlantic Ocean. Then we studies interannual and decadal variability in the flux fields and compared it with that which is present in the COADS fluxes for the corresponding period. COADS fluxes were evaluated from the individual COADS long marine reports by using bulk formulas. The main aim is to avoid consideration of mean fluxes, reasonably different in NCEP/NCAR and COADS, and to search the variability patterns which are typical for both sea-air flux sources. This can help to assess climatic signals in the North Atlantic ocean–atmosphere flux fields which are not affected by the uncertainties and time-dependent biases inherent into the COADS and Reanalysis data. Variability is analysed and validated using statistical estimates of trends, spectra, EOF and SVD analysis. Special attention is given to the variability in the mid-latitudinal dipole structure in the net flux, which plays an important role in the large-scale ocean-atmosphere interaction in the North Atlantic. The strategy for the reconstruction of the anomalies of sea-air fluxes which are free from inhomogeneities of data sources is suggested.

Modelling the seasonal variability of the circulation and the hydrography in the Iceland–Faroe–Shetland overflow area
I. H. Harms, J. O. Backhaus and D. Quadfasel

As part of the interdisciplinary EU-project TASC a three-dimensional, prognostic baroclinic model (HAMSOM) was applied to simulate the circulation around Iceland, the Faroe Islands and the NW-European continental slope and shelf. The flow fields served as input for a Lagragian particle tracking model applied to the succession of the copepod Calanus finmarchicus to test the hypothesis that C. finmarchicus crosses the Iceland Scotland Ridge through the Faroe-Bank Channel in depths of about 600 m advected by the overflow waters in winter. The small-scale model, with a horizontal resolution of approx. 14 km, is running in a prognostic mode including sea surface heat fluxes and a relaxation to seasonal mean Levitus temperature and salinity data. Two meteorological data sets are applied as model forcing: (i) a so-called 'typical year', based on ECMWF climatological, daily mean values and (ii) NCEP data for 1996 and 1997. The model results show a strong variability, in particular in the surface flow. In subsurface layers, the model reproduces very well the main current systems like the NAC, the NCC and the EGC. The flow field below 600–800 m is partly dominated by southward flows along the Norwegian Shelf into the Faroe–Shetland Channel. A clear overflow signal can be observed in the Faeroe Bank Channel, across the Wyville Thomson Ridge and across the Iceland Faeroe Ridge. The three-dimensional structure of temperature and salinity evolves in a realistic way. The model leaves the smooth Levitus distribution and reveals distinct fronts, in particular east and north-east of Iceland. In deeper layers, southward flowing cold overflow water can be traced in the Faroe–Shetland trough system. Model results from both simulations will be presented and compared to observational data as far as possible. Special emphasis is given to anomalies in the in- and outflow through the Faroe–Shetland Channel during the year 1996/1997.

On the link between the North Atlantic Oscillation and Arctic sea ice
M. Hilmer and T. Jung

The North Atlantic Oscillation (NAO) describes the simultaneous strengthening (high NAO) and weakening (low NAO) of the Azores high and Icelandic low. Due to the shortness of observed sea ice time series relatively less is known about its link to the ice volume flux through Fram Strait, which represents the major source of freshwater for the North Atlantic. Here we present evidence for a recent change in the link between the NAO and Arctic sea ice export through Fram Strait during wintertime (1958–1997) from the analysis of simulated Arctic sea ice and observations. The pronounced intensification of the NAO from the 1960s towards the 1990s was accompanied by a north-eastward shift of the NAO's interannual centres of action, thereby increasing the coherency between the NAO and Arctic sea ice export through Fram Strait on the interannual timescale. This shift also led to a change in the near-surface temperature response pattern to interannual variability of the NAO.

Do we overestimate the anthropogenic CO_2 uptake in the North Atlantic?
J. Holfort and D.W.R. Wallace

Estimates of the inventory of anthropogenic CO_2 in the North Atlantic (10°N–80°N) are in the order of 20 PgC in 1983 (Gruber et al., 1996). Naively all this 20 PgC has entered the ocean through air-to-sea flux in the North Atlantic. One part of it associated with the ventilation of the thermocline in the subtropical gyre, another part associated with the formation of North Atlantic Deep Water.

Our viewpoint lies outside the North Atlantic, rather we are looking from the South Atlantic northwards. In the South Atlantic (11°S to 30°S) warm surface and intermediate water is transported northward, being compensated with North Atlantic Deep Water flowing southward. In the southward flowing NADW we find only traces of anthropogenic carbon while the northward flowing upper waters contain a large amount of anthropogenic carbon, the surface waters being almost at equilibrium with the present-day atmosphere. his leads to a northward transport of anthropogenic carbon of order 500 kmol/s in the 1990s (Holfort et al., 1998). With the simple assumption, that the profile of anthropogenic carbon scales with the atmospheric excess pCO2 and that the overturning has not changed, we can show, that from preanthropogenic time to the 1990's the northward anthropogenic carbon transport from the South Atlantic into the North Atlantic sums up to about 10 PgC.

From the total inventory of about 20 PgC, therefore about 50% had entered the North Atlantic from the south and the air-to-sea flux has only to account for 10 PgC instead of 20 PgC.

Although the formation of NADW is the cause of the penetration of anthropogenic carbon into the deep ocean, the uptake of that anthropogenic CO_2 to a large extent does not occur in the formation region because the water that arrives the formation regions in the upper branch of the global conveyer has already taken up the anthropogenic carbon on its journey. Conceivably, in small regions of the North Atlantic, the actual total CO_2 uptake associated with cooling of surface waters and later formation of NADW could be lower today then before 1870 due to the decreased buffering of CO_2 uptake. Formation of NADW could therefore even conceivably drive a negative local uptake of anthropogenic CO_2.

Interannual to decadal variability of poleward flowing Atlantic Water between Iceland and Scotland
N. Penny Holliday, Raymond Pollard and Jane Read

The exact pathways and fluxes of warm salty Atlantic waters flowing between Iceland and Scotland into the Nordic Seas as part of the thermohaline overturning remain controversial. The northward flow is dominated by two varieties of sub polar mode water, the fresher Western North Atlantic Water (WNAW) in the Iceland Basin, and the more saline Eastern North Atlantic Water (ENAW) in the Hatton–Rockall–Scotland region. They are separated by the frontal zone of the North Atlantic Current, and because they have rather different temperature and salinity characteristics they contribute varying amounts of salt and heat to the northward flux. The interannual to decadal variability of those fluxes, the relationship between the WNAW and the ENAW and the processes that affect their properties and distribution are being investigated.

The hydrography of the northern Rockall Trough has been surveyed extensively since 1975 by a repeat section at 57°N. The ENAW temperature and salinity vary by ±0.3°C and ±0.04 psu over that time (after removing the seasonal cycle). The mean northward transport is 3.7 Sv but may be as high as 10 Sv in exceptional years.

The shelf edge current at that location carries around 80% of that volume flux. There is significant variability of the salinity and temperature fluxes carried by the ENAW, with unusually high fluxes in 1980, 1990 and 1998.

The variability of the WNAW at those latitudes is less well understood, but three WOCE sections from Iceland to Scotland via Rockall are being analysed to determine the changing nature and horizontal extent of both the WNAW and ENAW. In particular we hope to determine the relative impact on the poleward fluxes of interannual to decadal variability due to atmospheric influences and due to circulation changes.

How does the warm water return flow of the MOC influence the tropical/subtropical pathways?
Markus Jochum and Paola Malanotte-Rizzoli

The GFDL ocean general circulation model is used in idealised studies of the Atlantic circulation in a square basin. The subtropical/tropical/equatorial gyres are produce by forcing the model with a wind stress profile having only latitudinal dependence. The goal is to understand the effect of the meridional Overturning circulation (MOC) on the Atlantic intergyre exchanges. The MOC is imposed by prescribing a barotropic inflow all along the southern boundary and possibility for outflow at the northern one. The results indicate that the northward flow of the MOC has a crucial effect on the subtropical/tropical pathways. In the idealised configuration the North Atlantic wind field creates a basinwide potential vorticity barrier. Therefore, the water subducted in the North Atlantic has to flow to the western boundary before turning equatorward, as shown by the trajectories of floats injected in a band of northern latitudes/longitudes. Under such a wind curl, no interior pathways to the tropics are possible.

When the MOC is superimposed to the wind-driven circulation, in the western boundary the return flow sweeps most of the water northward, reducing the inflow of North Atlantic waters into the equator from 12 Sv in the purely wind-driven case to 3 Sv. Thus, with the MOC, the Equatorial UnderCurrent (EUC) is mostly supplied by water from the Southern Atlantic. The analysis of synthetic floats pathways reveals two distinct routes for the return flow of the MOC, the first one occurring in the intermediate layers along the western boundary and the second all across the basin in the surface layer. The surface path starts with water subducting in the South Atlantic subtropical gyre, flowing within the North Brazil Current to the equator, entering the EUC, getting entrained into the tropical mixed layer and finally flowing northward in the Ekman layer. The contribution of thermocline water to the MOC return flow is on the other side negligible.

A new view of the circulation in Denmark Strait with special reference to the source of the Denmark Strait Overflow Water
Steingrimur Jonsson

A remarkable feature of the Denmark Strait Overflow Water (DSOW) plume is its apparent stability. It shows very little variability on time scales longer than a few days. In particular no seasonal signal has been detected in the plume and there also seems to be little interannual variability. This raises questions on the source for this steady plume upstream from the sill and indicates that the source probably does not show significant seasonal or interannual signal. Current meter records from a section in the northern part of the strait indicate that the flow is towards the south-west over the whole deeper part of the section. Over the Greenland slope the current shows a very pronounced seasonal signal with the current even reversing during the summer. This makes it very unlikely that this part of the circulation contributes to the DSOW. On the other hand the current meter over the Iceland slope shows similar behaviour to the one observed in the plume. It shows no seasonal nor interannual variability. This would indicate that there is very little, if any, water recirculating back into the Iceland Sea from the East Greenland Current after it crosses this section. Furthermore this suggests that the DSOW has its source at the eastern edge of the EGC and thus a large part of it could be originating from the Iceland Sea.

Interdecadal changes of the NAO and its relationship to the Atlantic thermohaline circulation
Thomas Jung, Carsten Eden, Jürgen Willebrand and Eberhard Ruprecht

It is still under debate whether interdecadal changes of the Atlantic thermohaline circulation (THC) are passively driven by the NAO or if both phenomena are inherently coupled. Here we present results from observational and modelling studies which support the hypothesis that interdecadal changes of the THC during the 20th century are the passive response of the ocean to a low-frequency forcing by the NAO.

An OGCM of the Atlantic were forced with reconstructed NAO-related monthly fields of the net heat flux, wind stress and freshwater flux for the period 1865–1997. In agreement with previous studies SST anomalies along the North Atlantic Current develop against the anomalous heat flux forcing by the atmosphere during two periods: the twenties and sixties of this century. These anomalous developments can be associated with maxima and minima of the THC and meridional heat transport. Cross-spectral analysis reveals that the THC lags the NAO by approximately 90° on the interdecadal time scale. Since the response to an anomalous oceanic forcing is expected to occur instantaneously, the phase-lag between the NAO and THC supports the hypothesis of a passive ocean to a NAO-like forcing on the interdecadal time scale.

Instability and eddy formation in the overflow
Johann Jungclaus and Rolf Käse

The earliest current meter recordings from the Denmark Strait overflow demonstrated a remarkable temporal variability with typical timescales of a few days. More recent hydrographic observations with high spatial resolution showed that the overflow consists of anticyclonic and cyclonic eddies. The latter have been confirmed by satellite IR imagery. Several mechanisms have been proposed to explain the generation of these eddies, among them baroclinic instability. In our numerical experiments we use a sigma-coordinate general circulation model to simulate a cold bottom boundary current (a dense filament) on a sloping bottom in a periodic channel. We show that the filament gets unstable and breaks off into a chain of anticyclonic and cyclonic eddies if it is initially perturbed by a temperature anomaly with a wavelength that is consistent with baroclinic instability theory.

The anticyclonic eddies form within the filament as was earlier reported from experiments with layer models. The cyclones, however, form initially in the ambient water but wrap dense overflow water around their centre during their development. Therefore the anticyclones are rich of dense overflow water whereas the cyclones are a mixture of overflow and ambient water. Eddies of both signs travel along the topography with the shallower water to their right. Their self-propagation and their specific mixing behaviour contributes to the overflow transports and the water mass modification in the overflow.

Tracer observations in the Labrador Sea
Samar Khatiwala, Peter Schlosser and Martin Visbeck

Two distinct aspects of deep convection in the Labrador Sea are studied using hydrographic and transient tracer observations.

(1) The post-convection evolution of potential density on fixed pressure surfaces is used to study the eddy-induced overturning circulation set up in response to winter time convection. The overturning circulation driven by the slumping of isopycnals consists of a surface intensified flow transporting low salinity water from the boundary currents into the interior, downward motion in the central Labrador Sea, and an "outflow" at depth transporting newly ventilated Labrador Sea Water towards the boundaries. Typical eddy-induced velocities, assuming adiabatic motion and continuity, are estimated to be roughly 0.5 cm/s for the surface inflow, 1 metre/day for the vertical motion, and 0.1 cm/s for the deeper outflow, in surprisingly good agreement with those calculated in a simple numerical model of the Labrador Sea. The outflow velocity corresponds to a ventilation time scale of 3 years, similar to idealised age tracers simulated in the model.

(2) Time series of temperature, salinity, tritium, and helium data from the Labrador Sea collected between 1991 and 1996 are used to infer the history of deep convection in the 1990s. Between 1991 and 1993, even as convection penetrated to progressively deeper levels, the θ/S properties of Labrador Sea Water (LSW) stayed nearly constant as surface cooling and mixing down of freshwater was balanced by excavating into the warmer and saltier North East Atlantic Deep Water. Paradoxically, the tritium-helium age of LSW increased in this period of increasing convection. The extreme winter of 1993 produced above average sea ice on the Labrador Shelf resulting in lower than average salinity in the following spring. Because of the excess freshwater and a milder winter, convection in 1994 failed to penetrate below 2000 m. After 1994, convection was restricted to the upper 800 m. The evolution of tritium-helium age below 1000 m is similar to that of a stagnant water body.

Geostrophic boundary current transports in the subpolar North Atlantic
D. Kieke and Monika Rhein

Based on hydrographic data obtained in the Labrador Sea during the period 1950–1997, a time series of baroclinic transports (calculated below σ_θ=27.80) has been created. An objective method is chosen to fill up data gaps and bottom triangles. A comparison with corresponding transports from the Irminger Sea shows that the temporal transport variability differs in the two basins. Estimates from the Labrador Sea gave values between 3 Sv and 11 Sv in the 1950s and 1960s, with strong variations between the years. Such high values haven't been found in the Irminger Sea in this period. A comparison of transports during the 1970s and 1980s is difficult, due to very little data. But the results of the 1990s show that the geostrophic transports in the Labrador Sea are again higher than in the Irminger Sea.

Integral effects of open ocean deep convection in the Central Labrador Sea – investigated by ocean acoustic thermometry
D. Kindler and U. Send

Results of an ongoing acoustic tomography experiment in the central Labrador Sea will be presented. The Central Labrador Sea is a region of weak density stratification. During winter it is further destabilised near the ocean surface due to heat loss by atmospheric cooling. After such a 'preconditioning' sudden events of additional extreme heat loss like wind bursts can locally (on a horizontal scale of 10 km) result in deep convection reaching depths of 1000–2000 m. This deep mixing phase is followed by restratification of the mixed area resulting in an enhanced dynamic variability. To investigate the integral effects of such small scale convective processes an ocean tomography mooring array consisting of 4 tomography transceivers (400 Hz) was installed in August 1996 and redeployed in summer 1997 and 1998 in order to measure acoustic travel times over distances of typically 170–300 km. Time series of horizontally integrated properties like ocean heat content and temperature stratification are estimated by inverting travel time into sound speed and hence into temperature. These large scale properties will be used to study the interannual variability of ocean heat budget and water masses formed in close connection to deep convection and the ensuing renewal of Labrador Sea Water (LSW) [Clarke, R. A., and J. C. Gascard, JPO, 13, 1764—1778, 1983]. The Work is supported by Deutsche Forschungsgemeinschaft.

An approach for the data assimilation of statistical characteristics into eddy-resolving ocean models
A. Köhl and J. Willebrand

The study investigates perspectives of the parameter estimation problem in eddy resolving models. An adjoint method suitable for the assimilation of statistical characteristics of data and applicable on longer time scales than the forecast range is presented. The approach assumes a larger predictability for planetary scales which were isolated by spatial and temporal averaging. Since the usefulness of adjoint models is limited to the validity of the tangent linear approximation, the adjoint to a prognostic model for statistical moments is essential. Coarse resolution versions of eddy resolving models were used for this purpose.

Identical twin experiments were performed with a quasi-geostrophic model to evaluate the performance and general limitations of this approach in improving models by estimating parameters. Annual mean SSH-variance from TOPEX/POSEIDON and ERS-1 were assimilated in association with climatological data from Boyer and Levitus 1997 with the same experimental design into the CME North Atlantic model configuration. The method is shown to perform efficiently in minimising cost function values although only approximations to the gradients are employed. It is demonstrated that assimilating SSH variance can introduce in comparison to climatological data complementary but consistent information about the main frontal structures.

About the seasonality of the LSW arrival west of the Mid-Atlantic-Ridge at 47°
K.-P. Koltermann and G. Stelter

Several years of data from moorings west of the Mid-Atlantic-Ridge on the 48°N section WHP-A2 reveal that the newly formed Labrador Sea Water LSW arrives only in early spring of each year. Temperatures and salinities during these periods show little variations, indicating a rather homogeneous water mass. The changes from periods dominated by the LSW to those dominated by waters from the subtropical gyre are abrupt and occur within a week. For the rest of the year the warm and salty waters from the south show strong variations in temperature and salinity of 20–30 days periods. The vertical temperature profiles at the mooring sites are dominated by long warming and short cooling phases. Additional data from C-PALACE floats in the vicinity of the moorings provide valuable information on the development of temperature and salinity for the top 1500 m layer, particularly in winter.

Propagation of temperature anomalies along the North Atlantic Current
Gerd Krahmann, Martin Visbeck and Gilles Reverdin

A general circulation ocean model has been used to study the formation and advection mechanisms of North Atlantic Oscillation-related temperature anomalies along the North Atlantic Current. In a series of experiments we have applied patterns of wind vector, windspeed and windstress modulated by idealised fixed-frequency NAO-amplitudes. The forcing anomalies generate temperature anomalies in the upper ocean, spreading much like observed temperature anomalies which have been found to cross the basin in approximately 10 years. Our analysis of the heat budget reveals that the upper 440 m heat content anomalies are mostly formed by anomalous divergences of the oceanic heat transport. These divergences themselves arise from anomalous currents which are caused by the windstress anomalies. After their formation the temperature anomalies are advected with the mean currents.

The surface heat fluxes contribute only 1/3 of the total changes. Temperature anomalies of opposite sign are formed in the first and second half of the pathway of the North Atlantic Current, respectively. The ratio between the fixed forcing period and the advective timescale between the two parts of the pathway determines how the locally formed and the advected anomalies interfere in the second half of the pathway. For short forcing periods they are mainly determined by the local forcing while for long periods advected anomalies from the first half of the pathway become dominant. Maximal amplitudes of the temperature anomalies are found when both timescales agree.

Interhemispheric exchange and interaction with zonal flows in a modelled deep equatorial Atlantic
Jürgen Kröger and Claus W. Böning

A robust feature of model solutions for the deep equatorial Atlantic (e.g., CME, DYNAMO) is the presence of a system of zonal currents with alternating direction at annual and semiannual periods, caused by the oscillating zonal wind stresses. While mean eastward flow at depth is usually weak, tracer (e.g., salinity) distributions at NADW levels often reveal an eastward tongue along the equator. In the present study, we use an open-boundary, high-resolution model of the tropical Atlantic that was developed as part of the FLAME-(Family of Linked Atlantic Model Experiments) hierarchy, to examine the interhemispheric transport of NADW and its interaction with the equatorial current variability. A trajectory algorithm with a time-stepping scheme adapting to the highly variable flow speed is used to simulate pathways of water parcels released in the DWBC north of the equatorial regime. In contrast to the Eulerian mean picture which suggests a continuous DWBC across the equator, a large fraction of the model floats undergo elongated, zonal excursions in several bands north and south of the equator. The effect of these zonal flows on the spreading of tracers is investigated in a suite of sensitivity experiments.

Mechanisms of heat, freshwater, oxygen and nutrient transports at 24.5°N in the subtropical North Atlantic
A. Lavín, H. Bryden and G. Parrilla

Transports are estimated from hydrographic measurements taken across a section at 24.5°N occupied by the B.I.O. Hespérides in July–August 1992. Description of the hydrographic conditions and changes from earlier conditions measured on hydrographic sections in 1957 and 1981 have been presented by Parrilla et al., (1994), and Bryden et al., (1996). Meridional heat transport was recently calculated by Lavín et al. (1998). Following (Bryden and Imawaki, 1999), the meridional transports have been separated into baroclinic, horizontal and Ekman components and evaluated for the fluxes of heat, salt, oxygen and nutrients. The baroclinic contribution due to overturning circulation is responsible for the largest amount of poleward heat transport, with warmer thermocline waters flowing poleward and cooler deep water flowing equatorward. The barotropic flows associated to the Bering Straits, net precipitation and Ekman transports are the main components in the southward freshwater transport, which is larger than estimated in previous studies. The horizontal transport associated with the large-scale gyre circulation is the main contribution to southward oxygen flux. In the case of nutrients, the baroclinic component due to overturning circulation is principally responsible for the southward transports of silica, nitrate and phosphate.

Annual formation cycle of subtropical underwater in the North Atlantic
K. Leaman

Approximately 35 profiling ALACE floats, most with salinity and temperature sensors, have been deployed in the North Atlantic from about 18–30° N and 25–65°W to observe the annual variation of heat and salt content in the formaton region for Subtropical Underwater (STUW), and to observe the surrounding currents. The annual variation in heat content anomaly in the upper 200 metres relative to the time average for the floats follows well the climatological heating cycle from, for example, COADS monthly climatology. On the other hand, the salt content variability in the same layer (or the inferred evaporation minus precipitation) is highly irregular and suggests that the fresh-water inputs are strongly locally modified by, for example, convective precipitation events. However, it is still possible to see the overall pattern of formation of STUW under high-evaporation conditions (intensified trade winds) and the southward motion of this water at depths of 100–150 metres. The high-salinity core reaches the surface as the mixed layer deepens proceeding through the winter season in the north-eastern part of the above region.

The role of pre-existing mesoscale eddies in Labrador Sea convection
Sonya Legg and Jim McWilliams

Mesoscale eddies shed from the boundary currents, or persisting as remnants of previous convective chimneys, fill the Labrador sea prior to the onset of convection. Through a series of numerical simulations, we examine the role these eddies play during convective overturning driven by wintertime heat loss. Weakly stratified eddies may localise deep convection within their cores. Pre-existing eddies are destabilised to baroclinic instability following the erosion of stratification by convection, and break-up into smaller fragments, energising a barotropic velocity field, and mixing buoyancy in the horizontal. If pre-existing eddies have distinct T/S properties compared to the surrounding fluid, the eddy break-up leads to intrusions with large T/S variability but little associated density variability. The energetic small-scale barotropic velocity field ultimately homogenises most of the fluid in the horizontal. However, a few isolated eddies persist long after convection ceases, and protect the fluid within from mixing with the surroundings.

The structure of interior Labrador Sea eddy field
J. M. Lilly and P. B. Rhines

Analysis of currents from a mooring in the central Labrador Sea during 1994–1998 reveals energetic baroclinic eddies imbedded within a lower frequency barotropic flow. We employ both spectral and wavelet analysis to investigate the structure of these currents; the time-localised nature of the wavelet analysis is advantageous for highly non-stationary, episodic time series such as these. Both methods reveal a transition near 2 pw^{-1}=10 days. At shorter periods, the Fourier spectra of velocity have w^{-2} slope, while at longer periods the energy levels are elevated and have a roughly w^{-1} slope. The wavelet analysis also shows a transition at 10 days, energy at shorter periods being concentrated in localised events, but lower frequency energy having a more band-like character. The energetic events in the higher frequency band have been shown in a preceding work to be primarily advected coherent eddies. The nature of the low frequency flow is more difficult to determine, but simple analytical models of eddy advection show it cannot be due merely to interacting mesoscale eddies alone. Comparisons of the mooring data with laboratory convection regarding these two frequency bands is currently underway.

The eddy field is variable in time, with advection of convectively-generated coherent anticyclonic monopoles common during the non-convecting part of the year. During convection, the flow field is disorganised, and such coherent monopoles are never observed. Yet wintertime velocity impulses associated with warm, salty water from the boundary current are occasionally observed. The details of the origins of these eddies are unknown, and is a subject of current research.

Interannual and climate variability of volume, heat and freshwater transport estimates at 48°N in the North Atlantic
Katja Lorbacher and Klaus-Peter Koltermann

From the hydrographic dataset of five realisations of the WOCE/A2-section (along ca. 48°N in the North Atlantic) and from two previous cruises in 1957 and in 1982 we derived a significant temporal variability in the thermohaline structure and in the Meridional Overturning Circulation (MOC) on interannual and decadal scales. The section lies in the divergence zone of the subpolar and subtropical gyres that is marked by the line of zero wind stress curl.

At decadal, climate relevant time scales, the variability of volume transports reflects primarily a bimodal structure of the vertical profile of the MOC: a single meridional cell in 1982 with higher volume transports of the upper and deeper layers than the intermediate layer, the Labrador Sea Water (LSW) and two meridional cells in 1957 and in 1993 with a more pronounced LSW transport, whilst the upper and deep transports are drastically reduced. Comparisons with volume transport estimates at 36°N and 24.5°N in the North Atlantic at the same three times show that the switch of MOC between these two states is governed by changing overflow transports from the Greenland Sea.

At interannual time scales the variability of the MOC shows a rapid local response to the external, atmospheric forcing. High frequency, large amplitude fluctuations in the windfield over the North Atlantic – quantified by the NAO-index - effect mainly the position of the line of zero wind stress curl. During a negative NAO-index (weak westerlies) the subpolar gyre contracts (spins-down) and the subtropical gyre expands (spins-up). In this case the line is lying further north and the dynamics at 48°N are more influenced by the anticyclonic circulation of the subtropical gyre. This shift leads to a stronger southward transport east of the western boundary current and its recirculation which reduces the total northward transport of heat and of the upper layer of the MOC, the meridional overturning rate. At 48°N the dynamic response follows the changes in the NAO-index with a time lag of one year and was most pronounced for the largest change in the NAO-index since the beginning of the time series in 1864. This happened when the NAO-index dropped down from a maximum value in the winter of 1995 to a minimum value in the winter of 1996. Subsequently we find a maximum heat transport and overturning rate in 1996 and, only one year later, a reduction by 60% and 40%, respectively.

Changes in heat and salt contents at 48°N during the WOCE period show that the temporal variability of heat and freshwater transports is not dominated by advected subtropical temperature and salt anomalies in the upper layer. Responsibility for the observed temporal variability of heat and freshwater transports in the nineties are not the transported changes of volume characteristic but the changes in the rates of transported volume.

Subtropical/tropical water mass pathways in a numerical simulation of the Atlantic Ocean
Paola Malanotte-Rizzoli

A primitive equation, hydrostatic, terrain-following coordinate ocean general circulation model (OGCM)is used to investigate the mean water mass pathways from the subtropics to the tropics in the Atlantic Ocean. The OGCM is endowed with a free surface and with the planetary mixed layer parameterisation of Large et al. (1994). The OGCM is used in a fully realistic configuration of the Atlantic Ocean, from 30°S to 65°N and with realistic bathymetry. Surface forcing functions from the COADS climatology are used , which include the monthly means of wind stress, heat and freshwater fluxes. The model is initialised with the Levitus climatology (1994). At the northern and southern boundaries temperature and salinity are relaxed to the monthly Levitus climatology in 3°-wide buffer zones. A non eddy-resolving numerical simulation is analysed which has 3/4 degree horizontal resolution and 20 terrain-following vertical levels. The OGCM reaches a wind-driven spun-up state in about 5 years and properties are examined for the yearly average of the 10th year of simulation. Subtropical/tropical water mass pathways are not simply direct meridional routes; the existence of the tropical current system, quite realistic in the model, complicates the pathways. Theoretical ideas extending the ventilated thermocline theory to the equatorial band and the Equatorial UnderCurrent (EUC) are tested by evaluating the Bernoulli function on isopycnal surfaces outcropping in the subtropics and by injecting floats at different northern and southern latitudes. The Bernoulli isolines are streamlines of subducted geostrophic flow. The fact that velocity vectors are parallel to the Bernoulli streamlines in the basin interior, away from the near-equatorial band, shows that the subducted interior flow is indeed geostrophic.

The theoretical framework leads to the definition of three “windows” for the subtropical/tropical northern and southern ocean. The first one is the “recirculating window” in which all the northern/southern floats recirculate in the subtropical gyres. The second one is the “western boundary exchange window” in which subducted floats reach the western boundary before turning equatorward to be entrained into the EUC at the equator. The third one is the “interior exchange window” where floats reach the EUC directly in the ocean interior.

In the Northern Atlantic floats injected south of about 22°N, and between 22 and 35°W, migrate south-westward to the western boundary, and they reach the EUC following a zig-zag pattern determined by the tropical current system. It is impossible to distinguish between the western boundary and the interior exchange windows, as they are merged together and the floats trajectories cover a 10-degree broad longitudinal band. This implies a considerable transport from the subtropics to the tropics and the EUC on the warm, shallow isopycnals that outcrop south of about 22°N. The exchange window shrinks and is confined to the western boundary for the floats injected more northward and disappears for the floats injected north of about 30°N, that recirculate in the subtropical gyre In the Southern Atlantic all the floats injected between 6 and 15°S migrate to the western boundary where they are entrained in the North Brazil Current (NBC) . There is no interior exchange window. These floats migrate north-westward in the NBC. At the equator, some are directly entrained into the EUC, some overshoot but then retroflect at about 8°N to join the EUC in a pattern that had been confirmed observationally. Finally, the Atlantic InterTropical Convergence Zone (ICTZ), which has strong seasonal variations, has a profound effect on the float trajectories. The summer ICTZ, shifted northward between 10 and 20°N, creates a potential vorticity (PV) barrier, which is reflected in the yearly average. The ICTZ upwelling in fact creates a region of high PV in the surface layer, producing an “island” of closed Bernoulli contours with a very weak cyclonic circulation. The floats subducted at and north of 20°N cannot penetrate below the PV barrier but are constrained by PV conservation to flow all around it to reach the equator. The important transport to the EUC in the Northern Atlantic contradicts the observational evidence indicating that most of the EUC water is of southern origin. The Meridional Overturning Circulation (MOC) of the Atlantic seems to be responsible for inhibiting the pathway to the equator from the northern subtropics through its upper northward return flow. The model MOC, even though unrealistically shifted southward, has nevertheless a somewhat realistic upper return flow of about 12 Sv. We conjecture that the route to the equator from the northern subtropics may be completely blocked if a more realistic MOC were superimposed to the wind-driven circulation by prescribing a northward flow at the southern boundary.

Satellite tracked drifters and “Great Salinity Anomalies” in the subpolar gyre and the Norwegian Sea
Svend-Aage Malmberg and Hedinn Valdimarsson

The drift of three selected SVP WOCE drifters is described, all deployed in Icelandic waters in August/ September 1995. All together 120 drifters were deployed seasonally in Icelandic waters during the years 1995–

1998. Just a few drifters had a lifetime exceeding one year not to speak about more than three years as those described in the present paper. Their drift into the Labrador Sea and further around the Subpolar Gyre and respectively into the Norwegian Sea as far north as to Spitzbergen is discussed in comparison to the “Great Salinity Anomalies” in the seventies and eighties.

Recent variability of the North Atlantic thermohaline circulation inferred from surface heat and freshwater fluxes
Bob Marsh

A surface buoyancy-forced component of the North Atlantic overturning is diagnosed from observed surface heat and freshwater fluxes (subsetted from the SOC climatology). A climatological mean of this diagnostic indicates the steady overturning rates for those water masses which are principally formed by surface buoyancy forcing: 6.3 Sv of Greenland Sea Deep Water (GSDW), 3.4 Sv of Labrador Sea Water (LSW) and 7.1 Sv of 18 Degree Water (STMW). Obtained for each year over 1980–97, the diagnostic reveals interannual variability in the renewal and overturning in density ranges characteristic of these water masses. Total overturning over 1980–97 appears to have been relatively invariant at around 15.5 Sv, although a decreasing trend is evident over much of the period 1990–97. More dramatic changes are apparent in the overturning of different water masses. The overturning of STMW exhibits large-amplitude interannual variability, with rates ranging from 2–3 Sv (in 1980 and 1986) to 15-16 Sv (in 1987 and 1996). A background positive trend is dominated by variance of nearly 11 Sv. By contrast, the overturning rates of LSW and GSDW, while less noisy on interannual timescales, exhibit decadal-timescale trends. LSW overturning rates increase from near zero in the early 1980s to a maximum of ~10 Sv in 1990, and return to near zero by 1997. In an apparently opposite phase, GSDW overturning rates decline from a peak rate of ~11 Sv in 1981 to a minimum of ~3.5 Sv in 1991, and then increase somewhat up to 1997. Variability in these overturning rates is related to changes in the North Atlantic Oscillation (NAO) and the Arctic Oscillation (AO). Correlation coefficients between total overturning rate and three versions of the NAO-index (r=0.61, 0.66, 0.70) are significant at a 99% confidence level (based on a Student’s t-test). The overturning of STMW is more weakly (and not significantly) anti-correlated with NAO indices (r=-0.27, -0.39, -0.45). Co-variability of LSW overturning and the AO-index is highly significant (r=0.63). The overturning of LSW and GSDW is significantly anti-correlated (r=-0.53): strong GSDW overturning is obtained in years when NAO-indices are relatively low, while LSW is most strongly renewed at NAO-index maxima – i.e., surface-forced renewal rates for LSW and GSDW vary in anti-phase, as suggested by hydrographic evidence.

The surface circulation on the eastern North Atlantic as observed with satellite tracked drifters
C. S. Martins and A. Fiúza

A kinematic description of the near-surface circulation and its properties is obtained from the analysis of a drifting buoy data set in the Eastern North Atlantic between the Iberian Peninsula, the Azores and the Canary Islands.

Data from surface WOCE-TOGA drifters equipped with holey-sock drogues centred at 15 m depth were collected during a period of 22 months. The drifters sampled a velocity field with a weak mean flow regime and eddies of different scales. They meandered southward everywhere in the study region, except in the Iberian coastal transition zone. All important mean currents are reproduced by the near-surface mean velocity field obtained with these drifters, including the poleward Portugal Coastal Countercurrent during the autumn, winter and early spring off western and northern Iberia, the slow offshore equatorward flow of the Portugal Current during the whole year, the south-westward Canary Current, and the zonal eastward Azores Current, confirming the eastward extension of this current up to the vicinity of the African coast in the Gulf of Cadiz. Mean velocity values and the standard error about the mean are calculated on a regional basis. Discrete eddies were studied in order to map and describe their geographical distribution and characteristics on the Eastern North Atlantic. The eddy kinetic energy provides the largest part of the total kinetic energy.

The rate of dispersion is estimated from the Lagrangian statistics of the drifting buoys. The dispersion of the drifters in the study region is well modelled by a simple description of eddy diffusion, according to the theory of Taylor [1921]. Ensemble mean diffusivities (K) as well as the space-time Lagrangian integral scales (L,T) were obtained for the zonal and meridional directions. Testing least squares fits to $K \propto u^2 \cdot T_L$ and $K \propto u \cdot L$, where u^2 represents the velocity variance, leads to the conclusion that simple parameterisations relate the scales of motion of the random velocity field to the diffusivity. A linear dependence was found between the eddy diffusivity and the eddy kinetic energy.

Comparisons of high resolution POP simulations and WOCE data in the North Atlantic
Julie McClean, Mathew Maltrud, Wieslaw Maslowski and Albert J. Semtner

A suite of high resolution Los Alamos Parallel Ocean Program (POP) simulations will be used to examine the thermohaline overturning and fluxes in the North Atlantic. These models have different forcing, resolution, and configurations, however together they can be used to address a variety of issues which would not be possible with only one model. The highest resolution, almost-global (77°S to 77°N) POP simulation available has a nominal resolution of 1/6-degree and was forced with daily European Centre for Medium-Range Weather Forecasts (ECMWF) wind stresses and monthly Barnier climatological heat fluxes for 1993–1997. Surface salinity was restored to Levitus [1982] values. It was initialised using a 35-year spin-up from a lower resolution run followed by nearly thirty more years at the present resolution. Recently, a fully-global 1/3-degree version with a displaced North Pole grid was forced with ECMWF reanalysis wind stresses, heat and freshwater fluxes for 1979–1993, and with ECMWF operational products for 1994–1997. It was spun up for thirty years using a climatology created from the reanalysis products. Deep acceleration of the tracers was active below 1000 m for the first 20 years of the spin-up, producing an order of magnitude increase in tracer spin-up. Finally, a 1/10-degree North Atlantic basin simulation, using the same forcing as the 1/6-degree case, was run for 1985–1997, following a 5-year spin-up. Although not useful for studying longer term water mass variability, this model can be used to evaluate the effect of increased resolution on the fluxes.

Individual hydrographic sections will be compared with co-located 1/3- and 1/6-degree model output in terms of water mass composition. The 1/3-degree model will be used to examine variability using volumetric temperature/salinity analyses and empirical orthogonal functions (EOFs). Model fluxes will be calculated along sections co-located with those used in inverse studies (Ganachaud et al.) and the model/data fluxes and flux divergences compared. Finally, a comparison of 1/6- and 1/10-degree heat fluxes will be used to assess the effect of increased resolution.

Observations of vertical currents and convection
C. Mertens, F. Schott, J. Fischer and U. Send

The process of deep water formation in the central Labrador Sea has been observed by means of moored current meters and temperature/salinity recorders over several annual cycles.

Acoustic Doppler current profilers (ADCPs), recording the three-dimensional currents associated with deep mixing, show a large number of convective plumes with downward velocities from 2 to 8 cm/s during February and March. The mean vertical velocity of all observed plume events is of about 4.5 cm/s. Vertical velocities exceeding 4 cm/s are only found at night, when the largest surface heat fluxes occur. The horizontal scales of the observed convective plumes range from 200 to 1000 m, with a mean of about 650 m. Fluctuations of vertical velocity and temperature during periods of intense convection activity show a small but significant correlation resulting in a net upward transport of heat that varies with the surface heat flux.

Repeated CTD surveys confirm considerable interannual variability of vertical stability in the Labrador Sea Water layer (200 to 2000 m). The magnitude of these variations is found to be of the same order as the variability of the surface buoyancy fluxes.

The alkalinity to salinity relation in the northern North Atlantic Ocean: comparison of data from the WOCE era with the TTO-NAS study
L. Mintrop, A. Körtzinger, E. Lewis, and D. W. R. Wallace

Surface water total alkalinity generally shows a strong correlation with salinity, resulting from the mainly conservative behaviour of this parameter. Biological processes can affect this quantity by the uptake/release of nitrate and formation/dissolution of carbonate shells. These two processes, often occurring simultaneously, have opposite effects on alkalinity and can partly cancel each other. The freshwater (S=0) alkalinity end-member of an alkalinity-salinity regression reflects the average alkalinity input by river runoff. This intercept is mostly found to be constant in the North Atlantic, except for Labrador Sea and East Greenland Current surface waters which have a higher value.

Deep water total alkalinity reflects these surface origins together with the integrated effect of any dissolution of carbonate over time, added to the 'preformed' values. Resulting from uptake of anthropogenic CO_2, the total dissolved inorganic carbon concentration in seawater (CT) is expected to increase with time, and, depending on the penetration depth of the anthropogenic signal, this increase is expected to show up in deeper layers after some time. Alkalinity to the contrary is believed to remain unchanged by anthropogenic impact. A prerequisite for any simple interpretation of a change in CT between historical and recent data and also for any sophisticated method of calculating anthropogenic CO_2 from CT and oxygen data is an unchanged alkalinity.

In this poster, surface and deep water alkalinities and especially their relations to salinity are compared between the TTO North Atlantic Study (1981) and data from WOCE cruises and cruises within the SFB (special research programme) 460 from 1997. Consideration is given to whether observed differences are due to analytical artefacts or are ‘real’.

Decadal signals in upper layer temperature structure from expendable bathythermograph transects
Robert L. Molinari and Derrick Snowden

Expendable bathythermograph (XBT) representations of upper layer temperature structure in the Atlantic Ocean are available since the mid-1960s. Two types of sampling are used to illustrate decadal signals in temperature patterns. Low resolution sampling of the western subtropical Atlantic shows the presence of decadal variability in temperatures above 400 m. In contrast to model studies that suggest planetary wave propagation plays an important role in establishing these signals, much of the western Atlantic signal is explainable by local Ekman pumping dynamics. Several Voluntary Observing Ship transects have been occupied since the late 1960s. In particular, a line between the east coast of the US and Bermuda includes a decadal signal in upper layer temperature that is caused by lateral movements in the position of the Gulf Stream. Another line crossing the Atlantic at about 32°N includes a decadal signal with some suggestion of eastward propagation. Other lines will be reviewed for similar time-scale anomalies.

Thermohaline variability in the Irminger Sea
John Mortensen and Hedinn Valdimarsson

During the period May 1997 to May 1999 the VEINS (Variability of Exchanges In the Northern Seas, an EU project under the MAST III programme) hydrographic section Faxaflói between Greenland and Iceland across the Irminger Sea has been repeated seven times. The Faxaflói section covers the northern part of the Subpolar Gyre System in the north-western North Atlantic and plays an important role in monitoring thermohaline overturning of Atlantic Water which is believed to influence the long-term changes in the climate system. The poster will focus on thermohaline variability observed in the section. In addition deep overflow pulses and eddies connected to the overflow are discussed.

On the branching of the Iceland–Scotland Overflow east of Charlie Gibbs Fracture Zone: First results and future observations
Thomas J. Müller, Sylvia Becker and Walter Zenk

From its source regions the Iceland Scotland overflow parallels the eastern flank of the Reykjanes Ridge as a deep western boundary current ultimately approaching Charlie Gibbs Fracture Zone (CGFZ). This transform fault in the Mid Atlantic Ridge represents a topographic gap through which a major fraction of Iceland–Scotland Overflow Water (ISOW) escapes into the Irminger Basin.

However, as waters with ISOW characteristics are also found south of the CGFZ, part of this current must continue flowing southward. From two new highly resolved hydrographic sections (May/June 1997, August 1998) running normal to the ridge and an array of three current meter moorings just north of CGFZ (May 1997 to August 1998), we conclude that north of CGFZ the ISOW already appears to be split into two separate jets. The western jet seems to feed the flow through CGFZ with 1.7 Sv over 100 km width. The existence of the eastern jet already upstream of CGFZ, must be caused by the aforementioned eastward shift of the Mid Atlantic Ridge by four degrees in longitude at the latitude of CGFZ (~53°N). An array of four moorings has been set south of CGFZ on the eastern flank of the Mid Atlantic Ridge in August 1998 to measure directly the transport of the southward proceeding jet of ISOW. An additional array of four moorings is planned during a revisit of the site in June 1999 to observe the main jet leaving the Iceland Basin through CGFZ. Seeding of deep RAFOS floats will further be used to visualise spreading paths of ISOW in the southern Iceland Basin.

On the origin and pathway of the saline inflow to the Nordic Seas
A. L. New, S. Barnard, P. Herrmann and J.-M. Molines

Three high-resolution ocean circulation models of the North Atlantic, differing in their description of the vertical coordinate, have been investigated in the DYNAMO project to elucidate the origins and pathways of the saline inflows into the Nordic Seas. In two of the models, Mediterranean Overflow Water (MOW) flows northwards, but only as far as the Porcupine Bank (53°N). In one of the models, the MOW also invades the Rockall Trough.

However, none of the models allows the MOW into the Nordic Seas. Instead, they are unanimous in showing that the saline inputs to the Nordic Seas derive from near-surface water masses and result partly from branches of the North Atlantic Current (NAC), and partly from a poleward "Shelf Edge Current" (SEC) around the European continental slopes. The highest salinities are set and carried northwards by the SEC itself, which transports Eastern North Atlantic Water from the Bay of Biscay region. The high salinities on density surfaces appropriate to the MOW in the Nordic Seas result from the transport of saline waters in the SEC/NAC system and subsequent downward wintertime mixing, primarily in the Faeroe-Shetland Channel.

Does the potential vorticity distribution constrain the spreading of floats in the North Atlantic?
Jane O'Dwyer

Float trajectories are compared with the distribution of climatological potential vorticity, Q, on approximate isentropic surfaces for intermediate waters in the North Atlantic. The time-mean displacement and eddy dispersion are calculated for clusters of floats in terms of their displacements along and across Q contours. For float clusters with significant mean velocities, the mean flow crosses Q contours at an angle typically less than 20° and 30° in magnitude in the ocean interior. The implied Peclet number in the ocean interior ranges from 1 to 19 with a weighted mean value of 4.4. This mean Peclet number suggests that there is significant eddy mixing in the ocean interior: tracers should be quasi-conserved along mean streamlines over the sub-basin scale rather than the basin scale. The mean flow strongly crosses Q contours, assumed to be zonal, near the western boundary in the tropics with an implied Peclet number of 0.7; this may be a lower bound since Q contours are assumed to be zonal and relative vorticity is neglected. Float clusters with a lifetime greater than 200 days show anisotropic dispersion with greater dispersion along Q contours than across them. In summary, our diagnostics suggest that floats preferentially spread along Q contours over a sub-basin scale and imply that passive tracers should likewise preferentially spread along Q contours in the ocean interior.

Decadal variability in the Nordic Seas the last 50 years as observed in the Fram Strait and at OWS M in the Norwegian Sea
Svein Østerhus

Results from a 50 year long time of ice transport through the Fram Strait shows a strong decadal variability. The 50 year long hydrographical time series from station M (66°N, 2°E) in the Norwegian Sea shows that the layers below 1000 m is warming and the upper 1000 m is freshening.

Atlantic inflow to the Nordic Seas during 1995-1999: Transport estimates and structure
Kjell Arild Orvik, Oystein Skagseth and Martin Mork

The study is a part of the VEINS programme and deals with the inflow of Atlantic water to the Nordic Seas. This inflow of warm and saline water is an important factor for climate, ecology and biological production in Northern Europe. The investigations are carried out in the Svinøy Section just to the north of the Faroe-Shetland Channel cutting through the core of the Atlantic inflow to the Norwegian Sea. Different branches of the topographically steered inflow merges in the shelf break area off Svinøy. The Svinøy Section also intercepts the meandering front farther offshore that separates the Atlantic water and the Arctic water. This makes the Svinøy Section very suitable for monitoring the Atlantic inflow. Based on current measurements in 3–5 moorings for the period 1995–1999 across the continental slope of the Svinøy Section in water depths between 490 m and 990 m, long term transport estimates are obtained. Shipboard ADCP, SeaSoar-CTD and CTD transects were taken to reveal spatial features. The combined shipboard instrumentation on RV "Haakon Mosby" with SeaSoar towed profiling CTD and RDI-ADCP, has made it feasible to perform a near synoptic survey of the hydrographic and current field of the Atlantic inflow. A two-branch Norwegian Atlantic Current has been revealed in the Svinøy Section, an eastern and a western branch. The eastern branch has the properties of a narrow topographically trapped nearly barotropic 30–50 km wide current with a maximum speed of 117 cm/s. The western branch about 30 km wide appears to be a frontal jet with a maximum speed of 87 cm/s. In between these two prominent branches, the observations show an energetic eddy field with a recirculation to the south-west, features not revealed in the hydrography. Transport estimates from the current records in the eastern branch show an annual mean inflow of 5.1 Sv with variations on a 25 hours time scale ranging, from -1.2 Sv to 13.8 Sv and between 2.9 Sv and 9.6 Sv on a monthly time scale. The four-year time series of the eastern branch shows evidence of a systematic annual cycle with summer to winter variations of about 100% (except for the first year). Comparisons of sea level pressure differences between Portugal and Iceland (a hybrid NAO index) and the Atlantic inflow on a three-month time scale, show a strong relation for most of the record, reflecting the strong influence of the westerly winds. Transport estimates of the western branch are inferred from hydrography (Fofonoff potential) as well as ADCP and moored observations. Our findings show a yearly mean baroclinic transport of 4 Sv with no systematic annual cycle in this western branch. Thus our investigations to data show a yearly mean Atlantic inflow of 9 Sv in the Svinøy Section.

Vivaldi 1996 – a survey of the Subpolar Gyre of the North Atlantic
R. T. Pollard, N. P. Holliday, J. F. Read and H. Leach

As part of its contribution to WOCE, the UK carried out two hydrographic surveys of the North Atlantic in which the WOCE standard of full depth CTDs every 50 km was traded for wider spatial coverage with high quality CTD and other underway data every 4 km, but limited to the top 400–500 m of the water column. The first survey, Vivaldi 1991 (Pollard et al., 1996), covered the inter-gyre region northeast of the Azores, and consisted of 5 nearly north-south lines 300 km apart running from 39°N to 54°N. The second, Vivaldi 1996, extended the survey further north, from 54°N to Iceland and from Greenland to the UK.

In view of the proven usefulness of running SeaSoar + ADCP lines under altimetric satellite tracks (Challenor et al., 1996), the Vivaldi 1996 grid was modified to follow TOPEX/POSEIDON tracks wherever possible, whilst more or less retaining full depth CTDs on a 300 km grid, some duplicating those of Vivaldi 1991. An initial estimate of circulation and transports from the full depth CTDs has been published (Pollard et al., 1998). Here we show data from the ship's track along the ascending T/P track running from the Bay of Biscay to the Reykjanes Ridge, hence crossing the North Atlantic Current where it turns from (roughly) east to north to the south-west of Hatton Bank. The varying stratification along the track is shown (significantly weaker south-east of the NAC in the Eastern North Atlantic Water) and the ADCP data. The variability of the NAC during the entire period of the T/P mission can then be derived.

Mixing in the overflow plume of the Faroe-Bank Channel
Detlef Quadfasel and Dagmar Hainbucher

During April 1999 the overflow plume in and west of the Faroe-Bank Channel was mapped using hydrographic and current profiling instrumentation. With speeds of up to 1 m/s the plume descended down the continental slope and split into two branches at a topographic bump some 150 km west of the channel's exit. East of this bump the plume appeared to meander in the cross-slope direction with a time-scale of 5–7 days, as revealed by moored temperature and current records. The entrainment of ambient warm Atlantic Water into the cold overflow was strongest just east of the topographic bump in the region of steepest bottom slope.

North Atlantic mixing processes: an eddy in the Iceland Basin
Jane Read and Raymond Pollard

The modification of upper ocean water masses in the Northeast Atlantic is generally described as a slow progression around the subpolar gyre from subtropical to subpolar mode water, the dominant processes being cooling and freshening of the surface layer. However, both detailed surveys and large-scale coast to coast sections have revealed eddies and mesoscale structures. These are particularly evident in satellite images of the region. Thus small-scale processes also have a role to play.

During June 1998 a detailed survey was made of a large anticyclonic eddy in the Iceland Basin. Situated at 60°N, 21°W with a surface signature approximately 100 km in diameter, it was in near solid-body rotation with velocities up to 50 cm/s. The temperature and salinity characteristics of the eddy core were significantly different to the surrounding water, exhibiting unusually low stratification. In contrast, the core was encircled by tongues of water with extensive interleaving. The characteristics of both the core and the surrounding water suggest strong mixing and water mass modification. Some quantification of the processes is being attempted.

The formation and longevity of the eddy are unclear from its water mass characteristics. A drifting buoy rotated in the eddy for three months before moving away from it. Two short hydrographic/current sections were worked along TOPEX/POSEIDON satellite tracks to provide calibration information for the altimeter signal. From the time-series of altimeter data it is hoped that the origin and fate of the eddy can be identified, providing clues to the formation mechanism.

Estimates of LSW formation rates by the CFC inventory in the subpolar North Atlantic, 1997
M. Rhein, J. Fischer, C. Mertens, D. H. Min, A. Putzka, W. Roether, W. M. Smethie, D. Smythe-Wright, A.Sy and R.F.Weiss.

Numerous hydrographyic surveys in the subpolar North Atlantic in 1997 provided an unique quasi-synoptic hydrographic, chlorofluorocarbon (CFC, component CFC-11), and Palace float data set. Float trajectories and the CFC distribution in Labrador Sea Water (LSW), both appear to follow f/h contours. Thus a topography-following interpolation scheme is applied to calculate gridded CFC-11 and thickness fields for upper LSW (bounded by σ_θ=27.74-77) and lower LSW (bounded by σ_θ=27.77-80). From the gridded fields we determine the CFC-11 inventory of these layers from 40–65°N, and 10–60°W), which resulted in 2160±270 tons of CFC-11. These must be introduced into the LSW by deep convection since the 1930s. Assuming 100% CFC-11 saturation during convection, and neglecting CFC losses by export of LSW out of the subpolar gyre, by transfer to higher density classes through entrainment and vertical mixing, a lower limit of LSW formation rates is estimated to 3.5–4.5 Sv. If lower LSW is ventilated only during years with high NAO, the minimum formation rate of lower LSW during these periods would be approximately 5–7 Sv.

Deep water mass variability in the subpolar North Atlantic
M. Rhein, F. Schott, L. Stramma, C. Mertens and J. Fischer

As part of the IfM Kiel programme SFB 460 “Dynamics of the Thermohaline Circulation” hydrographic surveys of the Labrador Sea and surrounding seas have been carried out annually since 1996. The objectives of the investigations are to study the variability of the deep water masses Labrador Sea Water (LSW), Gibbs Fracture Zone Water (GFZW), and Denmark Strait Overflow Water (DSOW). We present maps of hydrographic property distributions averaged for key isopycnal layers, based on the SFB cruises. Due to weak or absent LSW formation in the last winters, the LSW-layer thickness decreased while its salinity and temperature increased. Even the DSOW in the Labrador Sea shows clear year to year variability.

The dense northern overflows
Peter M. Saunders

We review the state of knowledge of the major dense northern overflows of the northern North Atlantic, those overflowing the sills of the Denmark Strait and of the Faroe Bank Channel. The property changes between the sills and Cape Farewell (60°N) are summarised but the principal emphasis is on the overflow transports and their downstream changes. We make use of current meter measurements from 7 arrays in both the Irminger and Iceland Basins, at which sites transport time-series have been constructed along with estimates of variability. The topics of the control of overflow transports at the sills and the nature of mixing and entrainment beyond the sills are touched on. Current numerical models are shown to represent the evolution of the overflows poorly, level models mix away the dense water too rapidly and isopycnal models have the opposite defect, allowing dense water to propagate unrealistically far. These problems must be overcome before realistic representation of the large scale overturning of the North Atlantic can be constructed.

A coupled ocean-ice-atmosphere oscillation with decadal time scale in the North Atlantic area
Torben Schmith

The dominant mode of atmospheric variability in the North Atlantic region is the North Atlantic Oscillation (NAO). The NAO index, defined as the normalised pressure difference between Iceland and Azores and averaged over the winter, is available since the middle of the previous century. Spectral analysis yields a basically red spectrum, however with enhanced power between 6 and 10 years and below 3 years (e.g. Hurrell, 1997). This indicates that the ocean takes an active or passive role in the NAO.

In this work, a hypothesis is presented to account for the quasi-decadal variability, based on analysis of observed atmospheric and oceanic data. Propagation of salinity/sea temperature signals in the East Greenland Current is shown to be consistent with variations in sea ice cover along the mean ice border. These variations represent a thermal forcing of the atmosphere by preventing the turbulent heat fluxes directed from the ocean to the atmosphere. The Labrador Sea is identified to be particular effective, i.e. a heat flux anomaly gives a large atmospheric response. This is both indicated from observations and from GCM studies (Lopez et al., 1998)

This lead us to propose a coupled oscillation with 8–10 year period whose main elements are as follows: propagation of sea-ice anomaly from Barents Sea to Labrador Sea, forcing of positive/negative NAO pattern in the atmosphere through thermal forcing, enhanced heat transport to the Barents Sea, both in the ocean and in the atmosphere. After two loops the whole cycle is run through. The mechanism is described in more detail in Schmith et al. (1998).

On the transport of Mediterranean Outflow Water
D. R. Slater and H. L. Bryden

The influence of Mediterranean Outflow Water (MOW) can clearly be seen stretching northwards and westwards on maps of North Atlantic hydrography (Worthington, 1976). It was hypothesised by Reid (1979) that MOW is transported polewards in an eastern boundary undercurrent, outcropping in the Nordic Seas. This poleward transport has since been observed, although only as far as the Porcupine Bank (53°N) (McCartney and Mauritzen, 1998). We are seeking to determine how much of the MOW flows northwards and how much flows westwards.

Data from three hydrographic sections (24.5°N in 1992, 20°W in 1988, 41.5°N in 1997) were used to construct a 3-sided box (the Medbox) around the Strait of Gibraltar to investigate the transport of MOW. The influence of the MOW can be seen at mid-depths across the entire north edge of the Medbox (41.5°N). It is concentrated in a northward flowing current between 600 m and 1500 m depth east of 12°W, which has 2 distinctive cores centred on 800 m depth and 1200 m depth. The upper core is characterised by a temperature maximum (>11.5°C) and the lower core is characterised by a salinity maximum (>36.2 ppt). A westward flowing current of lower core MOW crosses the western boundary (20°W) at 700–1500 m depth, between 35°N and 40°N. Also observed on this boundary are two Meddies at 25-27°N.

By calculating the outflow salinity transport over the MOW depths, we have initially determined that the amount of MOW flowing northwards across 41.5°N and westwards across 20°W is approximately 40% and 60% respectively. There is no appreciable southward transport of MOW across 24.5°N.

Meridional distribution of CFCs in the western subtropical Atlantic Ocean
William M. Smethie, Jr.

During July and August of 1997, hydrographic/tracer sections were run along 52° and 66° W in the western subtropical Atlantic as part of the Atlantic Circulation and Climate Experiment. Chlorofluorocarbons (CFCs) 11, 12 and 113 were measured along these lines. At the northern ends of the lines, three subsurface maxima were present along the continental slope. The upper maxima was associated with Upper Labrador Sea Water, the middle maxima with Classical Labrador Sea Water and the deep maxima with overflow water from Denmark Strait and the Iceland-Scotland Ridge. The upper two maxima merge into a single maximum south of the boundary and this maximum extends across the entire basin with concentration generally decreasing in the southward direction and then increasing at the southern boundary in the DWBC. Relatively high CFC concentrations extend to 35°S, well seaward of the DWBC indicating substantial recirculation from the boundary. Isolated lobes of high CFC water near 31°N also appear to be a recirculation feature, but it is too far south to be part of the Gulf Stream recirculation. There is a well defined salinity minimum in the θ/S plot for the northern ends of the two sections associated with the upper CFC maximum indicating the presence of Classical Labrador Sea Water that formed during the early 1990s. However, this salinity minimum is not present in the upper CFC maximum at the southern boundaries of the sections suggesting that the recently formed Classical Labrador Sea Water had not reached this far south in 1997. The deep CFC maximum is highest at the northern and southern ends of the sections; it extends across the entire basin along 66°W, but not along 52°W indicating the presence of older deep and bottom water of southern origin at the central part of the 52°W section. As for the upper maximum, relatively high CFC concentrations in the deep maximum extend from the northern end of the sections to about 35°N indicating substantial recirculation from the western boundary.

North Atlantic circulation and transports in eddy-permitting and eddy-resolving models of the North Atlantic
Richard D. Smith and Frank O. Bryan

We will present analyses of the circulation and transports in a 0.1° resolution simulation of the North Atlantic Ocean using a level-coordinate general circulation model forced with daily ECMWF winds covering the period 1985–1998. The results are compared to corresponding simulations at 0.2° and 0.4° resolution, and to available in situ and remote sensing observations. The 0.1° simulation shows substantial improvements in both the time-mean circulation and its variability as compared to the 0.2 and 0.4° simulations and to previous eddy-permitting simulations. The model shows good agreement with observations of the magnitude and geographical distribution of eddy kinetic energy and sea-surface height variability. The Gulf Stream separation at Cape Hatteras, and its structure and transport between Cape Hatteras and the Grand Banks are realistically simulated, though the mean path position is displaced somewhat south of the observed position. The North Atlantic Current is remarkably well simulated in the model; it exhibits meanders and troughs in its time-mean path that are in good agreement with observations. The Azores Current appears in the simulation, with time-mean position, total transport and eddy variability that are consistent with observational estimates. A significant shortcoming of the simulation is an unrealistically stable Gulf of Mexico Loop Current and an associated diversion of Caribbean outflow from the Yucatan Strait to Windward Passage.

Observations in the eastern North Atlantic along the 20°W meridian and in the Rockall Trough
Denise Smythe-Wright

A repeat occupation of the 20°W line from 20°N to Iceland was made in May 1998 within CHAOS (a Chemical and Hydrographic Atlantic Ocean Survey). This was followed by four zonal sections along the length of the Rockall Trough and a section across the Rockall Plateau and Hatton Bank. Full depth CTDO/LADCP and water bottle measurements were made at a total of 138 stations and water samples analysed for a range of chemical parameters including CFC and nutrient tracers, naturally produced halogenated gases, CO_2, plant pigments and biological species. In addition, underway ADCP, XBT atmospheric gas and meteorological measurements were made.

Comparison with data collected during Oceanus Cruise 202, 10 years previously, shows that there has been little change in the overall temperature and silicate structure over the 10 year period, but that there are differences in other parameters. Not unexpectedly, there is much greater depth penetration of the CFC signal; but most interesting is the more distinct signature of Labrador Seawater in the CHAOS data. This is seen as low salinity ‘blobs’ at around 1800 m between 47–54°N and is also reflected in high oxygen, nitrate and CFC concentrations.

Comparison of the 4 zonal sections across the Rockall Trough, notionally at 52°N, 54°N, 56°N and 57°N, show that cold silicate rich bottom water, probably a derivative of Antarctic Bottom Water, extends into the Trough at far as 56°N becoming warmer and less silicate rich as it moves north. Other interesting features are low salinity, oxygen rich patches between 1800-2000 m at 52°N and 54°N which represent the flow of Labrador Seawater. The data suggest that Labrador Seawater circulates around the Trough with a northern extremity close to 56°N; although previously collected data show evidence of Labrador Seawater occasionally at 57°N (Holliday et al., submitted). There is also evidence of high/low salinity interleaving at 1000 m at 54°N which is also reflected in the CFC signal. We speculate that this interleaving is competition between Mediterranean Water flowing northwards and Antarctic Intermediate Water flowing from the west. In addition, it would seem from a first look at the data that Mediterranean Water does not penetrate through the Rockall Trough into the Nordic Seas as suggested by Reid (1979) which agrees with the findings from model output from the DYNAMO project (New et al., 1999).

Lagrangian floats in the Labrador Sea
Elisabeth L. Steffen and Eric A. D’Asaro

During the winters of 1997 and 1998 a total of twenty-four Lagrangian floats were deployed in the Labrador Sea. Designed to match the buoyancy and compressibility of seawater, these floats measure temperature and three dimensional position (pressure for vertical position and RAFOS acoustic tracking for latitude and longitude) as they follow water motions. From this data excellent estimates of vertical velocity can be made as well as direct observation of mixed layer depth. In addition, estimates of heat flux to the atmosphere can be derived in several ways and compared to other data.

Although active convection was observed during both winters, the patterns revealed are quite distinct, perhaps as a response to the very different atmospheric conditions of the two winters. The floats deployed in 1997 witnessed a rapidly deepening mixed layer from the time of their deployment, reaching up to 1000 m. In 1998, the mixed layer was so shallow (400 m) at the time of deployment that the floats were trapped below the mixed layer. They were gradually entrained into the convecting layer (which eventually extended down to 750 m) providing an excellent record of internal waves as well as documenting mixed layer motions during 1998. Vertical velocities were much higher in 1997, with a w rms of 1.67 cm/s compared to only 1.02 cm/s in the mixed layer for 1998. The differences between the two winters extend to the horizontal as well; both years data show a drift of almost 200 km from the deployment location, but the 1998 data reveals a rich eddy field absent in the 1997 data, despite the reduction in heat flux and vertical vigour of convection.

Ventilation of Denmark Strait Overflow Water
James H. Swift

The Arctic Ocean and Nordic Seas transform their source waters to higher density and send the modified waters south to the other oceans. The northern components of the dense outflows from Denmark Strait include waters from intermediate depth that are annually replenished from the sea surface in the Nordic Seas. Water mass transformations in the Arctic Ocean also reach densities of the outflow waters. A compilation of sections of dissolved oxygen throughout the Nordic Seas and Arctic Ocean shows that ventilation within the Norwegian Atlantic Current is substantial, but the Nordic gyre regimes and Arctic shelf seas also contribute effectively to the transformation and ventilation of DSOW.

Long-term variability of the upper ocean thermal structure of the North Atlantic
Martin Stolley and Alexander Sy

Since May 1988 Expandable Bathythermograph (XBT) measurements have been carried out along lines from Europe to Halifax/New York (line AX3) and from Europe to Brazil (AX11) as a German contribution to the WOCE Voluntary Observing Ship programme. Having a temporal resolution of 2 to 10 weeks for subsequent cruises and a spatial resolution from 10 to 30 (AX3) and up to 60 (AX11) nautical miles, most of the profiles exceed a depth of 750 m. Measurements along AX3 cover the transition zone between the sub-polar and the sub-tropical gyre while AX11 intersects the eastern part of the sub-tropical gyre and the equatorial Atlantic from 40°N to 10°S. The seasonal and interannual variability of the mixed layer is analysed and anomalies of heat content of the upper 750 m are calculated.

As one of the most striking features the time series of heat content anomaly along AX3 shows fluctuations on interannual timescales with periods of 4–5 years while heat content estimates along AX11 provide indications of a gradual warming during the last ten years.

Evolution of the thermohaline structure and geostrophic mass fluxes at 36°N in the North Atlantic during the 1970–80s
V. P. Tereschenkov and A. V. Arkhipkin

Ten years (1970–80s) of temperature and salinity observations at the 36° N cross Atlantic Ocean section, spanning the upper 1500 m layer, were analysed in terms of the water mass properties. It was found that the waters originating within the subpolar gyre (subpolar mode and lower thermocline waters) experienced significant cooling and freshening, whereas the water masses formed in the subtropical gyre (Mediterranean and 18° waters) were subjected to opposite tendencies. Associated estimates of the geostrophic mass transport across the section indicate significant strengthening of the Gulf Stream flux to the north, resulting in an increase of the total cross-section flux. In the eastern part of the section, characterised by small variations of the meridional mass transport, pronounced changes of the vertical flux structure were detected, revealing the weakening of the Mediterranean water transport to the north.

The North Atlantic Oscillation and sea ice
Sannie V. Thorsen and Aksel Walløe Hansen

The North Atlantic Oscillation (NAO) has a strong impact on the climate in the North Atlantic sector. The atmospheric pressure oscillation is connected to changes in storm tracks, SAT (surface air temperature), SST (sea surface temperature), precipitation and sea ice. A correlation analysis between NAO and sea ice concentration in the Arctic and North Atlantic are performed. 5 sub-areas in the North Atlantic region have been chosen for further analysis. For each of these the time-lagged correlation between NAO and the sea ice concentration is computed. The results of the analysis show a map with a seesaw pattern between the eastern and western part of the North Atlantic. Furthermore the sea ice in all sub-areas lags the NAO. The lag varies from place to place, depending on the mechanism determining the sea ice concentration in the specific area. In the Greenland Sea, the sea ice concentration depends on the transport of Arctic ice and low salinity water through the Fram Strait. This process is related to the regional atmospheric circulation in the polar region and consequently a time lag of 1–2 years is found. In the Baltic Sea the ice is solely determined by local temperatures and no time lag is found. Finally in the Barents Sea both advection and SST are important and the time lag is approximately one year. The above data analysis has been applied to show the atmospheric impact on the sea ice. In order to study the influence from the sea ice on the atmosphere an atmospheric GCM (Arpege) is used. The model is forced with prescribed SST and sea ice. Preliminary results from this study are shown.

Causes of and relationships in North Atlantic variability using a 20 year (79–98) global ocean simulation
Robin Tokmakian and Albert Semtner

We have investigated the variability of the North Atlantic by jointing using a model simulation and observational data. The model is the 1/4 degree average resolution Parallel Ocean Climate Model (Semtner and Chervin, 1992; Stammer et al., 1996). Forced with realistic momentum, heat, and freshwater fluxes (derived from ECMWF re-analyses and operational fields), the model realistically simulates the variability seen in observational data. The simulation shows that the steric height change (related to the density in the top 200 m) at a given location, is dominated both at the short and long periods by the applied heat flux. The momentum flux also plays a role at high latitudes (above 45°) as well as in the tropics. For example, between 40 and 60°N, the correlation between the North Atlantic Oscillation (NAO) Index and the model's estimate of meridional heat flux is 0.6. By examining changes at the surface in the simulation and how these changes relate to and effect the subsurface fields downstream, we may be able to develop a set of predictive oceanic indices for understanding the low frequency, climatic change in the deeper levels of the ocean. As an example, in the Labrador Sea, the changes in model sea surface height (verified by altimetry) correlates with the NAO pattern. Below the surface, the thickness of the Labrador Sea Water (LSW) at 53°N, increases beginning around 1982, reaches a maximum around 1988 and then decreases towards 1998. A similar pattern of increasing LSW thickness is seen at 36°N, but beginning in 1987. A lag of approximately 4.5 years is found between the two latitudes in LSW thickness. Further studies will use the 20 year simulation to place WOCE observations into the context of longer period changes.

Inter-annual to decadal variability of Eastern North Atlantic Central Water along the European Ocean Margin (repeat areas AR12 and AR16)
Hendrik M. van Aken

Hydrographic data from the eastern North Atlantic Ocean have been assembled in a data base, with emphasis on the European Ocean Margin. Data from the ocean margin in the Bay of Biscay south-west of Brittany in WOCE repeat area AR12 are available annually from 1992 to 1998. From the Iberian margin west of Galicia in repeat area AR16 data are available since 1977, with at least an annual coverage from 1986 to the winter of 1999.

The θ-S curves of the Eastern North Atlantic Central Water (ENACW) from the permanent thermocline in both areas show variations in salinity at fixed temperatures of over 0.05 with a characteristic time scale of several years. Occasionally high near surface temperatures were lacking in the Mode Water in the Bay of Biscay, especially in 1994 (θ<11.7°C). In the preceding winter deep convection had reached a maximum pressure of about 450 dbar. In that year also the maximal near surface salinity in the mode water started to be reduced. In 1995 and 1996 the salinity of the central water at fixed temperatures decreased. It had its maximal salinity in 1992 and 1993. In 1997 and 1998 the salinity of the central water started to increase again, and the ENACW reached to higher temperatures of the mode Water again in 1997 and 1998 (θ>12.5°C). However the high salinity of ENACW in 1992/93 was not yet reached in 1998.

Near the west Iberian Margin similar hydrographic variations were observed, but here in the temperature range 11<θ<15° C. As in the Bay of Biscay the stratification along the Iberian margin decreased strongly in the winter of 1994, and the near surface salinity was reduced from ~35.95 to ~35.75. and similarly the salinity at constant temperature of the ENACW decreased in 1995 and 1996, followed by an increase until the winter of 1999. The temperature range where the concept of a narrow band of ENACW in θ-S space can be used varied from year to year, as in the Bay of Biscay. It was very small in 1984, 1991, and 1994, after deep convection events in the preceding winter to a pressure of 150 to 200 dbar. Not only the position, but also the slope of the ENACW θ-S band varied here from year to year.

The apparent correlation of ENACW along the European margin indicates that the formation and subduction of this water mass is a large-scale process, where strong convection events in winter may play an important role.

Modelling anthropogenic CO_2 penetration in the North Atlantic
Christoph Voelker, Carsten Eden and Jürgen Willebrand

The penetration of anthropogenic CO_2 into the deeper North Atlantic was modelled using a medium-resolution model of the circulation in the Atlantic from 70° south to 70° north that treats anthropogenic CO_2 as an inert tracer. We studied the sensitivity of uptake rates and modelled anthropogenic CO_2 distributions against parameterisations of gas exchange, of turbulent advection and of a bottom boundary layer. We further studied interannual variability by performing model runs using time series of surface forcing fields constructed from NCEP-reanalyses from 1958 to 1996. The higher model resolution compared to standard global carbon models results in a better reproduction of the observed difference in penetration depth of anthropogenic carbon in the eastern and western basins of the North Atlantic. Model results are compared to data-based estimates of anthropogenic CO_2 and to CO_2-transports obtained in other models.

Atlantic warm water pathways through the Caribbean passages
W. Douglas Wilson, W. E. Johns and E. Johns

Heat and fresh water transport across the equator by the upper ocean limb of the Atlantic Meridional Overturning Circulation have a significant impact on North Atlantic Ocean conditions and climate. Numerous mechanisms are proposed to transport these waters through the tropics, viz. direct western boundary currents, eddies and rings, rectification of seasonally modulated Ekman transport, but distribution among these pathways is unknown. The first easily measured choke point for the upper ocean flow, and the region where the thermohaline and wind-driven circulations interact, are the passages between the Atlantic Ocean and the Caribbean Sea. A programme of direct observations of transport and water mass properties in the passages was conducted from 1991–1998, yielding stable mean transports for passages south of the Virgin Islands (18.4 Sv), including an estimate of 11.7 in the passages south of Dominica , where southern hemisphere water dominates the inflow (Wilson and W. Johns, 1997). Analysis of shipboard ADCP data in the upper 200 m from transits through the region during 1984–1996 gave consistent results (E. Johns, Wilson, and Molinari, 1999). Recent direct observations are also consistent with geostrophic transports from historical data, suggesting little long-term change. Differences between direct/geostrophic and predicted Sverdrup transport for the region suggest a superimposed upper ocean MOC transport of 13–15 Sv. To better understand transport variability, a pilot programme is underway to continuously monitor Grenada Passage transport by measuring voltage induced in an existing telephone cable spanning the passage. With plans in place by IfM investigators to monitor meridional transport at 16°N via dynamic height moorings, we suggest that a complementary programme of transport monitoring in the Atlantic Caribbean passages be implemented as well.

Transports and fluxes in the northern North Atlantic in autumn 1994
S. Woelk and J. Meincke

From October to December 1994 hydrographic measurements along the WOCE sections A1 (Meteor 30/3) and A2 (Meteor 30/2) forming a triangle between Newfoundland, Greenland and Europe, were carried out on a quasisynoptic timescale. Consequently, three boxes bounded by sections and continents exist: a subpolar North Atlantic, a Labrador Sea and an Arctic Ocean box. On this basis, transports and fluxes were estimated by applying an inverse box model and a sensitivity study reveals uncertainties of the model outputs. We constrained the box model to conserve salt only, thus remaining imbalances in heat and volume can be interpreted as fluxes between ocean and atmosphere.

At 48° N (WOCE section A2), we estimated an overturning rate of 17.4 ±1.5 Sv and a northward east- and southward freshwater flux of 0.58 ±0.07 PW and 0.17 ±0.04 Sv respectively. The box model heat loss in the section triangle (0.11 ±0.06 PW) is in good agreement with the annual mean flux derived from meteorological data (0.12 PW). The freshwater flux is only 0 ±0.02 Sv, which is less than the atmospheric flux (0.04 Sv). However, time series show that advected freshwater anomalies produced by interannual variability in the net precipitation off east USA and in the ice export through Fram Strait could account for this difference.

In summary the transports and fluxes in comparison with values from literature show that the model is able to resolve the large-scale circulation of the subpolar North Atlantic.

Where should we look for changes in the North Atlantic thermohaline circulation due to global warming?
Richard A. Wood, Ann B. Keen, John F.B . Mitchell and Jonathan M. Gregory

It is widely recognised that global warming due to increasing atmospheric greenhouse gases could weaken the North Atlantic thermohaline circulation (THC). Since the THC carries much of the northward heat transport in the North Atlantic, this could result in a reduced rate of climate warming in Western Europe. However coupled GCMs vary widely in their predictions of the amount of THC weakening, so there is still a great deal of uncertainty in this area. Two particular criticisms which have been made of climate models are their need to use unphysical ‘flux adjustments’ in order to maintain a stable and realistic climate state, and their inability to model the source regions of North Atlantic Deep Water (NADW) with any realism. Many climate models have only one source of NADW, often around the Irminger Sea, with little dense overflow from the Nordic Seas into the North Atlantic.

In this poster we present results from the new Hadley Centre coupled model HadCM3. The model has an ocean resolution of 1.25°, finer than most previous coupled models, and produces a stable surface climatology without use of flux adjustments, thanks to its accurate simulation of large scale heat transports. For the first time in a coupled GCM, the model's NADW is produced by Nordic Sea overflows and by Labrador Sea convection, as in reality. The model transports of dense water compare well with observational estimates at three key sites: Nordic Sea overflows, Cape Farewell and 24°N. Decadal variability at Cape Farewell is also consistent with recent observational estimates.

When the model is forced with increasing greenhouse gases, the convection in the Labrador Sea shuts off, and the deep boundary flow around the Labrador Sea also disappears. However the Nordic Sea overflow remains stable. In the model these changes reach an observable level during the early decades of the 21st century. Overall the THC weakens by about 25% by 2100, and Western Europe warms at a similar rate to the global mean.

The spatial pattern in the response is potentially an observable 'fingerprint' of anthropogenic climate change. While there are still many modelling uncertainties, the model appears to have reached a level of realism where it can make useful input to the design of observing systems to monitor the THC.

[Wood, R. A., A. B. Keen, J. F. B. Mitchell and J. M. Gregory: Changing spatial structure of the thermohaline circulation in response to atmospheric CO_2 forcing in a climate model. To appear in Nature (10 June 1999)].

Variable pathways of Labrador Sea Water entering and spreading in the Iceland Basin

Walter Zenk, Sylvia Becker and Thomas J. Müller

Labrador Sea Water represents a major water mass in the Iceland Basin. After its yearly formation by deep convection in the central Labrador Sea one core of this water mass is advected on the cold side of the North Atlantic Current eastward towards Charlie Gibbs Fracture Zone (~53°N). From there this low salinity water reaches the Iceland Basin at intermediate depth (~15000 m) where it enables substantial water mass transformations. Subpolar Mode Water, Overflow Water, lower Deep Water and remainders of Mediterranean Water are all involved in the final dissolution of the eastward and north-eastward penetrating Labrador Sea Water.

In our presentation we compile first results from an ongoing Lagrangian experiment aiming at direct observations of this spreading and mixing process. The already available float and hydrographic data indicate two preferred modes of spreading. On one hand, in the central Iceland Basin we find strong indications for diffusive pathways superimposed by intermediate eddies. There seems to be an increase of eddy variability towards the northern end of the basin, i.e. south of the overflow channels. On the other hand, there are clear indications for topographically controlled flow paths along the Rockall Plateau and east of the Reykjanes Ridge at the level of Labrador Sea Water. Repeat releases from an innovative RAFOS float park raise the question of the representativeness of single Lagrangian observations in this part of the subpolar gyre of the North Atlantic.

WOCE International Project Office
Southampton Oceanography Centre
Empress Dock
Southampton SO14 3ZH
UK
Tel: +44-(0)2380-596789
Fax: +44-(0)2380-596204
e-mail: woceipo@soc.soton.ac.uk